

## A scale-down study of the industrial penicillin fermentation using quantitative metabolomics

de Jonge, Lodewijk

**DOI**

[10.4233/uuid:bc496c02-d234-46d8-bcfe-8fd3e4c65bf5](https://doi.org/10.4233/uuid:bc496c02-d234-46d8-bcfe-8fd3e4c65bf5)

**Publication date**

2016

**Document Version**

Final published version

**Citation (APA)**

de Jonge, L. (2016). *A scale-down study of the industrial penicillin fermentation using quantitative metabolomics*. [Dissertation (TU Delft), Delft University of Technology].  
<https://doi.org/10.4233/uuid:bc496c02-d234-46d8-bcfe-8fd3e4c65bf5>

**Important note**

To cite this publication, please use the final published version (if applicable).  
Please check the document version above.

**Copyright**

Other than for strictly personal use, it is not permitted to download, forward or distribute the text or part of it, without the consent of the author(s) and/or copyright holder(s), unless the work is under an open content license such as Creative Commons.

**Takedown policy**

Please contact us and provide details if you believe this document breaches copyrights.  
We will remove access to the work immediately and investigate your claim.

# A scale-down study of the industrial penicillin fermentation using quantitative metabolomics

## Proefschrift

ter verkrijging van de graad van doctor  
aan de Technische Universiteit Delft,  
op gezag van de Rector Magnificus prof.ir. K.C.A.M. Luyben,  
voorzitter van het College voor Promoties,  
in het openbaar te verdedigen op  
dinsdag 17 mei 2016 om 15:00 uur

door

**Lodewijk Philip DE JONGE**

Master of Science in de Life Science & Technology  
geboren te Leiden

Dit proefschrift is goedgekeurd door de  
promotor: Prof. dr. ir. J.J. Heijnen en  
copromotor: Dr. W.M. van Gulik

Samenstelling van de promotiecommissie:

Rector Magnificus	voorzitter
Prof. dr. ir. J.J. Heijnen	Technische Universiteit Delft, promotor
Dr. W.M. van Gulik	Technische Universiteit Delft, copromotor

Onafhankelijke leden:

Prof. dr. P. Neubauer	Technische Universität Berlin
Prof. dr. ir. H.J. Noorman	Technische Universiteit Delft, DSM
Prof. dr. G.J. Witkamp	Technische Universiteit Delft
Dr. S. Noack	Forschungszentrum Jülich
Dr. A.F.J. Ram	Universiteit Leiden
Prof.dr. W.R. Hagen	Technische Universiteit Delft, reservelid

The studies described in this thesis were financially supported by the Netherlands Ministry of Economic Affairs and the B-Basic partner organizations ([www.b-basic.nl](http://www.b-basic.nl)) through B-Basic, a public private NWO-ACTS programme (ACTS: Advanced Chemical Technologies for Sustainability). This project was carried out within the research programme of the Kluyver Centre for Genomics of Industrial Fermentation which is part of the Netherlands Genomics Initiative / Netherlands Organization for Scientific Research.

ISBN 978-94-028-0166-8

De afbeelding op de omslag is een schilderij (Compositie, 1970, olieverf op doek) van Willem Hussem (1900-1974). De foto is ter beschikking gesteld door dhr. John Stoel, en is afgedrukt met toestemming van dhr. Frank Hussem.

# Table of contents

	List of abbreviations	5
Chapter 1	General introduction	7
Chapter 2	Intracellular metabolite determination in the presence of extracellular abundance: application to the penicillin biosynthesis pathway in <i>Penicillium chrysogenum</i>	19
Chapter 3	Optimization of cold methanol quenching for quantitative metabolomics of <i>Penicillium chrysogenum</i>	43
Chapter 4	Reconstruction of the oxygen uptake and carbon dioxide evolution rates of microbial cultures at near-neutral pH during highly dynamic conditions	63
Chapter 5	Scale-down of penicillin production in <i>Penicillium chrysogenum</i>	99
Chapter 6	The organization of metabolism by <i>Penicillium chrysogenum</i> in feast/famine conditions	129
Chapter 7	Outlook	171
	Summary	177
	Samenvatting	181
	List of publications	185
	Curriculum vitae	187
	Acknowledgements	189



# List of abbreviations

The following abbreviations have been used throughout this thesis.

2PG	2-phosphoglycerate
3PG	3-phosphoglycerate
6-APA	6-aminopenicillanic acid
6PG	6-phosphogluconate
8-HPA	8-hydroxypenicillic acid
AAA	L-alpha amino adipate
ACV	L- $\alpha$ -( $\delta$ -aminoadipyl)-L- $\alpha$ -cysteinyl-D- $\alpha$ -valine
ACVS	ACV synthetase
ADP	adenosine diphosphate
AMP	adenosine monophosphate
ATP	adenosine triphosphate
CoA	co-enzyme A
Cys	L-cysteine
DO	dissolved oxygen (concentration)
DTT	dithiothreitol
E4P	erythrose 4-phosphate
EDTA	ethylenediaminetetraacetic acid
F6P	fructose 6-phosphate
FBP	fructose 1,6-bisphosphate
F26bP	fructose-2,6-bis-phosphate
G1P	glucose 1-phosphate
G3P	glycerol 3-phosphate
G6P	glucose 6-phosphate
g <sub>DW</sub>	gram of dry weight biomass
IAT	Acyl Coenzyme A:Isopenicillin N Acyltransferase
IDMS	isotope dilution mass spectrometry
IPN	isopenicillin-N
IPNS	IPN synthetase
KOH	potassium hydroxide
M1P	mannose 1-phosphate
M6P	mannose 6-phosphate

Mtl-1P	mannitol-1-phosphate
Mtl1P-DH	mannitol-1-phosphate 5-dehydrogenase
o-OH-PAA	ortho-hydroxyphenylacetic acid
OPC	6-oxopiperidine-2-carboxylic acid
PAA	phenylacetic acid
PCL	phenylacetate-CoA ligase
PenG	penicillin-G
PEP	phosphoenolpyruvate
PGI	glucose-6-phosphate isomerase
PGM	phosphoglucomutase
PMI	mannose-6-phosphate isomerase
PP <sub>i</sub>	pyrophosphate
Pyr	pyruvate
PTV	programmed temperature vaporizer
R5P	ribose 5-phosphate
S7P	sedoheptulose 7-phosphate
T6P	trehalose 6-phosphate
TCEP	tris(2-carboxyethyl)phosphine
TOC	Total Organic Carbon
Val	L-valine.
αKG	α-ketoglutarate

# **Chapter 1**

---

## General introduction

---



# 1 Industrial biotechnology

## 1.1 Micro-organisms and bioprocess technology

Micro-organisms are capable of synthesizing a wide variety of products which are useful for humans. The product range includes the living micro-organism itself (e.g. yeast used for making bread), cell extracts (e.g. for adding flavor), enzymes and other proteins and peptides, hormones, vitamins, pharmaceuticals and small chemical compounds. Some micro-organisms are very efficient in synthesizing these products by nature, but usually they have been adapted by man to become more efficient and/or more productive. This adaptation may be the result of simple selection of the best producer strain from the natural variation, or by selecting from variation which is introduced on purpose by mutagenesis. The latter method is often referred to as classical strain improvement. Micro-organisms can also be adapted by making rational changes or improvements to the metabolic capabilities of the organism by genetic engineering techniques based on knowledge of their genetic, biochemical and metabolic characteristics.

To produce an interesting microbial product, it is not sufficient to have a micro-organism with the right metabolic capabilities to synthesize it. For high yields and production rates, the micro-organism has to be brought and kept in the optimal environment. The conditions of this environment usually need to be controlled within certain limits in order for the micro-organism to exhibit its desired metabolic capability. The conditions which need to be controlled include the temperature, the pressure, the concentration of one or more substrates, the pH, the concentrations of dissolved oxygen and dissolved CO<sub>2</sub>, the concentration of (by)products, and mechanical forces, including shear forces. Therefore, the production is usually performed in bioreactors designed and equipped to control a desired constant environment around the micro-organism.

The contents of bioreactors are usually actively mixed by any kind of mixing system (for example impellers) to ensure that substrates are well distributed over the liquid phase of the bioreactor and are kept available for the micro-organisms. Without mixing, the concentrations of substrates close to the micro-organism would decrease, and consequently conversion rates would decrease. Mixing is especially important if substrate, oxygen (air) and/or pH controlling agents (acid or base) are supplied to the bioreactor during the process. Limiting the substrate supply to the bioreactor is a way to control the substrate concentration within an optimal range during the process, which is required in many bioprocesses to ensure optimal conversion of the substrate to the desired product and minimize byproduct formation. A process operated in such a way is called a fed-batch process.

A biotechnological production process can be regarded as the combination of the selection of a micro-organism (or part thereof) capable of producing a desired product, the selection of a substrate, and the definition of the process conditions and the ways to control them. A production process making use of micro-organisms is also called fermentation. The field of bioprocess technology aims at studying, designing and optimizing biotechnological processes (bioprocesses) and equipment (e.g. bioreactors) used for the manufacturing of products with the use of cells (including micro-organisms) or components thereof.

## 1.2 Industrial scale fermentations and inhomogeneity

If large quantities of a microbial product are desired, then bioreactors are often operated at a high biomass concentration to provide high volumetric productivity. Moreover, production is performed at large scale, because it provides the benefits of economy of scale. Industrial bioreactors can have volumes of up to hundreds of cubic meters, and in some cases even several thousands of cubic meters. Going from smaller to larger scale, not all aspects of the process can be kept the same, which is called the scale-up problem [1-4]. Usually, a choice has to be made which process parameter is kept constant during scale-up. This could be the concentration of dissolved oxygen, power input per volume (as alternative expression of mixing intensity), or impeller tip speed (if shear force is important) for example [5,6]. These choices are called the scale-up criteria.

Another scale-up phenomenon is that it becomes increasingly difficult to ensure adequate mixing. This is a direct consequence of the larger dimensions of the bioreactor, because the size of broth recirculation loops in the reactor become larger, while the flow rate in these loops is not increased to the same level, because that would require an impractically high volumetric power input. So, it is unavoidable that mixing times (the time required to reach a certain level of homogeneity in a certain concentration) increase during scale-up. Mixing times of a few minutes are common for industrial scale bioprocesses [7,8].

The fact that many bioprocesses are operated at high biomass concentration is a contributing factor to long mixing times, because an increase in cell density can lead to an increase of the broth viscosity. This is especially the case for cultures of filamentous fungi, as a result of their filamentous morphology [9-11]. In addition, a high biomass concentration leads to high volumetric conversion rates.

The combination of long mixing times and high volumetric conversion rates are the cause for the formation of gradients in concentrations of components which are supplied to (or removed from) the bioreactor. Whether or not this will happen in a particular bioprocess, can be examined by regime analysis [12,13] whereby the mixing time is compared to the characteristic depletion time for a consumed component and the characteristic doubling

time of a produced compound. Again, the high metabolic activity of micro-organisms, and the high biomass concentration contribute to small characteristic times for conversion at production scale. If the mixing time is of the same order or larger, then concentration gradients or zones of higher and lower concentrations are likely to occur. Gradients may exist for [7]:

- Concentration of substrate, in case of a substrate-limited fed-batch process. The substrate concentration near the entry point of the highly concentrated substrate solution is high, but decreases steeply at distances further away from the entry point.
- pH: higher concentrations of acid/base are present near the entry point [14].
- Dissolved concentration of O<sub>2</sub>: high(er) dissolved oxygen concentration exists at zones of high oxygen transfer rate. This is where gas bubbles have high partial pressure of O<sub>2</sub>, so close to the sparger, and where power input for creating bubble surface area is high, so close to the impellers. Outside of the sparger and impeller region, O<sub>2</sub> concentrations are lower. The change of the hydrostatic pressure along the height of a large scale bioreactor forms another reason for gradients in the dissolved concentrations of O<sub>2</sub>, because it affects the solubility of gases [15].
- Dissolved concentration of CO<sub>2</sub>: the opposite compared to the dissolved concentration of O<sub>2</sub>, but the extent of the gradients is much lower because the dissolved concentration of CO<sub>2</sub> is usually much higher than that of oxygen due to the higher solubility of CO<sub>2</sub>. Like for oxygen, the solubility of CO<sub>2</sub> is higher near the bottom of the tank than near the top of the tank, because the hydrostatic pressure increases going from the top towards the bottom of the bioreactor.
- Temperature: lower temperatures near surfaces where heat is removed (cooling jacket or coils).
- Shear stress: high liquid shear forces exist in the impeller zone(s), where kinetic energy is transferred to the broth, while the shear stress is reduced at distances further away from the impeller(s) where liquid flow is lower.

Cells circulating in bioreactors are continuously confronted with a change in their environment as a result of these gradients. Their presence may be beneficial for the process, because of their effect on cellular properties or metabolism [10,16,17], or for the product, because it makes the micro-organisms exposed to heterogeneities more stress-tolerant [18]. However, heterogeneities are often found to have a negative effect on product yield [19,20] or product quality [21].

### 1.3 Penicillin fermentations and *Penicillium chrysogenum*

One of the first modern aerobic industrial bioprocesses was the production of penicillin. Penicillins, such as penicillin G and V are, together with cephalosporins, the main representatives of the class of beta-lactam antibiotics. The major part of the production is carried out using the filamentous fungi *Penicillium chrysogenum* and *Acremonium chrysogenum* (also called *Cephalosporium acremonium*).

A lot is known about the metabolic pathway for the biosynthesis of PenG, the genes and enzymes involved in it, and the regulation of the enzymes and the pathway flux [22,23]. The biosynthetic pathway consists of three main steps (see Figure 1). First, three amino acids which are formed in central metabolic pathways,  $\alpha$ -aminoadipic acid (AAA), cysteine (Cys) and valine (Val), are condensed into a tripeptide called  $\delta$ -(L- $\alpha$ -amino-adipyl)-L-cysteinyl-D-valine (ACV). Secondly, one four- and one five-membered ring are closed in an oxidative step forming isopenicillin-N (IPN) by the enzyme IPNS. Finally, if the side chain precursor phenylacetic acid (PAA) is supplied to the cultivation the AAA side chain is replaced by PAA through the action of the enzyme acyltransferase (AT) to form PenG, which is secreted into the fermentation broth.

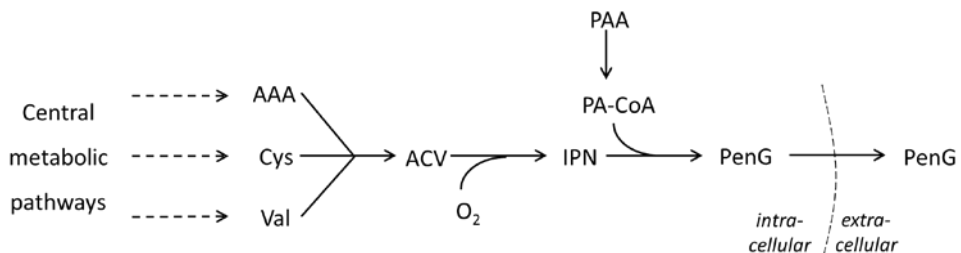


**Figure 1** Simple schematic overview of the penicillin biosynthetic pathway.

The way of operation of the penicillin fermentation process has changed a lot since 1940, when industrial production started, until now: the operation mode changed from batch to fed-batch, the bioreactor size increased to several hundreds of cubic meters, substrates were replaced to cheaper feedstocks, various automated process monitoring and control tools were introduced, and increasingly more productive strains were developed [24]. In the 1980s, Gist-Brocades (currently part of DSM) was producing with the high yielding strain DS12975, and strain DS17690 was obtained from the first by continued cultivation. These two strains have been used extensively in the past 20 years for research focusing on various aspects of industrial penicillin fermentations [25-32]. DS17690 was also used in the research presented in this thesis.

## 1.4 Gradients in industrial scale penicillin fermentations

Penicillin fermentations at industrial scale also suffer from heterogeneities in the bioreactor as discussed above. Two process parameters received particular attention in the literature: dissolved oxygen concentration and shear rate.

Oxygen is needed not only for cellular growth and maintenance of *P. chrysogenum*, but is also required as substrate in the enzymatic formation of IPN (see Figure 1). It has been reported that the specific penicillin formation rate is not affected by the oxygen level at dissolved oxygen (DO) levels above 30% of air saturation, but decreases drastically below DO levels of 30% [20,33]. No penicillin formation occurs at DO levels of about 5%-10%, although *P. chrysogenum* continues to consume oxygen at these levels for cellular growth and maintenance [20,33]. When the DO drops below the level of 30% air saturation, the penicillin synthesis rate can be restored to its maximal level by increasing the DO again above 30%, although various investigators reported that the capacity to produce penicillin was irreversibly lost once the DO drops below the 5%-10% level [20,34]. Vardar and Lilly mimicked the gradients in DO as they could exist in large scale penicillin fermentations by fluctuating the DO around the critical level of 30% air saturation and found that the penicillin production rate was reduced compared to the situation of a constant DO at 30% air saturation [20]. Larsson and Enfors [35] found that *P. chrysogenum* was irreversibly damaged, in terms of a lost respiratory capacity, if the cells resided in anoxic zones for periods of 5 to 10 minutes, but not for periods of less than 2 minutes.

The transfer of oxygen from the gas to the liquid phase strongly depends on the agitation rate, and higher agitation rates should favor the rates of cell growth and penicillin formation by increasing the supply rate of oxygen. However, the shear forces resulting from agitation were also found to be destructive for the hyphae of *P. chrysogenum*, and a negative correlation was reported to exist between the frequency of mycelia passing through the impeller region and penicillin production [36]. This can be explained in several ways. First, to compensate for the destruction of biomass, more energy has to be directed towards biomass formation and maintenance at the cost of penicillin formation. This could be expressed in a different way by stating that, the actual specific biomass formation rate (=intended growth rate + death rate) is higher at increased shear forces, resulting in an increased destruction rate of the mycelium. It was found that the relation between the specific penicillin production rate and the growth rate has an optimum (around  $0.03 \text{ h}^{-1}$  [25]) and thus the result of increased shear could be that the cultivation moves away from that optimum. Finally, the shear forces cause the hyphal branches to become shorter due to fragmentation [36], and penicillin formation is believed to be highest in subapical regions [37]; so it may be that the reduction of penicillin production at high agitation rates is due to

a reduction of productive subapical regions due to the destructive fragmentation of hyphal branches.

## 2 Aim and outline of this thesis

The effects of the presence of zones of high and low dissolved oxygen concentration and high and low shear forces in penicillin fermentations have received quite some attention in the literature, as outlined above. Surprisingly, the effects of substrate concentration gradients in penicillin fermentations has not been investigated systematically. The recent improvements in techniques to quantify intracellular metabolite levels offer interesting opportunities to investigate the intracellular metabolic effects of such substrate concentration gradients. Therefore the aim of the work described in this thesis was to study, through scale-down experiments, the effect of substrate gradients on the overall penicillin production, the behavior of central metabolism in terms of metabolic fluxes and metabolite levels and the consequences of this for the penicillin pathway flux. To this end, several experimental tools had to be developed first.

An analytical technique to quantify the intermediates and (by)products of the penicillin pathway was recently developed [38]. A number of these metabolites are not only present intracellularly, but also accumulate to significant levels in the extracellular medium. Chapter 2 presents the development of a method to efficiently remove these large extracellular amounts, which allow the accurate quantification of the intracellular amounts. The new method employs fast filtration instead of washing by centrifugation, using a cold aqueous methanol solution to keep metabolic reactions quenched.

The quenching of metabolic reactions is a key step in the sampling procedure for quantitative metabolomics to obtain a snapshot of the metabolic state of a culture. Various cold quenching solutions have been applied in literature, but it has become apparent that metabolites sometimes leak from the quenched cells into the quenching solution. The extent of leakage is dependent on the composition of the quenching liquid and the quenching temperature. Chapter 3 presents the results of the optimization of the quenching procedure which can be applied for leakage free quenching of cultures of *P. chrysogenum*.

Important physiological information, for example about the effects of substrate concentration gradients, can be obtained from the determination of the rates of oxygen uptake and CO<sub>2</sub> production of a culture. These can be obtained from measurements of the dissolved concentration of oxygen and measurements of the concentrations of oxygen and CO<sub>2</sub> in the gas entering and leaving the bioreactor. These rates may change rapidly during

transient conditions, and changes in the measured concentrations can be detected and used to calculate the rates from the material balances for O<sub>2</sub> and CO<sub>2</sub> over the gas and the liquid phase. However, the measurements of O<sub>2</sub> and CO<sub>2</sub> in the offgas of the bioreactor suffer from time delays and distortions, and furthermore the dissolved CO<sub>2</sub> can react to bicarbonate. During penicillin fermentations the pH is controlled near 6.5, and under this condition the pool of bicarbonate is significant. Chapter 4 presents an algorithm to reconstruct on a time-scale of minutes the rates of oxygen uptake and CO<sub>2</sub> production taking the measurement distortions and CO<sub>2</sub> conversion to bicarbonate into account.

The results of scale-down experiments, aimed to mimic the presence of substrate concentration gradients in large-scale fermentations, are presented chapters 5 and 6. The scale-down experiments were performed in a one-fermenter system on which a cyclic intermittent feeding regime was imposed to mimic the gradients in time instead of fermentor space. Chapter 5 focusses on the effects on the penicillin formation and the regulation of the penicillin pathway. In chapter 6 the effects of substrate gradients on central metabolism are investigated with emphasis on the metabolite pools, such as storage carbohydrates and intermediates of central metabolism, to which consumed carbon is shuttled during each feeding cycle.

Suggestions for future research following from the results and findings obtained from the research presented in this thesis are given in chapter 7.

## References

- [1] J.Y. Oldshue, Fermentation Mixing Scale-Up Techniques, *Biotechnol. Bioeng.* 8 (1966) pp. 3-24.
- [2] M. Charles, Fermentation Scale-Up - Problems and Possibilities, *Trends Biotechnol.* 3 (1985) pp. 134-139.
- [3] F.R. Schmidt, Optimization and scale up of industrial fermentation processes, *Appl. Microbiol. Biotechnol.* 68 (2005) pp. 425-435.
- [4] C.J. Hewitt and A.W. Nienow, The scale-up of microbial batch and fed-batch fermentation processes, *Adv. Appl. Microbiol.* 62 (2007) pp. 105-135.
- [5] L.A. Palomares, O.T. Ramirez, and M.C. Flickinger, *Bioreactor Scale-Up*, Encyclopedia of Industrial Biotechnology, John Wiley & Sons, Inc., 2009.
- [6] D.J. Pollard, T.F. Kirschner, G.R. Hunt, I.T. Tong, R. Stieber, and P.M. Salmons, Scale up of a viscous fungal fermentation: Application of scale-up criteria with

- regime analysis and operating boundary conditions, *Biotechnol. Bioeng.* 96 (2007) pp. 307-317.
- [7] A.R. Lara, E. Galindo, O.T. Ramirez, and L.A. Palomares, Living with heterogeneities in bioreactors, *Mol. Biotechnol.* 34 (2006) pp. 355-381.
- [8] D.J. Groen, *Macromixing in Bioreactors*, Delft University of Technology, 1994, PhD thesis.
- [9] M.R. Marten, K.S. Wenger, and S.A. Kahn, Rheology, Mixing Time, and Regime Analysis for a Production-Scale *Aspergillus Oryzae* Fermentation, in: A.W. Nienow (Ed.), 4th International Conference in Bioreactor & Bioprocess Fluid Dynamics, MECHANICAL ENGINEERING PUBLICATIONS LIMITED, Bury St Edmonds, UK, 1997, 295-313.
- [10] S. Bhargava, M.P. Nandakumar, A. Roy, K.S. Wenger, and M.R. Marten, Pulsed feeding during fed-batch fungal fermentation leads to reduced viscosity without detrimentally affecting protein expression, *Biotechnol. Bioeng.* 81 (2003) pp. 341-347.
- [11] A.I. Galaction, D. Cascaval, C. Oniscu, and M. Turnea, Evaluation and modeling of the aerobic stirred bioreactor performances for fungus broths, *Chem. Biochem. Eng. Q.* 19 (2005) pp. 87-97.
- [12] N.M.G. Oosterhuis, *Scale-Up of Bioreactors: a Scale-Down Approach*, Delft University of Technology, 1984, PhD thesis.
- [13] A.P.J. Sweere, K.C.A.M. Luyben, and N.W.F. Kossen, Regime Analysis and Scale-Down - Tools to Investigate the Performance of Bioreactors, *Enzyme Microb. Technol.* 9 (1987) pp. 386-398.
- [14] C. Langheinrich and A.W. Nienow, Control of pH in large-scale, free suspension animal cell bioreactors: Alkali addition and pH excursions, *Biotechnol. Bioeng.* 66 (1999) pp. 171-179.
- [15] R. Takors, Scale-up of microbial processes: Impacts, tools and open questions, *J. Biotechnol.* 160 (2012) pp. 3-9.
- [16] S. Bhargava, K.S. Wenger, K. Rane, V. Rising, and M.R. Marten, Effect of cycle time on fungal morphology, broth rheology, and recombinant enzyme productivity during pulsed addition of limiting carbon source, *Biotechnol. Bioeng.* 89 (2005) pp. 524-529.
- [17] S. Bhargava, K.S. Wenger, and M.R. Marten, Pulsed addition of limiting-carbon during *Aspergillus oryzae* fermentation leads to improved productivity of a recombinant enzyme, *Biotechnol. Bioeng.* 82 (2003) pp. 111-117.



- [18] P.V. Attfeld, Stress tolerance: The key to effective strains of industrial baker's yeast, *Nat. Biotechnol.* 15 (1997) pp. 1351-1357.
- [19] F. Bylund, E. Collet, S.O. Enfors, and G. Larsson, Substrate gradient formation in the large-scale bioreactor lowers cell yield and increases by-product formation, *Bioprocess Eng.* 18 (1998) pp. 171-180.
- [20] F. Vardar and M.D. Lilly, Effect of Cycling Dissolved-Oxygen Concentrations on Product Formation in Penicillin Fermentations, *Eur. J. Appl. Microbiol. Biotechnol.* 14 (1982) pp. 203-211.
- [21] J.A. Serrato, L.A. Palomares, A. Meneses-Acosta, and O.T. Ramirez, Heterogeneous conditions in dissolved oxygen affect N-glycosylation but not productivity of a monoclonal antibody in hybridoma cultures, *Biotechnol. Bioeng.* 88 (2004) pp. 176-188.
- [22] A.A. Brakhage, Molecular regulation of beta-lactam biosynthesis in filamentous fungi, *Microbiol. Mol. Biol. Rev.* 62 (1998) p. 547-+.
- [23] A.A. Brakhage, P. Sprote, Q. Al-Abdallah, A. Gehrke, H. Plattner, and A. Tuncher, Regulation of penicillin biosynthesis in filamentous fungi, *Adv. Biochem. Eng. Biotechnol.* 88 (2004) pp. 45-90.
- [24] R.P. Elander, Industrial production of beta-lactam antibiotics, *Appl. Microbiol. Biotechnol.* 61 (2003) pp. 385-392.
- [25] W.M. van Gulik, W.T.A.M. De Laat, J.L. Vinke, and J.J. Heijnen, Application of metabolic flux analysis for the identification of metabolic bottlenecks in the biosynthesis of penicillin-G, *Biotechnol. Bioeng.* 68 (2000) pp. 602-618.
- [26] W.M. van Gulik, M.R. Antoniewicz, W.T.A.M. Delaat, J.L. Vinke, and J.J. Heijnen, Energetics of growth and penicillin production in a high-producing strain of *Penicillium chrysogenum*, *Biotechnol. Bioeng.* 72 (2001) pp. 185-193.
- [27] U. Nasution, W.M. van Gulik, R.J. Kleijn, W.A. Van Winden, A. Proell, and J.J. Heijnen, Measurement of intracellular metabolites of primary metabolism and adenine nucleotides in chemostat cultivated *Penicillium chrysogenum*, *Biotechnol. Bioeng.* 94 (2006) pp. 159-166.
- [28] U. Nasution, W.M. van Gulik, C. Ras, A. Proell, and J.J. Heijnen, A metabolome study of the steady-state relation between central metabolism, amino acid biosynthesis and penicillin production in *Penicillium chrysogenum*, *Metab. Eng.* 10 (2008) pp. 10-23.
- [29] R.J. Kleijn, F. Liu, W.A. Van Winden, W.M. van Gulik, C. Ras, and J.J. Heijnen, Cytosolic NADPH metabolism in penicillin-G producing and non-producing

- chemostat cultures of *Penicillium chrysogenum*, *Metab. Eng.* 9 (2007) pp. 112-123.
- [30] D.M. Harris, Z.A. van der Krogt, P. Klaassen, L.M. Raamsdonk, S. Hage, M.A. van den Berg, R.A.L. Bovenberg, J.T. Pronk, and J.M. Daran, Exploring and dissecting genome-wide gene expression responses of *Penicillium chrysogenum* to phenylacetic acid consumption and penicillinG production, *BMC Genomics* 10 (2009) p. 75.
- [31] R.D. Douma, J.M. Batista, K.M. Touw, J.A.K.W. Kiel, A.M. Krikken, Z. Zhao, T. Veiga, P. Klaassen, R.A.L. Bovenberg, J.M. Daran, J.J. Heijnen, and W.M. van Gulik, eDegeneration of penicillin production in ethanol-limited chemostat cultivations of *Penicillium chrysogenum*: A systems biology approach, *Bmc Systems Biology* 5 (2011).
- [32] Z. Zhao, A. ten Pierick, L. de Jonge, J.J. Heijnen, and S.A. Wahl, Substrate cycles in *Penicillium chrysogenum* quantified by isotopic non-stationary flux analysis, *Microbial Cell Factories* 11 (2012).
- [33] C.M. Henriksen, J. Nielsen, and J. Villadsen, Influence of the dissolved oxygen concentration on the penicillin biosynthetic pathway in steady-state cultures of *Penicillium chrysogenum*, *Biotechnol. Prog.* 13 (1997) pp. 776-782.
- [34] R.W. Squires, Regulation of the penicillin fermentation by means of a submerged oxygen-sensitive electrode, *Dev Ind Microbiol* 13 (1972) pp. 128-135.
- [35] G. Larsson and S.O. Enfors, Studies of Insufficient Mixing in Bioreactors - Effects of Limiting Oxygen Concentrations and Short-Term Oxygen Starvation on *Penicillium Chrysogenum*, *Bioprocess Eng.* 3 (1988) pp. 123-127.
- [36] J.J. Smith, M.D. Lilly, and R.I. Fox, The Effect of Agitation on the Morphology and Penicillin Production of *Penicillium-Chrysogenum*, *Biotechnol. Bioeng.* 35 (1990) pp. 1011-1023.
- [37] T.C. Zangirolami, C.L. Johansen, J. Nielsen, and S.B. Jorgensen, Simulation of penicillin production in fed-batch cultivations using a morphologically structured model, *Biotechnol. Bioeng.* 56 (1997) pp. 593-604.
- [38] R.M. Seifar, Z. Zhao, J. van Dam, W. van Winden, W. van Gulik, and J.J. Heijnen, Quantitative analysis of metabolites in complex biological samples using ion-pair reversed-phase liquid chromatography-isotope dilution tandem mass spectrometry, *J. Chromatogr. A* 1187 (2008) pp. 103-110.



## Chapter 2

---

# Intracellular metabolite determination in the presence of extracellular abundance: application to the penicillin biosynthesis pathway in *Penicillium chrysogenum*

---

Published as:

Douma RD\*, de Jonge LP\*, Jonker CTH, Seifar RM, Heijnen JJ, van Gulik WM. Intracellular metabolite determination in the presence of extracellular abundance: Application to the penicillin biosynthesis pathway in *Penicillium chrysogenum*. *Biotechnol Bioeng* 2010;107(1):105-15.

\*These authors contributed equally to this work.

## Abstract

Important steps in metabolic pathways are formed by the transport of substrates and products over the cell membrane. The study of *in vivo* transport kinetics requires accurate quantification of intra- and extracellular levels of the transported compounds. Especially in case of extracellular abundance, the proper determination of intracellular metabolite levels poses challenges. Efficient removal of extracellular substrates and products is therefore important not to overestimate the intracellular amounts. In this study we evaluated two different rapid sampling methods, one combined with cold filtration and the other with centrifugation, for their applicability to determine intracellular amounts of metabolites which are present in high concentrations in the extracellular medium. The filtration-based method combines fast sampling and immediate quenching of cellular metabolism in cold methanol, with rapid and effective removal of all compounds present outside the cells by means of direct filtration and subsequent filtration-based washing. In the centrifugation-based method, removal of the extracellular metabolites from the cells was achieved by means of multiple centrifugation and resuspension steps with the cold quenching solution. The cold filtration method was found to be highly superior to the centrifugation method to determine intracellular amounts of metabolites related to penicillin-G biosynthesis and allowed the quantification of compounds of which the extracellular amounts were 3 to 4 orders of magnitude higher than the intracellular amounts. Using this method for the first time allowed to measure the intracellular levels of the side chain precursor phenylacetic acid (PAA) and the product penicillin-G of the penicillin biosynthesis pathway, compounds of which the transport mechanism in *Penicillium chrysogenum* is still far from being sufficiently understood.

## 1 Introduction

Important and often rate-limiting steps in metabolic pathways are formed by membrane transport of substrates, precursors and end products. The study of *in vivo* transport kinetics requires quantification of intra- and extracellular levels of the transported compounds. Especially in case of extracellular abundance, the proper determination of the intracellular concentration poses challenges.

Many procedures have been described in literature to obtain intracellular metabolite concentrations, which generally consist of a number of steps: that is, sampling, sample processing, including extraction, and analysis [1]. The focus of this chapter will be exclusively on sampling and sample processing, that is, removal of extracellular

metabolites. Metabolite extraction [2-4] and subsequent analysis [5,6] have been well addressed in other articles.

The turnover time of many intracellular metabolites is in the order of seconds. To obtain a true 'snapshot' of the metabolome of a microbial culture at a certain time point, sampling should be rapid and metabolic reactions should be stopped immediately. A simple approach is to sample total broth into a solution with an extreme pH or a high temperature, to instantly stop all enzymatic activity [7-9]. These procedures combine quenching of metabolic activity with extraction of metabolites from the cells. Although simple and efficient, a serious disadvantage of such methods is that they do not allow separation of cells and supernatant. Therefore they are only suitable to measure intracellular compounds of which the amounts present in the supernatant are negligible compared to the intracellular amounts, which is often not the case. A well-known quenching method which allows separation of cells and supernatant is the cold methanol quenching method [10,11], which has the important advantage that the cells remain intact after quenching, allowing washing of the cells to remove extracellular metabolites.

Until now, quantitative metabolomics has focused mainly on intermediates of central metabolic pathways. Less attention has been paid to the intracellular levels of metabolites at the beginning and the end of metabolic processes, that is, substrates and (excreted) products. In many situations the extracellular amounts of substrates and products are much higher than the intracellular amounts and the extracellular fraction can be expected to be in the order of 99% or even higher. Extremely efficient removal of the extracellular fraction is therefore essential for proper determination of the intracellular amount of a substrate or product.

In many of the recent rapid sampling protocols the samples are quenched in cold aqueous methanol followed by separation of the cells and the quenching liquid by cold centrifugation [11,12]. After centrifugation a large part of the supernatant, and therewith the extracellular metabolites, is removed by decantation. Sometimes this is repeated once or twice. The efficiency of removal of extracellular compounds in this method is limited. Washing of the cells can also be carried out using filtration [12-14]. However, for determination of metabolites with rapid turnover, filtration should be performed at sufficiently low temperatures to keep the metabolism quenched.

The aim of this study was to compare the efficiency of the cold centrifugation and the cold filtration method, for the removal of compounds which are abundantly present in the extracellular medium, after rapid sampling and subsequent cold methanol quenching of *Penicillium chrysogenum* cells. To this end we focused on a set of nine metabolites related

to the penicillin-G biosynthesis pathway, including one precursor, two intermediates, one product and five byproducts. The reaction network connecting these metabolites is depicted in Figure 1. In the penicillin-G production process the side-chain precursor phenylacetic acid (PAA) is supplied in the feed and taken up by the mycelium. The product penicillin-G (PenG) is efficiently excreted. Five main byproducts are formed, three by spontaneous chemical reactions (benzylpenicillic acid (PIO), 8-hydroxybenzylpenicillic acid (8-HPA) and 6-oxopiperidine-2-carboxylic acid (OPC)) and two by enzyme catalyzed reactions (*ortho*-hydroxyphenyl acetic acid (*o*-OH-PAA) and 6-aminopenicillanic acid (6-APA)). Except for the two intermediates of the pathway, L- $\alpha$ -( $\delta$ -aminoadipyl)-L- $\alpha$ -cystenyl-D- $\alpha$ -valine (ACV) and isopenicillin-N (IPN), it can be expected that the extracellular amounts of these metabolites are much larger than the intracellular amounts.

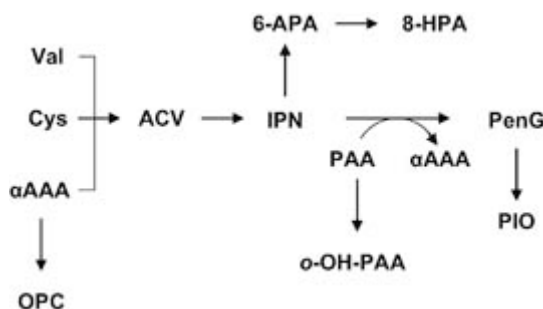


**Figure 1** A schematic overview of the penicillin synthesis pathway, including byproduct formation. Precursors are L-valine (Val), L-cysteine (Cys), and L- $\alpha$ -amino adipic acid ( $\alpha$ AAA). For other abbreviations see text.

## 2 Materials and methods

### 2.1 Strain

A high-yielding production strain of *P. chrysogenum* (code name DS17690) was kindly donated by DSM Anti-Infectives (Delft, the Netherlands) as spores from a culture grown on rice grains. The characteristics of this strain, in terms of productivity and biomass yield during chemostat cultivation, have been described earlier [11,15].

### 2.2 Media

Batch phase medium contained 16.5 g/L glucose-monohydrate, 5.0 g/L  $(\text{NH}_4)_2\text{SO}_4$ , 1.0 g/L  $\text{KH}_2\text{PO}_4$ , 0.5 g/L  $\text{MgSO}_4 \cdot 7\text{H}_2\text{O}$ , 0.41 g/L PAA and 2 mL/L of a trace elements solution. The trace elements solution contained 75.0 g/L  $\text{Na}_2\text{EDTA} \cdot 2\text{H}_2\text{O}$ , 10.0 g/L  $\text{ZnSO}_4 \cdot 7\text{H}_2\text{O}$ , 10.0 g/L  $\text{MnSO}_4 \cdot \text{H}_2\text{O}$ , 20.0 g/L  $\text{FeSO}_4 \cdot 7\text{H}_2\text{O}$ , 2.5 g/L  $\text{CaCl}_2 \cdot 2\text{H}_2\text{O}$ , 2.5 g/L

$\text{CuSO}_4 \cdot 5\text{H}_2\text{O}$ . The trace element solution was set to pH 6.0 with NaOH pellets. All the medium components except the glucose-monohydrate were dissolved in 3.7 L of demineralized water. The pH of the batch medium was set to 5.5 and the solution was sterilized for 40 minutes at 121°C. The glucose-monohydrate was dissolved in 200 mL of demineralized water and sterilized for 40 minutes at 110°C. The inoculum for the batch phase was prepared by suspending spores from 10 g of rice grains in 100 mL of demineralized water. The glucose solution and spore suspension were transferred to the reactor aseptically.

The composition of the chemostat feed medium was the same as the batch phase medium, except that the PAA concentration was changed as indicated in Table 1. The PAA was dissolved in 4 L of demineralized water by continuous stirring while adding KOH pellets until a pH of 5.5 was reached. The PAA solution was autoclaved for 40 minutes at 121°C. All other components were dissolved in 46 L of demineralized water, pH set to 5.5 with KOH pellets, and filter sterilized into the vessel containing the PAA solution using Supor DCF 0.2  $\mu\text{m}$  filters (Pall Gelman Sciences, East Hills, NY).

### 2.3 Chemostat cultivation

The strain was grown in a 7 L turbine-stirred bioreactor (Applikon, Schiedam, The Netherlands) with a working volume of 4 L under an aerobic glucose-limited regime at 25°C and a pH of 6.5 as described by Nasution et al. [11].

### 2.4 Centrifugation-based washing method

Cold methanol quenching combined with cold centrifugation for extracellular metabolite removal was performed according to Nasution et al. [11]. A schematic overview of the centrifugation method can be found in Figure 2. This method consists of rapid sampling of 1 mL of culture broth into 5 mL of a -40°C 60% (v/v) aqueous methanol solution. The quenched sample was centrifuged for 5 minutes at -20°C using a swing-out rotor, precooled at -40°C, at 4,800g. After centrifugation the supernatant was removed by decantation. Subsequently the cell pellet was washed by resuspension in 5 mL of -40°C 60% (v/v) aqueous methanol solution followed by a second cold centrifugation step and decantation of the supernatant to improve the efficiency of extracellular metabolite removal. To investigate the effect of additional washing steps on the measured intracellular amounts of metabolites related to penicillin biosynthesis, duplicate samples were subjected to one up to four additional washing steps (that is, a maximum of five washing steps). In case of five washing steps the complete washing procedure took approximately one hour.

Further processing of the cell pellet, metabolite extraction in boiling ethanol and sample concentration and storage, was performed as described in Nasution et al. [11].



## 2.5 Cold filtration-based washing method

A filtration set-up was designed for the rapid sampling, and cold methanol quenching, of *P. chrysogenum* broth from a bench scale fermentor, with the aim to quantify intracellular metabolites of which the extracellular amounts are high. A schematic overview of the filtration set-up can be found in Figure 2. A sampling port in the wall of the reactor was connected to a 50 cm long silicone tubing (Masterflex, L/S16, 3.1 mm inner diameter). Sample was withdrawn from the port with a Masterflex peristaltic pump at a flow rate of 300 mL/min, which corresponded with a residence time of the broth in the tubing of 0.8 seconds. In order to remove stagnant biomass from the tubing, the first 5 mL of broth was discarded before pumping approximately 10 g of sample in about two seconds into 50 mL of a -40°C 60% (v/v) aqueous methanol solution, present in a vacuum filtration unit placed on a balance. The balance was used to determine the exact weight of the sample. The filtration unit contained a glass fiber filter (type A/E, Pall Corporation, East Hills, NY, USA, 47 mm diameter, 1 µm pore size). Filtration was started about three seconds after sampling by applying vacuum to the filtration unit. Washing of the cell cake on the filter was accomplished by pouring 50 mL of fresh -40°C 60% (v/v) aqueous methanol on the cake as soon as the biomass fell dry. Up to three washings of the biomass on the filter could be performed within 1.5 minutes.

Once the final washing step was completed, 100 µL of a <sup>13</sup>C internal standard solution (0°C) was pipetted on top of the dry filter cake for accurate quantification purposes by IDMS [16]. The <sup>13</sup>C internal standard solution contained all relevant metabolites as U-<sup>13</sup>C-labeled isotopomers and was obtained from a *P. chrysogenum* fed-batch culture grown on 100 % U-<sup>13</sup>C-labeled glucose and PAA. Immediately after the addition of internal standard solution the filter with washed biomass cake was transferred, using tweezers, to a 50 mL tube containing 30 mL of a 73°C (just below boiling point) 75% (v/v) aqueous ethanol solution and completely submerged. The time to transfer the filter from the -40°C washing solution to the boiling ethanol never exceeded 5 seconds, making it unlikely for the temperature of the filter cake to rise much above -40°C. The whole procedure from sampling to submersion into ethanol took maximally 1.5 minutes for three washing steps. The tube was vigorously shaken by hand for approximately 5 seconds to disintegrate the filter and to maximize contact of the biomass with the ethanol solution. The tube was then placed for 3 minutes in a water bath at 95°C for extraction of the metabolites and inactivation of the enzymes. Subsequently the tube was cooled on ice and centrifuged for 8 minutes at 4°C and 4,400g. After decantation the solution was filtered using a 0.2 µm filter (FP30/0,2 CA-S; Whatman, Maidstone, England) to remove the glass fibers from the solution. The filtered solution was then concentrated under vacuum using a rapidVAP

(Labconco Corporation, Kansas City, MO) to a final volume of 500-1000  $\mu\text{l}$ . Subsequently, the sample was diluted to a final volume of 1000  $\mu\text{l}$  with demineralized water after which it was centrifuged for 5 minutes at 13,000g and the supernatant was stored at  $-80^{\circ}\text{C}$  until analysis.

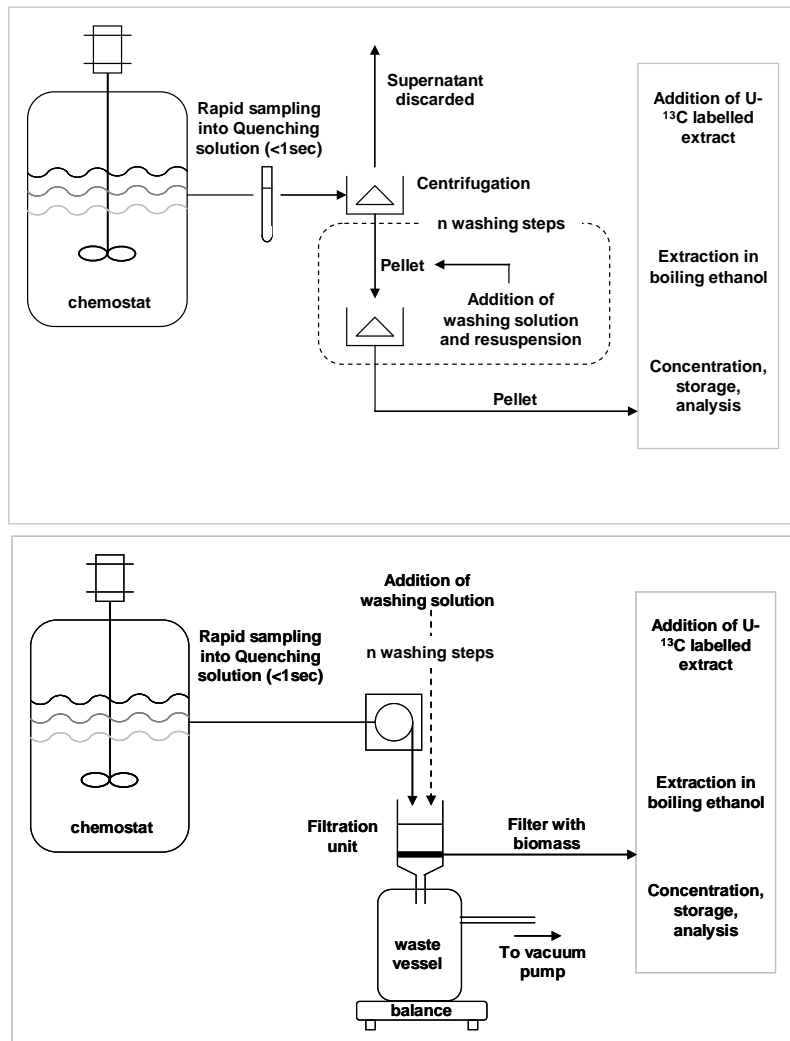


**Figure 2** A schematic overview of the conventional cold methanol sampling procedure with cold centrifugation (top) and the cold filtration-based sampling and processing procedure (bottom).

## 2.6 Determination of leakage

The extent of metabolite leakage induced by cold methanol quenching and washing with the cold filtration-based method was examined by carrying out metabolite measurements in the different sample fractions (total broth, mycelium, culture filtrate and quenching/washing liquid) and subsequent mass balancing, according to Canelas et al. [17]. For this evaluation all samples were taken in duplicate. Extracellular metabolite concentrations were determined in culture filtrates that were collected as described below in section 2.7. Sampling and sample processing for the determination of intracellular metabolite amounts was carried out as described in section 2.5, except that approximately 3 g of broth was sampled in 15 mL cold aqueous methanol and the cell cake was washed two times with 15 mL of washing solution. After collecting the filtrate a fraction of 300  $\mu\text{L}$  was transferred to an empty tube to which 100  $\mu\text{L}$  of the  $^{13}\text{C}$  internal standard solution was added. This fraction was subjected to the ethanol boiling procedure and sample concentration in the RapidVap to ensure that the final sample matrix would resemble the one of the samples for intracellular metabolite determination as close as possible. Finally, a total broth sample was obtained by sampling approximately 1 g of broth in 5 mL cold aqueous methanol using a rapid sampling device [18]. After thorough mixing (vortex), a fraction of 300  $\mu\text{L}$  was transferred to an empty tube to which the  $^{13}\text{C}$  internal standard solution was added. This fraction was subjected to the ethanol boiling procedure and sample concentration in the RapidVap. The reason for processing only a small part of the culture filtrate and total broth samples was that too high concentrations of sulfate and phosphate originating from the culture medium would interfere with our LC-MS/MS-based analysis method.

## 2.7 Rapid sampling for determination of extracellular metabolites

Rapid sampling for measurement of the extracellular metabolite concentrations was performed with the cold steel beads method as described earlier [19]. Approximately 2 mL of broth was rapidly (in less than 2 seconds) transferred from the reactor, through a sampling port in the reactor wall, into a syringe containing 32 g stainless steel beads (4 mm diameter) pre-cooled at  $-20^{\circ}\text{C}$ . This resulted in rapid cooling of the sample close to  $0^{\circ}\text{C}$ , without freezing. Thereafter the sample was immediately filtered through a Millex HV 0.45  $\mu\text{m}$  filter (Millipore, Billerica, MA, USA). After addition of the  $^{13}\text{C}$  internal standard solution, the obtained filtrate was stored in 2 ml cryovials at  $-80^{\circ}\text{C}$  until analysis.

## 2.8 Metabolite quantification

Quantification of amino acids was carried out using GC-MS [4]. Quantification of intermediates of glycolysis and the TCA-cycle [20] and the metabolites related to the penicillin pathway [21] was carried out using LC-MS/MS.

## 3 Results and discussion

### 3.1 Chemostat cultivations

Three chemostat cultivations were carried out at a dilution rate of  $0.05 \text{ h}^{-1}$  under aerobic glucose limited conditions. After three residence times a steady-state was reached with respect to the rates of oxygen consumption, carbon dioxide production and biomass concentration. The specific penicillin-G production rate however typically increased to a maximal value during the first 100 h of C-limited growth, corresponding to a period of five residence times, and then slowly decreased. This phenomenon is usually referred to as degeneration of product formation and was observed previously for penicillin production [22-24]. Table 1 shows the specific growth rate and specific glucose consumption rate and some relevant quantities at the moment of sampling for intracellular metabolites for the three chemostat cultivations. The carbon and degree of reduction balances closed within 5% for each of the three cultivations.

### 3.2 Centrifugation-based washing method

A chemostat culture of *P. chrysogenum* was run as described and used to determine the intracellular amounts of metabolites related to the penicillin biosynthesis pathway (chemostat 1). The extracellular concentrations of PenG and PAA at the time of sampling were determined to be 1.08 mM and 3.30 mM, respectively. Expressed per gram dry weight of biomass present in the chemostat, the extracellular amounts were  $180 \mu\text{mol/g}_{\text{DW}}$  of PenG and  $550 \mu\text{mol/g}_{\text{DW}}$  of PAA. Seifar et al. reported intracellular amounts of PenG and PAA of 9.6 and  $12.2 \mu\text{mol/g}_{\text{DW}}$  respectively for similar chemostat cultivations of *P. chrysogenum* [21]. Clearly the amounts of these compounds in the extracellular medium are one order of magnitude higher than the intracellular amounts, assuming that the values reported by Seifar et al., are realistic and not affected by carry over from the medium.

However, when using the conventional centrifugation method, as was done by Seifar et al. [21], it is unavoidable that about 0.1 to 0.3 mL of the 5 mL of the quenching or washing solution remains with the cell pellet (which originates from 1 mL of broth sample containing about  $6 \text{ g}_{\text{DW}}/\text{L}$  of biomass) in the test tube after decantation. Assuming a

specific cell volume of 2.5 mL/g<sub>DW</sub> [25,26], only 0.015 mL of the sample consists of mycelium.

**Table 1** Results of the chemostat experiments. Specific rates and concentrations are shown with 1 standard error.

Chemostat	General			At time of sampling				
	$\mu$ (h <sup>-1</sup> )	$-q_s$ (mmol Cmol <sup>-1</sup> h <sup>-1</sup> )	C <sub>PAA,in</sub> (mM)	Chemostat time (h)	C <sub>x</sub> (g L <sup>-1</sup> )	C <sub>ReusG</sub> (mM)	C <sub>PAA</sub> (mM)	q <sub>p</sub> (mmol Cmol <sup>-1</sup> h <sup>-1</sup> )
1	0.0495 ± 0.0002	19.9 ± 0.6	5.6	60	6.00 ± 0.10	1.08 ± 0.01	3.30 ± 0.01	0.25
2	0.0494 ± 0.0006	20.5 ± 0.6	4.5	90	5.79 ± 0.10	1.34 ± 0.02	2.75 ± 0.02	0.32
3	0.0518 ± 0.0003	19.7 ± 0.6	4.5	236	5.72 ± 0.02	1.04 ± 0.01	3.05 ± 0.24	0.23

This implies that, after decantation, the test tube contains only a small volume (0.015 mL) of cell pellet and a much larger volume (0.1 – 0.3 mL) of non-decanted broth/quenching fluid, resulting in a significant carry over of metabolites from the extracellular pool. Assuming that the intracellular amounts reported by Seifar et al. [21] represent the true amounts, it can be calculated for the above case of PAA and PenG that, after decantation of the quenching solution, at least two washings with 5 mL of quenching/washing solution are required to reduce the carry over to an amount which is insignificant compared to the intracellular amount (e.g. 2% or less). To verify this we took multiple samples from a steady state chemostat of *P. chrysogenum* and subjected each sample to a different number of washing steps. After extraction of the obtained cell pellets, the amounts of eight different metabolites associated with the penicillin biosynthesis pathway were determined.

The results are shown in Figure 3. The expectation was that the measured amounts would initially decrease with an increasing number of washing steps, whereafter they would stabilize to values representing the true intracellular amounts. However, the results do not show this expected behavior. Every additional washing step resulted in a further decrease in the amount of each measured metabolite. It is very unlikely that the extracellular amounts of the penicillin pathway related metabolites is so large compared to the intracellular amounts that more than five washing steps (that is, a dilution of ten million times) are needed to sufficiently reduce the extracellular pool. As the contact time of the cells with the cold methanol washing solution is increased with each additional washing step (up to one hour for the maximum of five washing steps), the observed continuous decrease has been most probably caused by leakage from the cells into the washing solution. Metabolite leakage into cold methanol has been observed for several micro-organisms, including eukaryotes as *Saccharomyces cerevisiae*, and the extent was found to be dependent on the time of exposure to cold methanol [17,27]. The above findings indicate that, unless these losses can be prevented by either modifying the composition of the washing liquid or drastically shortening the processing time, the centrifugation-based washing method appears impracticable.

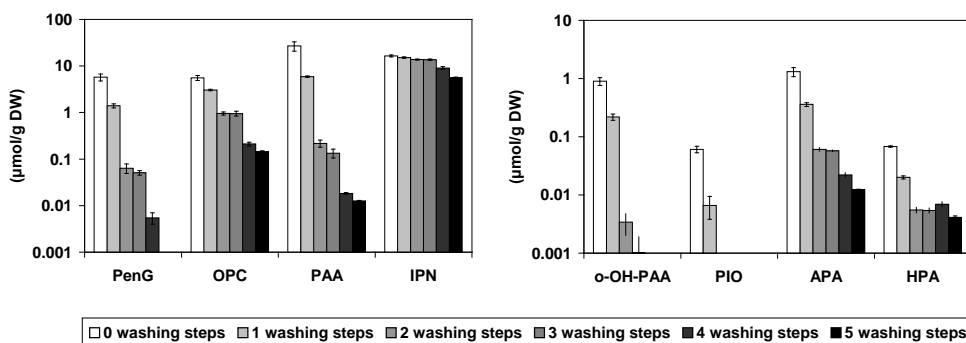


**Figure 3** Intracellular amounts of metabolites related to penicillin biosynthesis obtained with the centrifugation method after a different number of washing steps with a  $-40^{\circ}\text{C}$  60% (v/v) aqueous methanol solution. Data are averages  $\pm$  standard deviation of duplicate samples, each analyzed in duplicate.

### 3.3 Cold filtration-based washing method

Because centrifugation-based washing for removal of extracellular metabolites appeared impracticable for our purpose, a rapid sampling procedure was developed, combining cold methanol quenching with a filtration-based washing method. With this procedure, which is described in detail in the materials and methods section, the broth was sampled into an amount of cold methanol on top of a glass fiber filter. By immediate filtration after quenching of the sample, the contact time of the cells with the cold methanol could be significantly reduced. Because filtration allows a much more efficient removal of the surrounding liquid from the mycelium compared with centrifugation and subsequent decantation, it also allows a much more efficient removal of extracellular metabolites. To evaluate the performance of the cold filtration-based sampling method a similar experiment was carried out as for the evaluation of the centrifugation-based sampling method. Using the cold filtration method, multiple samples were taken within a short period of time (one hour), from a similar steady state chemostat of *P. chrysogenum* (chemostat 2), whereby either zero, one, two or three washing steps with 50 mL cold methanol solution were applied. The same set of metabolites was measured as described above. Although multiple washing steps result in increased exposure to the cold methanol solution, the maximum exposure time to cold methanol, that is, in case of three washing steps, was only 1.5 minutes and thus significantly lower than for the conventional centrifugation-based quenching and washing procedure.

The results are shown in Figure 4. It can be seen from this Figure that for IPN and ACV the measured amounts were the same for the four washing conditions, showing that they represent the true intracellular amounts of these compounds. For the other metabolites the measured amounts were significantly higher when the filter cake was not washed, compared to the results after a single washing with 50 mL of cold methanol solution. These amounts did not decrease further after applying additional washing steps. The intracellular amounts of PIO and 8-HPA could not be quantified because the levels were below the detection limits (which were, respectively, 1.76 and 1.88 nmol/g<sub>DW</sub>, for PIO and 8-HPA) in the samples which were washed at least once. Washing of the biomass cake by filtration removes the extracellular metabolites in a plug flow manner. This is orders of magnitude more effective than the centrifugation method where the cell pellet is each time resuspended and centrifuged. Furthermore, the stabilization of the measured metabolite levels after a single washing step strongly indicates that application of the cold filtration method does not lead to significant metabolite leakage from the cells.

The need for thorough washing of the cell cake for proper measurement of the intracellular amounts of most of the metabolites associated with penicillin biosynthesis can be clearly illustrated by comparing the intracellular and extracellular amounts of these metabolites. These were measured in a separate steady state chemostat (chemostat 3) carried out under identical conditions as the previous two. To facilitate comparison, the metabolite amounts measured in the culture filtrate as well as in the cell extracts were expressed in  $\mu\text{mol}$  per gram biomass dry weight present in the chemostat. Mycelium samples were obtained using the cold filtration method with two washings with 50 mL cold methanol solution. The results are presented in Table 2. The differences in intracellular metabolite amounts with

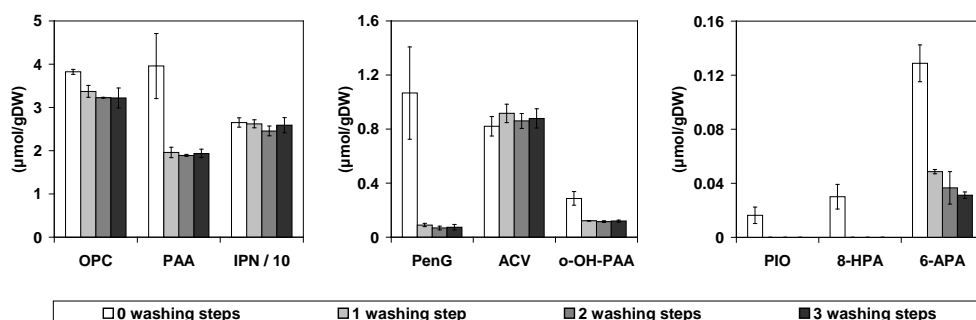


**Figure 4** Intracellular amounts of metabolites related to penicillin biosynthesis obtained with the cold filtration method after a different number of washing steps with a  $-40^{\circ}\text{C}$  60% (v/v) aqueous methanol solution. As indicated the IPN amount is 10 times higher than depicted in the graph. Data are averages  $\pm$  standard deviation of triplicate samples, each analyzed in duplicate.



the ones in Figure 4 can be explained by the difference in culture age. Although the fermentations are very reproducible, the penicillin productivity changes with culture age as described before by Van Gulik et al. [23]. Table 2 clearly shows that the extracellular amounts of all metabolites, except for IPN and ACV, are 1 to nearly 4 orders of magnitude larger. Clearly, with the proposed cold filtration method such a good washing efficiency can be obtained that it can easily remove such large extracellular amounts.

### 3.4 Validation of the cold filtration-based method with respect to metabolite leakage

To confirm whether metabolite leakage was indeed insignificant during cold filtration-based sampling, an additional experiment was performed to quantify whether metabolite leakage into the cold methanol occurred during cold filtration of *P. chrysogenum* cells. Unfortunately, most of the metabolites associated with penicillin biosynthesis are present in such high amounts in the extracellular medium that quantification of leakage from the cells is infeasible. Therefore the occurrence of leakage was checked for a set of primary metabolites of which the extracellular amounts were known to be low compared to the intracellular amounts. This set contained metabolites with highly different properties and consisted of large and small phosphorylated compounds, organic acids and amino acids (polar, non-polar, aromatic, and charged). The amounts of these metabolites were measured in samples of total broth, extracellular medium, cell extract, and quenching/washing filtrate. This allowed to accurately quantify leakage by comparison of metabolite amounts measured in the cell extract with amounts measured in total broth minus the amounts measured in the extracellular medium. Significantly lower amounts in the cell extract, corresponding with increased amounts in the filtrate after quenching, would be a proof for leakage. The results are shown in Figure 5. It can be seen from this Figure that there is no difference between the metabolite amounts measured in total broth (left bars) and the amounts measured in the cell extract plus the quenching liquid (right bars). Furthermore, there is no significant difference between the dark grey and the black areas, which respectively represent the calculated intracellular amounts (total broth minus filtrate) and the amounts measured in the cell extract. Unfortunately the presence of salts and the large dilution factors of the total broth and filtrate samples resulted in relatively large standard errors for these measurements. Nevertheless the results show clearly that metabolite leakage is not significant in *P. chrysogenum* for this set of metabolites with very diverse properties, using the cold filtration-based washing procedure.

**Table 2** Intracellular amounts using the cold filtration method and extracellular concentrations of metabolites in steady-state

Metabolite	Intracellular amount ( $\mu\text{mol/gDW}$ )	Extracellular concentration (mM)	Extracellular amount ( $\mu\text{mol/gDW}$ )	Ratio of amounts (Ex/In) (-) a)	Ratio of concentrations (Ex/In) (-) b)
PenG	$0.037 \pm 0.006$	$1.038 \pm 0.003$	$181.5 \pm 0.8$	$4905 \pm 796$	$71 \pm 11$
6-APA	$0.017 \pm 0.006$	$0.45 \pm 0.06$	$79 \pm 10$	$4628 \pm 1746$	$67 \pm 27$
PIO	$0.003 \pm 0.001$	$0.015 \pm 0.001$	$2.6 \pm 0.2$	$874 \pm 297$	$15 \pm 4$
o-OH-PAA	$0.17 \pm 0.01$	$0.33 \pm 0.02$	$58 \pm 4$	$339 \pm 29$	$4.9 \pm 0.3$
OPC	$1.13 \pm 0.04$	$0.24 \pm 0.01$	$42 \pm 2$	$37 \pm 2$	$0.53 \pm 0.04$
PAA	$2.97 \pm 0.18$	$3.05 \pm 0.24$	$533 \pm 42$	$180 \pm 18$	$2.6 \pm 0.3$
HPA	$0.0029 \pm 0.0002$	$0.023 \pm 0.003$	$4.0 \pm 0.5$	$1387 \pm 205$	$20.5 \pm 3.2$
ACV	$0.39 \pm 0.02$	$0.0001 \pm 0.0001$	$0.02 \pm 0.02$	$0.045 \pm 0.045$	$0.001 \pm 0.001$
IPN	$1.08 \pm 0.03$	$0.008 \pm 0.001$	$1.4 \pm 0.2$	$1.3 \pm 0.2$	$0.019 \pm 0.002$

Samples were taken in triplicate and each was analyzed in duplicate. The numbers show the average of the three samples  $\pm 1$  standard deviation.

a) The amount ratio is calculated as extracellular amount ( $\mu\text{mol}$  extracellular/gDW) divided by intracellular amount ( $\mu\text{mol}$  intracellular/gDW).

b) The ratio is calculated as extracellular concentration (mM) divided by intracellular concentration (mM). For the intracellular concentration a homogeneous distribution of metabolites within the cells and a cell specific volume of 2.5 mL/gDW (Jaklitsch et al., 1986; Packer et al., 1992b) was assumed.

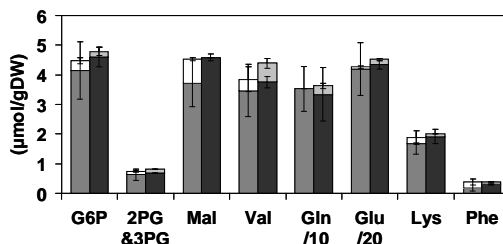


**Figure 5** Mass balances for glucose-6-phosphate (G6P), 2-phosphoglycerate and 3-phosphoglycerate (2PG&3PG), malate (Mal), valine (Val), glutamine (Gln), glutamate (Glu), lysine (Lys) and phenylalanine (Phe). The left bars represent the measured amounts of metabolites in total broth, whereby the white part represents the measured amounts in the culture filtrate and the dark grey part the calculated intracellular amount (total broth – extracellular). The right bars show the measured intracellular amounts (black part) and the amounts measured in the quenching/washing solutions (light grey). As indicated the Gln amount is 10 times higher than depicted and the Glu amount is 20 times higher than depicted. Error bars indicate standard deviations for duplicate samples.

### 3.5 Intracellular amounts of metabolites related to penicillin biosynthesis

The concentration ratio (table 2) shows that the intracellular concentration of PenG was about two orders of magnitude lower than its extracellular concentration. This is in agreement with the conclusion of others that PenG is actively transported out of the cell [28,29]. Uptake of PAA is nowadays believed to occur through passive diffusion of the undissociated acid over the cell membrane [30], although earlier studies concluded there is a specific uptake mechanism for undissociated PAA [31]. It can be calculated that in case of passive diffusion of the undissociated acid, for a culture pH of 6.5 and assuming a for filamentous fungi typical cytosolic pH of 7.2 [32-35], the ratio of the extracellular to the intracellular concentration of PAA at thermodynamic equilibrium is equal to 0.20. The observed ratio of  $2.6 \pm 0.3$  implies that the free energy for import is negative which agrees with the direction of PAA transport. Furthermore, the system is relatively far from thermodynamic equilibrium, which indicates that PAA transport might be limiting. This could, for example, be caused by a low membrane permeability coefficient in case of passive diffusion or the existence of a specific facilitated transport system for PAA.

The turnover times for the metabolites in the penicillin biosynthesis pathway can be calculated from the measured intracellular amounts and the specific rates of PenG production, 6-APA production and PAA uptake. These turnover times are presented in Table 3. For a number of the metabolites, like 6-APA and PenG, the turnover time appears to be only a few tens of seconds. This is surprising because it shows that not only primary but also secondary metabolites can have short turnover times. This shows that realistic values of their intracellular amounts can only be obtained when proper rapid sampling and

quenching procedures are applied. With the proposed cold filtration-based sampling method the time until quenching is approximately 0.8 seconds, which is sufficiently lower than the turnover time of all metabolites involved in the penicillin biosynthesis pathway.

**Table 3** Turnover times of metabolites related to penicillin biosynthesis.

Metabolite	Turnover time (s)
IPN	$3 \times 10^2$
PAA	$9 \times 10^2$
ACV (total)	$1 \times 10^2$
6-APA	$3 \times 10^1$
Pen-G	$2 \times 10^1$

### 3.6 Different conditions require different protocols

Many sampling protocols exist that aim at the quantification of intracellular metabolite amounts. A proper sampling protocol should be sufficiently effective in preventing changes in the amounts of the intracellular metabolites of interest after sampling, that is, by immediate quenching of all enzymatic activity, and removal of extracellular amounts of these metabolites, if present. Figure 6 shows which characteristics of a sampling protocol are important for different combinations of the intra- and extracellular abundance and turnover time of the metabolites to be quantified. The way different metabolites are distributed among the scenarios in Figure 6 is highly organism and cultivation condition dependent. The examples given in the Figure are specific for the *P. chrysogenum* strain cultivated in this study. Preventing changes in the amounts of the intracellular metabolites of interest (that is, quenching) is of absolute importance in case of rapid turnover of metabolites, that is, in scenarios I, II and V. Efficient removal of extracellular metabolites is of high importance in case of high extracellular amounts, that is, for scenarios IV and V. To our best knowledge none of the existing methods is suitable for proper quantification of intracellular metabolites in case of scenario V (very high extracellular amounts compared to the size of the intracellular pool). The cold filtration method described in this chapter complies with the prerequisites of scenario V, namely immediate quenching and highly effective washing.

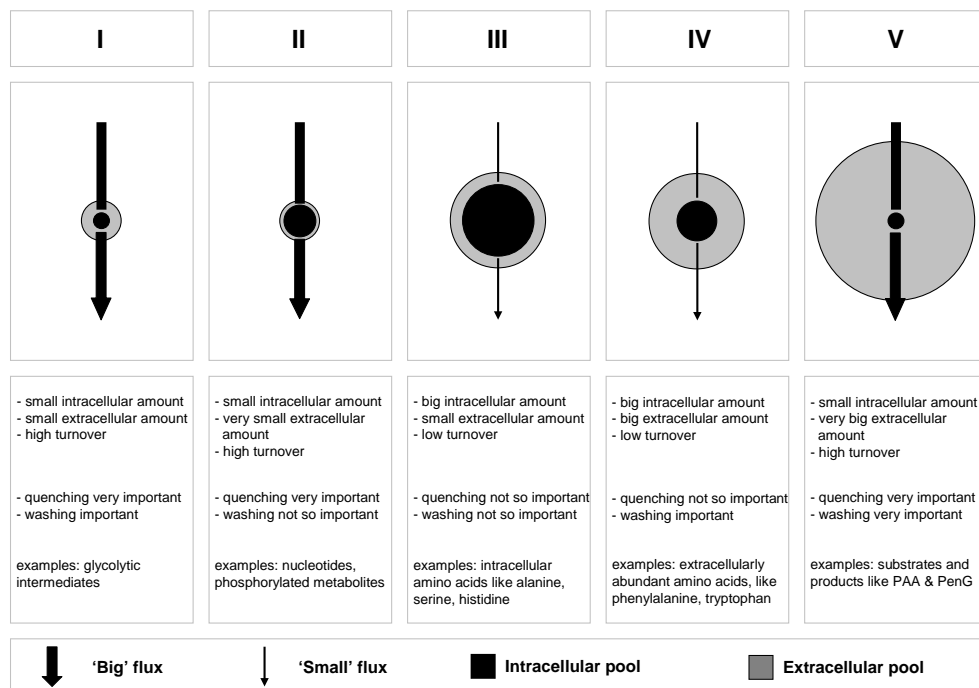


**Figure 6** Different scenarios for intracellular metabolite sampling. The width of the arrows indicates the magnitude of the flux. The area of the black part of the circle indicates the size of the intracellular pool and the area of the grey part of the circle the size of the extracellular pool. The mentioned examples are specific for *P. chrysogenum* as cultivated in this study.

Although a few sampling protocols have been described in literature that somewhat resemble the cold filtration protocol described here, they would, to our opinion, be ineffective for quantification of the set of metabolites investigated in this study. Wittman et al. applied rapid filtration and subsequent washing with a 0.9% NaCl washing solution at room temperature for *Corynebacterium glutamicum* [14]. Because their procedure did not include a quenching step it was only possible to quantify metabolites with large turnover times. For our set of metabolites, the rapid turnover of some of them necessitates quenching. Sáez and Lagunas used filtration and washing of the cell cake of *S. cerevisiae* with  $-40^{\circ}\text{C}$  50% (v/v) aqueous methanol to remove extracellular metabolites [13]. However, instead of immediately quenching metabolism by directly sampling into cold aqueous methanol, they only minimized the sample processing time by dividing their samples in ten portions which are processed separately. Ruijter and Visser developed a procedure in which *Aspergillus niger* cells are rapidly sampled in cold methanol and

extracellular metabolites were separated by vacuum filtration [36]. However, vacuum filtration was not carried out immediately, but 5 to 10 minutes after sampling. The authors presented results to show the absence of leakage within 30 minutes after sampling for the 14 metabolites they analyzed. This is, however, not surprising as 11 of the 14 metabolites analyzed were phosphorylated compounds, and relatively large compounds like  $\text{NAD}^+$  and NADH. It was demonstrated for *S. cerevisiae* that phosphorylated, charged and bulky metabolites leak insignificantly into cold methanol [17]. In contrast to these 13 metabolites, the intracellular amount of pyruvate, which is small and not phosphorylated and therefore more likely to leak, was reported to drop from 0.2 to 0.1 nmol/mL [12]. As shown in Figure 5, no metabolite leakage could be detected for our cold filtration method for a set of metabolites with highly different properties.

Our cold filtration-based washing protocol can in principle be applied to measure all metabolites in organisms which do not show cold-shock behavior or significant metabolite leakage during short term exposure to cold solvent/water mixtures. The protocol especially enables to measure intracellular substrate levels, when the amounts of substrates in the extracellular medium are relatively high. This is of particular interest in strains, which are metabolically engineered to grow on non-natural substrates and for which the capacity of transport systems might still be a bottleneck (e.g., yeast strains able to grow on C5 sugars like xylose and arabinose). Such limitations would be revealed by a very low intracellular substrate concentration. Also intracellular amounts of other medium components like ammonium or phosphate can be determined, allowing the study of their transport kinetics. Furthermore, our sampling method allows the study of transport energetics and kinetics of secreted products (e.g. penicillin-G) under in-vivo conditions. Another advantage of the cold filtration method is that extracellular salts from the medium are more thoroughly removed from the sample, which reduces problems with interference of these compounds with LC-MS/MS-based analysis methods. Drawback of the current method is that, due to the many manual handlings, the number of samples that can be withdrawn in certain timeframe is limited. This is a problem for stimulus response experiments when rapid changes in metabolite amounts need to be observed. However, if the procedure would be (partly) automated this problem could be solved.

## 4 Conclusions

A method combining rapid sampling with cold methanol quenching and cold filtration-based washing was developed and found to be especially suitable for the determination of intracellular amounts of metabolites which abundantly appear in the extracellular environment of the cells. The washing efficiency of the method appeared much higher than washing by repeated resuspension, cold centrifugation and decantation as applied in the conventional cold methanol quenching procedure. Our method allows immediate cold filtration and washing after quenching of the sample, and thus assures a short contact time (maximum 1.5 minutes in case of three washings) of the cells with the washing liquid, thereby minimizing metabolite leakage. The results obtained with this method proved to be reproducible. A surprising result was that the turnover time of several metabolites in a secondary metabolic pathway, that is, penicillin biosynthesis, was only a few tens of seconds. Because of its high washing efficiency, this method is very well suited for the study of *in vivo* kinetics of transport of substrates and products.

## Acknowledgements

The authors would like to thank Zheng Zhao for providing *P. chrysogenum* U-13C-labeled cell extract.

## References

- [1] M.R. Mashego, K. Rumbold, M. de Mey, E. Vandamme, W. Soetaert, and J.J. Heijnen, Microbial metabolomics: past, present and future methodologies, *Biotechnol. Lett.* 29 (2007) pp. 1-16.
- [2] S.G. Villas-Bôas, J. Hojer-Pedersen, M. Akesson, J. Smedsgaard, and J. Nielsen, Global metabolite analysis of yeast: evaluation of sample preparation methods, *Yeast* 22 (2005) pp. 1155-1169.
- [3] C.L. Winder, W.B. Dunn, S. Schuler, D. Broadhurst, R. Jarvis, G.M. Stephens, and R. Goodacre, Global metabolic profiling of *Escherichia coli* cultures: An evaluation of methods for quenching and extraction of intracellular metabolites, *Anal. Chem.* 80 (2008) pp. 2939-2948.
- [4] A.B. Canelas, A. ten Pierick, C. Ras, R.M. Seifar, J.C. van Dam, W.M. van Gulik, and J.J. Heijnen, Quantitative Evaluation of Intracellular Metabolite Extraction Techniques for Yeast Metabolomics, *Anal. Chem.* 81 (2009) pp. 7379-7389.

- 
- [5] J.M. Buscher, D. Czernik, J.C. Ewald, U. Sauer, and N. Zamboni, Cross-Platform Comparison of Methods for Quantitative Metabolomics of Primary Metabolism, *Anal. Chem.* 81 (2009) pp. 2135-2143.
- [6] W.B. Dunn and D.I. Ellis, Metabolomics: Current analytical platforms and methodologies, *Trends Anal. Chem.* 24 (2005) pp. 285-294.
- [7] K.E. Weibel, J.R. Mor, and A. Fiechter, Rapid Sampling of Yeast-Cells and Automated Assays of Adenylate, Citrate, Pyruvate and Glucose-6-Phosphate Pools, *Anal. Biochem.* 58 (1974) pp. 208-216.
- [8] U. Theobald, W. Mailinger, M. Reuss, and M. Rizzi, *In Vivo* Analysis of Glucose-Induced Fast Changes in Yeast Adenine-Nucleotide Pool Applying A Rapid Sampling Technique, *Anal. Biochem.* 214 (1993) pp. 31-37.
- [9] D. Weuster-Botz, Sampling tube device for monitoring intracellular metabolite dynamics, *Anal. Biochem.* 246 (1997) pp. 225-233.
- [10] W. De Koning and K. Van Dam, A Method for the Determination of Changes of Glycolytic Metabolites in Yeast on A Subsecond Time Scale Using Extraction at Neutral pH, *Anal. Biochem.* 204 (1992) pp. 118-123.
- [11] U. Nasution, W.M. van Gulik, R.J. Kleijn, W.A. van Winden, A. Proell, and J.J. Heijnen, Measurement of intracellular metabolites of primary metabolism and adenine nucleotides in chemostat cultivated *Penicillium chrysogenum*, *Biotechnol. Bioeng.* 94 (2006) pp. 159-166.
- [12] G.J.G. Ruijter and J. Visser, Determination of intermediary metabolites in *Aspergillus niger*, *J. Microbiol. Meth.* 25 (1996) pp. 295-302.
- [13] M.J. Sáez and R. Lagunas, Determination of Intermediary Metabolites in Yeast - Critical-Examination of Effect of Sampling Conditions and Recommendations for Obtaining True Levels, *Mol. Cell. Biochem.* 13 (1976) pp. 73-78.
- [14] C. Wittmann, J.O. Kromer, P. Kiefer, T. Binz, and E. Heinzle, Impact of the cold shock phenomenon on quantification of intracellular metabolites in bacteria, *Anal. Biochem.* 327 (2004) pp. 135-139.
- [15] W.M. van Gulik, W.T.A.M. De Laat, J.L. Vinke, and J.J. Heijnen, Application of metabolic flux analysis for the identification of metabolic bottlenecks in the biosynthesis of penicillin-G, *Biotechnol. Bioeng.* 68 (2000) pp. 602-618.
- [16] L. Wu, M.R. Mashego, J.C. van Dam, A.M. Proell, J.L. Vinke, C. Ras, W.A. van Winden, W.M. van Gulik, and J.J. Heijnen, Quantitative analysis of the microbial metabolome by isotope dilution mass spectrometry using uniformly C-13-labeled cell extracts as internal standards, *Anal. Biochem.* 336 (2005) pp. 164-171.



- [17] A.B. Canelas, C. Ras, A. ten Pierick, J.C. van Dam, J.J. Heijnen, and W.M. van Gulik, Leakage-free rapid quenching technique for yeast metabolomics, *Metabolomics* 4 (2008) pp. 226-239.
- [18] H.C. Lange, M. Eman, G. van Zuijlen, D. Visser, J.C. van Dam, J. Frank, M.J.T. de Mattos, and J.J. Heijnen, Improved rapid sampling for in vivo kinetics of intracellular metabolites in *Saccharomyces cerevisiae*, *Biotechnol. Bioeng.* 75 (2001) pp. 406-415.
- [19] M.R. Mashego, W.M. van Gulik, J.L. Vinke, and J.J. Heijnen, Critical evaluation of sampling techniques for residual glucose determination in carbon-limited chemostat culture of *Saccharomyces cerevisiae*, *Biotechnol. Bioeng.* 83 (2003) pp. 395-399.
- [20] J.C. van Dam, M.R. Eman, J. Frank, H.C. Lange, G.W.K. van Dedem, and S.J. Heijnen, Analysis of glycolytic intermediates in *Saccharomyces cerevisiae* using anion exchange chromatography and electrospray ionization with tandem mass spectrometric detection, *Anal. Chim. Acta* 460 (2002) pp. 209-218.
- [21] R.M. Seifar, Z. Zhao, J. van Dam, W. van Winden, W. van Gulik, and J.J. Heijnen, Quantitative analysis of metabolites in complex biological samples using ion-pair reversed-phase liquid chromatography-isotope dilution tandem mass spectrometry, *J. Chromatogr. , A* 1187 (2008) pp. 103-110.
- [22] R.C. Righelato, Selection of Strains of *Penicillium chrysogenum* with Reduced Penicillin Yields in Continuous Cultures, *J. Appl. Chem. Biotechnol.* 26 (1976) pp. 153-159.
- [23] W.M. van Gulik, M.R. Antoniewicz, W.T.A.M. De Laat, J.L. Vinke, and J.J. Heijnen, Energetics of growth and penicillin production in a high-producing strain of *Penicillium chrysogenum*, *Biotechnol. Bioeng.* 72 (2001) pp. 185-193.
- [24] R.D. Douma, P.J.T. Verheijen, W.T.A.M. De Laat, J.J. Heijnen, and W.M. van Gulik, Dynamic Gene Expression Regulation Model for Growth and Penicillin Production in *Penicillium chrysogenum*, *Biotechnol. Bioeng.* 106 (2010) pp. 608-618.
- [25] W.M. Jaklitsch, W. Hampel, M. Rohr, C.P. Kubicek, and G. Gameraith, Alpha-Amino adipate Pool Concentration and Penicillin Biosynthesis in Strains of *Penicillium-Chrysogenum*, *Canadian Journal of Microbiology* 32 (1986) pp. 473-480.
- [26] H.L. Packer, E. Keshavarzmoore, M.D. Lilly, and C.R. Thomas, Estimation of Cell-Volume and Biomass of *Penicillium chrysogenum* Using Image-Analysis, *Biotechnol. Bioeng.* 39 (1992) pp. 384-391.

- [27] C.J. Bolten, P. Kiefer, F. Letisse, J.C. Portais, and C. Wittmann, Sampling for metabolome analysis of microorganisms, *Anal. Chem.* 79 (2007) pp. 3843-3849.
- [28] M.A. van den Berg, R.A.L. Bovenberg, A.J.M. Driessen, W.N. Konings, T.A. Schuurs, M. Nieboer, and I. Westerlaken, Method for Enhancing Secretion of Beta-Lactam Transport, 2001.
- [29] J.F. Martin, J. Casqueiro, and P. Liras, Secretion systems for secondary metabolites: how producer cells send out messages of intercellular communication, *Curr. Opin. Microbiol.* 8 (2005) pp. 282-293.
- [30] D.J. Hillenga, H.J.M. Versantvoort, S. Vandermolen, A.J.M. Driessen, and W.N. Konings, *Penicillium chrysogenum* Takes Up the Penicillin-G Precursor Phenylacetic Acid by Passive Diffusion, *Appl. Environ. Microbiol.* 61 (1995) pp. 2589-2595.
- [31] J.M. Fernández-Cañón, A. Reglero, H. Martinezblanco, and J.M. Luengo, Uptake of Phenylacetic Acid by *Penicillium-Chrysogenum* Wis 54-1255 .1. A Critical Regulatory Point in Benzylpenicillin Biosynthesis, *Journal of Antibiotics* 42 (1989) pp. 1398-1409.
- [32] T.L. Legerton, K. Kanamori, R.L. Weiss, and J.D. Roberts, Measurements of Cytoplasmic and Vacuolar pH in *Neurospora* Using Nitrogen-15 Nuclear Magnetic Resonance Spectroscopy, *Biochemistry* 22 (1983) pp. 899-903.
- [33] M. Legisa and J. Kidric, Initiation of Citric Acid Accumulation in the Early Stages of *Aspergillus niger* Growth, *Appl. Microbiol. Biotechnol.* 31 (1989) pp. 453-457.
- [34] U. Pilatus and D. Techel, <sup>31</sup>P-NMR-studies on Intracellular pH and Metabolite Concentrations in Relation to the Circadian Rhythm, Temperature and Nutrition in *Neurospora crassa*, *Biochim. Biophys. Acta* 1091 (1991) pp. 349-355.
- [35] D. Sanders and C.L. Slayman, Control of Intracellular pH - Predominant Role of Oxidative Metabolism, Not Proton Transport, in the Eukaryotic Microorganism *Neurospora*, *J. Gen. Physiol.* 80 (1982) pp. 377-402.
- [36] G.J.G. Ruijter and J. Visser, Determination of intermediary metabolites in *Aspergillus niger*, *J. Microbiol. Meth.* 25 (1996) pp. 295-302.



## Chapter 3

---

# Optimization of cold methanol quenching for quantitative metabolomics of *Penicillium chrysogenum*

---

Published as:

de Jonge LP, Douma RD, Heijnen JJ, van Gulik WM. Optimization of cold methanol quenching for quantitative metabolomics of *Penicillium chrysogenum*. *Metabolomics* 2012;8(4):727-35.

## Abstract

A sampling procedure for quantitative metabolomics in *Penicillium chrysogenum* based on cold aqueous methanol quenching was re-evaluated and optimized to reduce metabolite leakage during sample treatment. The optimization study included amino acids and intermediates of the glycolysis and the TCA-cycle. Metabolite leakage was found to be minimal for a methanol content of the quenching solution of 40% (v/v) while keeping the temperature of the quenched sample near -20°C. The average metabolite recovery under these conditions was 95.7% ( $\pm 1.1\%$ ). Several observations support the hypothesis that metabolite leakage from quenched mycelia of *P. chrysogenum* occurs by diffusion over the cell membrane. First, a prolonged contact time between mycelia and the quenching solution lead to a somewhat higher extent of leakage. Second, when suboptimal quenching liquids were used, increased metabolite leakage was found to be correlated with lower molecular weight and with lower absolute net charge. The finding that lowering the methanol content of the quenching liquid reduces metabolite leakage in *P. chrysogenum* contrasts with recently published quenching studies for two other eukaryotic micro-organisms. This demonstrates that it is necessary to validate and, if needed, optimize the quenching conditions for each particular micro-organism.

## 1 Introduction

Quantitative metabolome analysis is an important tool in microbial systems biology and metabolic engineering, such as for the determination of *in vivo* kinetic parameters and in isotopic nonstationary  $^{13}\text{C}$  flux analysis [1,2]. Metabolomics of micro-organisms involves a number of steps. These include at least sampling, quenching of metabolic activity, metabolite extraction from the cells and quantification, but may include additional sample processing steps, such as washing of cells to prevent interference of the exometabolome, and sample concentration [3,4].

The turnover time of many intermediates of both primary and secondary metabolism of micro-organisms is in the range of sub seconds to several tens of seconds [5-7]. Sampling and quenching of metabolic activity should therefore be sufficiently rapid to prevent (inter)conversion. Several rapid sampling devices and protocols have been developed in the past decades to achieve sub second sampling times [8,9]. Fast quenching of metabolic activity in cold aqueous methanol [10] has become very popular, because it has the advantage that, provided that the cells remain intact, it allows washing of the cells to remove extracellular metabolites by centrifugation or filtration. This is required if the

extracellular amounts of metabolites are significant compared to the corresponding intracellular amounts, to prevent overestimation of the intracellular amounts [6,7,11].

Nevertheless, it has become apparent that contact of cells with cold aqueous methanol will not seldom lead to a loss of metabolites from the cells [11-17]. From the studies performed on this subject so far, it seems that the underlying mechanism is different for prokaryotes and eukaryotes. For the former, the sudden (<1 s) change in temperature alone appears to be enough to induce release of intracellular metabolites [18], which is therefore usually referred to as the cold shock phenomenon. Despite some conflicting reports [10,19,20], metabolite leakage during cold methanol quenching was also clearly demonstrated for the eukaryote *Saccharomyces cerevisiae* [13,15]. The loss of metabolites from these eukaryotic cells seems to occur through a process of diffusion over the cell membrane, in which the time of exposure, quenching temperature, properties of the cold aqueous methanol solution (e.g. ionic strength) and physicochemical properties of the metabolites (e.g. size and polarity) are factors that determine the extent of leakage [15].

Recently a protocol for quantitative metabolomics in *Penicillium chrysogenum* relying on cold aqueous methanol quenching was published [21]. Until now this protocol has not been evaluated for a large set of metabolites. The aim of our study was to critically evaluate the applicability of cold methanol quenching for quantitative metabolomics of *P. chrysogenum*. Hereby a mass balance based approach was used as proposed by Canelas et al. [15]. For this, the fate of a large set of metabolites with various physicochemical properties was followed during sample treatment by analyzing different samples and sample fractions, including quenched total broth samples, quenched and washed cell pellets and supernatants.

## 2 Materials and methods

### 2.1 Solvents and chemicals

HPLC-grade methanol and ethanol were obtained from Baker (The Netherlands). Analytical grade standards were obtained from Sigma-Aldrich.

### 2.2 Strain

A strain of *P. chrysogenum* (DS17690) with a high penicillin yield was kindly donated as spores from a culture grown on rice grains by DSM Anti-Infectives (Delft, The Netherlands). This strain has been well characterized in terms of its productivity and yields during chemostat cultivation [21,22].

### 2.3 Media and chemostat cultivations

The batch medium contained per L of demineralized water: 15.0 g glucose, 5.0 g  $(\text{NH}_4)_2\text{SO}_4$ , 1.0 g  $\text{KH}_2\text{PO}_4$ , 0.5 g  $\text{MgSO}_4$ , 0.41 g PAA and 2 mL of trace element solution. The trace element solution contained per L 75.0 g  $\text{Na}_2\text{EDTA}\cdot 2\text{H}_2\text{O}$ , 10.0 g  $\text{ZnSO}_4\cdot 7\text{H}_2\text{O}$ , 10.0 g  $\text{MnSO}_4\cdot \text{H}_2\text{O}$ , 20.0 g  $\text{FeSO}_4\cdot 7\text{H}_2\text{O}$ , 2.5 g  $\text{CaCl}_2\cdot 2\text{H}_2\text{O}$ , 2.5 g  $\text{CuSO}_4\cdot 5\text{H}_2\text{O}$ . The pH of the trace element solution was set to 6.0 with NaOH pellets. All batch medium components except the glucose were dissolved in 3.6 L demineralized water. The pH was set to 5.6 and the solution was sterilized for 40 min at 121°C. The glucose was dissolved separately and demineralized water was added to bring the weight of the solution to 300 g. This solution was sterilized for 40 min at 110 °C. For inoculation, 10 g of rice grains were submerged in 100 mL demineralized water for one hour. The batch medium, glucose solution and inoculum were introduced aseptically into the reactor.

The composition of the chemostat medium was the same as that of the batch medium except that the concentration of PAA was 0.76 g/L PAA. The PAA concentration in the batch and chemostat media were designed to achieve a (residual) concentration of approximately 3 mM, which is not limiting for penicillin production, nor inhibiting for cell growth [22]. The required amount of PAA for 50 L of medium was dissolved in 4 L of demineralized water by continuous stirring while adding KOH pellets to set the pH to 5.6. This solution was sterilized in a 55 L vessel for 40 min at 121°C. All other medium components were dissolved in 46 L of demineralized water. After setting the pH to 5.6 with KOH pellets, this solution was added to the PAA solution by filter sterilization (Supor DCF 0.2  $\mu\text{m}$  filters, Pall Gelman Sciences, East Hills, NY). This medium supported a steady state biomass concentration of about 6  $\text{g}_{\text{DW}}/\text{L}$ .

Cultivations were carried out in a 7 L fermentor (Applikon, The Netherlands) with a working volume of 4 L under an aerobic glucose-limited regime at 25°C, a pH of 6.5 and a dilution rate of 0.05  $\text{h}^{-1}$  as described by Nasution et al. [21].

### 2.4 Sampling and sample treatment procedures

Samples for analysis of intracellular metabolites (IC) were taken essentially as described by Nasution et al. [21]. Samples of  $\pm 1$  g of broth were quickly ( $\pm 0.7$  s) withdrawn from the reactor and sprayed into a tube containing a quenching liquid using a rapid sampling device [23]. Three variations were made with respect to the quenching liquid. The sampling tubes were filled either with 5 mL -40°C 60% (v/v) aqueous methanol, 5 mL -40°C pure methanol or 10 mL -25°C 40% (v/v) aqueous methanol. After sampling the content of each tube was immediately ( $<1$  s after sampling) mixed by vortexing (for 2-5 s, until a vortex was established) and directly placed back in the cryostat. The exact amounts of sample were

determined by weighing. Subsequently, the tubes were centrifuged for 5 min at 4,800g in a cooled centrifuge at -20°C using a swing-out rotor, precooled at -40°C. After decanting, the cell pellets were resuspended by vortexing in 5 mL of a washing liquid that had the same temperature and composition as the quenching liquid and the tubes were centrifuged again. The supernatants of the first (from now on called quenching solution, QS) and second (washing solution, WS) centrifugation step were collected and weighed. The cell pellets, quenching and washing solutions were placed in the cryostat until further treatment. 100 µL of a <sup>13</sup>C internal standard solution (0°C) was added to the washed cell pellets to compensate for losses and degradation of metabolites during further sample treatment and for accurate quantification purposes by IDMS [24]. The <sup>13</sup>C internal standard solution contained all relevant metabolites as U-<sup>13</sup>C-labeled isotopologues and was obtained from a *P. chrysogenum* fed-batch culture grown on >99% U-<sup>13</sup>C-labeled glucose (Campro Scientific, Veenendaal, the Netherlands) and <sup>13</sup>C-labeled PAA with all carbon atoms of the aromatic ring labeled (Sigma-Aldrich). The washed cell pellets containing the <sup>13</sup>C internal standards were then extracted using boiling 75% (v/v) ethanol and further treated as described earlier [21].

300 to 500 µL of the collected quenching solutions (QS) and washing solutions (WS) were transferred to clean tubes. Subsequently 100 µL of the <sup>13</sup>C internal standard solution was added to each of them. The QS and WS samples were subjected to the boiling ethanol treatment to denature possible enzymes present in the supernatant, thereby preventing conversion of metabolites. These samples were further processed in the same way as the cell pellet samples.

Total broth (TB) samples were taken by sampling ±1 g of broth in 5 mL -40°C 60% (v/v) aqueous methanol. After weighing, 300 µL of the homogenized suspension was transferred to clean tubes and, after addition of 100 µL of the <sup>13</sup>C internal standard solution, the broth samples were subjected to the boiling ethanol treatment and were further processed in the same way as the cell pellets. Broth samples for quantification of extracellular metabolite levels (EX) were immediately cooled to 0 °C and filtered to remove the cells, using the cold steel bead method [25] with the difference that the filtrate was directly injected into a 5 mL solution of -40°C 60% (v/v) aqueous methanol and vortexed thoroughly. Subsequently 300 µL of this mixture was combined with 100 µL of the <sup>13</sup>C internal standard solution, subjected to ethanol boiling and further treated in the same way as the cell pellets. In the second experiment investigating the effect of quenching time (see section 3.2), TB and EX samples were taken in 10 mL of -25°C 40% (v/v) aqueous methanol instead of in 5 mL of -40°C 60% (v/v) aqueous methanol.



## 2.5 Analysis

Three different analytical platforms were used. GC-MS was used to analyze the free amino acid pools of ornithine and the twenty proteinogenic amino acids except arginine, cysteine and valine, by using the EZ:Faast kit for free amino acid analysis from Phenomenex (Torrance, CA, USA). In one experiment, anion-exchange LC-ESI-MS/MS was used for the analysis of G6P, F6P, M6P, FBP, T6P, 6PG, PEP G3P, pyruvate,  $\alpha$ KG, succinate, fumarate, malate, and the combined pools of citrate+isocitrate, 2PG+3PG and G1P+M1P [26]. In a second experiment, another GC-MS method was used for the analysis of G6P, F6P, M6P, FBP, T6P, PEP, pyruvate,  $\alpha$ KG, succinate, fumarate, malate, citrate, isocitrate, 2PG, 3PG, R5P, S7P and E4P [27]. All analyses were performed at least in duplicate and quantification of the metabolites was based on the use of U- $^{13}$ C-labeled cell extract as internal standard [24,28].

## 2.6 Mass balance calculations

Metabolite amounts were quantified in the above mentioned samples and sample fractions. Standard deviations were estimated from two (first experiment) or three (second experiment) replicate samples taken from the same chemostat culture. Because  $^{13}$ C labeled internal standard mix was added to all sample fractions before the metabolite extraction procedure, possible partial degradation of metabolites was effectively corrected for. Therefore a mass balance can be established for every metabolite  $i$  and quenching protocol variation  $j$  which states that the metabolite amount measured in total broth (TB) samples equals the sum of the amounts measured in cell pellets (IC), and quenching (QS) and washing supernatants (WS):

$$M_i(\text{TB}) = M_{i,j}(\text{IC}) + M_{i,j}(\text{QS}) + M_{i,j}(\text{WS}) \quad (1)$$

Furthermore, the amount which was released from cells into the quenching and washing solutions during sample treatment can be calculated from a second balance:

$$M_{i,j}(\text{leakage}) = M_i(\text{TB}) - M_i(\text{EX}) - M_{i,j}(\text{IC}) \quad (2)$$

$$\text{With } M_{i,j}(\text{leakage}) \geq 0$$

If no metabolite leakage occurs, the metabolite amount in the cell pellet (IC) is equal to the difference between the amounts in total broth samples (TB) and culture filtrate samples (EX). Leakage becomes evident when the amount in the cell pellet is smaller than the difference between TB and EX. Hence the inequality for the amount of leaking metabolites.

Since, except for the leakage term, all terms in both balances were measured, the data set contained redundant information, allowing statistical testing of the consistency of the measurements. For both experiments described in this study, this was done by calculating the  $\chi^2$  distributed consistency index  $h$  for each metabolite in a single protocol variation at a significance level of 0.05 [29]. Subsequently, the data that were not rejected by the test were reconciled. The reconciliation was achieved by least squares minimization of the differences between measured and estimated metabolite amounts, weighed by their measurement errors and subjected to the constraints expressed by equations 1 and 2 [17].

## 3 Results and discussion

### 3.1 Effect of methanol concentration

The first experiment aimed at evaluating the extent of metabolite leakage, when using the conventional quenching solution (-40°C, 60% v/v aqueous methanol) as proposed in the protocol for quantitative metabolomics in *P. chrysogenum* of Nasution et al. [21]. In addition, two other quenching liquids were tested for comparison. Cold pure methanol (-40°C) was tested for the reason that it was reported to be the optimal quenching liquid for *S. cerevisiae* [15], which is also a eukaryotic micro-organism. To further assess the effect of the methanol content, an aqueous solution with a lower methanol content of 40% (v/v) was tested too. Due to its higher freezing point, the 40% (v/v) aqueous methanol solution was precooled to -25°C instead of -40°C. To prevent that the temperature of the mixture of the broth sample and quenching liquid would rise above -20°C during sampling, a volume ratio of broth sample to quenching liquid of 1:10 (1 mL sample + 10 mL quenching liquid) was used in this case. We considered -20 °C as upper limit because Wellerdiek et al. showed that metabolic activity was absent at -20°C in the case of quenched *Corynebacterium glutamicum* cells [18].

The extent of leakage of metabolites from cells quenched in these three liquids was evaluated using a quantitative mass balance approach (see section 2.6). As an example, the mass balances for the three applied quenching liquids and three selected metabolites with different physicochemical properties are shown in Figure 1. Note that the metabolite amounts of all sample fractions are expressed in  $\mu\text{mol}/\text{g}_{\text{DW}}$  to be able to compare them. In Figure 1, the metabolite amounts measured in the quenched and washed cell pellet (IC, direct determination of the intracellular amount) should be compared to the amount calculated from the difference between the amounts in the total broth and culture filtrate (TB – EX, indirect determination) which is considered to be the best estimate of the “true”

intracellular amount. Obtaining the intracellular amount by this subtraction procedure is known in literature as the differential method [6,11].

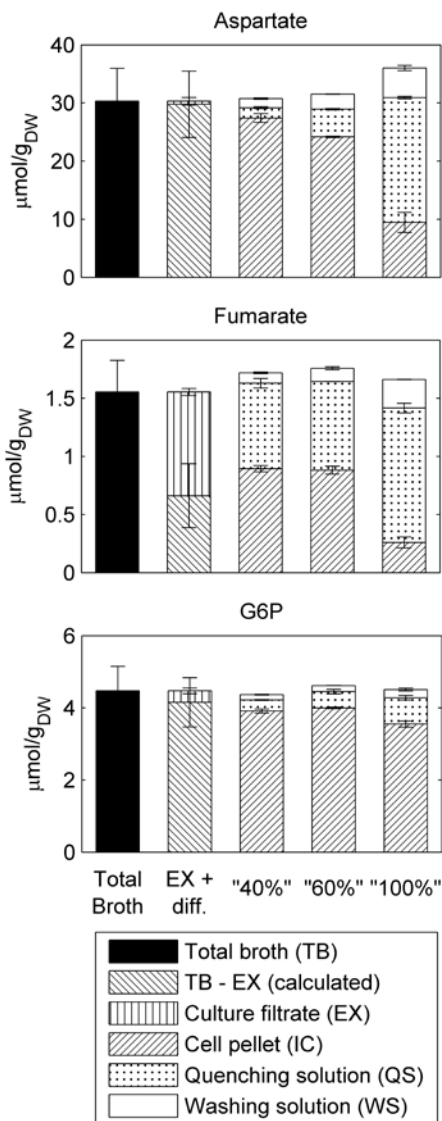


**Figure 1** Mass balances of G6P, aspartate and fumarate for the three protocol variations. “40%”: quenching of 1 mL sample in 10 mL -25°C 40% (v/v) aqueous methanol; “60%”: quenching of 1 mL sample in 5 mL -40°C 60% (v/v) aqueous methanol; “100%”: quenching of 1 mL sample in 5 mL -40°C pure methanol. Error bars give the standard errors for duplicate samples, each analyzed in duplicate.

From the results shown in Figure 1 it can be seen that, when pure methanol was used as quenching liquid (“100%”), the amounts of fumarate and aspartate found in the cell pellet were considerably lower than the amounts obtained with the differential method (further on referred to as reference amount). Furthermore, for all three metabolites in this condition, as well as for aspartate in the “60%” condition, the sum of the amounts measured in the quenching and washing solutions were notably higher than the amounts measured in the culture filtrate. These observations indicate that metabolite leakage into the cold quenching liquid occurred under these conditions. Finally, it can be seen from this Figure that no or hardly any G6P and fumarate leaked into the quenching liquids with 40% and 60% methanol. Note that the standard errors of the total broth samples in Figure 1 are large relative to those of the other sample fractions. This may be due to the fact that only a part of the quenched total broth sample was used in the extraction step, which was done to limit the carry-over of sulfate and phosphate (originating from the medium), because too high concentrations of these salts interfere with the MS-based analysis [26]. An overview of the metabolite levels measured in the various sample fractions is given in the Appendix (Table A1).

To verify the quality of the measurements, the consistency of the data was tested (see section 2.6) to detect gross measurement errors. Only data that passed the test were included in the evaluation. For a better comparison of the results, those data were also reconciled under the constraints expressed in equations 1 and 2.

To compare the performance of the three quenching liquids, the ratio of the metabolite amount in the cell pellet (IC) and the reference amount obtained by the differential method (TB – EX) was calculated for every metabolite for each of the three quenching liquids. These ratios can be considered as recoveries. For the complete set of evaluated metabolites, the average recoveries ( $\pm$  standard error) were 95.7% ( $\pm 1.1\%$ ), 84.3% ( $\pm 3.1\%$ ), and 49.8% ( $\pm 6.6\%$ ) when quenching was performed using  $-25^{\circ}\text{C}$  40% (v/v) aqueous methanol,  $-40^{\circ}\text{C}$  60% (v/v) aqueous methanol and  $-40^{\circ}\text{C}$  pure methanol, respectively. In Figure 2a, the sets of metabolite-specific recoveries are represented by boxplots for all evaluated metabolites; on the left side, the results were calculated from the (consistent) raw data, and on the right side the recoveries were obtained from the reconciled data. Clearly, the best agreement between metabolite amounts found in the cell pellet and the reference amounts was obtained when  $-25^{\circ}\text{C}$  40% (v/v) aqueous methanol was used as the quenching liquid.

In Figure 2b–d, the evaluated metabolites are separated into three classes, namely phosphorylated metabolites, organic acids and amino acids. In both the raw and the reconciled data it is observed that for all three compound classes the recoveries obtained by quenching in  $-25^{\circ}\text{C}$  40% (v/v) aqueous methanol were closest to 100%, while those

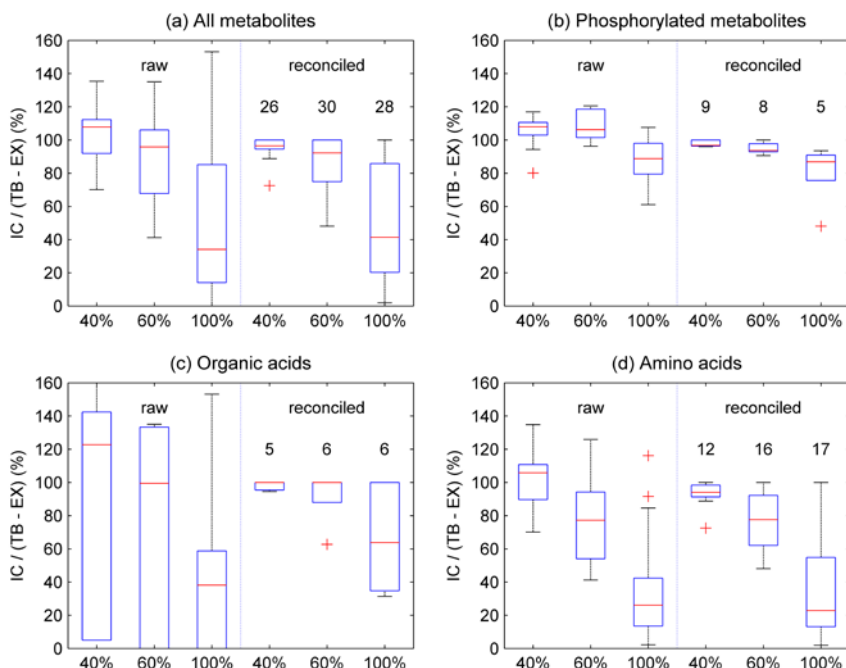


**Figure 2** Boxplots of the ratios between the intracellular amounts measured in quenched and washed cell pellets (IC) and the reference amounts calculated from the difference between the amounts measured in total broth and culture filtrate (TB-EX) for the three protocol variations. “40%”: quenching with 10 mL  $-25^{\circ}\text{C}$  40% (v/v) aqueous methanol; “60%”: quenching with 5 mL  $-40^{\circ}\text{C}$  60% (v/v) aqueous methanol; “100%”: quenching with 5 mL  $-40^{\circ}\text{C}$  pure methanol. The boxplots are shown both for the consistent raw (left) and the reconciled (right) data and indicate the median, the first and third quartile. The whiskers indicate the most extreme point from the first and third quartile within a distance of 1.5 times the distance between the first and third quartile; points at a greater distance are indicated by red crosses. The numbers above the boxplots on the right refer to the number of metabolites evaluated in that condition and apply also for the consistent raw data on the left. The four panels show results of (a) all evaluated metabolites, (b) only phosphorylated metabolites, (c) only organic acids and (d) only free amino acids.

obtained with  $-40^{\circ}\text{C}$  pure methanol as quenching liquid were quite widely distributed. Especially the amounts of organic acids (Figure 2c) and amino acids (Figure 2d) recovered from the quenched and washed cell pellets were found to be reduced compared to the reference amounts when 60% (v/v) aqueous methanol or pure methanol was used for quenching. In the case of 40% (v/v) aqueous methanol, almost all metabolites had a recovery (calculated from reconciled data) higher than 90%, except for Gln (88.7%) and Gly (72.5%). All in all, it was concluded that  $-25^{\circ}\text{C}$  40% (v/v) aqueous methanol was the

best performing of the three quenching liquids tested, although for some metabolites, especially amino acids, it did not completely prevent leakage.

The present finding that higher recoveries are obtained when the methanol fraction in the quenching liquid is reduced to 40%, contrasts with the findings of leakage studies performed on two other eukaryotic microorganisms [15,17,30]. For *S. cerevisiae* it was found that a higher methanol content and a lower temperature lead to a lower extent of leakage, with -80 °C pure methanol being the optimal quenching liquid [15]. For cultures of *Pichia pastoris* it was found that the methanol content of the quenching liquid did not significantly affect the recovery of metabolites from cell pellets [17,30]. These examples demonstrate that a dedicated validation of quenching liquids is required for every microorganism before it is applied in a quantitative metabolomics study.

### 3.2 Prolonged exposure to quenching liquid

Results of a study with *S. cerevisiae* have suggested that leakage can occur by diffusion of metabolites over the cell membrane [15]. In that case, the extent of leakage would increase if quenched cells are not processed immediately, but are kept in the quenching solution for a longer period of time. Therefore, in a second experiment, the degree of metabolite loss was evaluated for the situation that cells are exposed to the quenching solution for a prolonged period of time. To study this, samples were taken from another chemostat culture operated under the same conditions. Using 10 mL -25°C 40% (v/v) aqueous methanol as the quenching liquid, one set of triplicate samples was processed immediately and another set was left in the cryostat at -25°C for 30 min before proceeding to the centrifugation and washing steps.

The results are summarized in Figure 3. The average recoveries ( $\pm$  standard deviation) of the samples that were processed immediately (“0 min”) and with a 30 min delay (“30 min”) were 92.8% ( $\pm$ 1.1%) and 88.0% ( $\pm$ 1.3%), respectively (calculated from the reconciled data). The small difference between these averages and the distribution of the recoveries show that the extent of metabolite leakage increased due to the prolonged contact time with the quenching liquid. This finding supports the hypothesis that metabolite leakage can occur by diffusion over the cell membrane as suggested by Canelas et al. [15]. It also means that sample treatment should proceed as quickly as possible to the boiling ethanol step for extraction and enzyme inactivation.

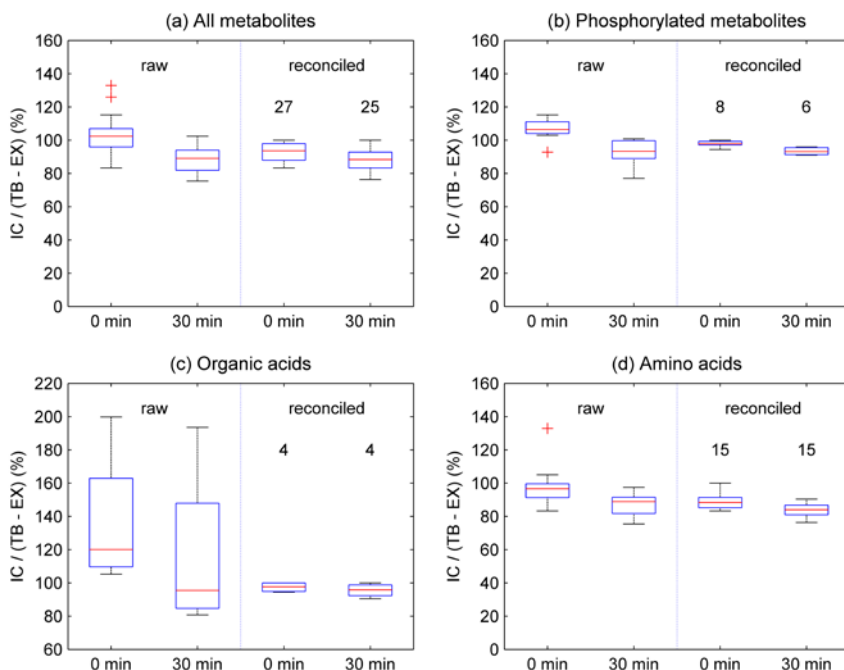


**Figure 3** Influence of the contact time of cells quenched with  $-25^{\circ}\text{C}$  40% (v/v) aqueous methanol on the extent of leakage. Samples were either processed immediately (0 min) or were left for 30 minutes in the quenching solution at  $-25^{\circ}\text{C}$  before being processed (30 min). The boxplots are plotted as in Figure 2. The four panels show results of (a) all evaluated metabolites, (b) only phosphorylated metabolites, (c) only organic acids and (d) only free amino acids. Note that the range of the vertical axis in panel c was adjusted.

### 3.3 Factors influencing the extent of metabolite leakage

Canelas et al. based their hypothesis that metabolite leakage in *S. cerevisiae* is driven by diffusion not only on the observation that the extent of leakage increased with quenching time, but also on the finding that smaller metabolites leaked more than larger ones, which corresponds with the fact that the diffusivity of smaller molecules is higher [15]. We plotted the extent of leakage versus molecular weight for our data in Figure 4a. Molecular weight was used as proxy for molecular size. The extent of leakage was calculated from the reconciled data as the percentage difference between the reference amount (TB-EX) and the amount in the cell pellets treated with 60% (v/v) aqueous methanol and pure methanol. Figure 4a shows the trend that smaller molecules leak more, which further supports the hypothesis that also in the case of *P. chrysogenum* leakage of metabolites from quenched biomass is driven by diffusion.

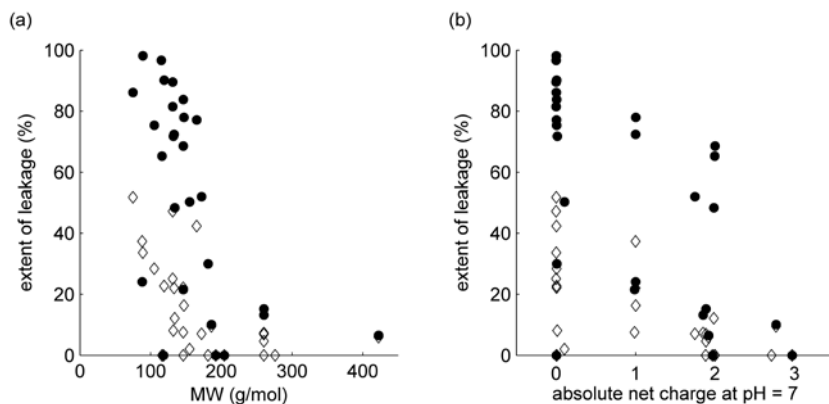


**Figure 4** Extent of leakage versus molecular weight (a) and versus absolute net charge (b). The extent of leakage was calculated from the reconciled data as the percentage difference between metabolite levels in the cell pellets and the reference amount (TB-EX). Each symbol represents the extent of leakage for one metabolite under the condition of using 60% (v/v) aqueous methanol (open diamonds) or pure methanol (solid circles) for quenching.

If metabolites leak from cells by diffusion, they have to pass the hydrophobic cell membrane, which is expected to be less likely to happen when they are electrically charged. Indeed a trend of a lower extent of leakage with higher absolute net charge can be observed in Figure 4b. Here, the absolute net charge was calculated from the pKa values and an assumed intracellular pH of 7 (theoretical pKa values obtained from the software MarvinSketch 5.5.1.0 were used in case experimentally determined pKa values were not available, for example in the case of 2PG). The metabolites plotted as having an absolute net charge of close to 0 were zwitterionic free amino acids without a charged side-group but with a positively charged amino group and a negatively charged carboxyl group. The class of amino acids was found to show the largest extent of leakage in this study (see also Figures 2d and 3d).

Canelas et al. observed that the extent of leakage from *S. cerevisiae* cells decreased when the methanol content of the quenching liquid was increased [15]. Methanol is not as good a solvent as water for most metabolites, because they are mostly charged and polar. In combination with observations on the effects of the temperature and the ionic strength of the quenching liquid on metabolite leakage, they suggested that reduction of the solubility of the metabolites in the quenching liquid would decrease the extent of leakage. However, Carnicer et al. did not observe a significant difference in leakage for different methanol content of the cold aqueous methanol quenching solution in case of *P. pastoris* [17], while



we find that the extent of leakage from *P. chrysogenum* cells increases with an increase in the methanol content, which is the exact opposite of the finding of Canelas et al. [15]. These results make it doubtful whether solubility must be considered as a factor of importance in metabolite leakage.

### 3.4 The advantage of using a quantitative mass balance approach

In this work the extent of metabolite leakage during cold aqueous methanol quenching was evaluated using a quantitative mass balance approach. With this approach the amounts of metabolites are quantified in different sample fractions such that losses of metabolites from cells during methanol quenching can be detected and quantified. Several other studies aiming at minimization of leakage reported in literature only compared the amounts recovered from the cell pellet when using different quenching liquids [31,32]. With such an approach it is possible to find the quenching procedure which results in the highest metabolite levels. However, the advantages of the mass balance approach are that the extent of leakage is also estimated and that it allows to check the consistency of the data. Furthermore, the use of <sup>13</sup>C labeled cell extract as internal standard in all samples and standards is recommended, because it corrects for partial degradation of metabolites during sample processing and storage and improves the precision of the mass spectrometric based quantification, as was also concluded by others [18,33,34].

## 4 Concluding remarks and recommendations

For quantitative metabolomics studies in *P. chrysogenum*, -25°C 40% (v/v) aqueous methanol was found to be the optimal quenching and washing liquid of the three liquids compared in this work, because its use resulted in the highest recovery of metabolites from quenched and washed cell pellets. The volume ratio of sample to this quenching liquid should preferably be 1:10 to avoid that the temperature of the mixture rises above -20°C. Sample treatment should proceed as quickly as possible to metabolite extraction and definitive enzyme inactivation, because prolonged contact time between quenched cells and the quenching liquid can lead to increased metabolite losses.

Besides the contact time with the quenching liquid, the extent of leakage was found to depend on factors affecting the diffusivity, namely molecular weight and net charge, suggesting that metabolite leakage from quenched mycelia of *P. chrysogenum* is driven by diffusion.

## Acknowledgements

The authors would like to thank Zheng Zhao and Amit Deshmuk for providing *P. chrysogenum* <sup>13</sup>C-labeled cell extract and Angela ten Pierick, Cor Ras and Zhen Zeng for excellent analytical support.

## References

- [1] K. Nöh, K. Grönke, B. Luo, R. Takors, M. Oldiges, and W. Wiechert, Metabolic flux analysis at ultra short time scale: Isotopically non-stationary C-13 labeling experiments, *J. Biotechnol.* 129 (2007) pp. 249-267.
- [2] J. Schaub, A. Mauch, and M. Reuss, Metabolic flux analysis in *Escherichia coli* by integrating isotopic dynamic and isotopic stationary C-13 labeling data, *Biotechnol. Bioeng.* 99 (2008) pp. 1170-1185.
- [3] M.R. Mashego, K. Rumbold, M. De Mey, E. Vandamme, W. Soetaert, and J.J. Heijnen, Microbial metabolomics: past, present and future methodologies, *Biotechnol. Lett.* 29 (2007) pp. 1-16.
- [4] B. Álvarez-Sánchez, F. Priego-Capote, and M.D. Luque de Castro, Metabolomics analysis II. Preparation of biological samples prior to detection, *Trac-Trends in Analytical Chemistry* 29 (2010) pp. 120-127.
- [5] K.E. Weibel, J.R. Mor, and A. Fiechter, Rapid Sampling of Yeast-Cells and Automated Assays of Adenylate, Citrate, Pyruvate and Glucose-6-Phosphate Pools, *Anal. Biochem.* 58 (1974) pp. 208-216.
- [6] H. Taymaz-Nikerel, M. De Mey, C. Ras, A. ten Pierick, R.M. Seifar, J.C. van Dam, J.J. Heijnen, and W.M. van Gulik, Development and application of a differential method for reliable metabolome analysis in *Escherichia coli*, *Anal. Biochem.* 386 (2009) pp. 9-19.
- [7] R.D. Douma, L.P. de Jonge, C.T.H. Jonker, R.M. Seifar, J.J. Heijnen, and W.M. van Gulik, Intracellular Metabolite Determination in the Presence of Extracellular Abundance: Application to the Penicillin Biosynthesis Pathway in *Penicillium chrysogenum*, *Biotechnol. Bioeng.* 107 (2010) pp. 105-115.
- [8] F. Schädel and E. Franco-Lara, Rapid sampling devices for metabolic engineering applications, *Appl. Microbiol. Biotechnol.* 83 (2009) pp. 199-208.

- [9] W.M. van Gulik, Fast sampling for quantitative microbial metabolomics, *Curr. Opin. Biotechnol.* 21 (2010) pp. 27-34.
- [10] W. De Koning and K. Van Dam, A Method for the Determination of Changes of Glycolytic Metabolites in Yeast on A Subsecond Time Scale Using Extraction at Neutral pH, *Anal. Biochem.* 204 (1992) pp. 118-123.
- [11] C.J. Bolten, P. Kiefer, F. Letisse, J.C. Portais, and C. Wittmann, Sampling for Metabolome Analysis of Microorganisms, *Analytical Chemistry* 79 (2007) pp. 3843-3849.
- [12] C. Wittmann, J.O. Kromer, P. Kiefer, T. Binz, and E. Heinzle, Impact of the cold shock phenomenon on quantification of intracellular metabolites in bacteria, *Anal. Biochem.* 327 (2004) pp. 135-139.
- [13] S.G. Villas-Bôas, J. Hojer-Pedersen, M. Akesson, J. Smedsgaard, and J. Nielsen, Global metabolite analysis of yeast: evaluation of sample preparation methods, *Yeast* 22 (2005) pp. 1155-1169.
- [14] M. Faijes, A.E. Mars, and E.J. Smid, Comparison of quenching and extraction methodologies for metabolome analysis of *Lactobacillus plantarum*, *Microbial Cell Factories* 6 (2007).
- [15] A.B. Canelas, C. Ras, A. ten Pierick, J.C. van Dam, J.J. Heijnen, and W.M. van Gulik, Leakage-free rapid quenching technique for yeast metabolomics, *Metabolomics* 4 (2008) pp. 226-239.
- [16] C.A. Sellick, R. Hansen, A.R. Maqsood, W.B. Dunn, G.M. Stephens, R. Goodacre, and A.J. Dickson, Effective Quenching Processes for Physiologically Valid Metabolite Profiling of Suspension Cultured Mammalian Cells, *Analytical Chemistry* 81 (2009) pp. 174-183.
- [17] M. Carnicer, A.B. Canelas, A. ten Pierick, Z. Zeng, J. van Dam, J. Albiol, P. Ferrer, J.J. Heijnen, and W. van Gulik, Development of Quantitative Metabolomics for *Pichia Pastoris*, 2011.
- [18] M. Wellerdiek, D. Winterhoff, W. Reule, J. Brandner, and M. Oldiges, Metabolic quenching of *Corynebacterium glutamicum*: efficiency of methods and impact of cold shock, *Bioprocess Biosystems Eng.* 32 (2009) pp. 581-592.
- [19] B. Gonzalez, J. Francois, and M. Renaud, A rapid and reliable method for metabolite extraction in yeast using boiling buffered ethanol, *Yeast* 13 (1997) pp. 1347-1355.
- [20] H. Hajjaj, P.J. Blanc, G. Goma, and J. Francois, Sampling techniques and comparative extraction procedures for quantitative determination of intra- and

- extracellular metabolites in filamentous fungi, *FEMS Microbiol. Lett.* 164 (1998) pp. 195-200.
- [21] U. Nasution, W.M. van Gulik, R.J. Kleijn, W.A. Van Winden, A. Proell, and J.J. Heijnen, Measurement of intracellular metabolites of primary metabolism and adenine nucleotides in chemostat cultivated *Penicillium chrysogenum*, *Biotechnol. Bioeng.* 94 (2006) pp. 159-166.
- [22] W.M. van Gulik, W.T.A.M. De Laat, J.L. Vinke, and J.J. Heijnen, Application of metabolic flux analysis for the identification of metabolic bottlenecks in the biosynthesis of penicillin-G, *Biotechnol. Bioeng.* 68 (2000) pp. 602-618.
- [23] H.C. Lange, M. Eman, G. van Zuijlen, D. Visser, J.C. van Dam, J. Frank, M.J.T. de Mattos, and J.J. Heijnen, Improved rapid sampling for in vivo kinetics of intracellular metabolites in *Saccharomyces cerevisiae*, *Biotechnology and Bioengineering* 75 (2001) pp. 406-415.
- [24] L. Wu, M.R. Mashego, J.C. van Dam, A.M. Proell, J.L. Vinke, C. Ras, W.A. Van Winden, W.M. van Gulik, and J.J. Heijnen, Quantitative analysis of the microbial metabolome by isotope dilution mass spectrometry using uniformly C-13-labeled cell extracts as internal standards, *Anal. Biochem.* 336 (2005) pp. 164-171.
- [25] M.R. Mashego, W.M. van Gulik, J.L. Vinke, and J.J. Heijnen, Critical evaluation of sampling techniques for residual glucose determination in carbon-limited chemostat culture of *Saccharomyces cerevisiae*, *Biotechnol. Bioeng.* 83 (2003) pp. 395-399.
- [26] J.C. van Dam, M.R. Eman, J. Frank, H.C. Lange, G.W.K. van Dedem, and J.J. Heijnen, Analysis of glycolytic intermediates in *Saccharomyces cerevisiae* using anion exchange chromatography and electrospray ionization with tandem mass spectrometric detection, *Anal. Chim. Acta* 460 (2002) pp. 209-218.
- [27] C. Cipollina, A. ten Pierick, A.B. Canelas, R.M. Seifar, A.J.A. van Maris, J.C. van Dam, and J.J. Heijnen, A comprehensive method for the quantification of the non-oxidative pentose phosphate pathway intermediates in *Saccharomyces cerevisiae* by GC-IDMS, *J. Chromatogr. B Analyt. Technol. Biomed. Life. Sci.* 877 (2009) pp. 3231-3236.
- [28] M.R. Mashego, L. Wu, J.C. van Dam, C. Ras, J.L. Vinke, W.A. Van Winden, W.M. van Gulik, and J.J. Heijnen, MIRACLE: mass isotopomer ratio analysis of U-C-13-labeled extracts. A new method for accurate quantification of changes in concentrations of intracellular metabolites, *Biotechnol. Bioeng.* 85 (2004) pp. 620-628.

- [29] R.T.J.M. van der Heijden, B. Romein, J.J. Heijnen, C. Hellinga, and K.C.A.M. Luyben, Linear Constraint Relations in Biochemical Reaction Systems: II. Diagnosis and Estimation of Gross Errors, *Biotechnol. Bioeng.* 43 (1994) pp. 11-20.
- [30] G.D. Tredwell, B. Edwards-Jones, D.J. Leak, and J.G. Bundy, The Development of Metabolomic Sampling Procedures for *Pichia pastoris*, and Baseline Metabolome Data, *Plos One* 6 (2011).
- [31] S.G. Villas-Bôas and P. Bruheim, Cold glycerol-saline: The promising quenching solution for accurate intracellular metabolite analysis of microbial cells, *Anal. Biochem.* 370 (2007) pp. 87-97.
- [32] J. Spura, L.C. Reimer, P. Wieloch, K. Schreiber, S. Buchinger, and D. Schomburg, A method for enzyme quenching in microbial metabolome analysis successfully applied to gram-positive and gram-negative bacteria and yeast, *Anal. Biochem.* 394 (2009) pp. 192-201.
- [33] J.M. Büscher, D. Czernik, J.C. Ewald, U. Sauer, and N. Zamboni, Cross-Platform Comparison of Methods for Quantitative Metabolomics of Primary Metabolism, *Analytical Chemistry* 81 (2009) pp. 2135-2143.
- [34] N. Zamboni and U. Sauer, Novel biological insights through metabolomics and C-13-flux analysis, *Curr. Opin. Microbiol.* 12 (2009) pp. 553-558.

## Appendix

Table A1.

Measured metabolite amounts in the different sample fractions. Shown are the averages  $\pm$  standard errors of duplicate samples. Numbers in red are measurements which were judged to be inconsistent with the TB and EX measurements according to the consistency check.

Metabolite	Quenching in -25 °C 40% (v/v) aqueous methanol						
	Total broth, TB ( $\mu\text{mol/gdw}$ )	Culture filtrate, EX ( $\mu\text{mol/gdw}$ )	Differential, TB-EX ( $\mu\text{mol/gdw}$ )	Cell pellet, IC ( $\mu\text{mol/gdw}$ )	Quenching solution, QS ( $\mu\text{mol/gdw}$ )	Washing solution, WS ( $\mu\text{mol/gdw}$ )	
G6P	4.47 $\pm$ 0.68	0.32 $\pm$ 0.08	4.15 $\pm$ 0.68	3.91 $\pm$ 0.06	0.31 $\pm$ 0.01	0.15 $\pm$ 0.01	
G1P+M1P	0.816 $\pm$ 0.098	0.210 $\pm$ 0.003	0.606 $\pm$ 0.098	0.680 $\pm$ 0.011	0.137 $\pm$ 0.037	0.028 $\pm$ 0.004	
F6P	0.587 $\pm$ 0.079	-	0.587 $\pm$ 0.079	0.646 $\pm$ 0.011	-	0.025 $\pm$ 0.003	
FBP	0.197 $\pm$ 0.033	0.132 $\pm$ 0.006	0.065 $\pm$ 0.034	<b>0.565 <math>\pm</math> 0.001</b>	<b>0.064 <math>\pm</math> 0.005</b>	<b>0.009 <math>\pm</math> 0.001</b>	
M6P	1.32 $\pm$ 0.21	0.07 $\pm$ 0.02	1.25 $\pm$ 0.21	1.46 $\pm$ 0.02	0.08 $\pm$ 0.01	0.05 $\pm$ 0.01	
T6P	0.390 $\pm$ 0.057	-	0.390 $\pm$ 0.057	0.412 $\pm$ 0.005	0.005 $\pm$ 0.002	0.010 $\pm$ 0.002	
6PG	0.260 $\pm$ 0.051	0.165 $\pm$ 0.092	0.094 $\pm$ 0.106	0.075 $\pm$ 0.006	0.125 $\pm$ 0.023	0.017 $\pm$ 0.003	
G3P	0.748 $\pm$ 0.070	0.477 $\pm$ 0.016	0.271 $\pm$ 0.071	0.292 $\pm$ 0.014	0.354 $\pm$ 0.002	0.020 $\pm$ 0.002	
2PG+3PG	0.735 $\pm$ 0.132	0.108 $\pm$ 0.021	0.628 $\pm$ 0.134	0.690 $\pm$ 0.022	0.114 $\pm$ 0.016	0.023 $\pm$ 0.002	
PEP	0.294 $\pm$ 0.021	0.024 $\pm$ 0.002	0.270 $\pm$ 0.021	0.291 $\pm$ 0.016	0.007 $\pm$ 0.001	0.007 $\pm$ 0.001	
Pyruvate	0.148 $\pm$ 0.143	-	0.148 $\pm$ 0.143	0.243 $\pm$ 0.005	-	0.015 $\pm$ 0.010	
Citrate	11.50 $\pm$ 0.23	13.10 $\pm$ 2.21	-1.60 $\pm$ 2.22	<b>3.03 <math>\pm</math> 0.02</b>	<b>11.63 <math>\pm</math> 0.29</b>	<b>0.90 <math>\pm</math> 0.06</b>	
$\alpha$ -KG	1.324 $\pm$ 0.152	0.762 $\pm$ 0.108	0.563 $\pm$ 0.186	0.427 $\pm$ 0.004	0.516 $\pm$ 0.107	0.076 $\pm$ 0.014	
Succinate	5.92 $\pm$ 0.49	6.48 $\pm$ 0.43	-0.56 $\pm$ 0.65	1.17 $\pm$ 0.01	5.16 $\pm$ 0.14	0.38 $\pm$ 0.04	
Fumarate	1.554 $\pm$ 0.273	0.893 $\pm$ 0.030	0.661 $\pm$ 0.274	0.894 $\pm$ 0.026	0.735 $\pm$ 0.041	0.089 $\pm$ 0.006	
Malate	4.53 $\pm$ 0.57	0.81 $\pm$ 0.04	3.71 $\pm$ 0.57	4.56 $\pm$ 0.06	0.77 $\pm$ 0.04	0.26 $\pm$ 0.01	
Ala	48.1 $\pm$ 7.0	2.8 $\pm$ 1.4	45.2 $\pm$ 7.1	39.5 $\pm$ 0.4	4.2 $\pm$ 0.1	1.8 $\pm$ 0.1	
Gly	6.31 $\pm$ 0.27	1.32 $\pm$ 0.99	4.99 $\pm$ 1.02	3.50 $\pm$ 0.03	2.05 $\pm$ 0.25	0.45 $\pm$ 0.04	
Leu	1.214 $\pm$ 0.086	0.215 $\pm$ 0.030	0.999 $\pm$ 0.091	<b>0.608 <math>\pm</math> 0.013</b>	<b>0.020 <math>\pm</math> 0.017</b>	<b>0.031 <math>\pm</math> 0.004</b>	
Ile	0.521 $\pm$ 0.018	0.206 $\pm$ 0.029	0.315 $\pm$ 0.034	<b>0.270 <math>\pm</math> 0.004</b>	<b>0.064 <math>\pm</math> 0.017</b>	<b>0.019 <math>\pm</math> 0.002</b>	
Thr	9.70 $\pm$ 1.20	0.79 $\pm$ 0.18	8.90 $\pm$ 1.21	8.18 $\pm$ 0.14	0.97 $\pm$ 0.06	0.54 $\pm$ 0.04	
Ser	9.46 $\pm$ 0.69	3.17 $\pm$ 1.13	6.29 $\pm$ 1.33	6.61 $\pm$ 0.25	2.53 $\pm$ 0.29	0.41 $\pm$ 0.02	
Pro	2.30 $\pm$ 0.27	0.24 $\pm$ 0.22	2.06 $\pm$ 0.35	<b>1.17 <math>\pm</math> 0.04</b>	<b>0.21 <math>\pm</math> 0.02</b>	<b>0.08 <math>\pm</math> 0.01</b>	
Asn	2.34 $\pm$ 0.44	-	2.34 $\pm$ 0.44	2.61 $\pm$ 0.04	-	0.13 $\pm$ 0.01	
Asp	30.3 $\pm$ 4.0	0.5 $\pm$ 0.5	29.8 $\pm$ 4.0	27.4 $\pm$ 0.5	1.8 $\pm$ 0.1	1.6 $\pm$ 0.1	
Met	0.090 $\pm$ 0.006	-	0.090 $\pm$ 0.006	0.064 $\pm$ 0.010	-	0.004 $\pm$ 0.001	
Glu	85.2 $\pm$ 12.5	1.4 $\pm$ 0.5	83.8 $\pm$ 12.5	89.4 $\pm$ 0.3	3.8 $\pm$ 0.2	4.0 $\pm$ 0.3	
Phe	0.376 $\pm$ 0.012	0.190 $\pm$ 0.076	0.186 $\pm$ 0.077	<b>0.128 <math>\pm</math> 0.002</b>	<b>0.193 <math>\pm</math> 0.001</b>	<b>0.012 <math>\pm</math> 0.001</b>	
Gln	35.3 $\pm$ 5.3	-	35.3 $\pm$ 5.3	38.8 $\pm$ 0.3	3.0 $\pm$ 0.6	2.0 $\pm$ 0.2	
Orn	2.15 $\pm$ 0.10	0.37 $\pm$ 0.05	1.78 $\pm$ 0.11	1.85 $\pm$ 0.02	<b>0.25 <math>\pm</math> 0.01</b>	<b>0.11 <math>\pm</math> 0.01</b>	
Lys	1.89 $\pm$ 0.20	0.20 $\pm$ 0.16	1.69 $\pm$ 0.26	1.85 $\pm$ 0.02	0.18 $\pm$ 0.01	0.08 $\pm$ 0.01	
His	1.67 $\pm$ 0.13	0.16 $\pm$ 0.02	1.51 $\pm$ 0.13	1.78 $\pm$ 0.02	0.13 $\pm$ 0.12	0.07 $\pm$ 0.01	
Tyr	0.231 $\pm$ 0.029	0.128 $\pm$ 0.018	0.103 $\pm$ 0.035	0.139 $\pm$ 0.017	0.059 $\pm$ 0.034	0.010 $\pm$ 0.001	
Trp	0.235 $\pm$ 0.011	0.289 $\pm$ 0.024	-0.054 $\pm$ 0.026	<b>0.031 <math>\pm</math> 0.003</b>	<b>0.243 <math>\pm</math> 0.002</b>	<b>0.013 <math>\pm</math> 0.001</b>	

Table A1 continued

Metabolite	Quenching in -40 °C 60% (v/v) aqueous methanol			Quenching in -40 °C pure methanol		
	Cell pellet, IC ( $\mu\text{mol/g}_{\text{DW}}$ )	Quenching solution, QS ( $\mu\text{mol/g}_{\text{DW}}$ )	Washing solution, WS ( $\mu\text{mol/g}_{\text{DW}}$ )	Cell pellet, IC ( $\mu\text{mol/g}_{\text{DW}}$ )	Quenching solution, QS ( $\mu\text{mol/g}_{\text{DW}}$ )	Washing solution, WS ( $\mu\text{mol/g}_{\text{DW}}$ )
G6P	3.99 ± 0.02	0.45 ± 0.06	0.17 ± 0.01	3.55 ± 0.08	0.73 ± 0.08	0.23 ± 0.04
G1P+M1P	0.705 ± 0.020	0.173 ± 0.010	0.034 ± 0.002	<b>0.808 ± 0.032</b>	<b>0.227 ± 0.042</b>	<b>0.051 ± 0.004</b>
F6P	0.708 ± 0.005	0.008 ± 0.005	0.027 ± 0.001	<b>0.933 ± 0.026</b>	<b>0.139 ± 0.020</b>	<b>0.093 ± 0.015</b>
FBP	<b>0.427 ± 0.001</b>	<b>0.131 ± 0.025</b>	<b>0.004 ± 0.001</b>	<b>0.381 ± 0.005</b>	<b>0.111 ± 0.013</b>	<b>0.001 ± 0.001</b>
M6P	1.24 ± 0.01	0.12 ± 0.02	0.05 ± 0.01	1.18 ± 0.04	0.19 ± 0.03	0.06 ± 0.01
T6P	0.403 ± 0.001	0.019 ± 0.013	0.009 ± 0.001	0.419 ± 0.003	0.025 ± 0.005	0.005 ± 0.001
6PG	0.177 ± 0.005	0.169 ± 0.032	0.023 ± 0.002	<b>0.665 ± 0.032</b>	<b>0.112 ± 0.015</b>	<b>0.016 ± 0.003</b>
G3P	0.288 ± 0.002	0.680 ± 0.158	0.023 ± 0.001	0.165 ± 0.011	0.719 ± 0.096	0.067 ± 0.003
2PG+3PG	0.664 ± 0.021	0.149 ± 0.015	0.029 ± 0.001	0.557 ± 0.002	0.140 ± 0.014	0.030 ± 0.001
PEP	<b>0.287 ± 0.003</b>	<b>0.040 ± 0.002</b>	<b>0.012 ± 0.001</b>	<b>0.307 ± 0.008</b>	<b>0.085 ± 0.014</b>	<b>0.026 ± 0.003</b>
Pyruvate	0.200 ± 0.005	0.087 ± 0.036	0.043 ± 0.001	0.227 ± 0.049	0.056 ± 0.006	0.011 ± 0.006
Citrate	2.78 ± 0.02	8.92 ± 0.61	0.58 ± 0.04	2.75 ± 0.07	9.40 ± 0.81	0.56 ± 0.01
$\alpha$ -KG	0.557 ± 0.009	0.482 ± 0.019	0.132 ± 0.001	0.208 ± 0.040	1.182 ± 0.220	0.197 ± 0.011
Succinate	1.30 ± 0.09	4.79 ± 0.12	0.38 ± 0.04	0.54 ± 0.05	5.83 ± 0.86	0.45 ± 0.04
Fumarate	0.881 ± 0.034	0.763 ± 0.001	0.113 ± 0.012	0.260 ± 0.047	1.156 ± 0.152	0.246 ± 0.002
Malate	3.71 ± 0.12	1.00 ± 0.06	0.32 ± 0.01	2.18 ± 0.20	2.41 ± 0.41	0.61 ± 0.03
Ala	30.6 ± 0.1	14.0 ± 0.2	4.3 ± 0.3	1.0 ± 0.3	55.4 ± 4.8	4.3 ± 0.5
Gly	2.43 ± 0.02	3.67 ± 1.01	0.84 ± 0.01	0.70 ± 0.24	5.13 ± 0.87	0.55 ± 0.18
Leu	0.501 ± 0.013	0.325 ± 0.203	0.073 ± 0.005	0.143 ± 0.062	1.033 ± 0.100	0.242 ± 0.061
Ile	0.235 ± 0.014	0.207 ± 0.139	0.034 ± 0.001	0.065 ± 0.034	0.393 ± 0.061	0.096 ± 0.029
Thr	6.87 ± 0.03	1.84 ± 0.16	0.97 ± 0.01	1.07 ± 0.25	9.39 ± 0.84	1.42 ± 0.26
Ser	4.86 ± 0.56	5.44 ± 1.53	0.83 ± 0.04	1.71 ± 0.72	7.05 ± 1.32	1.42 ± 0.41
Pro	0.85 ± 0.01	0.81 ± 0.18	0.21 ± 0.01	0.08 ± 0.04	2.54 ± 0.27	0.22 ± 0.05
Asn	2.23 ± 0.09	-	0.28 ± 0.01	0.85 ± 0.15	1.75 ± 0.26	0.46 ± 0.06
Asp	24.2 ± 0.1	4.8 ± 0.1	2.6 ± 0.1	9.4 ± 1.2	21.5 ± 3.2	5.1 ± 0.3
Met	<b>0.060 ± 0.008</b>	<b>0.092 ± 0.013</b>	<b>0.008 ± 0.001</b>	<b>0.023 ± 0.005</b>	<b>0.109 ± 0.014</b>	<b>0.014 ± 0.003</b>
Glu	76.7 ± 0.3	10.1 ± 0.7	6.2 ± 0.1	21.8 ± 4.0	85.3 ± 11.0	17.4 ± 0.8
Phe	0.107 ± 0.006	0.272 ± 0.113	0.018 ± 0.002	0.057 ± 0.024	0.303 ± 0.032	0.068 ± 0.022
Gln	32.8 ± 0.2	5.9 ± 0.5	3.5 ± 0.1	6.8 ± 1.4	34.7 ± 6.9	6.7 ± 0.7
Orn	<b>2.08 ± 0.03</b>	<b>1.01 ± 0.14</b>	<b>0.11 ± 0.02</b>	2.07 ± 0.17	0.04 ± 0.01	0.14 ± 0.09
Lys	1.69 ± 0.02	0.26 ± 0.08	0.10 ± 0.01	1.55 ± 0.09	0.54 ± 0.09	0.12 ± 0.01
His	1.60 ± 0.01	0.22 ± 0.12	0.09 ± 0.01	0.90 ± 0.13	0.86 ± 0.15	0.25 ± 0.03
Tyr	0.130 ± 0.020	0.122 ± 0.075	0.011 ± 0.001	0.087 ± 0.030	0.117 ± 0.021	0.050 ± 0.011
Trp	0.034 ± 0.004	0.241 ± 0.027	0.013 ± 0.001	0.030 ± 0.006	0.237 ± 0.029	0.025 ± 0.006

## Chapter 4

---

# Reconstruction of the oxygen uptake and carbon dioxide evolution rates of microbial cultures at near-neutral pH during highly dynamic conditions

---

Published as:

de Jonge LP, Heijnen JJ, van Gulik WM. Reconstruction of the oxygen uptake and carbon dioxide evolution rates of microbial cultures at near-neutral pH during highly dynamic conditions. *Biochem Eng J* 2014;83:42-54.



## Abstract

The reconstruction of the dynamically changing rates of O<sub>2</sub> uptake and CO<sub>2</sub> production during short term bioreactor perturbation experiments, from dissolved oxygen and offgas O<sub>2</sub> and CO<sub>2</sub> measurements, requires a model describing the mass transfer and dispersion of O<sub>2</sub> and CO<sub>2</sub> in the system as well as the sensor dynamics. Additionally, if perturbation experiments are carried out at near-neutral pH levels, also the inter conversion of dissolved carbon dioxide and bicarbonate needs to be taken into account. While developing such a model we found that for an accurate description of the systems dynamic response on a time-scale of seconds, it is required to incorporate not only the mass transfer between gas bubbles and broth, but also between headspace and broth. The delay and dispersion in the measurements of the gas analyser, due to the length and complexity of the offgas system, was accounted for by determining the impulse response of the offgas system. This model fitted excellently to an identification data set, used to identify a limited number of 10 parameters. Finally the model was successfully applied to reconstruct the dynamic rates of O<sub>2</sub> uptake and CO<sub>2</sub> production of a culture of *Penicillium chrysogenum*, which was perturbed by a glucose pulse.

## 1 Introduction

One of the goals of microbial systems biology is to unravel the different levels of metabolic control by which cells adapt to changes in their environment. In an industrial setting, knowledge of these control mechanisms can be used to redesign micro-organisms to improve production rates and yield. The metabolic control mechanisms which are relevant at short time scales (sub seconds to minutes) are related to the affinities of enzymes for their substrates and products, to allosteric mechanisms and to covalent modifications. These can be identified and studied by short (30 – 400 seconds) perturbation experiments, e.g. by injecting a concentrated substrate solution in a substrate limited chemostat culture [1-8]. The transient metabolic response to a perturbation is usually studied in terms of changes in the intra- and extracellular metabolite concentrations (to quantify rates), which can be used to quantify metabolic fluxes or to fit a kinetic model which describes the control mechanisms mathematically. Also measurement of concentration changes in the offgas from a perturbed aerobic (i.e. O<sub>2</sub> and CO<sub>2</sub>) or anaerobic (N<sub>2</sub>-flushed) bioreactor (i.e. only CO<sub>2</sub>) are important to quantify changes in O<sub>2</sub> uptake rate (OUR) and CO<sub>2</sub> evolution rate (CER). These provide additional data to obtain more accurate information on the flux dynamics. However, proper quantification of the short term dynamics of the OUR and CER from measurements of O<sub>2</sub> and CO<sub>2</sub> concentrations in the offgas is hampered by the

residence time of the gas in the headspace of the fermentor and the offgas analysis system, back mixing, and the response times of the O<sub>2</sub> and CO<sub>2</sub> sensors in the gas analyser.

Bloemen et al. [9] and Wu et al. [10] have presented algorithms to reconstruct the OUR and CER from delayed and highly dynamic measurements of the offgas concentrations and the dissolved O<sub>2</sub> concentration during short term perturbation experiments. In their approach, reconstruction calculations are performed with the help of a model which describes the transport processes of O<sub>2</sub> and CO<sub>2</sub> in the bioreactor and the offgas system to account for time delays and distortion of the measurements. They account for example for the turnover time of gas in the headspace of the bioreactor, which is usually in the order of one to several minutes, and for the characteristic time for O<sub>2</sub> transfer from the gas to the liquid phase and the response time of the DO probe, which are both typically in the order of several tens of seconds. However, both algorithms were developed for, and applied to, cultures of *Saccharomyces cerevisiae* grown at a pH of 5. At that pH value the concentration of bicarbonate in equilibrium with the concentration of dissolved CO<sub>2</sub> is in the order of 5% of the dissolved CO<sub>2</sub> concentration, and therefore the exchange between these two pools was neglected in the calculations. At more neutral pH levels, however, the bicarbonate concentration is of the same order of magnitude as the dissolved CO<sub>2</sub> concentration. Moreover, the characteristic time for bicarbonate formation, in terms of the reciprocal of the rate constant for CO<sub>2</sub> hydration, is several tens of seconds (depending on the temperature) [11], which is relevant in the time window of a short perturbation experiment. Clearly, at near-neutral pH levels, the inter conversion of bicarbonate and dissolved CO<sub>2</sub> should be incorporated in the model.

Spérandio and Paul [12] and Kovács et al. [13] followed this approach of incorporating the inter conversion of dissolved CO<sub>2</sub> and bicarbonate in a model used to calculate the CER under non-steady state conditions. However, they carried out perturbation experiments over longer time periods (minutes to hours), which required less detail with respect to modelling the short-term dynamics. Therefore, in their models the delay times related to the offgas analysis (due to the residence time of the gas in the tubing between the outlet of the reactor and the analyser) could be neglected.

The aim of this work is to develop a model suitable for the reconstruction of the highly dynamic OUR and CER during short perturbation experiments of microbial cultures grown at pH values where significant inter conversion of dissolved CO<sub>2</sub> and bicarbonate occurs. To achieve this, the physical and chemical processes taking place in the reactor and the offgas system have to be modelled accurately. The procedure is applied to reconstruct the OUR and CER of a glucose perturbed chemostat culture of *Penicillium chrysogenum* grown at a pH of 6.5.

## 2 Modelling

### 2.1 Model development

#### 2.1.1 System description

A scheme of the experimental set-up is shown in Figure 1. The model was developed such that it reproduces the sensor outputs (DO and offgas  $O_2$  and  $CO_2$  concentrations) from the OUR, CER and input  $O_2$  and  $CO_2$  mole fractions, for given experimental conditions and initial state. During perturbation experiments, which are typically carried out in well mixed bench scale bioreactors, the DO and the pH in the broth can be measured on-line with little to no time delay. In contrast to this, the measurement of the concentrations of  $O_2$  and  $CO_2$  in the offgas is subjected to significant time delay and distortion, because the gas has to travel through the headspace of the bioreactor and a system of tubing, filters, valves, a dryer etc., before arriving at the analyzer. In view of the complexity of the offgas system, we divided the model into two parts. The first part describes the physical and (bio)chemical processes occurring in the bioreactor and the initial part of the offgas system until point B in Figure 1, while the second part describes the response of the offgas system from point B until the offgas analyzer.

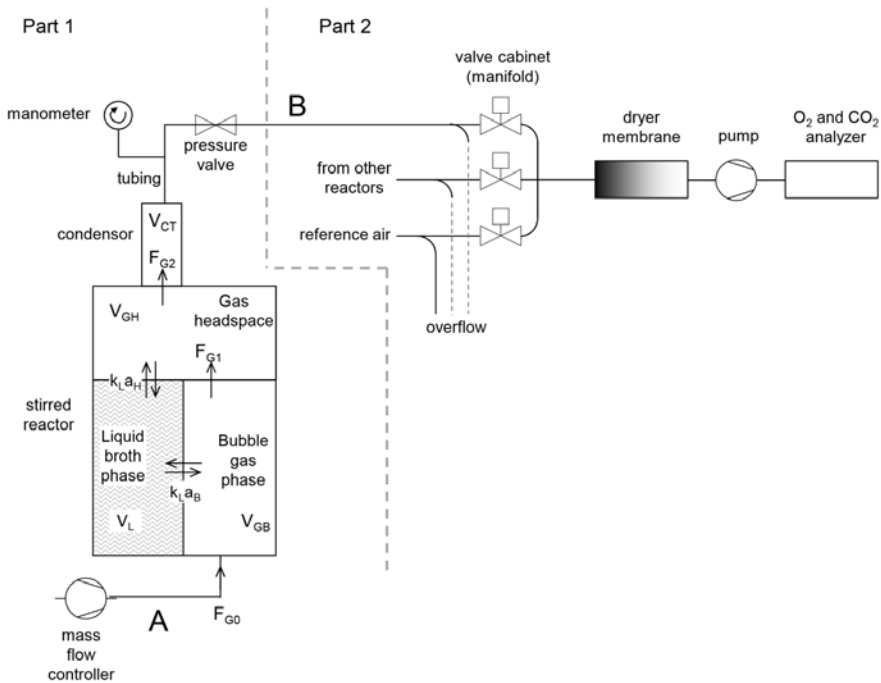


**Figure 1** Schematic overview of the system.

### 2.1.2 Gas and liquid phases

The first part of the model contains four compartments, namely (1) the fermentation broth, (2) the homogeneously dispersed gas bubbles in the broth, (3) the gas phase above the broth (headspace) and (4) the gas outlet (condenser), filter, pressure valve and tubing towards the offgas analysis system (see Figure 1). These four compartments are assumed to have a fixed volume and compartments one and two (broth and gas bubbles) are assumed to be ideally mixed. We have measured that the liquid mixing in this reactor under the applied operating conditions (stirrer speed and airflow rate) was complete in less than 5 seconds [14]. In such a well-mixed small bench scale bioreactor, the gas present in the bubbles may be considered well mixed and uniform as well.

The gas in the headspace is, however, only mixed by the movement of the turbulent liquid surface and the flow of gas from bubbles that arrive at the liquid surface, so the headspace may in fact not be ideally mixed. Furthermore, the condenser and tubing of the initial part of the offgas system are expected to respond as a plug flow reactor rather than as an ideally stirred tank. However, this part of the system (headspace, condenser, tubing) can be approximated to respond as a series of ideally stirred tanks plus a pure time delay. It was shown by Bloemen et al. [9] that for the currently used setup two ideally stirred tanks are sufficient, but the number can be increased as needed for other setups. It should be noted that these two ideally stirred tanks correspond to the abovementioned third (headspace) and fourth (initial part of the offgas system) model compartments. Also, it should be noted that the volumes of the two ideally stirred tanks are now model parameters which are not necessarily equal to the physical volumes of the headspace and the condenser.

The model describes the concentrations of several molecular and ionic species in these four model compartments. Oxygen, carbon dioxide and nitrogen are present in the three gas compartments and, in dissolved form, in the liquid phase. Water vapour in the gas compartments is modelled implicitly by taking into account the water vapour pressure. The changes in the concentrations of the following ions in the liquid phase are modelled: bicarbonate, hydronium, hydroxide, monohydrogenphosphate and dihydrogenphosphate. We will now first describe the transport processes of  $O_2$ ,  $CO_2$  and  $N_2$  between the four compartments.

### 2.1.3 Gas flows and mass transfer between gas and liquid phase

Dry air enters the reactor at a fixed flow rate and is dispersed by the stirrers into small bubbles. At the broth surface the bubbles merge with the gas in the headspace which leaves the reactor towards the offgas system. It should be realized that transfer of  $O_2$ ,  $CO_2$  and  $N_2$  does not only take place across the gas-liquid interface of the gas bubbles, but also at the

surface between the broth and the headspace. The mole fractions of O<sub>2</sub>, CO<sub>2</sub> and N<sub>2</sub> in the gas bubbles can then be described by the following mass balance equation (in which each term is expressed in m<sup>3</sup> of gas i per second):

$$V_{GB} \frac{dx_{GB,i}}{dt} = F_{G0} \cdot x_{G0,i} - F_{G1} \cdot x_{GB,i} - k_L a_{B,i} \cdot V_L \cdot \left( \frac{x_{GB,i}}{m_i} - c_{L,i} \cdot \frac{RT}{P} \right), \quad i = O_2, CO_2, N_2 \quad (1)$$

It should be noted that all volumetric gas flow rates and gas volumes are defined at the pressure and temperature in the reactor. In a comparable way, we can write for the headspace:

$$V_{GH} \frac{dx_{GH,i}}{dt} = F_{G1} \cdot x_{GB,i} - F_{G2} \cdot x_{GH,i} - k_L a_{H,i} \cdot V_L \cdot \left( \frac{x_{GH,i}}{m_i} - c_{L,i} \cdot \frac{RT}{P} \right), \quad i = O_2, CO_2, N_2 \quad (2)$$

And for the third gas compartment (condensor, tubing and pressure valve) we write:

$$V_{CT} \frac{dx_{CT,i}}{dt} = F_{G2} \cdot (x_{GH,i} - x_{CT,i}), \quad i = O_2, CO_2, N_2 \quad (3)$$

For the model, it is assumed that the volumes ( $V_{GB}$ ,  $V_{GH}$ ,  $V_{CT}$ ,  $V_L$ ), the pressure ( $P$ ) and the temperature ( $T$ ) are constant and that all gases behave as an ideal gas. Consequently, the total amount of gas in the system remains constant, which leads to the following coupling mass balance relation:

$$F_{G1} = F_{G0} - \sum_i k_L a_{B,i} \cdot V_L \cdot \left( \frac{x_{GB,i}}{m_i} - c_{L,i} \cdot \frac{RT}{P} \right) + F_w, \quad i = O_2, CO_2, N_2 \quad (4)$$

It may reasonably be assumed that the gas bubbles are saturated with water vapour and therefore

$$\frac{F_w}{F_{G1}} = \frac{P_w}{P} \quad (5)$$

which transforms equation 4 into

$$F_{G1} = \left( F_{G0} - \sum_i k_L a_{B,i} \cdot V_L \cdot \left( \frac{x_{GB,i}}{m_i} - c_{L,i} \cdot \frac{RT}{P} \right) \right) / \left( 1 - \frac{P_w}{P} \right), \quad i = O_2, CO_2, N_2 \quad (6)$$

If also the gas leaving the headspace is saturated with water vapour, then

$$F_{G2} = \left( \left( 1 - \frac{P_w}{P} \right) F_{G1} - \sum_i k_L a_{H,i} \cdot V_L \cdot \left( \frac{x_{GH,i}}{m_i} - c_{L,i} \cdot \frac{RT}{P} \right) \right) / \left( 1 - \frac{P_w}{P} \right), \quad i = O_2, CO_2, N_2 \quad (7)$$

### 2.1.4 Reactions, liquid phase balances, DO and pH probe

In aerobic cultivations, the micro-organisms in the broth consume  $O_2$  and produce  $CO_2$ . The dissolved  $CO_2$  can be converted into bicarbonate according to two spontaneous reactions [11,15-21]



For the current study in which a near-neutral pH region is considered, the concentration of carbonate can be neglected. The reaction rates are related by the chemical equilibrium constants  $K_1^*$  and  $K_2^*$  and the water dissociation constant  $K_w$  according to the following equations:

$$K_w = c_{L,H^+} \cdot c_{L,OH^-} \quad (10)$$

$$K_1^* = \frac{c_{L,HCO_3^-} \cdot c_{L,H^+}}{c_{L,CO_2}} = \frac{k_{1f}}{k_{1r}} \quad (11)$$

$$K_2^* = \frac{c_{L,HCO_3^-}}{c_{L,CO_2} \cdot c_{L,OH^-}} = \frac{k_{2f}}{k_{2r}} = \frac{K_1^*}{K_w} \quad (12)$$

The liquid flows into and out of the reactor are assumed to be equal for convenience. Taking also the mass transfer into account, the liquid phase balances for  $N_2$ ,  $O_2$ ,  $CO_2$  and bicarbonate can be written as:

$$V_L \frac{dc_{L,N_2}}{dt} = F_L \cdot (c_{L0,N_2} - c_{L,N_2}) + k_L a_{B,N_2} \cdot V_L \cdot \left( \frac{P \cdot x_{GB,N_2}}{RTm_{N_2}} - c_{L,N_2} \right) + k_L a_{H,N_2} \cdot V_L \cdot \left( \frac{P \cdot x_{GH,N_2}}{RTm_{N_2}} - c_{L,N_2} \right) \quad (13)$$

$$V_L \frac{dc_{L,O_2}}{dt} = F_L \cdot (c_{L0,O_2} - c_{L,O_2}) + k_L a_{B,O_2} \cdot V_L \cdot \left( \frac{P \cdot x_{GB,O_2}}{RTm_{O_2}} - c_{L,O_2} \right) + k_L a_{H,O_2} \cdot V_L \cdot \left( \frac{P \cdot x_{GH,O_2}}{RTm_{O_2}} - c_{L,O_2} \right) - OUR \cdot V_L \quad (14)$$

$$\begin{aligned}
V_L \frac{dc_{L,CO_2}}{dt} = & F_L \cdot (c_{L0,CO_2} - c_{L,CO_2}) + k_L a_{B,CO_2} \cdot V_L \cdot \left( \frac{P \cdot x_{GB,CO_2}}{RTm_{CO_2}} - c_{L,CO_2} \right) \\
& + k_L a_{H,CO_2} \cdot V_L \cdot \left( \frac{P \cdot x_{GH,CO_2}}{RTm_{CO_2}} - c_{L,CO_2} \right) + CER \cdot V_L \\
& - (k_{If} + k_{2f} \cdot c_{L,OH^-}) \cdot c_{L,CO_2} \cdot V_L + (k_{Ir} \cdot c_{L,H^+} + k_{2r}) \cdot c_{L,HCO_3^-} \cdot V_L
\end{aligned} \tag{15}$$

$$\begin{aligned}
V_L \frac{dc_{L,HCO_3^-}}{dt} = & F_L \cdot (c_{L0,HCO_3^-} - c_{L,HCO_3^-}) \\
& + (k_{If} + k_{2f} \cdot c_{L,OH^-}) \cdot c_{L,CO_2} \cdot V_L - (k_{Ir} \cdot c_{L,H^+} + k_{2r}) \cdot c_{L,HCO_3^-} \cdot V_L
\end{aligned} \tag{16}$$

DO probes are known to show a significant lag and their dynamic response is usually modelled well by the combination of a first order response and a pure time delay [9,22,23].

$$\frac{dc_{s,O_2}}{dt} = k_{DO} (c_{L,O_2} - c_{s,O_2}) \tag{17}$$

$$c_{DO}[t + d_{DO}] = c_{s,O_2}[t] \tag{18}$$

The hydronium concentration  $c_{L,H^+}$  can be obtained from the activity of hydronium ( $a_{L,H^+}$ ), which is measured by the pH probe. In this study, a pH probe was used with negligible lag, for which only a pure time delay needed to be taken into account (possibly due to time needed for data acquisition).

$$c_{L,H^+}[t] = \frac{a_{s,H^+,m}[t + d_{pH}]}{\gamma_{H^+}} \tag{19}$$

### 2.1.5 Offgas system impulse responses

The model equations presented above describe the relevant physical and (bio)chemical processes taking place in the reactor (broth and gas phases) and the initial part of the offgas system (up to point B in Figure 1) as well as the DO sensor output. To complete the model, it should also describe the output of the gas analyzer. That output is affected by the characteristics of the offgas analysis system, which in this study was a complex sequence of filters, valves, a dryer membrane and a pump, connected by tubing, all of which give rise to molecular dispersion of the analytes (i.e.  $O_2$  and  $CO_2$ ). Therefore, instead of trying to describe this part of the system by multiple ideal mixers with dead volumes, it was simply characterized in terms of its residence time distribution (RTD). At a constant gas flow, this part of the system is linear and time-invariant, and in that case the RTD is equal to the impulse response. In reality, there are small variations in the gas outflow due to gas production/consumption and transfer which cause time shifts (delays/advancements) in the

response. However, if the variation in the gas outflow is below 1%, then the time shifts are of sub-second order and can be neglected in the context of this study. The model output of the gas analyzer can then be obtained by convolving the model state variables  $x_{CT,O_2}$  and  $x_{CT,CO_2}$  (given by eq. 3) with their respective impulse responses.

$$x_{a,j}[t + d_{\text{gas}}] = \frac{x_{CT,j}[t]}{1 - \frac{P_w}{P}} \otimes E_j, \quad j = O_2, CO_2 \quad (20)$$

The parameter  $d_{\text{gas}}$  is the pure time delay corresponding to the initial part of the offgas system (up to point B in Figure 1), and is equal for  $O_2$  and  $CO_2$ . The expected time delay in the offgas system between point B and the analyzer is included in the impulse responses  $E_j$ . It should be noted that  $x_{a,j}$  gives the modelled analyzer output as mole fractions of the dried gas, whereas  $x_{CT,j}$  represents mole fractions of undried gas, as they occur until point B.

## 2.2 Identification of parameters and impulse responses

The aim of the model is to use it together with the measurements (DO, pH, offgas  $O_2$  and  $CO_2$ ) obtained during a perturbation experiment to reconstruct the course of the OUR and CER (see section 3.2.5). The model equations presented so far are sufficient to carry out this reconstruction calculation, except that its parameters and the offgas system impulse responses need to be identified beforehand.

### 2.2.1 Identification of the impulse responses of the offgas analysis system

The impulse responses for  $O_2$  and  $CO_2$  of the offgas analysis system have to be obtained from an identification experiment in which the analyzer response to known changes in the  $O_2$  and  $CO_2$  concentration in the flow at point B (see Figure 1) is recorded. Experimentally it is easiest to apply a step change in the concentrations, for example by changing from a (water vapour saturated) flow of nitrogen to a (water vapour saturated) flow of a defined gas mixture containing  $O_2$  and  $CO_2$ . The measured step response is then defined by (subscript m denotes the measured values)

$$F_j[t] = \frac{x_{a,j,m}[t]}{x_{a,j,m}[t_{\text{end}}]}, \quad j = O_2, CO_2 \quad (21)$$

$x_{a,j,m}[t_{\text{end}}]$  is the measured mole fraction at the end of the step experiment and is equal to the mole fraction in the defined gas mixture. Subsequently, a continuous function should be found which describes the measured step response function. Taking the first derivative of that function yields the impulse response function:

$$E_j[t] = \frac{dF_j[t]}{dt}, \quad j = O_2, CO_2 \quad (22)$$



### 2.2.2 Experimental conditions and physical parameters

A part of the model parameters is related to the applied experimental conditions and their values are set by the experimenter. Table 1 gives the conditions which are relevant for the model calculations of the particular glucose pulse experiment which is used as a case study in this chapter. Another set of parameters depends on these experimental conditions, especially on the temperature, on the ionic strength and on the composition of the broth. Empirical values of these parameters or functions describing how these parameters depend on the experimental conditions can be obtained from the literature. Table 2 shows this set of parameters with their values as used in the model calculations and the corresponding references.

**Table 1** Some experimental conditions of the perturbation experiment

Quantity	Value	Unit
$F_{G0}$	$33.3 \cdot 10^{-6}$	$\text{m}^3/\text{s}$ at normal conditions
$F_L$	$55 \cdot 10^{-9}$	$\text{m}^3/\text{s}$
$V_L$	$4.00 \cdot 10^{-3}$	$\text{m}^3$
$P$	$1.30 \cdot 10^5$	Pa
$T$	298.15	K
$x_{G0,O2}$	0.20950	mol/mol
$x_{G0,CO2}$	0.00045	mol/mol
$x_{G0,N2}$	0.79005	mol/mol

**Table 2** Used empirical parameter values taken or calculated from literature

Quantity	Value	Unit	References
$P_w$	$3.2 \cdot 10^3$	Pa	[24]
$K_w$	$1.2 \cdot 10^{-8}$	$\text{mol}^2/\text{m}^6$	[25]
$\gamma_{H^+}$	0.743	-	[26]
$m_{O2}$	33.31	-	[27], [28], [29]
$m_{CO2}$	1.166	-	[30], [28], [29]
$m_{N2}$	65.87	-	[27], [28], [29]
$k_{1f}$	0.03593	$\text{s}^{-1}$	[11]
$k_{2r}$	$40 \cdot 10^{-5}$	$\text{s}^{-1}$	[11]
$D_{O2}$	$2.317 \cdot 10^{-9}$	$\text{m}^2/\text{s}$	[31]
$D_{CO2}$	$1.920 \cdot 10^{-9}$	$\text{m}^2/\text{s}$	[32]
$D_{N2}$	$2.302 \cdot 10^{-9}$	$\text{m}^2/\text{s}$	[33]

For reasons given by Bloemen et al. [9], volumetric  $O_2$  mass transfer coefficients can best be obtained from measurements of the offgas  $O_2$  concentration and the dissolved  $O_2$  concentration in a steady state of a living (respiring) culture. In the currently developed model there are two coefficients, one for transfer between gas bubbles and broth and one for transfer between head space and broth. Unfortunately, without the simultaneous knowledge of the steady state  $O_2$  concentrations in the gas bubbles, the headspace and the liquid phase, it is not possible to identify both  $k_L a_{B,O_2}$  and  $k_L a_{H,O_2}$ . However, intuitively one can understand that  $k_L a_{B,O_2}$  should be much larger than  $k_L a_{H,O_2}$ , because the total surface area of the bubbles is significantly larger than the liquid surface. Therefore, in a steady state  $x_{GH,O_2}$  is only slightly smaller than  $x_{GB,O_2}$ , and the following approximation can be made:

$$x_{GB,O_2}^{ss} \approx x_{GH,O_2}^{ss} = x_{a,O_2,m}^{ss} \left( \frac{P - P_w}{P} \right) \quad (23)$$

With this approximation, the driving forces in the  $O_2$  transfer terms in equations 1 and 2 become equal. In this case an overall mass transfer coefficient,  $k_L a_{O_2}$ , can be defined as the sum of the two  $O_2$  mass transfer coefficients (for bubbles and headspace respectively):

$$k_L a_{O_2} = k_L a_{B,O_2} + k_L a_{H,O_2} \quad (24)$$

The combination of equation 1, 2, 23 and 24 and rearranging allows calculation of  $k_L a_{O_2}$  from steady state measurements:

$$k_L a_{O_2} = \frac{F_{G0} \cdot x_{G0,O_2} - F_{G2}^{ss} \cdot x_{GH,O_2}^{ss}}{V_L \cdot \left( \frac{x_{GH,O_2}^{ss}}{m_{O_2}} - c_{DO,m}^{ss} \frac{RT}{P} \right)} \quad (25)$$

Considering that transport of  $N_2$  via the liquid phase is negligible,  $F_{G2}^{ss}$  can be calculated from a  $N_2$  balance as:

$$F_{G2}^{ss} = F_{G0} \frac{(1 - x_{G0,O_2} - x_{G0,CO_2})}{(1 - x_{a,O_2,m}^{ss} - x_{a,CO_2,m}^{ss})(1 - P_w/P)} \quad (26)$$

In a dynamic state, the larger turnover time of the gas volume in the headspace compared to that of the total volume of the gas bubbles and the amount of gas-liquid mass transfer (which may be considerable) can cause the difference between  $x_{GB,i}$  and  $x_{GH,i}$  to become

much larger than in a steady state. Therefore, with the constraint of the value of their sum given by equations 24 and 25, a dynamic state offers the possibility to identify the individual values of  $k_L a_{B,O_2}$  and  $k_L a_{H,O_2}$ , which will be treated in section 2.2.3. For convenience, the fraction  $\alpha$  is introduced:

$$k_L a_{B,O_2} = \alpha \cdot k_L a_{O_2}, \quad 0 \leq \alpha \leq 1 \quad (27)$$

$$k_L a_{H,O_2} = (1 - \alpha) \cdot k_L a_{O_2}, \quad 0 \leq \alpha \leq 1 \quad (28)$$

The penetration film theory relates the overall volumetric mass transfer coefficients for  $CO_2$  and  $N_2$  to that of  $O_2$  according to:

$$k_L a_k = k_L a_{O_2} \sqrt{D_k / D_{O_2}}, \quad k = CO_2, N_2 \quad (29)$$

This relation is supported by experimental evidence presented by Kordač and Linek [34]. References for the values used for the diffusion coefficients are given in Table 2. The extent of chemical enhancement of  $O_2$  absorption and  $CO_2$  desorption due to respiration of biomass in the liquid boundary film with the gas phases, which affect the mass transfer coefficients, can be calculated [35,36]. For our system it was concluded that these effects are small and can be neglected in the model, but this may not be true if much higher biomass concentrations are used. Also the extent of the chemical enhancement of  $CO_2$  desorption due to dehydration of bicarbonate in the boundary film was calculated to be small and it is therefore neglected [37].

### 2.2.3 Parameter estimation

This leaves the following model parameters to be identified:  $V_{GB}$ ,  $V_{GH}$ ,  $V_{CT}$ ,  $K_1^*$ ,  $k_{DO}$ ,  $d_{DO}$ ,  $d_{pH}$ ,  $d_{gas}$  and  $\alpha$ . These parameter values can be obtained by fitting the dynamic response of the model to the measured dynamic response of the system to known changes in the input. A separate identification experiment has to be performed to obtain this measured response. Since the experimenter has no direct control over the model inputs OUR and CER, the identification experiment consists of applying changes to the inputs  $x_{G0,O_2}$  and  $x_{G0,CO_2}$ . Ideally, the identification experiment is performed with a living broth under exactly the same conditions, i.e. viscosity and dissolved compounds, as during the perturbation experiment, because these conditions affect the mass transfer coefficients, the solubilities of gases and the chemical equilibrium constants. In the case of *P. chrysogenum* this approach is not possible, because changes in especially the partial pressure of  $CO_2$  lead to (unknown) changes in the physiology and respiratory rates [38-40]. Therefore, the respiratory rates were made constant (and equal to zero) by inactivating the biomass prior to the

identification experiment by exposing the broth overnight to an anoxic atmosphere. It was assumed that this procedure had no significant effect on the relevant physical and chemical properties of the broth.

The chemical equilibrium constant  $K_1^*$  depends on the temperature and the specific composition of the broth, especially the concentration and charge of all the ions. In view of the complex composition of the broth,  $K_1^*$  can better be obtained by optimization than by calculation from empirical relations. However, identification of  $K_1^*$ , and also of  $d_{pH}$ , requires that the model gives the pH (or the hydronium activity  $a_{s,H^+}$ ) as an output rather than that the model uses the measured pH as an input, as was stated above (eq. 19). To allow the model to describe the pH as an output, it should also take into account the presence of buffering agents in the medium. The dominant buffer in many media, including the one used in this study, is that of the couple  $HPO_4^{2-}/H_2PO_4^-$ , with equilibrium constant  $K_p^*$ . The following equations should therefore be included in the model and replace eq. 19 for the purpose of parameter identification. Note that in this case the liquid flow is zero, because the identification experiment is performed on a dead, inactivated broth.

$$K_p^* = \frac{c_{L,HPO_4^{2-}} \cdot c_{L,H^+}}{c_{L,H_2PO_4^-}} = \frac{k_{pf}}{k_{pr}} \quad (30)$$

$$\begin{aligned} \frac{dc_{L,H^+}}{dt} = & k_{if} \cdot c_{L,CO_2} - k_{1r} \cdot c_{L,HCO_3^-} \cdot c_{L,H^+} + k_{2f} \cdot c_{L,CO_2} \cdot c_{L,OH^-} - k_{2r} \cdot c_{L,HCO_3^-} \\ & + k_{pf} \cdot c_{L,H_2PO_4^-} - k_{pr} \cdot c_{L,HPO_4^{2-}} \cdot c_{L,H^+} \end{aligned} \quad (31)$$

$$\frac{dc_{L,HPO_4^{2-}}}{dt} = k_{pf} \cdot c_{L,H_2PO_4^-} - k_{pr} \cdot c_{L,HPO_4^{2-}} \cdot c_{L,H^+} \quad (32)$$

$$c_{L,H_2PO_4^-} = c_{L,phosph,tot} - c_{L,HPO_4^{2-}} \quad (33)$$

$$a_{s,H^+} = \gamma_{H^+} \cdot c_{L,H^+} \quad (34)$$

For the same reason as for  $K_1^*$ , the value of  $K_p^*$  has to be obtained by optimization. Since equations 32 and 33 describe fast (de)protonation reactions,  $k_{pf}$  can simply be chosen such that  $k_{pf} \gg k_{1f}$ . The total concentration of phosphate  $c_{L,phosph,tot}$  can be assumed equal to the concentration in fresh medium, because only a very small amount of phosphate ends up in biomass.

## 3 Material and methods

### 3.1 Experimental procedures

#### 3.1.1 Experimental setup

The experiments were carried out in a 6.8 L fermentor (Applikon Biotechnology B.V., Schiedam, The Netherlands) with 4 L working volume. Air or defined gas mixtures (from cylinders) were sparged at 2.00 Ln/min (5.35 mol/h) through the reactor which was stirred by two 6-bladed Rushton-type impellers at 500 rpm. The reactor was equipped with three baffles and electrodes for pH (type: InPro3030/120, Mettler-Toledo, Switzerland) and dissolved oxygen (type: AppliSens, Applikon Biotechnology B.V., Schiedam, The Netherlands). The reactor temperature was controlled at 25 °C. Offgas left the reactor via a condenser (5 °C), a cotton filter and a pressure valve, which maintained an overpressure of 0.30 bar in the reactor, before it arrived in a valve cabinet/manifold (constructed in-house) which was controlled by a MUX multiplexer unit (B. Braun Biotech, Germany). The valve cabinet was designed to receive multiple gas streams (offgas from several reactors and reference air) and connect them one by one, via a drying module (Perma Pure LLC, USA), to a gas analyzer (NGA 2000, Rosemount, USA). From each gas stream a limited flow of 0.200 Ln/min was passed to the analyser via a pump, the surplus was vented to the environment via an overflow. Also all non-measured gas streams were vented to the environment.

#### 3.1.2 Fermentation and glucose pulse perturbation

A strain of *Penicillium chrysogenum* (DS17690) with a high penicillin yield was kindly donated by DSM Anti-Infectives (Delft, The Netherlands).

A glucose-limited aerobic chemostat culture, aerated at 2.00 Ln/min (5.35 mol/h), with a biomass concentration of  $\pm 5.7$  g<sub>DW</sub>/L was grown at a dilution rate of 0.05 h<sup>-1</sup> and at a controlled pH of 6.5 (by automatic addition of 4 M KOH) as described [41]. The physiological behaviour of this strain under these conditions has been described elsewhere [14,41-43].

After 230 h of chemostat cultivation, the culture was perturbed by the addition of 16 mL of a 62.5 g/L glucose solution, while at the same moment the fresh medium feed was stopped. This pulse raised the glucose concentration from a negligible amount to 250 mg/L. Sensor data (including pH, DO, offgas O<sub>2</sub> and CO<sub>2</sub>) were acquired and logged approximately every second over a time period stretching from several hundred seconds before the perturbation until 500 seconds after the perturbation.

### 3.1.3 Identification experiments

After the perturbation experiment, the medium feed and pH control were stopped and the reactor was sparged with N<sub>2</sub> for several minutes to remove all O<sub>2</sub> and to inactivate the biomass. The stirrer speed was then reduced to 100 rpm and the reactor was kept in the N<sub>2</sub> atmosphere overnight at an overpressure of  $\pm 0.3$  bar by clamping off the gas in- and outlet. The following day, the broth was re-aerated (stirring at 500 rpm) and the offgas measurements were compared to reference air to confirm absence of respiratory (metabolic) activity.

The first of two identification experiments was then carried out by alternatingly sparging the reactor with one of two defined gas mixtures (Linde Gas Benelux B.V., Dieren, The Netherlands), while logging the sensor measurements every second. The point at which the gases were switched is indicated in Figure 1 by the letter A. An in-house built device controlling two electric valves was used to instantly switch from one gas to the other without interruption of the flow. The first gas consisted of 20.975% O<sub>2</sub>, 2.975% CO<sub>2</sub> and 76.050% N<sub>2</sub>, the second consisted of 20.416% O<sub>2</sub>, 1.956% CO<sub>2</sub> and 77.628% N<sub>2</sub>. During this experiment the conditions in the reactor were the same as during the fermentation, except that the pH was not controlled and there was no inflow of liquid medium, nor outflow of broth. To monitor drift of the sensors, care was taken that apart from measurements of the transient states, also sufficient measurements were taken of the steady states corresponding to the two gases and that the experiment ended with the steady state of the first gas.

In the second identification experiment, the response of the offgas system was measured by alternating the composition of the gas flow at point B in Figure 1, i.e. after the pressure valve. In this case, step changes were made between the defined gas mixture consisting of 20.975% O<sub>2</sub>, 2.975% CO<sub>2</sub> and 76.050% N<sub>2</sub> and pure N<sub>2</sub>, which had both been humidified by passing them through a stirred reactor with water (25 °C) and a condenser (5 °C) before they arrived at point B. The flow rate of the dry gases before humidification was 2.00 Ln/min.

## 3.2 Calculatory procedures

### 3.2.1 Resampling and data pre-processing

All measurements of the perturbation and identification experiments were resampled at 1 second intervals by linear interpolation of the raw data. Furthermore, the data were corrected for offsets, atmospheric pressure changes and linear trends that could be attributed to drift of the sensors.

### 3.2.2 Impulse responses of the offgas analysis system

The response in terms of the measured  $O_2$  and  $CO_2$  concentration to one of the step changes from  $N_2$  to the defined gas mixture was normalized to the respective concentrations in the defined gas mixture. Subsequently, a continuous function was fitted to these normalized step responses. In this case, the function consisted of the product of a generalized extreme value cumulative distribution function with a function of the form

$$f(t) = 1 - a_1 \times \exp(a_2(t - a_3)) - b_1 \times \exp(b_2(t - b_3)) \quad (35)$$

The impulse response  $E_j$  was then found as the first derivative of the continuous function. The discrete time impulse response was found by sampling the continuous response at a discrete interval, which was 1 second in this case.

### 3.2.3 Parameter estimation

The parameters  $V_{GB}$ ,  $V_{GH}$ ,  $V_{CT}$ ,  $K_1^*$ ,  $K_p^*$ ,  $k_{DO}$  and  $\alpha$  were estimated by fitting the model to the first identification data set, using these seven parameters as the degrees of freedom. The objective function value that had to be minimized was determined as follows. First, after each simulation the arrays of  $x_{CT,O_2}$  and  $x_{CT,CO_2}$  were convolved with their respective offgas system impulse responses to obtain the modelled gas analyzer data (not yet corrected for the time-shift  $d_{gas}$ ; see eq. 20). Then, for a range of integer values for the time-shifts  $d_{DO}$ ,  $d_{pH}$  and  $d_{gas}$ , the sum of squared differences between measured and time-shifted simulated sensor data, weighted by the respective variance of the measurements, was calculated and the lowest weighted sum of squares from each range was selected. The value of the objective function was obtained by summing the three (for DO, pH and gas measurements) selected weighted sums of squares.

### 3.2.4 Deconvolution of impulse response from glucose pulse data

The offgas measurements carried out during the glucose pulse (perturbation) experiment were deconvolved by the offgas system impulse responses using a water level regularization scheme [44]. Shortly, the offgas measurements and the impulse responses for  $O_2$  and  $CO_2$  were converted to their Fourier transform (FT). Then, the amplitudes of frequencies in the impulse response FT which were lower than a threshold “water level” were replaced by the water level amplitude. Finally the offgas measurement FT was divided by the adjusted impulse response FT and the deconvolved signal was obtained by taking the inverse FT.

### 3.2.5 Reconstruction by Kalman filtering

The reconstruction calculation was performed following the same procedure as described by Bloemen et al. [9]. For this, the continuous-time, time-invariant, nonlinear model described by equations 1-19 was replaced by a discrete-time, time-varying, linear model (obtained by linearization and discretization) and expanded with state equations for OUR and CER. Using the measured pH (corrected by the time-shift  $d_{\text{pH}}$ ) as input to the model and the deconvolved offgas measurements as observations, the OUR and CER were reconstructed by Extended Kalman Filtering with correction by the Bryson-Frazier formulas [45].

## 4 Results and discussion

Before it is possible to reconstruct the OUR and CER from the measurements of a perturbation experiment, it is necessary to obtain a model which is able to describe accurately the transport processes and reactions of  $\text{O}_2$  and  $\text{CO}_2$  taking place in the system. As explained in the modelling section 2, the system was divided into two parts for this purpose: one part models the processes taking place in the bioreactor, in terms of a system of ODEs, and a second part is described in terms of the impulse response of the offgas system. Below, the results of the identification of the offgas system impulse responses are presented first. Then the results of the parameter identification are shown and finally the reconstruction results for the perturbation experiment are presented.

### 4.1 Impulse responses of the offgas analysis system

For the identification of the offgas system impulse response, a number of step changes between a humidified  $\text{N}_2$  flow and a humidified flow of a defined gas mixture containing  $\text{O}_2$ ,  $\text{CO}_2$  and  $\text{N}_2$  were applied at the entrance of the offgas system, that is, directly after the pressure valve at point B indicated in Figure 1. The measured mole fractions of  $\text{O}_2$  and  $\text{CO}_2$  are shown in Figure 2a and b, respectively.

The measured responses to the last step change from  $\text{N}_2$  to defined gas mixture, applied at  $t = 6177$  s, were normalized and approximated with continuous functions to describe the  $\text{O}_2$  and  $\text{CO}_2$  step responses. The form of the continuous functions used in this particular case is given in section 3.2.2 and their parameters were obtained by fitting. Taking the first time derivative of the (normalized) functions yielded the impulse responses ( $E_{\text{O}_2}(t)$  and  $E_{\text{CO}_2}(t)$ ), which are shown in Figure 2c (only the first 100 seconds) and 2d (zoomed in on the vertical axis). It follows from these two plots that the largest part of the gas entering the offgas system had a residence time of less than one hundred seconds, but a small part of the gas



had a residence time of several hundreds of seconds. These long residence times were the result of the various units, such as valves, filters and a membrane dryer, aligned in the offgas system. To demonstrate the accuracy of the determined impulse responses, their convolution with the applied step changes is also plotted in Figure 2a and b for comparison to the measured step responses.

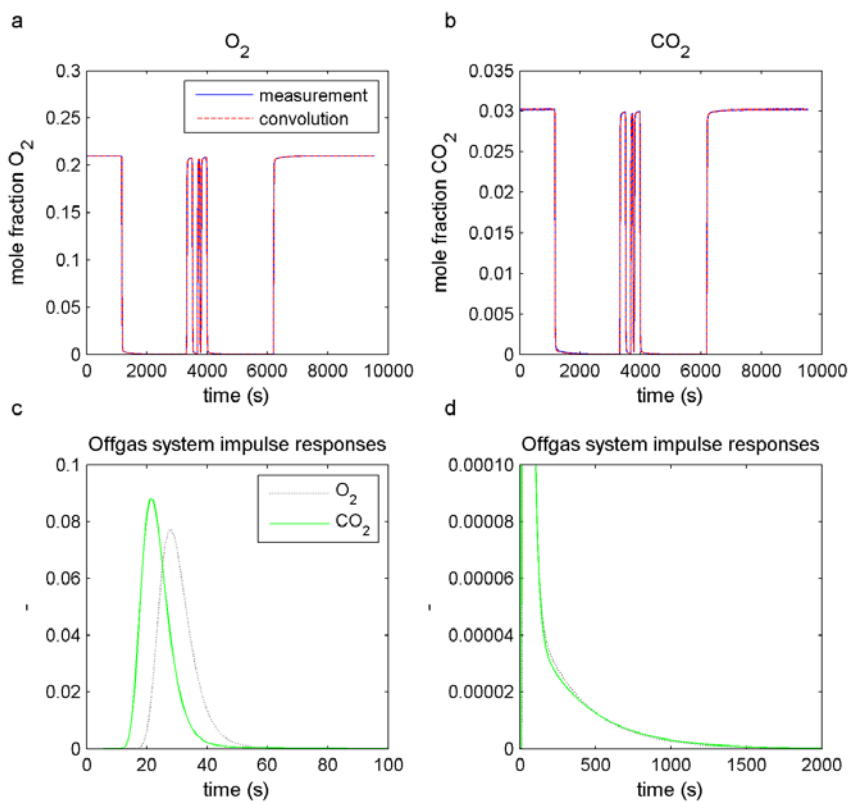


**Figure 2** Offgas system response. (a)  $O_2$  and (b)  $CO_2$  mole fraction measured by the gas analyzer in response to step changes in the input concentrations of  $O_2$  and  $CO_2$  at the beginning of the offgas system (blue line), and the convolution of the impulse response with the input mole fractions (red dashed line). (c) The offgas system impulse responses for  $O_2$  ( $E_{O_2}(t)$ ) and  $CO_2$  ( $E_{CO_2}(t)$ ), limited to the first 100 seconds. (d) Offgas system impulse responses for  $O_2$  ( $E_{O_2}(t)$ ) and  $CO_2$  ( $E_{CO_2}(t)$ ), zoomed in on the vertical axis.

Since the  $O_2$ -measurement cell of the combined  $O_2/CO_2$  analyzer was placed in series with (behind) the  $CO_2$ -measurement cell, the average response time of the  $O_2$  measurement was approximately 7 seconds longer than that of  $CO_2$ , as can be seen from Figure 2c.

Furthermore, this plot shows that for the largest part of the responses, the configuration of the offgas system caused a dispersion in the response of several tens of seconds.

## 4.2 Parameter identification

The overall oxygen transfer coefficient,  $k_L a_{O_2}$ , can be obtained from steady state measurements using equation 25. To obtain a reliable value for the parameter  $k_L a_{O_2}$ , an average was calculated, using equation 25, from measurements obtained from several steady state chemostat cultures carried out under identical conditions. This resulted in  $k_L a_{O_2} = 0.139 \text{ s}^{-1}$ .

The remaining parameters were obtained by fitting the model to the measured response of the identification experiment. Figure 3 shows this measured response in terms of the sensor data (offgas  $O_2$ , offgas  $CO_2$ , DO and pH ) as well as the modelled response for the entire time range of the identification experiment; the residuals between the measurements and the model output are plotted on the right-hand side of Figure 3. It is clear from these plots that a good fit was obtained for the offgas mole fractions and the pH. The steady states of the DO probe are also well described, but the transient periods of the DO measurement are not captured well by the model (see Figure 3). Possibly, the first order model by which the probe response was modelled is too simple to describe the response to the relatively small changes in the dissolved  $O_2$  concentration.

The optimized parameters are given by the numbers in the first column of Table 3. Seven parameters were optimized to fit the model. Although this may seem to be a relatively high number, the comparison of the residuals with the estimated standard deviations of the measurements (plots on the right-hand side of Figure 3) shows that still not all of the behaviour of the measured signals is captured by the model, especially not for  $CO_2$  and DO.

The following remarks can be made with respect to the optimized values in the first column of Table 3.  $V_{GB}$  is optimized to a value of 0.389 L, which would mean that the gas hold-up in the reactor amounts approximately 9.7%, which is not unrealistic for an intensely stirred lab-scale reactor aerated at 0.5 vvm. Although the parameter  $V_{GH}$  (as well as  $V_{CT}$ ) is a non-physical parameter of the model, it is reassuring that the sum of the (optimized) parameters,  $V_L$ ,  $V_{GB}$  and  $V_{GH}$  amounts 6.9 L, which is very close to the real reactor volume of 6.8 L. The parameter  $V_{CT}$  is optimized to a very low value, which means that for this particular setup this parameter could also be omitted. The parameter  $\alpha$  is optimized to 0.974, which means that  $k_L a_{B,i}$  is 38 times larger than  $k_L a_{H,i}$ . This is in line with previously made

assumption that the coefficient for mass transfer between broth and headspace is much smaller than that for mass transfer between broth and bubbles.

**Table 3** Estimated parameter values for the complete model, the model without bicarbonate reactions, and the model without mass transfer between broth and headspace

Parameter	Estimated values for complete model	Estimated values without CO <sub>2</sub> /bicarbonate interconversion	Estimated values without headspace mass transfer	Unit
$V_{GB}$	$3.89 \cdot 10^{-4}$	$4.68 \cdot 10^{-4}$	$9.47 \cdot 10^{-4}$	m <sup>3</sup>
$V_{GH}$	$2.52 \cdot 10^{-3}$	$4.22 \cdot 10^{-3}$	$1.98 \cdot 10^{-3}$	m <sup>3</sup>
$V_{CT}$	$1.02 \cdot 10^{-6}$	$6.84 \cdot 10^{-7}$	$1.08 \cdot 10^{-6}$	m <sup>3</sup>
$k_{DO}$	$2.35 \cdot 10^{-2}$	$1.78 \cdot 10^{-2}$	$2.25 \cdot 10^{-2}$	s <sup>-1</sup>
$K_1^*$	$7.25 \cdot 10^{-4}$	Not applicable	$7.50 \cdot 10^{-4}$	mol/m <sup>3</sup>
$K_p^*$	$1.54 \cdot 10^{-4}$	Not applicable	$1.52 \cdot 10^{-4}$	mol/m <sup>3</sup>
$\alpha$	0.974	0.965	1 (constraint)	-
$d_{DO}$	10	10	10	s
$d_{pH}$	10	Not applicable	6	s
$d_{gas}$	9	5	5	s
Value of objective function including contribution from pH	438521	Not applicable	1450488	-
Value of objective function excluding contribution from pH	414192	45387624	1398713	-

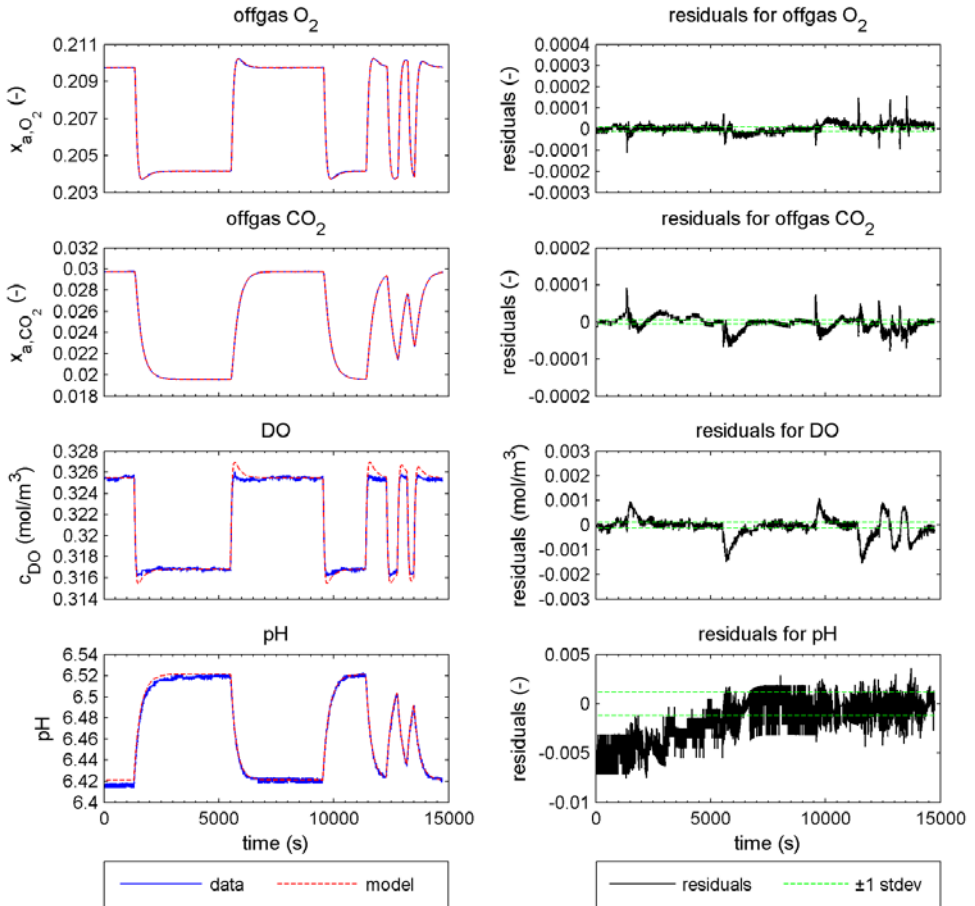


**Figure 3** Fit of the optimized complete model to the measured identification data. Left: measurements and model output. Right: residuals of the difference between measurements and model output.

Based on extensive potentiometric measurements in dilutions of seawater, Millero et al. [46] presented an empirical equation to calculate  $K_1^*$  from temperature and ionic strength. For our culture conditions, this equation gives a value of  $(8.50 \pm 0.11) \cdot 10^{-4} \text{ mol/m}^3$ , which is higher than our optimized value of  $7.25 \cdot 10^{-4} \text{ mol/m}^3$ . The reason for the difference may be the much more complex composition of the broth, the presence of other ionic species with higher charges and interactions of ions with charged macromolecules in the broth.

### 4.3 Importance of the bicarbonate reactions

The most important difference of the currently developed model with the model presented in Bloemen et al. [9] is the incorporation of reactions for the inter conversion of dissolved  $\text{CO}_2$  and bicarbonate. To demonstrate the relevance of this extension, the model was optimized while taking out these reactions. The optimized parameter values in this condition are given in the second column of Table 3 and Figure 4 shows the optimized model output in comparison to the measured identification data. It is clear from the plot of the offgas  $\text{O}_2$ , as well as from the plots of the residuals (right-hand side of Figure 4), that this limited model is unable to fit the measured system response. The bad fit is also expressed in the objective function value (corrected to include only contributions from residuals for offgas  $\text{O}_2$ , offgas  $\text{CO}_2$  and DO, but excluding the contribution from pH), which is about 100 times larger than that obtained for the full model which includes the bicarbonate reactions (see Table 3). The parameter  $V_{\text{GH}}$  (corresponding to the headspace volume) is increased in the optimization to 4.22 L to fit the offgas  $\text{CO}_2$  measurements, but this is an unrealistically large value in view of the total reactor volume of only 6.8 L and a broth volume of 4.0 L. These results demonstrate that at near-neutral pH values it is important to include bicarbonate reactions in order to obtain a model which can accurately fit the measured response.

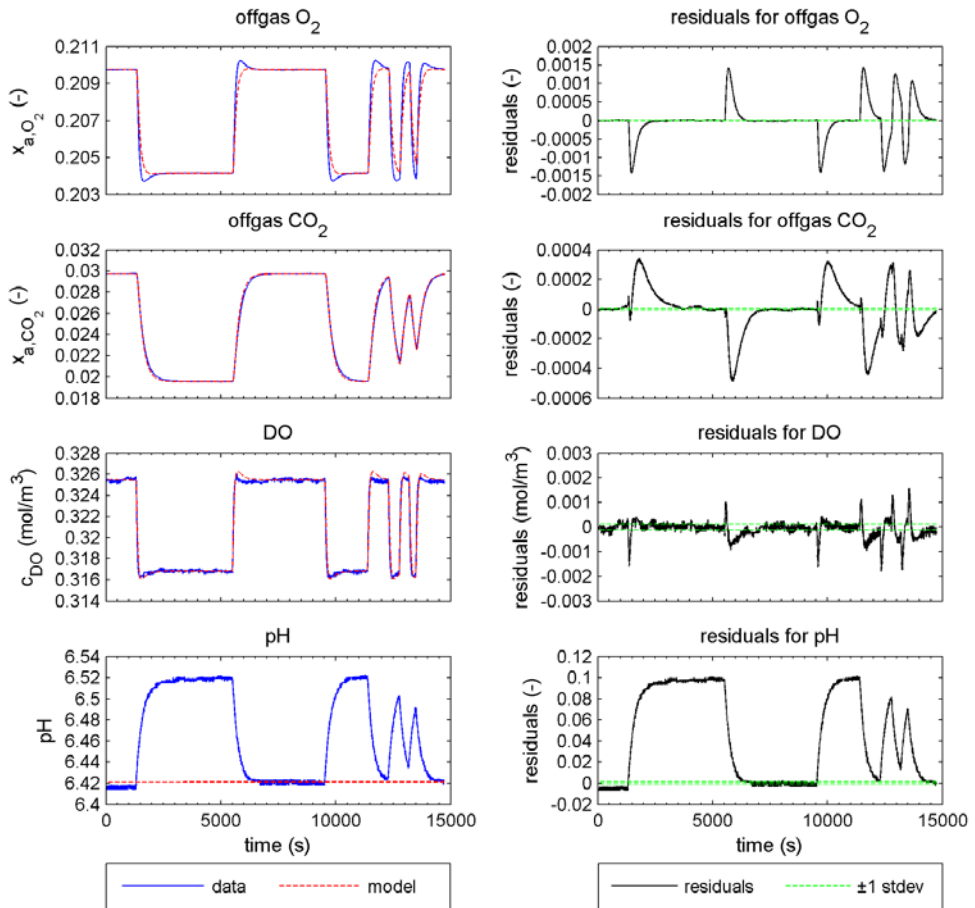


**Figure 4** Fit of the optimized model without bicarbonate reactions to the measured identification data. Left: measurements and model output. Right: residuals of the difference between measurements and model output.

#### 4.4 Importance of mass transfer between broth and head space

One specific aspect of the current model (with respect to other bioreactor models) is the incorporation of mass transfer terms for gas exchange between headspace and broth, apart from transfer between gas bubbles and broth. To demonstrate the importance of these additional mass transfer terms, the model was also optimized without the mass transfer between headspace and broth (by setting  $\alpha$  to 1). These optimization results are shown in Figure 5. The optimized parameter values are given in the third column of Table 3. It follows from a comparison of the residual plots obtained for the model without the mass transfer between headspace and broth (right-hand side of Figure 5) with the residual plots

of the full model (right-hand side of Figure 3) that the reduced model fits the measurements less well compared to the full model. This is also expressed in a much larger value of the objective function (Table 3). For this reduced model, the sum of the broth volume  $V_L$ , the bubble volume  $V_{GB}$  and headspace volume  $V_{GH}$  is 6.9 L, which is close to the real reactor volume of 6.8 L. However, a bubble volume  $V_{GB}$  of 0.947 L would mean that the gas hold-up is 24%, which is completely unrealistic. Clearly, the incorporation of mass transfer between broth and headspace allows the model to fit the measured response much more accurate and also makes the model description much more realistic.

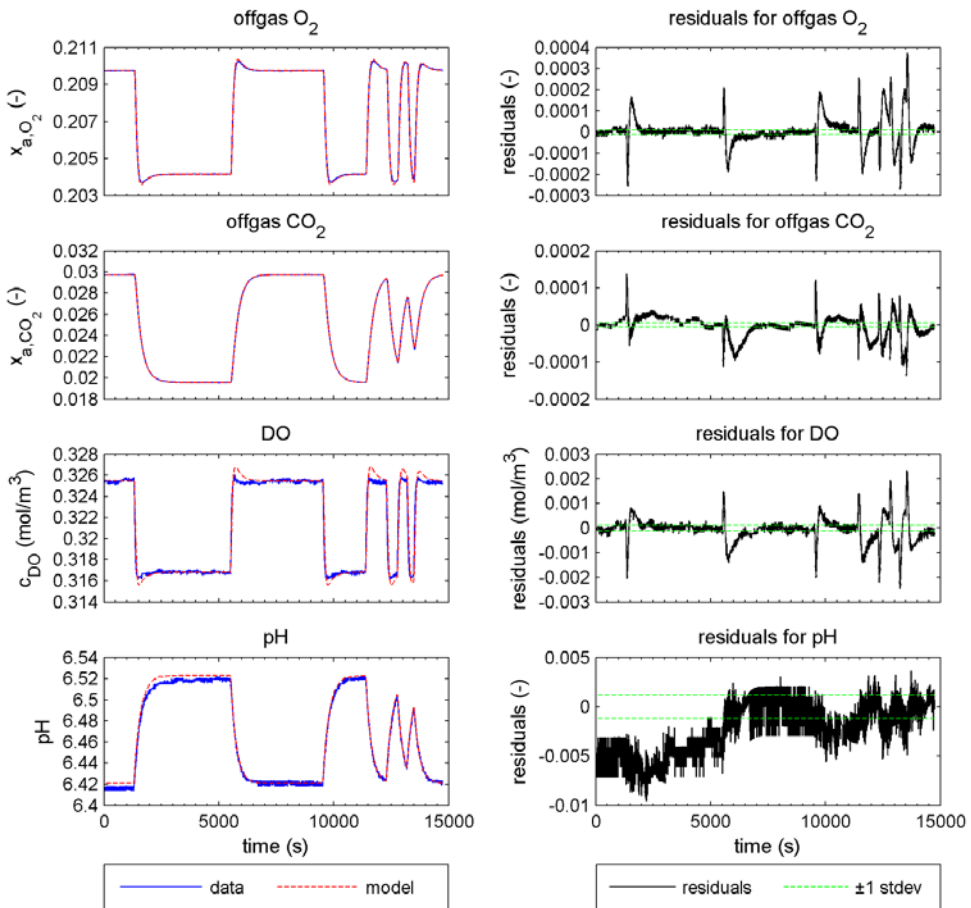


**Figure 5** Fit of the optimized model without gas transfer between broth and headspace to the measured identification data. Left: measurements and model output. Right: residuals of the difference between measurements and model output.

## 4.5 Reconstruction results

With all the parameters of the complete model identified, it is possible to use the model to make a reconstruction calculation of the OUR and CER during the dynamic condition of a perturbation experiment. In this case, a glucose-limited chemostat culture of *P. chrysogenum* was perturbed by a sudden increase of the extracellular glucose concentration (glucose pulse).

The reconstruction calculation was performed by means of Kalman filtering, for which the continuous-time nonlinear time-invariant model (the system of ODEs) was linearized (at every time step) and discretized. Furthermore, the offgas system impulse responses were deconvolved from the offgas measurements, because the convolution cannot be combined with the Kalman filter algorithm.

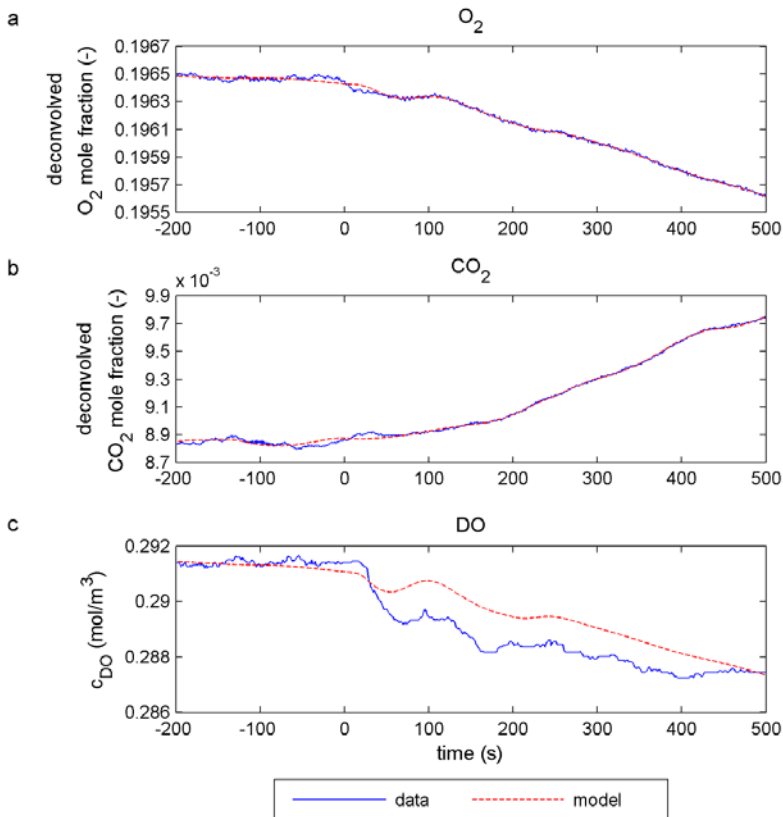


**Figure 6** Measured and reconstructed data. The glucose pulse was applied at  $t = 0$  s. a: deconvolved  $O_2$  offgas measurements and reconstructed output. b: deconvolved  $CO_2$  offgas measurements and reconstructed output. c: dissolved  $O_2$  concentration measurements and reconstructed output.



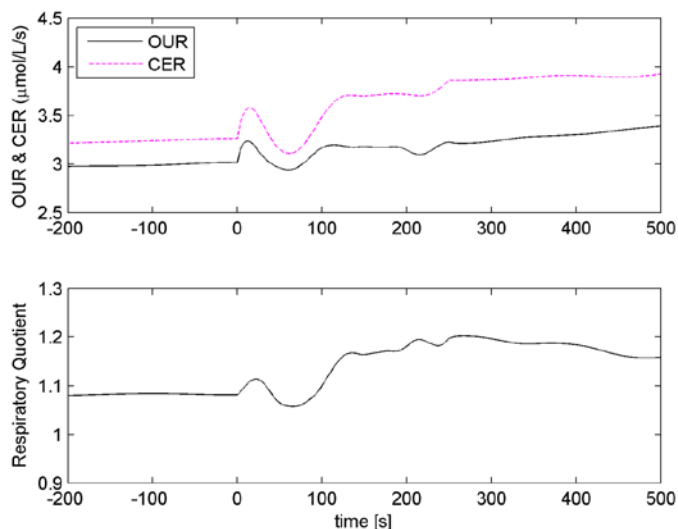


**Figure 7** Reconstructed OUR, CER and RQ. The glucose pulse was applied at  $t = 0$  s.

In principle, the observation vector, which is used to update the predicted model state (and in that way calculate the OUR and CER), can contain the DO measurements and the deconvolved offgas measurements for  $O_2$  and  $CO_2$ . However, it was observed that the optimized model did not fit the measured DO responses well (see Figures 3-5). Therefore, for this case, the DO measurements were not included in the observation vector, which thus only contained the deconvolved offgas measurements. The course of the DO was then calculated as one of the state variables according to the model, but the actual DO measurements were not used for the reconstruction calculation of the OUR and CER.

The (deconvolved) measurements and the reconstructed sensor data are plotted in Figure 6, and the reconstructed OUR, CER and respiratory quotient (RQ) in Figure 7. These plots show that the metabolic response to the sudden situation of glucose excess is very moderate in terms of the change in the respiratory rates, compared to the response of for example *S. cerevisiae* [9,10]. The plots show a few interesting points:

- Both the OUR and the CER increase over the first 30 seconds and then decrease until 70-90 seconds before they increase again. The concerted way by which the two rates change can be understood from the metabolic coupling of the rates via production and consumption of NADH in the TCA-cycle, and it is reassuring that the information for these concerted rate changes is also enclosed in the relatively small concentration changes of the offgas measurements.

- The decrease in the O<sub>2</sub> and the increase in the CO<sub>2</sub> mole fractions from 0 to 500 seconds is approximately equal (about 0.0009), but because of the higher solubility of CO<sub>2</sub> and the conversion of a part of the produced CO<sub>2</sub> to bicarbonate, the relative increase of the CER is higher than that of the OUR. Therefore the respiratory quotient increases from 1.08 during the steady state to about 1.18 towards the end of the experiment.
- The DO data are not well reconstructed, which was expected because it was already observed from the optimization results that the model didn't describe the DO-probe dynamics well. Nevertheless, some qualitative characteristics of the measured and the reconstructed DO data do match, such as the initial decrease after the glucose pulse is given and a peak at around 100 seconds. It is well possible that the steeper decrease in the measured DO (compared to the reconstructed DO) is caused by a slight decrease of the overpressure in the reactor due to the withdrawal of broth samples during the experiment: if the overpressure drops from 0.300 to 0.295 bar, then the DO drops by about 0.0018 mol/m<sup>3</sup>.

#### 4.6 Advantages and limitations of the model

Both Spérandio and Paul [12] and Kovács et al. [13] recognized the importance to incorporate the reactions describing the hydration of CO<sub>2</sub> and dehydration of bicarbonate in their models used to calculate the CER. Unfortunately, their models contain a number of inaccuracies which make them unsuitable to reconstruct the CER at short time scales (up to several minutes). First, they don't account for the change of the gas flow while it travels as bubbles through the liquid phase as a result of the gas transfer to (O<sub>2</sub>) and from (CO<sub>2</sub>) the liquid phase, like our model does in equations 6 and 7. This transfer can be considerable and therefore changes the gas flow rate. For this reason, it is important to model the fluxes of all the major constituents of the gas flow simultaneously, so O<sub>2</sub>, CO<sub>2</sub> and N<sub>2</sub>. Furthermore, effects of the presence of cells and spent medium components on the mass transfer coefficient were not taken into account by Kovács et al. [13], because it was determined in water instead of broth. Moreover, the delay time and the dispersion of gas in the offgas system were neglected by Spérandio and Paul [12] and Kovács et al. [13]. Finally, mass transfer between headspace and broth was not included in their models.

Soons et al. used monitoring of the offgas O<sub>2</sub> concentration to reconstruct OUR for online control of the medium feed for biomass growth [47]. They had to model the offgas system to correct for dispersion and delay in the measurements, especially because of the volume of the pilot-scale bioreactor with a large headspace. Compared to our approach, the

modelling of the offgas system was relatively simple, but our approach is probably too laborious to base an online control strategy on. Of course, our approach is meant as a research tool to facilitate the study of single bioreactor cultures, rather than an online control algorithm.

Nedbal et al. developed a model describing the CO<sub>2</sub> fluxes in algal cultures to study the effect of respiration and photosynthesis on dissolved CO<sub>2</sub> levels and CO<sub>2</sub> concentration in the offgas [48]. The model was used to simulate the effect of respiration and photosynthesis, but a reconstruction of the rates for uptake and release of CO<sub>2</sub> and bicarbonate from the measurements was not attempted. Our algorithm could be used for that and could be valuable in combination with other metabolic measurements, such as nutrient uptake, to study the metabolism related to these processes in algal systems.

## 5 Conclusion

An adapted model was developed which can be used to reconstruct the OUR and CER of microbial cultures growing at near-neutral pH levels and under dynamic conditions. The most prominent features of the model are that it includes the description of the inter conversion of dissolved CO<sub>2</sub> and bicarbonate and the exchange of gases by mass transfer between broth and headspace, in addition to the transfer between broth and submerged gas bubbles. It was shown that this model is able to fit the dynamic response of an identification experiment much better compared to models without the two mentioned features and its estimated parameter values seem realistic. The optimized model was successfully used to reconstruct the highly dynamic respiratory rates of a chemostat culture of *P. chrysogenum* perturbed by a glucose pulse.

## Chapter-specific list of symbols

$\alpha$	fraction	(-)
$\gamma_{H^+}$	hydronium activity constant	(-)
$a_{s,H^+}$	hydronium activity	(mol/m <sup>3</sup> )
CER	carbon dioxide evolution rate	(mol/m <sup>3</sup> /s)
$c$	molar concentration	(mol/m <sup>3</sup> )
$D$	diffusion coefficient	(m <sup>2</sup> /s)
$d_{DO}$	pure time delay for DO probe model	(s)
$d_{gas}$	pure time delay for offgas	(s)
$d_{pH}$	pure time delay for pH probe model	(s)
$E[t]$	impulse response function	(-)
$F$	volumetric flow rate	(m <sup>3</sup> /s)
$F[t]$	step response function	(-)
$K_1^*$	chemical equilibrium constant for hydration reaction of CO <sub>2</sub>	(mol/m <sup>3</sup> )
$K_2^*$	chemical equilibrium constant for reaction of CO <sub>2</sub> and hydroxide	(m <sup>3</sup> /mol)
$K_p^*$	chemical equilibrium constant for deprotonation of dihydrogenphosphate	(mol/m <sup>3</sup> )
$K_w$	water dissociation constant	(mol <sup>2</sup> /m <sup>6</sup> )
$k_{DO}$	first order rate constant for DO probe model	(s <sup>-1</sup> )
$k_{L,a_i}$	overall volumetric mass transfer coefficient	(s <sup>-1</sup> )
$k_{L,a_{B,i}}$	volumetric bubbles-broth mass transfer coefficient	(s <sup>-1</sup> )
$k_{L,a_{H,i}}$	volumetric headspace-broth mass transfer coefficient	(s <sup>-1</sup> )
$k_{1f}$	forward reaction rate constant	(s <sup>-1</sup> )
$k_{1r}$	backward reaction rate constant	(s <sup>-1</sup> ·m <sup>3</sup> /mol)
$k_{2f}$	forward reaction rate constant	(s <sup>-1</sup> ·m <sup>3</sup> /mol)
$k_{2r}$	backward reaction rate constant	(s <sup>-1</sup> )
$k_{pf}$	forward reaction rate constant	(s <sup>-1</sup> )
$k_{pr}$	backward reaction rate constant	(s <sup>-1</sup> ·m <sup>3</sup> /mol)
$L$	litre	
$Ln$	normal litre	
$m_i$	partition coefficient of $i$	(-)
OUR	oxygen uptake rate	(mol/m <sup>3</sup> /s)
$P$	total pressure in the reactor	(Pa)
$P_w$	water vapour pressure	(Pa)

R	universal gas constant	(J/mol/K)
T	temperature in reactor	(K)
t	time	(s)
V	volume	(m <sup>3</sup> )
x	mole fraction	(-)
⊗	denotes convolution operation	

*Subscripts*

a	offgas analyzer
CO <sub>2</sub>	carbon dioxide
CT	model compartment related to condenser, tubing and valve
G0	gas in the flow entering the bioreactor
G1	gas in the flow from gas bubbles to headspace
G2	gas in the flow from headspace to condenser and rest of the offgas system
GB	model compartment related to gas bubble phase
GH	model compartment related to gas headspace
H <sup>+</sup>	hydronium ion
HCO <sub>3</sub> <sup>-</sup>	bicarbonate ion
H <sub>2</sub> PO <sub>4</sub> <sup>-</sup>	dihydrogen phosphate
HPO <sub>4</sub> <sup>2-</sup>	monohydrogen phosphate
i, j, k	type of gas (O <sub>2</sub> , CO <sub>2</sub> , N <sub>2</sub> )
0	entering the reactor (via liquid phase or gas bubble phase)
L	liquid phase (broth)
L0	liquid in the medium flow into the bioreactor
m	measured value
N <sub>2</sub>	nitrogen
OH <sup>-</sup>	hydroxide ion
O <sub>2</sub>	oxygen
s	sensor
w	water (vapour)

*Superscripts*

+	positive charge
-	negative charge
ss	steady state

## References

- [1] M. De Mey, H. Taymaz-Nikerel, G. Baart, H. Waegeman, J. Maertens, J.J. Heijnen, and W.M. van Gulik, Catching prompt metabolite dynamics in *Escherichia coli* with the BioScope at oxygen rich conditions, *Metab. Eng.* 12 (2010) pp. 477-487.
- [2] M.R. Mashego, W.M. van Gulik, J.L. Vinke, D. Visser, and J.J. Heijnen, In vivo kinetics with rapid perturbation experiments in *Saccharomyces cerevisiae* using a second-generation BioScope, *Metab. Eng.* 8 (2006) pp. 370-383.
- [3] U. Nasution, W.M. van Gulik, A. Proell, W.A. Van Winden, and J.J. Heijnen, Generating short-term kinetic responses of primary metabolism of *Penicillium chrysogenum* through glucose perturbation in the bioscope mini reactor, *Metab. Eng.* 8 (2006) pp. 395-405.
- [4] M. Rizzi, U. Theobald, E. Querfurth, T. Rohrhirsch, M. Baltes, and M. Reuss, In vivo investigations of glucose transport in *Saccharomyces cerevisiae*, *Biotechnol. Bioeng.* 49 (1996) pp. 316-327.
- [5] S. Sunya, F. Delvigne, J.L. Uribelarrea, C. Molina-Jouve, and N. Gorret, Comparison of the transient responses of *Escherichia coli* to a glucose pulse of various intensities, *Appl. Microbiol. Biotechnol.* 95 (2012) pp. 1021-1034.
- [6] U. Theobald, W. Mailinger, M. Baltes, M. Rizzi, and M. Reuss, In vivo analysis of metabolic dynamics in *Saccharomyces cerevisiae* .1. Experimental observations, *Biotechnol. Bioeng.* 55 (1997) pp. 305-316.
- [7] D. Visser, G.A. van Zuylen, J.C. van Dam, M.R. Eman, A. Proll, C. Ras, L. Wu, W.M. van Gulik, and J.J. Heijnen, Analysis of in vivo kinetics of glycolysis in aerobic *Saccharomyces cerevisiae* by application of glucose and ethanol pulses, *Biotechnol. Bioeng.* 88 (2004) pp. 157-167.
- [8] D. Weuster-Botz, Sampling tube device for monitoring intracellular metabolite dynamics, *Anal. Biochem.* 246 (1997) pp. 225-233.
- [9] H.H.J. Bloemen, L. Wu, W.M. van Gulik, J.J. Heijnen, and M.H.G. Verhaegen, Reconstruction of the O<sub>2</sub> uptake rate and CO<sub>2</sub> evolution rate on a time scale of seconds, *AIChE J.* 49 (2003) pp. 1895-1908.
- [10] L. Wu, H.C. Lange, W.M. van Gulik, and J.J. Heijnen, Determination of in vivo oxygen uptake and carbon dioxide evolution rates from off-gas measurements under highly dynamic conditions, *Biotechnol. Bioeng.* 81 (2003) pp. 448-458.

- [11] X.G. Wang, W. Conway, R. Burns, N. McCann, and M. Maeder, Comprehensive Study of the Hydration and Dehydration Reactions of Carbon Dioxide in Aqueous Solution, *Journal of Physical Chemistry A* 114 (2010) pp. 1734-1740.
- [12] M. Sperandio and E. Paul, Determination of carbon dioxide evolution rate using on-line gas analysis during dynamic biodegradation experiments, *Biotechnol. Bioeng.* 53 (1997) pp. 243-252.
- [13] R. Kovács, F. ázi, Z. Csikor, and P. iháltz, Connection between oxygen uptake rate and carbon dioxide evolution rate in aerobic thermophilic sludge digestion, *PERIODICA POLYTECHNICA CHEMICAL ENGINEERING* 51 (2007) pp. 17-22.
- [14] U. Nasution, W.M. van Gulik, R.J. Kleijn, W.A. Van Winden, A. Proell, and J.J. Heijnen, Measurement of intracellular metabolites of primary metabolism and adenine nucleotides in chemostat cultivated *Penicillium chrysogenum*, *Biotechnol. Bioeng.* 94 (2006) pp. 159-166.
- [15] B.R.W. Pinsent and F.J.W. Roughton, The Kinetics of Combination of Carbon Dioxide with Water and Hydroxide Ions, *Transactions of the Faraday Society* 47 (1951) pp. 263-269.
- [16] B.R.W. Pinsent, L. Pearson, and F.J.W. Roughton, The Kinetics of Combination of Carbon Dioxide with Hydroxide Ions, *Transactions of the Faraday Society* 52 (1956) pp. 1512-1520.
- [17] D.M. Kern, The hydration of carbon dioxide, *Journal of Chemical Education* 37 (1960) pp. 14-23.
- [18] K.S. Johnson, Carbon-Dioxide Hydration and Dehydration Kinetics in Sea-Water, *Limnol. Oceanogr.* 27 (1982) pp. 849-855.
- [19] H.J. Noorman, G.C.A. Luijckx, K.C.A.M. Luyben, and J.J. Heijnen, Modeling and Experimental Validation of Carbon-Dioxide Evolution in Alkalophilic Cultures, *Biotechnol. Bioeng.* 39 (1992) pp. 1069-1079.
- [20] A.L. Soli and R.H. Byrne, CO<sub>2</sub> system hydration and dehydration kinetics and the equilibrium CO<sub>2</sub>/H<sub>2</sub>CO<sub>3</sub> ratio in aqueous NaCl solution, *Mar. Chem.* 78 (2002) pp. 65-73.
- [21] K.G. Schulz, U. Riebesell, B. Rost, S. Thoms, and R.E. Zeebe, Determination of the rate constants for the carbon dioxide to bicarbonate inter-conversion in pH-buffered seawater systems, *Mar. Chem.* 100 (2006) pp. 53-65.

- [22] P.A. Vanrolleghem and H. Spanjers, A hybrid respirometric method for more reliable assessment of activated sludge model parameter, *Water Science and Technology* 37 (1998) pp. 237-246.
- [23] C.F. Lindberg and B. Carlsson, Estimation of the respiration rate and oxygen transfer function utilizing a slow DO sensor, *Water Science and Technology* 33 (1996) pp. 325-333.
- [24] R.H. Perry, D.W. Green, and J.O. Maloney, *Perry's Chemical Engineers' Handbook*, McGraw-Hill, New York, 1984.
- [25] F.H. Sweeton, R.E. Mesmer, and C.F. Baes, Acidity Measurements at Elevated Temperatures. VII. Dissociation of Water, *Journal of Solution Chemistry* 3 (1974) pp. 191-214.
- [26] L. Pezza, M. Molina, M. deMoraes, C.B. Melios, and J.O. Tognolli, Ionic medium effects on equilibrium constants .1. Proton, copper(II), cadmium(II), lead(II) and acetate activity coefficients in aqueous solution, *Talanta* 43 (1996) pp. 1689-1695.
- [27] L.P.B.M. Janssen and M.M.C.G. Warmoeskerken, *Transport Phenomena Data Companion*, Arnold, London, 1987.
- [28] S. Weisenberger and A. Schumpe, Estimation of gas solubilities in salt solutions at temperatures from 273 K to 363 K, *AIChE J.* 42 (1996) pp. 298-300.
- [29] E. Rischbieter, A. Schumpe, and V. Wunder, Gas solubilities in aqueous solutions of organic substances, *Journal of Chemical and Engineering Data* 41 (1996) pp. 809-812.
- [30] J.J. Carroll, J.D. Slupsky, and A.E. Mather, The Solubility of Carbon-Dioxide in Water at Low-Pressure, *Journal of Physical and Chemical Reference Data* 20 (1991) pp. 1201-1209.
- [31] C.E. St-Denis and C.J.D. Fell, Diffusivity of Oxygen in Water, *Can. J. Chem. Eng.* 49 (1971) p. 885-&.
- [32] C.L. Yaws, *Handbook of Transport Property Data: Viscosity, Thermal Conductivity, and Diffusion Coefficients of Liquids and Gases*, Gulf Pub. Co., Houston, 1995.
- [33] P.T.H.M. Verhallen, L.J.P. Oomen, A.J.J.M. Vanderelsen, A.J. Kruger, and J.M.H. Fortuin, The Diffusion-Coefficients of Helium, Hydrogen, Oxygen and Nitrogen in Water Determined from the Permeability of A Stagnant Liquid Layer in the Quasi-Steady State, *Chem. Eng. Sci.* 39 (1984) pp. 1535-1541.
- [34] M. Kordac and V. Linek, Dynamic measurement of carbon dioxide volumetric mass transfer coefficient in a well-mixed reactor using a pH probe: Analysis of the



- salt and supersaturation effects, *Industrial & Engineering Chemistry Research* 47 (2008) pp. 1310-1317.
- [35] H. Yagi and F. Yoshida, Enhancement Factor for Oxygen Absorption Into Fermentation Broth, *Biotechnol. Bioeng.* 17 (1975) pp. 1083-1098.
- [36] J.C. Merchuk, Further Considerations on Enhancement Factor for Oxygen Absorption Into Fermentation Broth, *Biotechnol. Bioeng.* 19 (1977) pp. 1885-1889.
- [37] H. Yagi and F. Yoshida, Desorption of Carbon-Dioxide from Fermentation Broth, *Biotechnol. Bioeng.* 19 (1977) pp. 801-819.
- [38] S.J. Pirt and B. Mancini, Inhibition of Penicillin Production by Carbon-Dioxide, *J. Appl. Chem. Biotechnol.* 25 (1975) pp. 781-783.
- [39] C.S. Ho and M.D. Smith, Effect of Dissolved Carbon-Dioxide on Penicillin Fermentations - Mycelial Growth and Penicillin Production, *Biotechnol. Bioeng.* 28 (1986) pp. 668-677.
- [40] M. McIntyre and B. McNeil, Morphogenetic and biochemical effects of dissolved carbon dioxide on filamentous fungi in submerged cultivation, *Appl. Microbiol. Biotechnol.* 50 (1998) pp. 291-298.
- [41] L.P. de Jonge, N.A.A. Buijs, A. ten Pierick, A. Deshmukh, Z. Zhao, J.A.K.W. Kiel, J.J. Heijnen, and W.M. Gulik, Scale-down of penicillin production in *Penicillium chrysogenum*, *Biotechnology Journal* 6 (2011) pp. 944-958.
- [42] W.M. van Gulik, W.T.A.M. De Laat, J.L. Vinke, and J.J. Heijnen, Application of metabolic flux analysis for the identification of metabolic bottlenecks in the biosynthesis of penicillin-G, *Biotechnol. Bioeng.* 68 (2000) pp. 602-618.
- [43] W.M. van Gulik, M.R. Antoniewicz, W.T.A.M. Delaat, J.L. Vinke, and J.J. Heijnen, Energetics of growth and penicillin production in a high-producing strain of *Penicillium chrysogenum*, *Biotechnol. Bioeng.* 72 (2001) pp. 185-193.
- [44] R.C. Aster, B. Borchers, and C.H. Thurber, *Parameter Estimation and Inverse Problems*, Elsevier Academic Press, Boston, 2005.
- [45] T. Kailath, A.H. Sayed, and B. Hassibi, *Linear Estimation*, Prentice Hall, Upper Saddle River, NJ, 2000.
- [46] F.J. Millero, T.B. Graham, F. Huang, H. Bustos-Serrano, and D. Pierrot, Dissociation constants of carbonic acid in seawater as a function of salinity and temperature, *Mar. Chem.* 100 (2006) pp. 80-94.
- [47] Z.I.T.A. Soons, J. van den IJssel, L.A. van der Pol, G. van Straten, and A.J.B. van Boxtel, Scaling-up vaccine production: implementation aspects of a biomass

growth observer and controller, *Bioprocess Biosystems Eng.* 32 (2009) pp. 289-299.

- [48] L. Nedbal, J. Cervený, N. Keren, and A. Kaplan, Experimental validation of a nonequilibrium model of CO<sub>2</sub> fluxes between gas, liquid medium, and algae in a flat-panel photobioreactor, *J. Ind. Microbiol. Biotechnol.* 37 (2010) pp. 1319-1326.



## Chapter 5

---

# Scale-down of penicillin production in *Penicillium chrysogenum*

---

Published as:

de Jonge LP, Buijs NAA, ten Pierick A, Deshmukh A, Zhao Z, Kiel JAKW, Heijnen JJ, van Gulik WM. Scale-down of penicillin production in *Penicillium chrysogenum*. *Biotechnol J* 2011;6(8):944-58.

## Abstract

In large-scale production reactors the combination of high broth viscosity and large broth volume leads to insufficient liquid phase mixing, resulting in gradients in, for example, the concentrations of substrate and oxygen. This often leads to differences in productivity of the full scale process, compared to lab scale. In this scale-down study of penicillin production, the influence of substrate gradients on the process performance and cell physiology was investigated by imposing an intermittent feeding regime on a lab-scale culture of a high yielding strain of *Penicillium chrysogenum*. It was found that the penicillin production was reduced by a factor 2 in the intermittently fed cultures compared to constant feed cultivations, fed with the same amount of glucose per hour, while the biomass yield was the same. Measurement of the levels of the intermediates of the penicillin biosynthesis pathway along with the enzyme levels, suggested that the reduction of the flux through the penicillin pathway is mainly the result of a lower influx into the pathway, possibly due to inhibitory levels of AMP and pyrophosphate and lower activating levels of ATP during the zero substrate phase of each cycle of intermittent feeding.

## 1 Introduction

Many industrial microbial fermentation processes are carried out in large scale reactors with high cell densities, to obtain high volumetric productivities at low operational costs. High cell densities lead to a high broth viscosity, especially in cultures of filamentous fungi growing as dispersed mycelia [1]. The efficiency of the broth mixing in these fermentations is dependent on viscosity, working volume, tank geometry, power input and the type, number and position of the agitators. For reactors with working volumes up to 100 m<sup>3</sup> and above, the mixing time has been reported to be in the order of one to several minutes for broths of filamentous fungi [2-4]. Usually these fermentations are operated as substrate-limited fed-batch cultivations. When the consumption of substrate by the micro-organisms occurs faster than the substrate mixing, zones with a relatively high substrate concentration will arise near the feed point, while the concentration is low in regions farther away [5,6]. Cells circulating through the broth experience this as alternating situations of feast and famine. Imperfect mixing also causes gradients in pH [7] and in dissolved oxygen tension in aerobic processes [8], as reviewed in [9]. The result is that the metabolism of cells travelling through the reactor has to adapt continuously to the changing environment.

In contrast, process development and strain improvement studies are usually carried out in laboratory scale fermentors, which are well mixed. If the performance of a strain is found to be different after scale-up of the fermentation, it is likely that this is caused by imperfect

mixing and resulting gradients. Whether this is so can be investigated by scale-down studies in which the imperfect mixing conditions of the large-scale process are mimicked on laboratory scale.

There are several approaches to simulate the presence of substrate concentration gradients [9,10]. The simplest is to subject a well-mixed culture to an intermittent feeding pattern, which generates concentration gradients in time instead of space [11]. A more elaborate method is to recycle broth between two well-mixed fermentors, which maintain a different residual substrate level [12]. As a variation of such a two reactor system, one of the well-mixed fermentors can be exchanged for a plug flow reactor, in which the concentration decreases along the length of the reactor. It can be chosen to recycle the broth leaving the plug flow reactor back to the well-mixed reactor [13] or not [14,15].

In the design of scale-down experiments, certain aspects of the large-scale process should be mimicked closely to ensure that the results of the simulation experiments have any predictive value. One of these aspects can be the circulation time. In industrial fermentations, each cell experiences the alternating high (in the feed zone) and low substrate concentration at a different frequency and duration of exposure depending on the circulation loops it follows. For the whole culture, the distribution of these circulation times characterizes the mixing intensity and could be a criterion for the scale-down design. As a rule of thumb, circulation times are considered about 4 times lower than mixing times [16], so for broths of filamentous fungi they are typically between 10 and 50 s.

Another aspect in the design of the simulation experiments is the size of the gradients in the substrate concentration. For a 30 m<sup>3</sup> cultivation of *Saccharomyces cerevisiae* at a cell density of 10 g<sub>DW</sub>/L with feed supply from the top, glucose concentrations were reported to be 40.7 mg/L near the top and 4.3 mg/L near the bottom of the reactor [5]. For an *Escherichia coli* cultivation in a 12 m<sup>3</sup> reactor with a cell density of up to 30 g<sub>DW</sub>/L, the glucose concentration gradient ranged from 5 to 35 mg/L in case feed was added near the bottom of the reactor, while peak concentrations of up to 2000 mg/L were measured when feed was supplied from the top [6]. Both studies show that the difference between the highest and lowest concentration decreases with higher cell densities. Although such information is not described in the literature, the concentrations existing in the feed zone and the size of the feed zone are likely to be dependent on the substrate feed rate, mixing intensity and uptake rate of the cultivated micro-organism, which in turn depends on the maximum uptake capacity and affinity for the substrate.

One of the first modern biotechnological processes that were run on a large scale is the production of penicillin and other beta-lactam antibiotics, of which the global demand

continues to be high [17,18]. Surprisingly, only very few studies have been published about the effect of imperfect mixing in penicillin fermentations with *Penicillium chrysogenum* [19,20]. Yet, imperfect mixing can be expected to be a relevant issue for these fermentations, because especially broths of filamentous fungi are known to be extremely viscous [1]. Remarkably, all the reported investigations focus on the dissolved oxygen tension. Henriksen et al. [21], and Vardar and Lilly [20] found that there is a critical oxygen concentration (around 30% of air saturation) below which the specific penicillin production is sharply decreased. The latter also found that the specific penicillin production is decreased when the dissolved oxygen concentration is not kept constant but fluctuates around this critical level. Using a two compartment setup with one anaerobic plug flow reactor, Larsson and Enfors [19] found that exposing *P. chrysogenum* to long (5-10 min) periods of oxygen starvation decreased the respiratory capacity of the culture, while short periods (1-2 min) of exposure didn't have any irreversible effects. However, in that study the effect of fluctuations in dissolved oxygen on penicillin production was not investigated.

The aim of this study was to investigate the influence of substrate concentration gradients (feast/famine cycles) on penicillin production in a high producing strain of *P. chrysogenum*. Apart from monitoring the effect on the specific penicillin production rate and biomass yield, it was considered important to pay attention to the intracellular precursors and intermediates of the penicillin biosynthesis pathway and its enzyme levels, to obtain an understanding of the metabolic response to this condition. For that reason the intermittent feeding approach was used as scale-down method, because in such a system all cells experience the same environmental fluctuations, which allows following the cellular response in terms of the levels of enzymes and, on a timescale of seconds, the levels of intracellular metabolites. The intermittently fed cultures were compared to (continuously fed) chemostat cultures, representing a true and continuous substrate limited condition as a control.

## 2 Materials and methods

### 2.1 Strain

The high yielding *Penicillium chrysogenum* strain DS17690 [22] was kindly donated by DSM Anti-Infectives (Delft, the Netherlands) as spores on rice grains.

### 2.2 Media and inoculation

All media contained per L of demineralized water: 16.51 g glucose monohydrate, 5.0 g  $(\text{NH}_4)_2\text{SO}_4$ , 0.5 g  $\text{MgSO}_4$  heptahydrate, 1.0 g  $\text{KH}_2\text{PO}_4$ , and 2 mL of trace element solution

[23]. In addition, the media contained the following amounts of PAA per L: 0.408 g (batch medium), 0.681 g (chemostat medium), 0.545 g (medium for intermittent feeding regime). These amounts of PAA were aimed at obtaining a PAA concentration in the reactor of approximately 3 mM, which is neither limiting for PenG biosynthesis, nor toxic for cell growth [24]. These media supported a steady state biomass concentration of about 5.7 g<sub>DW</sub>/L.

For preparation of the media of the chemostat and intermittent feeding regimes, the PAA was first dissolved in 4 L of demineralized water by stirring and adding KOH pellets. After the PAA was completely dissolved, the pH of the solution was set to 5.6. This solution was autoclaved in a 50 L vessel for 40 min at 121 °C. The other medium components were dissolved in 46 L of demineralized water and the pH was set to 5.6. This solution was filter sterilized (Supor DCF 0.2 µm filters, Pall Gelman Sciences, East Hills, NY) and mixed with the PAA solution in the medium vessel.

All components of the batch medium except glucose, were dissolved in 3.6 L of demineralized water and autoclaved for 40 min at 121 °C. The glucose was dissolved separately and demineralized water was added to bring the weight of the solution to 300 g, before it was autoclaved for 40 min at 110 °C. A spore solution for inoculation was prepared by submerging approximately 10 g of the rice grains in 100 mL of demineralized water for 1 h with occasional shaking. The medium without glucose, the glucose solution, and the spore suspension were separately and aseptically transferred to the reactor.

### 2.3 Bioreactor setup

Two chemostat fermentations (see below) were run with the setup described in [25]. All other fermentations were carried out in a 7 L bioreactor (Applikon, Schiedam, the Netherlands), which was placed on a balance to control the culture weight at 4.00 kg. Effluent was removed by a peristaltic pump via a pneumatic valve in the bottom of the reactor. The reactor contained 3 baffles and the broth was stirred at 500 rpm by two six-bladed Rushton turbine stirrers (D = 85 mm). The broth was sparged with air at a rate of 5.35 mol/h (0.5 vvm), controlled by a mass flow controller. Offgas left the reactor via a condenser (4 °C), a valve which kept the overpressure in the reactor at 0.3 bar and a drying column (permapure, Perma Pure LLC, USA) before part of it passed through a gas analyzer (NGA 2000, Rosemount, USA) for measurement of the concentrations of O<sub>2</sub> and CO<sub>2</sub>. The pH was controlled at 6.5 by automatic addition of 4 M KOH. The temperature was controlled at 25 °C. Anti-foam (Basildon silicone anti-foam, Basildon Chemicals Ltd, UK) was supplied to the reactors at a rate of ±0.022 mL/h. The dissolved O<sub>2</sub> tension was



measured (Mettler-Toledo, Switzerland) but not controlled, because it was known that under these conditions it never dropped below 80% of air saturation.

#### 2.4 Continuous and intermittently fed cultivations

After inoculation with spores, each cultivation was started with a batch phase. Just before glucose in the batch medium was depleted, the chemostat regime or the intermittent feeding regime was imposed on the culture. In the chemostat regime, medium was pumped continuously into the reactor at a rate of 200 mL/h. In the intermittent feeding regime, the medium pump was set to a feeding rate of 2000 mL/h. In this case the pump was controlled by an industrial timer (PTC-1A Programmable Timing Controller, Omega Engineering Inc., USA) switching it on every first 36 seconds and off for the remaining 324 seconds of a 360 seconds cycle. This cyclic feeding regime was maintained throughout the cultivation. With this setup the overall dilution rate was the same for both systems (continuous and intermittent feeding), namely  $0.05 \text{ h}^{-1}$ .

#### 2.5 Sampling for measurement of dry-weight, TOC and extracellular PenG and PAA

The biomass dry-weight concentration was measured gravimetrically in triplicate, using glass fiber filters (type A/E; Pall Corporation, East Hills, NY; 47 mm diameter, 1  $\mu\text{m}$  pore size) pre-dried for 24 h at 70 °C. Pre-weighed filters were loaded with 5 g broth, washed with two times 10 mL of demineralized water and dried for 24 h at 70 °C. Before weighing, the filters were cooled down to room temperature in a dessicator. Part of the filtrate (2 vials of  $\pm 1 \text{ mL}$ ) was frozen in liquid nitrogen and stored until analysis of PAA and PenG by HPLC-UV [26]. Another part of the filtrate ( $\pm 5 \text{ mL}$ ) and broth ( $\pm 5 \text{ mL}$ ) were stored at -20 °C until analysis of the concentrations of total organic carbon (TOC) with a TOC analyzer (TOC-5050A, Shimadzu).

#### 2.6 Rapid sampling for extracellular glucose and excreted byproducts of penicillin biosynthesis

Culture filtrate was obtained by rapid sampling of broth with immediate cooling to 0 °C and fast filtration, using the cold steel bead method [27]. For measuring the extracellular glucose concentration, 20  $\mu\text{L}$  of the obtained filtrate samples were immediately transferred to a glass vial which contained 20  $\mu\text{L}$  of U- $^{13}\text{C}$ -labeled cell extract as internal standard. The vial was quickly frozen in liquid nitrogen to stop metabolite conversions and subsequently the sample was lyophilized and stored until analysis. For measuring the extracellular concentrations of the byproducts of the penicillin biosynthesis pathway, another 80  $\mu\text{L}$  were transferred to a separate sample vial which contained 20  $\mu\text{L}$  of U- $^{13}\text{C}$ -labeled cell extract as

internal standard. This vial was also quickly frozen in liquid nitrogen and stored until analysis.

## 2.7 Rapid sampling for measurement of intracellular metabolites

For the determination of the intracellular amounts of ACV, IPN, PAA and PenG, rapid sampling of broth, combined with cold methanol quenching and rapid cold filtration was applied as described previously [23], with the adaptation that broth samples of about 5 g were taken. After the extraction, 100  $\mu$ L of 100  $\mu$ M DTT or TCEP were added to reduce all oxidized forms of ACV [28]. For the determination of the intracellular amounts of amino acids and adenine nucleotides, broth samples of  $\pm 1.2$  g were taken using essentially the same rapid sampling and quenching procedure, except that washing of the cells was accomplished by cold centrifugation as described previously [29], with the adaptation that the cold aqueous methanol solutions consisted of 8 mL  $-25$  °C 40% (v/v) methanol. This adaptation was found to prevent leakage of intracellular metabolites into the quenching solution [30].

## 2.8 Metabolite analysis by mass spectrometry

The adenine nucleotides were analyzed by LC-MS/MS [31] and a modified LC-MS/MS method was used to analyze the intermediates and (by)products of the penicillin pathway [32]. For analysis of extracellular glucose and trehalose, the lyophilized samples were derivatized and analyzed by GC-MS as described elsewhere [33].

For analysis of amino acids, 100  $\mu$ L of sample were transferred to a glass vial, 30  $\mu$ L of 100 mg/mL NaCl were added and the mixture was lyophilized. 75  $\mu$ L acetonitril and 75  $\mu$ L of MTBSTFA (N-Methyl-N-(Tert-Butyldimethylsilyl)trifluoroacetamide, Thermo Scientific) were added and the vial was incubated for 1 h at 70 °C. Subsequently the sample was centrifuged in a Table top centrifuge (10000 rpm, 2 min) and 60  $\mu$ L of the supernatant were transferred to a GC glass vial with insert. The sample was then analyzed by GC-MS, carried out on a 7890A GC (Agilent, Santa Clara, CA, USA) coupled to a 5975C MSD single quadrupole mass spectrometer (Agilent, Santa Clara, CA, USA). The optimized conditions for the measurement of the metabolites of interest in the cell extracts were as follows: 1  $\mu$ L of sample was injected on a Zebron ZB-50 column (30 m  $\times$  250  $\mu$ m internal diameter, 0.25  $\mu$ m film thickness; Phenomenex, Torrance, CA, USA) using a programmed temperature vaporizer (PTV; Gerstel, Mühlheim, Germany) for injection in splitless mode. Straight glass liners with glass wool were used (Agilent). The PTV temperature was set to 100 °C with a splitless time of 1 min or in split mode with a split of 15 for highly concentrated amino acids. After injection, the PTV temperature was raised to 220 °C with a speed of 720 °C/min and kept at that temperature for 5 min. Subsequently the temperature was raised

with a speed of 720 °C/min to 300 °C for cleaning purposes. The carrier gas (helium) flow during the analysis was set at 1 mL/min. The GC temperature gradient for the separation of complex amino acid mixtures was set at 100 °C for 1 min and subsequently increased with a speed of 10 °C/min up to 320 °C and kept at that temperature for 1 minute. At the end of a GC run, the column was back flushed with 5 column volumes at 320 °C. The temperature of the transfer line to the MS was set at 250 °C, the MS source at 230 °C and the quadrupole at 150 °C. Electron ionization was operated with 70 eV. For quantitative measurements the MS was used in selected ion monitoring (SIM) mode. The mass resolution was 1 mass unit throughout the mass range 1–1050 amu.

Quantification of the metabolites was performed by IDMS, using U-<sup>13</sup>C-labeled cell extract as internal standard mix [34,35].

## 2.9 Sampling and quantification of enzyme levels of the penicillin biosynthetic pathway

40 mL of broth were centrifuged (4000 g, 4 °C, 10 min), and the cell pellet was washed twice with freeze buffer (100 mM potassium phosphate buffer pH 7.5, 2 mM EDTA, 4 °C). The pellet was resuspended in 5 mL freeze buffer and stored at -20 °C. For analysis, frozen samples were combined with 1 volume of a 25 % TCA solution, mixed thoroughly, and stored at -20 °C. After thawing on ice, from each sample three independent aliquots were taken and crude protein extracts were prepared as described previously [36]. Protein concentrations were determined using the RC/DC Protein Assay system (Bio-Rad) using bovine serum albumin as standard. Subsequently, Western blots were prepared in six-fold utilizing the three independently taken aliquots, with equal amounts of protein (30 µg) loaded per lane. SDS/PAGE and Western blotting were performed according to established procedures. Western blots were decorated with specific polyclonal antibodies against ACVS, IAT and IPNS. As secondary antibody anti-rabbit IgG-AP (Santa Cruz) was used with NBT/BCIP (Roche) as substrate. After detection, Western blots were scanned using a Bio-Rad GS-710 densitometer. Each ACVS, IAT and IPNS-specific band was quantified three times using ImageJ 1.40 (<http://rsbweb.nih.gov/ij/index.html>). After averaging, values were expressed as percentages of the value found for one the control chemostats, which was set to 100 %.

## 3 Results

### 3.1 General observations

To investigate the effect of substrate gradients, as they occur in non-ideally mixed large scale bioreactors, on the performance of a high penicillin-G producing *P. chrysogenum* strain, the strain was grown in a lab-scale bioreactor under an intermittent feeding regime. With the focus of this study being the metabolic response, the design of the intermittent feeding cycles was primarily directed at achieving transient substrate concentrations as they could exist in large-scale penicillin fermentations. The reported gradients in large-scale fermentations of *S. cerevisiae* [5] and *E. coli* [6] were used as a point of reference. Thus, the aim was to obtain glucose concentration differences in the order of 50 mg/L. To avoid a too high broth viscosity in our scale-down experiments, which could give rise to mixing problems and limited oxygen transfer, it was decided to use a moderate cell density with longer cycle times, which were not aimed at exactly mimicking the circulation times in large-scale reactors. The intended glucose concentration differences could be obtained by operating a well mixed bioreactor as a chemostat with discontinuous feeding in cycles of 360 seconds, whereby fresh medium was supplied during the first 36 seconds of each cycle. As a control, conventional carbon limited chemostat cultivations with continuous feeding were carried out, representing continuous substrate limited conditions. The medium composition for both systems was identical and the average dilution rate, and thus the average specific growth rate, of the intermittently fed cultures was the same as that of the control chemostats. For both cultivation modes four cultivations were carried out whereby biomass dry weight, O<sub>2</sub> consumption, CO<sub>2</sub> production, PenG production and PAA consumption were monitored over a period of at least 200 h. The maximum growth rate of this strain in the batch phase preceding the feeding phase was  $0.162 \pm 0.004 \text{ h}^{-1}$ . From the samples that were taken daily during the feeding phase, the carbon and degree-of-reduction balances were calculated and were found to close always between 94% and 106%.

The control chemostat cultures reached a steady state with respect to the concentration of biomass dry weight, O<sub>2</sub> consumption and CO<sub>2</sub> production after three residence times, as found previously [24,29,37].

Intermittent feeding resulted in periodic (360 seconds) fluctuations in the concentrations of dissolved O<sub>2</sub> and of O<sub>2</sub> and CO<sub>2</sub> in the offgas (see Figure 1). The mean of these periodic fluctuations and the biomass dry weight concentration became stable after three residence times.

In both feeding regimes the fungus grew as dispersed mycelia at a dry weight concentration of  $5.72 \pm 0.05$  g/L. No significant morphological differences were observed under the microscope.

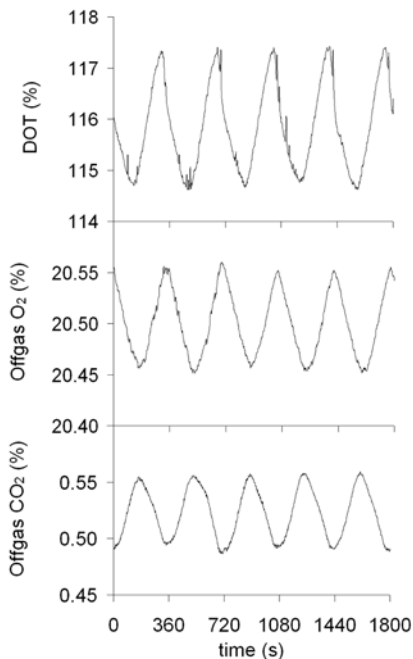


**Figure 1** Illustration of the fluctuations in the dissolved O<sub>2</sub> tension, O<sub>2</sub> concentration in the offgas and CO<sub>2</sub> concentration in the offgas, during several cycles (of 360 seconds) of intermittent feeding. Time 0 does not represent the start of a cycle.

### 3.2 Penicillin production

The specific PenG production rate of four cultures carried out under both feeding regimes was calculated from the measured PenG concentrations in the culture filtrate using a PenG mass balance, and the results are plotted against the cultivation age in Figure 2. Clearly, the development of the production rate was very reproducible for cultivations of the same regime, but the course was completely different for the two feeding regimes. In the control chemostat cultivations a peak in the production occurred after approximately 90 h of cultivation, after which the production rate declined. This decrease is known to occur and ascribed to the phenomenon of degeneration of product formation [38,39]. The intermittently fed cultures had a much lower biomass specific production over a period of 250 h which was slowly increasing during at least the first 200 h of the cultivation.

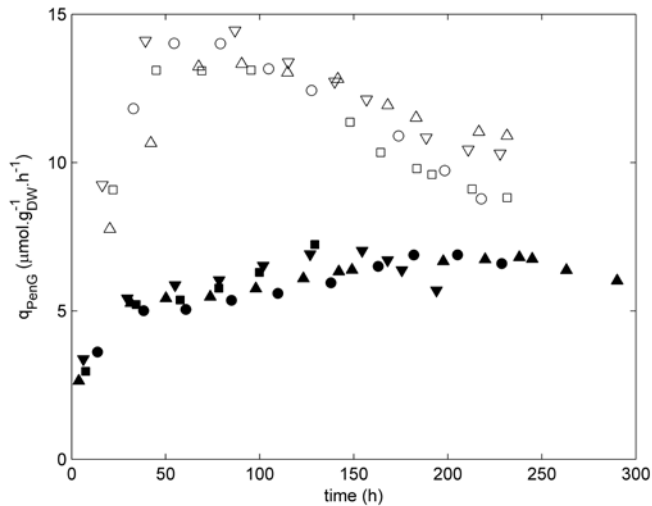


**Figure 2** Specific PenG production rate. For each cultivation, time 0 represents the start of the carbon limited phase. Each cultivation is represented by a separate symbol. Open symbols: control chemostat cultures; solid symbols: intermittently fed cultures.

### 3.3 Other specific rates and yields

For comparison of the physiological state of the cultures under the two regimes, the specific rates of consumption of glucose, PAA and  $O_2$  and of production of  $CO_2$ , PenG and byproducts of penicillin production as well as the biomass yield were calculated at a culture age of 90 h, when PenG production was maximal for the control chemostat cultures (table 1). In the intermittently fed cultures, the concentrations of glucose and  $O_2$  and  $CO_2$  in the offgas were changing periodically, so average rates were calculated by averaging concentrations over several cycles.

Remarkably, no significant differences were found between the two feeding regimes with respect to the biomass yield and (cycle averaged) specific rates of glucose uptake,  $O_2$  consumption and  $CO_2$  production (table 1). In agreement with the decrease in PenG production in intermittently fed cultures (Figure 2), the uptake of the side chain precursor PAA was found to be decreased. The excretion rate of the penicillin pathway intermediate IPN was also reduced, as well as that of the byproduct *o*-OH-PAA. *o*-OH-PAA is an intermediate of the homogentisate pathway for the catabolism of PAA. This pathway is inactive in industrial strains, due to a loss-of-function mutation of the first enzyme, a PAA 2-hydroxylase encoded by the gene *pahA* [40]. However, this enzyme or other enzymes may still exhibit some PAA 2-hydroxylase activity [41], responsible for the oxidation of

PAA to *o*-OH-PAA. Because of the inactivity of the homogentisate pathway, the PAA moiety is conserved in the compounds PAA, *o*-OH-PAA and PenG. Using the rates in Table 1, the PAA balance can be found to close for both feeding regimes, confirming that the homogentisate pathway is inactive. Furthermore, the formation rates of the byproducts OPC, 6-APA and 8-HPA were not found to be significantly different (table 1). Finally, the excretion rate of other carbon products was higher in the intermittently fed cultures (table 1). It has been found earlier for carbon-limited chemostat cultivations of this strain that the extracellular medium contains significant amounts of peptides/proteins and carbohydrates [24]. This can be partly attributed to cell lysis, but is also the result of the excretion of digestive enzymes. In its natural habitats, which include soil and decaying vegetation, *P. chrysogenum* excretes digestive enzymes to degrade plant material. Possibly, the feast/famine regime induced the expression and excretion of such enzymes.

**Table 1** Comparison of biomass-specific rates and the yield of biomass on glucose obtained from glucose-limited cultures grown at a dilution rate of  $0.05 \text{ h}^{-1}$  after 90 h of cultivation, operated under a regime of continuous feeding and of intermittent feeding.

	Continuous feeding regime	Intermittent feeding regime
$-q_{\text{Glucose}}$	$739 \pm 8^{\text{a}}$	$735 \pm 9^{\text{a,g}}$
$-q_{\text{O}_2}$	$1885 \pm 48^{\text{a}}$	$1881 \pm 24^{\text{a,g}}$
$q_{\text{CO}_2}$	$2038 \pm 28^{\text{a}}$	$1968 \pm 15^{\text{a,g}}$
$-q_{\text{PAA}}$	$16.5 \pm 0.3^{\text{a}}$	$6.2 \pm 0.2^{\text{a}}$
$q_{\text{PenG}}$	$13.9 \pm 0.4^{\text{a}}$	$5.7 \pm 0.2^{\text{a}}$
$q_{\text{OPC}}$	$3.6 \pm 0.3^{\text{b}}$	$3.5 \pm 0.7^{\text{c}}$
$q_{\text{IPN}}$	$0.86 \pm 0.17^{\text{b}}$	$0.22 \pm 0.06^{\text{c}}$
$q_{\text{(6-APA)}}$	$3.0 \pm 0.2^{\text{b}}$	$3.9 \pm 1.4^{\text{c}}$
$q_{\text{(8-HPA)}}$	$0.71 \pm 0.09^{\text{b}}$	$0.37 \pm 0.06^{\text{c}}$
$q_{\text{(o-OH-PAA)}}$	$3.09 \pm 0.28^{\text{b}}$	$0.46 \pm 0.09^{\text{c}}$
$q_{\text{(Other excreted organic carbon)}}$	$234 \pm 25^{\text{d}}$	$392 \pm 52^{\text{e}}$
Biomass yield	$0.379 \pm 0.005^{\text{f}}$	$0.379 \pm 0.007^{\text{f}}$

Given are the mean  $\pm$  standard error of the indicated number of cultivations.

<sup>a</sup>Based on four cultivations, expressed in  $\mu\text{mol}(\text{g}_{\text{DW}} \cdot \text{h})^{-1}$

<sup>b</sup>Based on two cultivations, expressed in  $\mu\text{mol}(\text{g}_{\text{DW}} \cdot \text{h})^{-1}$

<sup>c</sup>Based on three cultivations, expressed in  $\mu\text{mol}(\text{g}_{\text{DW}} \cdot \text{h})^{-1}$

<sup>d</sup>Based on two cultivations, expressed in  $\mu\text{Cmol}(\text{g}_{\text{DW}} \cdot \text{h})^{-1}$

<sup>e</sup>Based on three cultivations, expressed in  $\mu\text{Cmol}(\text{g}_{\text{DW}} \cdot \text{h})^{-1}$

<sup>f</sup>Based on four cultivations, expressed in  $\text{g}_{\text{DW}} (\text{g glucose consumed})^{-1}$

<sup>g</sup>Mean of cycle averages

### 3.4 Enzyme levels in the penicillin pathway

A likely reason for the lower penicillin production rate in intermittently fed cultures could be lower enzyme activities in the penicillin pathway. The expression of the enzymes ACVS and IPNS is known to be subject to glucose repression [42], which could have occurred in the intermittently fed cultures. Therefore the enzyme levels were compared by western blot analysis, using samples from two cultivations from both feeding regimes taken at a culture age of around 100 h (table 2). Due to the fact that samples from only duplicate cultivations were used in the analysis, a statistically significant difference could only be detected for the level of IPNS. The amount of this enzyme appeared to be decreased with about 33% in the intermittently fed cultures.

**Table 2** Relative enzyme abundance obtained by western blot analysis of the penicillin pathway enzymes ACVS, IPNS and IAT. Shown are the relative levels of two cultivations for both regimes. The levels were normalized to the level of one of the control chemostat cultures. The p-values of two-tailed unequal variance t-tests given in the bottom line indicate that only the decrease in the IPNS level was statistically significant.

	ACVS	IPNS	IAT
Control chemostat 1	100	100	100
Control chemostat 2	105.9	89.2	113.9
Intermittently fed culture 1	213.5	59.3	76.6
Intermittently fed culture 2	184.0	68.0	90.3
p-value	0.087	0.050*	0.138

### 3.5 Glucose uptake

To further characterize the metabolic behavior of this strain under the intermittent feeding regime, the uptake of glucose during the cycle was studied. For this, the extracellular glucose concentration was measured during a complete cycle. It was found that the concentration of glucose could not simply be measured by enzymatic analysis of the culture filtrates, because it appeared that trehalose (and possibly also other polymers of glucose) was enzymatically converted into glucose during sample processing (see the Appendix). Using an adapted rapid sampling procedure, involving quick freezing in liquid nitrogen to stop the enzymatic formation of glucose, this conversion was avoided. Using this procedure the extracellular glucose concentration during a cycle was found to follow the trend shown in Figure 3 (left panel). During the first 36 seconds of the cycle, the concentration increased due to the addition of fresh medium, and then decreased to practically zero around 200 s after the start of the cycle because of uptake. This profile, with the same slopes, was very



reproducible both at different culture ages within the same cultivation and among different cultivations.

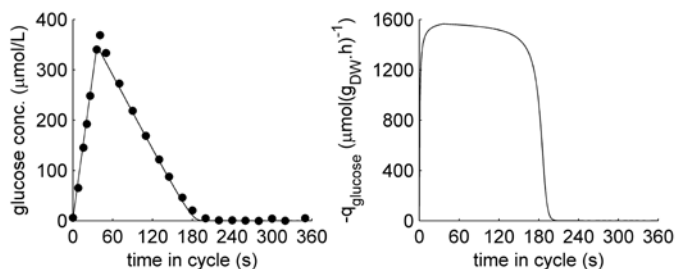


**Figure 3** Glucose uptake during a cycle. Left panel: extracellular glucose concentration profile during a cycle. Right panel: specific glucose uptake rate during a cycle according to fitted model with hyperbolic glucose uptake kinetics. Solid circles, measurements; solid line, fitted glucose uptake model.

It was assumed that the specific glucose uptake rate during a cycle was a hyperbolic function of the glucose concentration, according to:

$$-q_{\text{glucose}} = q_{\text{glucose}}^{\max} \left( \frac{c_{\text{glucose}}}{K_{\text{glucose}} + c_{\text{glucose}}} \right) \quad (1)$$

As is shown in the left panel of Figure 3, a good fit could be obtained with this equation. The estimated parameters with their 95% confidence intervals are  $q_{\text{glucose}}^{\max} = 1600 \pm 94 \mu\text{mol}(\text{g}_{\text{DW}}.\text{h})^{-1}$  and  $K_{\text{glucose}} = 7.8 \pm 2.8 \mu\text{mol/L}$ .

The residual glucose concentration of the control chemostat cultures was measured to remain at a stable level of  $6.8 \pm 0.4 \mu\text{mol/L}$ .

### 3.6 Precursors and intermediates of the penicillin pathway

The *in vivo* activities of the enzymes of the penicillin pathway depend on their levels but also on the concentrations of the metabolites and cofactors participating in each reaction. Therefore the intracellular levels of the adenine nucleotides as well as the precursors and intermediates of the penicillin pathway were measured in two cultures of both feeding regimes during the cultivation. From the intermittently fed cultures, samples were also taken during a cycle to examine whether the highly fluctuating glucose uptake rate (Figure 3) also caused periodic fluctuations in the levels of the intracellular metabolites. Such a periodic fluctuation was clearly observed for the nucleotides ATP, ADP and AMP, as well as for the penicillin pathway precursors AAA, Cys and Val (Figure 4). As is expected in a

cyclic feeding regime, the levels of these metabolites returned at the end of each cycle to the levels at the beginning of the cycle. In contrast to this oscillatory behavior, the amount of IPN was relatively stable during a cycle (Figure 4). The reason for this is that the turnover time of this pool is about 0.4 – 0.7 h (calculated using the excretion rates for IPN and PenG in Table 1). Unfortunately, the scatter in the measured values of intracellular ACV, PAA and PenG does not allow discerning a periodic pattern in the intracellular levels of these metabolites (Figure 4).

Although the levels of ATP, ADP and AMP fluctuated strongly, their sum was constant during the cycle and similar to the summed amount in continuously fed control chemostat cultures (Figure 4). Also the energy charge was changing strongly, from about 0.85 at the start and end of the cycle to about 0.95 between 60 and 240 s, while in chemostat cultures the energy charge was about 0.93.

The intracellular metabolite levels of the control chemostat cultures are plotted in Figure 5 as a function of culture age, together with the levels found in intermittently fed cultures which were sampled at 300 s of the cycle. The individual adenine nucleotides of the intermittently fed cultures are not plotted in Figure 5, because a comparison between their levels at 300 s of the cycle (Figure 4) and the chemostat levels is not meaningful because of the large fluctuations in the levels of these nucleotides within a cycle.

Intermittent feeding resulted in a significantly lower level of AAA and an increased level of Cys (Figure 5). The results of the third amino acid precursor Val were not consistent for the intermittently fed cultures, but at least one culture had similar levels as the control chemostat cultures. Also no significant difference was observed for the intracellular amount of the side-chain precursor PAA and that of the final product PenG. In contrast, the intermediates ACV and IPN are observed to accumulate in the first 100 h of chemostat cultivation followed by a decrease of their levels, while in the intermittent feeding regime these levels remain quite stable at a much lower level. Remarkably, the culture age at which the ACV and IPN levels are highest in the control chemostat cultures coincides with the maximum specific PenG production (Figure 2).

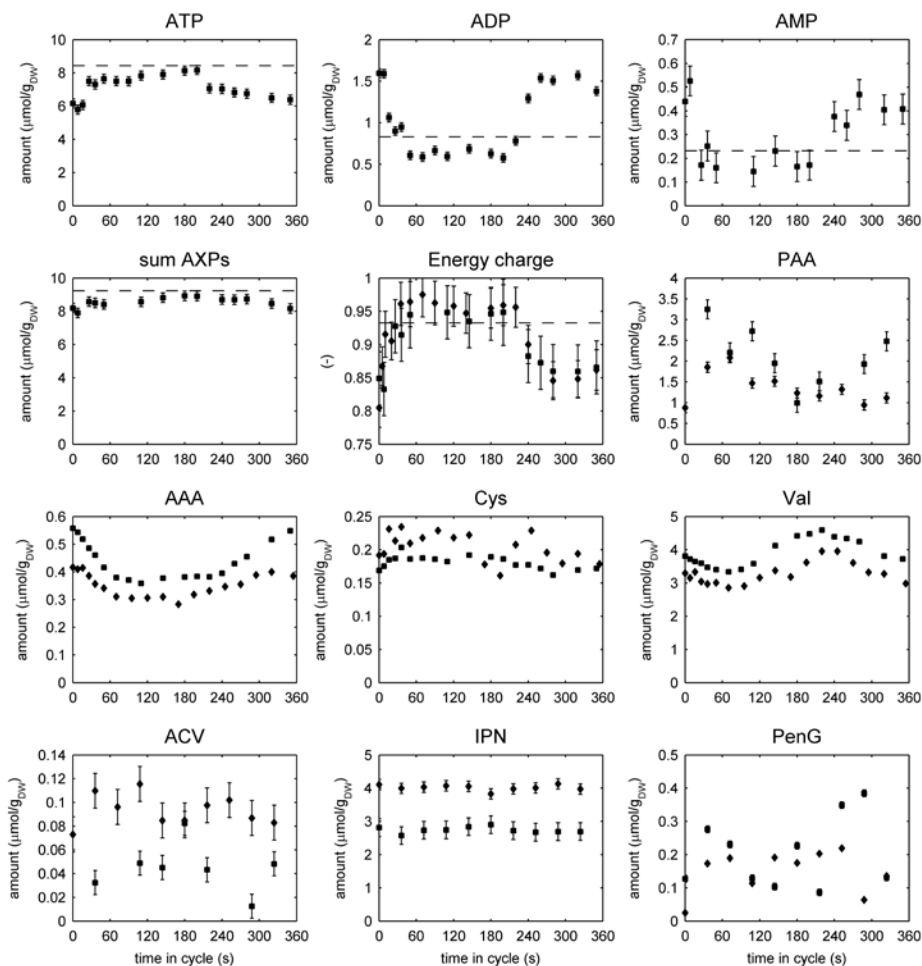


**Figure 4** Intracellular metabolite levels of intermittently fed cultures during a cycle. Squares and diamonds represent different cultivations. Dashed lines indicate the steady state level in control chemostat cultures. The sum of AXPs is the sum of the amounts of ATP, ADP and AMP. The energy charge is calculated from the amounts of ATP, ADP and AMP. Each data point represents a single sample and error bars give the standard deviation for replicate analysis. Data points without error bars represent single analytical replicates of single samples.

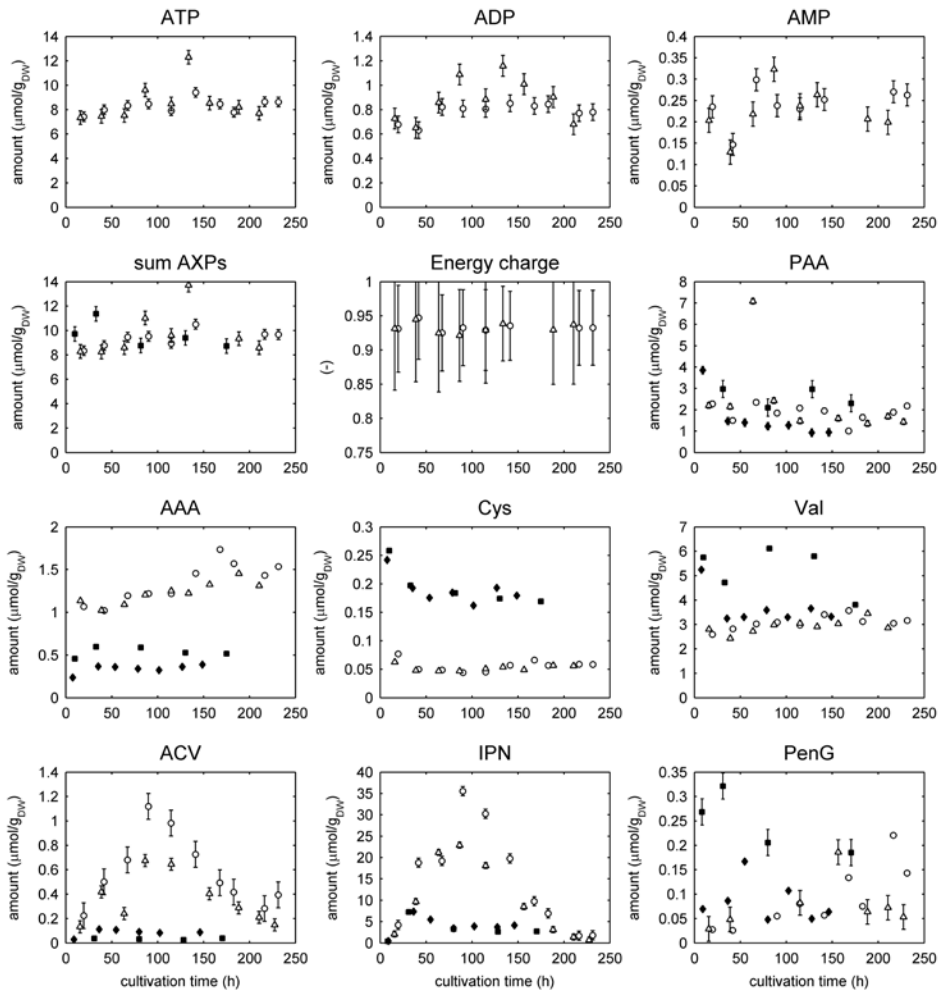


**Figure 5** Intracellular metabolite levels as a function of culture age in intermittently fed cultures (solid symbols) and control chemostats (open symbols). For each cultivation, time 0 represents the start of the carbon limited phase. Samples from intermittently fed cultures were taken 300 s after a cycle start. Each data point represents a single sample and error bars give the standard deviation for replicate analysis. Data points without error bars represent single analytical replicates of single samples.

## 4 Discussion

### 4.1 Characteristics of the glucose uptake system

In the intermittent feeding regime, the extracellular glucose concentration increased from 0 to approximately 380  $\mu\text{mol/L}$  ( $\approx 70 \text{ mg/L}$ ) during the 36 s of medium addition at the start of every cycle (see Figure 3, left panel). No information has been published about glucose concentration gradients in industrial penicillin fermentations of *P. chrysogenum*. However, for experiments with *S. cerevisiae* grown in a 30  $\text{m}^3$  reactor it was reported that the glucose concentration was approximately 30 to 40  $\text{mg/L}$  in the feed zone and around 5  $\text{mg/L}$  at the farthest point from the feed zone [5]. The difference between the lowest and highest concentration is therefore of the same order in this scale-down study.

In the right panel of Figure 3 it is shown that the glucose uptake rate is rapidly increasing from 0 to its estimated maximum of  $1600 \pm 94 \mu\text{mol}(\text{g}_{\text{DW}}\cdot\text{h})^{-1}$  at the start of each cycle. To verify whether this estimate represents a realistic value it can be compared to the value obtained for unlimited growth in batch culture. From the maximum growth rate of this strain during batch growth, the published maximum yield of biomass on glucose and the maintenance coefficient of this strain in [43] (and using a C-molar biomass weight of 28.05  $\text{g}_{\text{DW}}\cdot\text{Cmol}^{-1}$ ), a  $q_{\text{glucose}}^{\text{max}}$  during batch growth ( $q_{\text{PenG}} = 0$ ) can be calculated to be  $1504 \pm 48 \mu\text{mol}(\text{g}_{\text{DW}}\cdot\text{h})^{-1}$ . This value is not significantly different from the estimated  $q_{\text{glucose}}^{\text{max}}$  for the intermittently fed cultures. In contrast, the  $q_{\text{glucose}}^{\text{max}}$  was found to be only around 1283  $\mu\text{mol}(\text{g}_{\text{DW}}\cdot\text{h})^{-1}$  when the same strain was grown under continuous glucose limited conditions in a well-mixed chemostat culture, and was subsequently subjected to a (single) glucose pulse [44]. Apparently, cells grown for prolonged periods of time under glucose limited conditions decrease their maximum glucose uptake capacity. A possible reason is that under these conditions maintaining an unnecessarily high uptake capacity means a higher protein burden and cells with lower levels of glucose transporters have a competitive advantage. Such a difference in maximum glucose uptake capacity of chemostat cultures and intermittently fed cultures has also been found before for *Saccharomyces cerevisiae* [11].

The glucose uptake system had a high affinity for glucose, judging from the fitted parameter  $K_{\text{glucose}}$  of  $7.8 \pm 2.8 \mu\text{mol/L}$ . From the measured residual glucose concentration in the control chemostat cultures, it can be calculated using equation 1 that under continuous glucose limitation the cells have a similar high affinity for glucose with a  $K_{\text{glucose}}$  of approximately 5  $\mu\text{mol/L}$ . This result suggests that the same glucose uptake system is active in both feeding regimes and that cultures subjected to intermittent feeding maintain the high

uptake capacity present during batch growth, while chemostat cultures adapt by decreasing the enzyme levels of this uptake system.

#### 4.2 Enzyme levels of the penicillin pathway

The level of the second enzyme of the penicillin pathway, IPNS, was found to be about 33% lower in cultures subjected to the intermittent feeding regime compared to control chemostat cultures maintained under glucose limited conditions for about 100 h (table 2). The difference in the levels of the other two enzymes, ACVS and IAT, was not statistically significant (at a confidence level of 0.05). There are many factors that determine the level of an enzyme present in a cell. In general, it is a function of the expression level of its gene, the translation efficiency of the transcript and the degradation rate of the enzyme. Although the genes coding for the three enzymes are genetically organized in a cluster, each is transcribed separately from a different promoter [45]. The genes coding for ACVS, IPNS and IAT are known to be repressed by glucose [42,46], although it is not known from which concentration gene repression sets in and to which extent. Nevertheless, the relatively high extracellular glucose concentration during a large part of each cycle in the intermittent feeding regime (Figure 3) compared to the low residual concentration in the glucose limited control chemostats could have been the cause for the lower IPNS level.

Recently it was reported that inhibition of the cellular process of autophagy leads to higher levels of the enzymes of the penicillin biosynthesis pathway and a higher penicillin production rate in *P. chrysogenum* [47]. In filamentous fungi, autophagy is involved in the recycling of organelles and enzymes for nutrient replenishment during starvation [48]. It could be that the occurrence of a short starvation period during every cycle in the intermittent feeding regime leads to increased autophagy. Indeed, the IPNS level in the intermittently fed cultures was significantly lower than in the control cultures, but this was not the case for the enzymes ACVS and AT. Furthermore the penicillin production rate in the intermittently fed cultures was observed to increase slowly during 250 h of cultivation, which does not point at increased autophagy.

From an economic point of view it is interesting to note that in the intermittent feeding regime not only the formation rate of PenG was reduced, but also that of the byproduct *o*-OH-PAA (table 1), which can not be recycled. Possibly, the fluctuating glucose concentration leads to lower levels of enzymes with PAA 2-hydroxylase activity.

#### 4.3 What is controlling the flux through the penicillin pathway?

In the control chemostat cultures both the levels of intracellular ACV and IPN accumulated during the first 100 h (Figure 5). This indicates that the supply of these compounds was larger than the enzymatic capacity of the later enzymatic steps of the penicillin pathway,

e.g. the capacity of IAT, PCL or one of the transport activities over the peroxisomal membrane (see Figure 6 for a schematic overview of the penicillin pathway). It should be noted that the side-chain precursor PAA can enter the cells by passive diffusion over the membrane at a rate which is much higher than the flux through the pathway [49] and therefore PAA import is not expected to be limiting for PenG biosynthesis. Furthermore, the extracellular PenG concentration in these cultivations is two orders of magnitude larger than the intracellular concentration [23]. For that reason, the export of PenG from the mycelia is believed to be an energy requiring active process [50]. If PenG export was the limiting factor in the control chemostats, it would be expected that, due to accumulation, the intracellular PenG concentration would be higher than in the intermittently fed cultures. However, this was not the case as can be seen from the lower right panel of Figure 5.

In a different study, the same strain was used in shake-flask experiments with lactose as the main C-source [51]. It is known that lactose is non-repressing for the genes of the penicillin cluster [52]. It was concluded from this study that the activity mediating the import of the enzyme IAT into the peroxisomes and/or the availability of the CoA-activated side chain precursor could be the limiting step in the pathway, which is in agreement with our observations of the accumulation of intracellular ACV and IPN in the control chemostats. In these chemostats it was observed that after 100 h, the IPN and ACV levels were decreasing (Figure 5). However, this coincided with a decrease of the penicillin production rate (Figure 2) which does not point at an increase of the *in vivo* capacities of the steps downstream but rather at a decrease of the capacity of the earlier steps, i.e. that of ACVS and/or IPNS, and/or the supply of the precursor amino acids and cofactors. The time patterns of the intracellular levels of AAA, Cys and Val do not give any indication for a decreased supply of precursor amino acids; the levels of Cys and Val were stable throughout the entire cultivation period while the AAA level showed a slight increase. With respect to a possible decrease of the capacities of ACVS and/or IPNS, a time series analysis of the enzyme levels could give an indication for this. In prolonged ethanol-limited chemostat cultures it was observed that the productivity decreased tenfold within 30 generations, which coincided with a decrease of the levels of ACVS, IPNS and IAT [53].

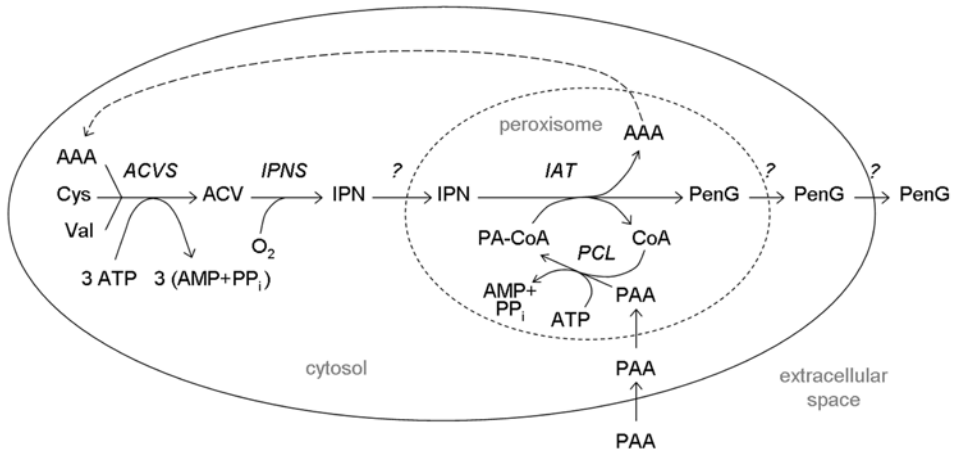


**Figure 6** Schematic overview of the penicillin pathway. ACV and IPN formation occur in the cytosol, activation of PAA and formation of PenG takes place in peroxisomes. Several transport steps over the cell membrane and the peroxisomal membrane are involved in the biosynthesis of PenG. PAA can pass the membranes by passive diffusion of the undissociated form. The mechanisms of the transport of IPN and PenG have not been elucidated yet. The formation of by-products is not shown for clarity.

Remarkably, accumulation of the pathway intermediates ACV and IPN did not occur during intermittent feeding (Figure 5), so apparently the capacities of the later enzymatic steps (IAT and PCL) were not flux limiting in this regime. Despite the significant reduction of the IPNS level with 33% (table 2), the absence of intracellular accumulation of ACV makes it also unlikely that this is the main cause of the decrease in the PenG production. This could imply that in this case the activity of the first enzymatic step (ACVS) is limiting the flux through the pathway. This would mean that either the capacity of the ACVS is decreased (lower enzyme level) and/or that it is less activated or inhibited by allosteric effectors or by the reactants of the reaction it catalyzes. However, there were no indications for a decreased ACVS level (table 2). Possible kinetic effects caused by changes in the concentrations of the amino acid precursors and cofactors involved in the reaction may be identified by comparison with affinity and inhibition constants. The affinity constants of *P. chrysogenum* ACVS determined *in vitro* were 45, 80 and 80  $\mu\text{M}$  for AAA, Cys and Val, respectively [54]. The whole-culture and whole-cell averaged level of AAA shown in Figure 5 can be converted into whole-culture and whole-cell averaged concentrations using a specific cell volume of 2.5 mL/g<sub>DW</sub> [55]. In the intermittent feeding regime, the AAA concentration fluctuates then between 0.12 and 0.24 mM, compared to an averaged concentration of 0.4 to 0.6 mM in the chemostat regime. Although the concentration of



AAA is lower in intermittently fed cultures, it is still well above the value of the affinity constant. The averaged concentration of Cys in intermittently fed cultures (around 70  $\mu\text{M}$ ) is in the order of the value of the affinity constant, but higher than the Cys level of the control chemostat cultures which was around 20  $\mu\text{M}$  (Figure 5). This concentration of Cys may therefore prevent ACVS to work at its maximum rate, but cannot be the reason for the decreased flux through the pathway under intermittent feeding conditions. The measured levels of Val were always high compared to the affinity constant (Figure 5). So, also the supply of amino acid precursors does not seem to be a cause for the lower flux.

It was observed that the level of ATP was also oscillating during cycles of intermittent feeding (Figure 4). In the *in vitro* characterization study of the *P. chrysogenum* ACVS, it was found that there is an optimum ATP concentration of 5 mM at which the enzyme activity was highest [54]. It can be calculated from our measurements that the whole-culture and whole-cell averaged concentration of ATP is always below this optimum value in the intermittently fed cultures, and fluctuates between 2.6 and 3.4 mM, while in the control chemostat the ATP level remains stable at an average concentration of about 3.5 mM. Per ACV formed, 3 ATP are converted to 3 AMP and 3 pyrophosphate. At the end of each cycle the level of AMP is twice as high as in the chemostats (see Figure 4), which could inhibit the *in vivo* ACVS activity. Indeed the ACVS of *Streptomyces clavuligerus* was reported to be strongly inhibited by AMP and pyrophosphate [56], but inhibition constants were not given. In addition, ACVS is a cytosolic enzyme and the fluctuation in the cytosolic concentrations of ATP, AMP and pyrophosphate may be even stronger than the fluctuation of the whole-cell-averaged levels shown in Figure 4, because of the strong fluctuation of the glycolytic flux which also takes place in the cytosol. It is therefore concluded that unfavorable ATP and AMP levels during the first 30 and last 180 seconds of the cycle are the most likely cause for the lower *in vivo* activity of ACVS in intermittently fed cultures.

#### 4.4 Implications for large-scale fermentation

In our scale-down experiments, the cells in the culture experienced the alternating high and low substrate concentrations in a cyclic manner and all at the same frequency. This was a prerequisite for a proper measurement of the metabolic response of the cells. As shown, *P. chrysogenum* was found to react to the applied fluctuations in glucose concentration. In large-scale fermentations, however, the times between experiencing high and low concentrations vary continuously for every cell, depending on the circulation flows the cell follows in the reactor. The average circulation time in reactors up to 200 m<sup>3</sup> is expected to be shorter than the cycle time used in our scale-down study. Whether the observed

metabolic effects would be similar at shorter and varying circulation times should be studied separately.

If cells in non-ideally mixed industrial reactors suffer from glucose concentration gradients, and fluctuations in ATP and AMP levels are indeed a cause for a lower production as argued above, there are two obvious ways to make the cells more robust. First, the glucose uptake system could be replaced by one with a lower affinity for glucose, which would result in less extreme oscillations in the uptake rate [5]. Second, the ACVS might be engineered to reduce the inhibitory effect of AMP and pyrophosphate.

## Acknowledgements

J.A.K.W.K. was financially supported by DSM, Delft, The Netherlands.

## References

- [1] A.I. Galaction, D. Cascaval, C. Oniscu, and M. Turnea, Evaluation and modeling of the aerobic stirred bioreactor performances for fungus broths, *Chem. Biochem. Eng. Q.* 19 (2005) pp. 87-97.
- [2] P.H. Jansen, S. Slott, and H. Gürtler, Determination of Mixing Times in Large Scale Fermentors Using Radioactive Isotopes, 1978.
- [3] M.R. Marten, K.S. Wenger, and S.A. Kahn, Rheology, Mixing Time, and Regime Analysis for a Production-Scale *Aspergillus Oryzae* Fermentation, in: A.W. Nienow (Ed.), 4th International Conference in Bioreactor & Bioprocess Fluid Dynamics, MECHANICAL ENGINEERING PUBLICATIONS LIMITED, Bury St Edmonds, UK, 1997, 295-313.
- [4] D.J. Pollard, T.F. Kirschner, G.R. Hunt, I.T. Tong, R. Stieber, and P.M. Salmons, Scale up of a viscous fungal fermentation: Application of scale-up criteria with regime analysis and operating boundary conditions, *Biotechnol. Bioeng.* 96 (2007) pp. 307-317.
- [5] G. Larsson, M. Tornkvist, E.S. Wernersson, C. Tragardh, H. Noorman, and S.O. Enfors, Substrate gradients in bioreactors: Origin and consequences, *Bioprocess Eng.* 14 (1996) pp. 281-289.
- [6] F. Bylund, E. Collet, S.O. Enfors, and G. Larsson, Substrate gradient formation in the large-scale bioreactor lowers cell yield and increases by-product formation, *Bioprocess Eng.* 18 (1998) pp. 171-180.

- [7] C. Langheinrich and A.W. Nienow, Control of pH in large-scale, free suspension animal cell bioreactors: Alkali addition and pH excursions, *Biotechnol. Bioeng.* 66 (1999) pp. 171-179.
- [8] N.M.G. Oosterhuis and N.W.F. Kossen, Dissolved-Oxygen Concentration Profiles in A Production-Scale Bioreactor, *Biotechnol. Bioeng.* 26 (1984) pp. 546-550.
- [9] A.R. Lara, E. Galindo, O.T. Ramirez, and L.A. Palomares, Living with heterogeneities in bioreactors, *Mol. Biotechnol.* 34 (2006) pp. 355-381.
- [10] P. Neubauer and S. Junne, Scale-down simulators for metabolic analysis of large-scale bioprocesses, *Curr. Opin. Biotechnol.* 21 (2010) pp. 114-121.
- [11] B.H.A. Van Kleeff, J.G. Kuenen, and J.J. Heijnen, Heat flux measurements for the fast monitoring of dynamic responses to glucose additions by yeasts that were subjected to different feeding regimes in continuous culture, *Biotechnol. Prog.* 12 (1996) pp. 510-518.
- [12] A.P.J. Sweere, Y.A. Matla, J. Zandvliet, K.Ch.A.M. Luyben, and N.W.F. Kossen, Experimental simulation of glucose fluctuations, *Appl. Microbiol. Biotechnol.* 28 (1988) pp. 109-115.
- [13] S. George, G. Larsson, and S.O. Enfors, A scale-down two-compartment reactor with controlled substrate oscillations: Metabolic response of *Saccharomyces cerevisiae*, *Bioprocess Eng.* 9 (1993) pp. 249-257.
- [14] D. Visser, G.A. van Zuylen, J.C. van Dam, A. Oudshoorn, M.R. Eman, C. Ras, W.M. van Gulik, J. Frank, G.W.K. van Dedem, and J.J. Heijnen, Rapid sampling for analysis of in vivo kinetics using the BioScope: A system for continuous-pulse experiments, *Biotechnol. Bioeng.* 79 (2002) pp. 674-681.
- [15] M.R. Mashego, W.M. van Gulik, J.L. Vinke, D. Visser, and J.J. Heijnen, In vivo kinetics with rapid perturbation experiments in *Saccharomyces cerevisiae* using a second-generation BioScope, *Metab. Eng.* 8 (2006) pp. 370-383.
- [16] R.M. Voncken, D.B. Holmes, and H.W. Denhartog, Fluid Flow in Turbine-Stirred, Baffled Tanks-II. Dispersion During Circulation, *Chem. Eng. Sci.* 19 (1964) pp. 209-213.
- [17] H. Kresse, M.J. Belsey, and H. Rovini, The antibacterial drugs market, *Nat. Rev. Drug Discov.* 6 (2007) pp. 19-20.
- [18] F.R. Schmidt, The Beta-Lactam Antibiotics: Current Situation and Future Prospects in Manufacture and Therapy, in: M. Hofrichter (Ed.), *Industrial Applications X, The Mycota*; Springer Verlag, Berlin Heidelberg, 2010, pp. 101-121.

- [19] G. Larsson and S.O. Enfors, Studies of Insufficient Mixing in Bioreactors - Effects of Limiting Oxygen Concentrations and Short-Term Oxygen Starvation on *Penicillium Chrysogenum*, *Bioprocess Eng.* 3 (1988) pp. 123-127.
- [20] F. Vardar and M.D. Lilly, Effect of Cycling Dissolved-Oxygen Concentrations on Product Formation in Penicillin Fermentations, *Eur. J. Appl. Microbiol. Biotechnol.* 14 (1982) pp. 203-211.
- [21] C.M. Henriksen, J. Nielsen, and J. Villadsen, Influence of the dissolved oxygen concentration on the penicillin biosynthetic pathway in steady-state cultures of *Penicillium chrysogenum*, *Biotechnol. Prog.* 13 (1997) pp. 776-782.
- [22] D.M. Harris, J.A. Diderich, Z.A. van der Krogt, M.A.H. Luttkik, U.M. Raamsdonk, R.A.L. Bovenberg, W.M. van Gulik, J.P. Van Dijken, and J.T. Pronk, Enzymic analysis of NADPH metabolism in beta-lactam-producing *Penicillium chrysogenum*: Presence of a mitochondrial NADPH dehydrogenase, *Metab. Eng.* 8 (2006) pp. 91-101.
- [23] R.D. Douma, L.P. de Jonge, C.T.H. Jonker, R.M. Seifar, J.J. Heijnen, and W.M. van Gulik, Intracellular Metabolite Determination in the Presence of Extracellular Abundance: Application to the Penicillin Biosynthesis Pathway in *Penicillium chrysogenum*, *Biotechnol. Bioeng.* 107 (2010) pp. 105-115.
- [24] W.M. van Gulik, W.T.A.M. De Laat, J.L. Vinke, and J.J. Heijnen, Application of metabolic flux analysis for the identification of metabolic bottlenecks in the biosynthesis of penicillin-G, *Biotechnol. Bioeng.* 68 (2000) pp. 602-618.
- [25] Z. Zhao, K. Kuijvenhoven, C. Ras, W.M. van Gulik, J.J. Heijnen, P.J.T. Verheijen, and W.A. Van Winden, Isotopic non-stationary C-13 gluconate tracer method for accurate determination of the pentose phosphate pathway split-ratio in *Penicillium chrysogenum*, *Metab. Eng.* 10 (2008) pp. 178-186.
- [26] L.H. Christensen, G. Mandrup, J. Nielsen, and J. Villadsen, A Robust Liquid-Chromatographic Method for Measurement of Medium Components During Penicillin Fermentations, *Anal. Chim. Acta* 296 (1994) pp. 51-62.
- [27] M.R. Mashego, W.M. van Gulik, J.L. Vinke, and J.J. Heijnen, Critical evaluation of sampling techniques for residual glucose determination in carbon-limited chemostat culture of *Saccharomyces cerevisiae*, *Biotechnol. Bioeng.* 83 (2003) pp. 395-399.
- [28] R.M. Seifar, A.T. Deshmukh, J.J. Heijnen, and W.M. van Gulik, Determination of delta-[L-alpha-aminoadipyl]-L-cysteinyl-D-valine in cell extracts of *Penicillium chrysogenum* using ion pair-RP-UPLC-MS/MS, *Journal of Separation Science* 35 (2012) pp. 225-230.

- [29] U. Nasution, W.M. van Gulik, R.J. Kleijn, W.A. Van Winden, A. Proell, and J.J. Heijnen, Measurement of intracellular metabolites of primary metabolism and adenine nucleotides in chemostat cultivated *Penicillium chrysogenum*, *Biotechnol. Bioeng.* 94 (2006) pp. 159-166.
- [30] L.P. de Jonge, R.D. Douma, J.J. Heijnen, and W.M. van Gulik, Optimization of cold methanol quenching for quantitative metabolomics of *Penicillium chrysogenum*, *Metabolomics* 8 (2012) pp. 727-735.
- [31] R.M. Seifar, C. Ras, J.C. van Dam, W.M. van Gulik, J.J. Heijnen, and W.A. Van Winden, Simultaneous quantification of free nucleotides in complex biological samples using ion pair reversed phase liquid chromatography isotope dilution tandem mass spectrometry, *Anal. Biochem.* 388 (2009) pp. 213-219.
- [32] R.M. Seifar, Z. Zhao, J. van Dam, W. van Winden, W. van Gulik, and J.J. Heijnen, Quantitative analysis of metabolites in complex biological samples using ion-pair reversed-phase liquid chromatography-isotope dilution tandem mass spectrometry, *J. Chromatogr. A* 1187 (2008) pp. 103-110.
- [33] C. Cipollina, A. ten Pierick, A.B. Canelas, R.M. Seifar, A.J.A. van Maris, J.C. van Dam, and J.J. Heijnen, A comprehensive method for the quantification of the non-oxidative pentose phosphate pathway intermediates in *Saccharomyces cerevisiae* by GC-IDMS, *J. Chromatogr. B Analyt. Technol. Biomed. Life. Sci.* 877 (2009) pp. 3231-3236.
- [34] M.R. Mashego, L. Wu, J.C. van Dam, C. Ras, J.L. Vinke, W.A. Van Winden, W.M. van Gulik, and J.J. Heijnen, MIRACLE: mass isotopomer ratio analysis of U-C-13-labeled extracts. A new method for accurate quantification of changes in concentrations of intracellular metabolites, *Biotechnol. Bioeng.* 85 (2004) pp. 620-628.
- [35] L. Wu, M.R. Mashego, J.C. van Dam, A.M. Proell, J.L. Vinke, C. Ras, W.A. Van Winden, W.M. van Gulik, and J.J. Heijnen, Quantitative analysis of the microbial metabolome by isotope dilution mass spectrometry using uniformly C-13-labeled cell extracts as internal standards, *Anal. Biochem.* 336 (2005) pp. 164-171.
- [36] J.A.K.W. Kiel, M.A. van den Berg, F. Fusetti, B. Poolman, R.A.L. Bovenberg, M. Veenhuis, and I.J. van der Klei, Matching the proteome to the genome: the microbody of penicillin-producing *Penicillium chrysogenum* cells, *Funct. Integr. Genomics* 9 (2009) pp. 167-184.
- [37] U. Nasution, W.M. van Gulik, C. Ras, A. Proell, and J.J. Heijnen, A metabolome study of the steady-state relation between central metabolism, amino acid biosynthesis and penicillin production in *Penicillium chrysogenum*, *Metab. Eng.* 10 (2008) pp. 10-23.

- [38] L.H. Christensen, C.M. Henriksen, J. Nielsen, J. Villadsen, and M. Egelmitani, Continuous Cultivation of *Penicillium-Chrysogenum* - Growth on Glucose and Penicillin Production, *J. Biotechnol.* 42 (1995) pp. 95-107.
- [39] R.C. Righelato, Selection of Strains of *Penicillium-Chrysogenum* with Reduced Penicillin Yields in Continuous Cultures, *J. Appl. Chem. Biotechnol.* 26 (1976) pp. 153-159.
- [40] M. Rodriguez-Saiz, J.L. Barredo, M.A. Moreno, J.M. Fernandez-Canon, M.A. Penalva, and B. Diez, Reduced function of a phenylacetate-oxidizing cytochrome P450 caused strong genetic improvement in early phylogeny of penicillin-producing strains, *J. Bacteriol.* 183 (2001) pp. 5465-5471.
- [41] D.M. Harris, Z.A. van der Krogt, P. Klaassen, L.M. Raamsdonk, S. Hage, M.A. van den Berg, R.A.L. Bovenberg, J.T. Pronk, and J.M. Daran, Exploring and dissecting genome-wide gene expression responses of *Penicillium chrysogenum* to phenylacetic acid consumption and penicillinG production, *BMC Genomics* 10 (2009) p. 75.
- [42] B. Feng, E. Friedlin, and G.A. Marzluf, A Reporter Gene Analysis of Penicillin Biosynthesis Gene-Expression in *Penicillium-Chrysogenum* and Its Regulation by Nitrogen and Glucose Catabolite Repression, *Appl. Environ. Microbiol.* 60 (1994) pp. 4432-4439.
- [43] W.M. van Gulik, M.R. Antoniewicz, W.T.A.M. Delaat, J.L. Vinke, and J.J. Heijnen, Energetics of growth and penicillin production in a high-producing strain of *Penicillium chrysogenum*, *Biotechnol. Bioeng.* 72 (2001) pp. 185-193.
- [44] U. Nasution, W.M. van Gulik, A. Proell, W.A. Van Winden, and J.J. Heijnen, Generating short-term kinetic responses of primary metabolism of *Penicillium chrysogenum* through glucose perturbation in the bioscope mini reactor, *Metab. Eng.* 8 (2006) pp. 395-405.
- [45] A.A. Brakhage, P. Sprote, Q. Al-Abdallah, A. Gehrke, H. Plattner, and A. Tuncher, Regulation of penicillin biosynthesis in filamentous fungi, *Adv. Biochem. Eng. Biotechnol.* 88 (2004) pp. 45-90.
- [46] J.E. Martin, J. Casqueiro, K. Kosalkova, A.T. Marcos, and S. Gutierrez, Penicillin and cephalosporin biosynthesis: Mechanism of carbon catabolite regulation of penicillin production, *Antonie Van Leeuwenhoek* 75 (1999) pp. 21-31.
- [47] M. Bartoszewska, J.A.K.W. Kiel, R.A.L. Bovenberg, M. Veenhuis, and I.J. van der Klei, Autophagy Deficiency Promotes beta-Lactam Production in *Penicillium chrysogenum*, *Appl. Environ. Microbiol.* 77 (2011) pp. 1413-1422.
- [48] J.K. Pollack, S.D. Harris, and M.R. Marten, Autophagy in filamentous fungi, *Fungal Genet. Biol.* 46 (2009) pp. 1-8.

- [49] D.J. Hillenga, H.J.M. Versantvoort, S. Vandermolen, A.J.M. Driessen, and W.N. Konings, Penicillium-Chrysogenum Takes Up the Penicillin-G Precursor Phenylacetic Acid by Passive Diffusion, *Appl. Environ. Microbiol.* 61 (1995) pp. 2589-2595.
- [50] M.A. van den Berg, R.A.L. Bovenberg, A.J.M. Driessen, W.N. Konings, T.A. Schuurs, M. Nieboer, and I. Westerlaken, Method for Enhancing Secretion of Beta-Lactam Transport., 2001.
- [51] J.G. Nijland, B. Ebbendorf, M. Woszczyńska, R. Boer, R.A.L. Bovenberg, and A.J.M. Driessen, Nonlinear Biosynthetic Gene Cluster Dose Effect on Penicillin Production by *Penicillium chrysogenum*, *Appl. Environ. Microbiol.* 76 (2010) pp. 7109-7115.
- [52] G. Revilla, M.J. Lopeznieto, J.M. Luengo, and J.F. Martin, Carbon Catabolite Repression of Penicillin Biosynthesis by *Penicillium-Chrysogenum*, *J. Antibiot.* 37 (1984) pp. 781-789.
- [53] R.D. Douma, J.M. Batista, K.M. Touw, J.A.K.W. Kiel, A.M. Krikken, Z. Zhao, T. Veiga, P. Klaassen, R.A.L. Bovenberg, J.M. Daran, J.J. Heijnen, and W.M. van Gulik, Degeneration of penicillin production in ethanol-limited chemostat cultivations of *Penicillium chrysogenum*: A systems biology approach, *Bmc Systems Biology* 5 (2011).
- [54] H.B.A. Theilgaard, K.N. Kristiansen, C.M. Henriksen, and J. Nielsen, Purification and characterization of delta-(L-alpha-aminoadipyl)-L-cysteiny-D-valine synthetase from *Penicillium chrysogenum*, *Biochem. J.* 327 (1997) pp. 185-191.
- [55] W.M. Jaklitsch, W. Hampel, M. Rohr, C.P. Kubicek, and G. Gamerith, Alpha-Aminoadipate Pool Concentration and Penicillin Biosynthesis in Strains of *Penicillium-Chrysogenum*, *Can. J. Microbiol.* 32 (1986) pp. 473-480.
- [56] J.Y. Zhang, S. Wolfe, and A.L. Demain, Biochemical-Studies on the Activity of Delta-(L-Alpha-Aminoadipyl)-L-Cysteiny-D-Valine Synthetase from *Streptomyces-Clavuligerus*, *Biochem. J.* 283 (1992) pp. 691-698.

## Appendix

### Sampling for extracellular glucose in carbon limited cultures of *Penicillium chrysogenum*

When the extracellular glucose concentration during a cycle of an intermittently fed culture (see main text) was measured enzymatically in culture filtrates obtained by the steel beads method [27], the concentration profile shown in Figure A1 was obtained. Remarkably, the concentration did not drop below about 60  $\mu\text{mol/L}$  during the starvation phase. We attributed this to an artefact of the measurement, because we could not think of any biological explanation why the fungus wouldn't consume this quite abundant amount of glucose. Spiking experiments excluded analytical errors in the enzymatic analysis (not shown).

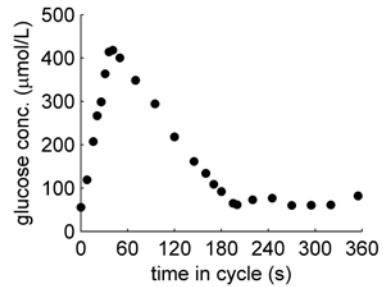


**Figure A1. Extracellular glucose concentration during one feeding cycle, measured enzymatically, in culture filtrate samples.**

It was then hypothesized that the glucose was formed in the sample after filtration by enzymatic hydrolysis of trehalose also present in the filtrate. The presence of trehalase activity in the filtrate was tested by adding 400  $\mu\text{mol}(\text{glucose-equivalents})/\text{L}$  of trehalose to a filtrate sample. After one hour of incubation (at RT), the sample was frozen in liquid nitrogen, lyophilized and further processed for analysis by GC-MS as explained in the Materials and methods section of the main text. It appeared that about 80% of the trehalose had been converted to glucose (left panel of Figure A2), which confirmed that there was trehalase activity in the culture filtrate.

The presence of trehalose in culture filtrates was verified by incubating a filtrate sample for 5 min in a water bath of 95  $^{\circ}\text{C}$  to denature enzymes present in the filtrate. Analysis by GC-MS showed that the heated sample contained approximately 10  $\mu\text{mol/L}$  of glucose and 13  $\mu\text{mol}(\text{glucose-equivalents})/\text{L}$  of trehalose (right panel of Figure A2). When trehalase was added to the heated sample, the trehalose was converted to glucose (right panel of Figure A2).

These experiments demonstrate that the concentration of glucose in the culture filtrate of *P. chrysogenum* can be significantly overestimated due to conversion of trehalose to glucose



by enzymatic activity of for example trehalases in the samples. The enzymatic activity remains, even when samples are frozen (for storage) and thawed again (for analysis).

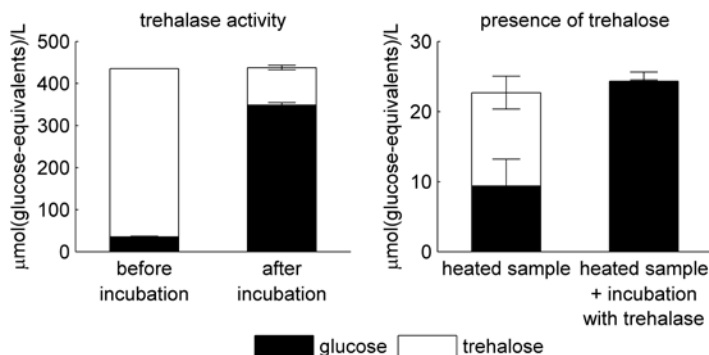


**Figure A2. Trehalase activity and presence of trehalose in filtrate samples.** Left panel: “before incubation”: 400  $\mu\text{mol}(\text{glucose-equivalents})/\text{L}$  of trehalose were added to a filtrate sample which (after addition of the trehalose solution) also contained about 35  $\mu\text{mol}/\text{L}$  of glucose. “after incubation”: after one hour of incubation, about 80% of the trehalose had been converted to glucose. Right panel: “heated sample”: shown are the concentrations of glucose and trehalose present in a sample of culture filtrate that was heated for 5 min in a water bath of 95 °C. “heated sample + incubation with trehalase”: 5  $\mu\text{L}$  of a trehalase suspension was added and the sample was incubated for 1 h at RT, resulting in the hydrolysis of trehalose to glucose. All analyses were performed by GC-MS.

To avoid this, an adapted sampling procedure is required which prevents such enzymatic activity. In our experiments this was achieved by quickly ( $\leq 20$  s) freezing the filtrate samples in liquid nitrogen. Furthermore it was chosen to analyze the samples by the GC-MS method described in the Materials and methods section of the main text, because then the water is removed from the sample by lyophilisation which elegantly prevents any further enzyme activity. Heating the sample in a water bath was found to be too slow to completely stop enzymatic activity in comparison to freezing in liquid nitrogen (not shown).

A number of questions could not be answered yet. Is the glucose formed only from trehalose, or also from other sources (e.g. glycogen)? What is the rate at which the glucose is formed? Is the rate the same in chemostat cultures and intermittently fed cultures, and is it constant throughout the cultivation? Is the conversion taking place only in the filtrate after sampling, or does it also take place in the reactor? Formation of glucose in the reactor was not included in the model fitting procedure discussed in section 3.5, because of the lack of this information.

## Chapter 6

---

The organization of metabolism by  
*Penicillium chrysogenum*  
in feast/famine conditions

---

## Abstract

The combination of long mixing times and high volumetric substrate uptake rates in large scale industrial fed-batch fermentations gives rise to the presence of zones of relatively high substrate concentration close to the feeding point of substrate into the bioreactor and zones which are practically depleted of substrate. Biomass passing through these two types of zones experiences a feast/famine regime. To investigate the metabolic response of a high-yielding strain of *Penicillium chrysogenum* to this condition during penicillin fermentations, the feast/famine condition was mimicked in a lab-scale bioreactor by imposing an intermittent feeding regime of 360 seconds cycles in which substrate was only fed during the first 36 seconds. All substrate in the form of glucose was consumed during the first 200 seconds of each cycle, and there was no glucose during the last 160 seconds. There was no excretion of metabolites which served as an extracellular carbon buffer during the period of glucose depletion. The respiratory rate was higher during the period of glucose excess, but respiration continued during the period of glucose depletion. About 11% of the carbon consumed in the form of glucose accumulated temporarily as intracellular mannitol during the period of glucose excess. Interestingly, the overall flux of carbon through the two most important pools of the storage carbohydrates, trehalose and mannitol, amounted approximately 18% of the glucose uptake rate and this was comparable (22%) to that of control chemostat cultures. However, in the feast/famine regime the overall flux through the trehalose pool was about 2-fold higher and the overall flux through the mannitol pool was 2-fold lower than in the chemostat regime. Finally, it was found that a significant amount of about 18% of the consumed carbon temporarily accumulated in intracellular pools of intermediates of central metabolic pathways. So, to cope with feast/famine cycles as experienced in non-homogeneously mixed, large-scale fermentors, *P. chrysogenum* has the capacity to absorb a large amount of carbon in intracellular pools of storage carbohydrates and central metabolic pathways during substrate-available periods, from which it can release carbon during periods of substrate depletion.

## 1 Introduction

The mixing time in large scale industrial fed-batch fermentations with viscous broths of high cell density microbial cultures is usually in the order of minutes. In substrate-limited conditions (fed-batch) the combination of this long mixing time with high substrate consumption rates gives rise to gradients in the concentration of substrate, with high concentrations close to the entry point of medium into the vessel and steeply decreasing concentrations and substrate free zones at larger distances from this entry point. For

individual cells following the circulation flows in the bioreactor, the gradients are experienced as a feast/famine-like regime. Some micro-organisms such as *Saccharomyces cerevisiae*, *Escherichia coli* and *Corynebacterium glutamicum* respond to such a dynamic environment with overflow metabolism.

Interesting experiments in which feast/famine effects were studied on a time scale of minutes were performed among others by Van Kleeff et al. with the yeasts *S. cerevisiae* and *Candida utilis* [1]. In contrast to *S. cerevisiae*, *C. utilis* does not exhibit overflow metabolism. In an intermittent feeding regime, the yield of biomass on glucose decreased by 25% for *S. cerevisiae* compared to a continuous feed regime, and respiratory rates increased. For *C. utilis*, no change in physiology was observed. This difference in the response of the two types of yeast was attributed to a difference in the affinity for glucose of the glucose uptake systems of the two yeast species. The metabolic effects of the intermittent feeding regime were not examined in this study.

The fungus *Penicillium chrysogenum* is widely applied for the industrial production of penicillins and does not exhibit overflow metabolism. Because penicillin production in *P. chrysogenum* is repressed by glucose [2,3], the industrial fermentation process for the production of penicillins is carried out in fed-batch mode, to keep the residual glucose concentration at a non-repressing level. Furthermore, fed-batch cultivation has the advantage that the growth rate can be controlled by controlling the feed rate, to achieve conditions where the productivity is maximal [4]. The disadvantage of substrate limited fed-batch cultivation is that substrate gradients occur, especially in large scale industrial fermentors. The effect of the exposure of *P. chrysogenum* to feast-famine cycles on the penicillin production has been investigated in a scale down study [5]. In this study the feast-famine regime was achieved in a well-mixed lab-scale bioreactor by applying a cyclic feeding pattern of 360 seconds, during which fresh medium was fed only during the first 36 seconds, and no feeding for the remaining 324 seconds. It was observed that the glucose concentration increased rapidly during the first 36 seconds of each cycle, when fresh medium was supplied. Due to rapid uptake by the cells, the glucose was completely consumed at about 200 seconds after the start of each cycle, and remained practically zero during the last 160 seconds until the start of a new cycle. The feast-famine regime had a clear negative effect on the penicillin production, as the penicillin production was approximately a factor 2 lower in the intermittently fed cultures. Remarkably, the yield of biomass on glucose, and the (cycle-averaged) biomass-specific rates of glucose uptake, O<sub>2</sub> uptake and CO<sub>2</sub> production were not significantly different.

In a second study, identical feast-famine experiments were combined with <sup>13</sup>C labeling to quantify the dynamic flux patterns in the glycolysis and pentose phosphate pathway and

connected storage metabolism [6]. Storage carbohydrates (including polyols) are known to have different roles. They can serve as intracellular substrate pools, function to control intracellular osmolarity, and serve as storage pools of reducing power [7]. For example, in *Aspergillus niger*, erythritol and arabitol were found to act predominantly as carbohydrate reserves, while mannitol had a role in balancing the cellular redox potential [8]. Furthermore, in *S. cerevisiae* glycogen and trehalose act as storage carbohydrates with roles during the cell cycle, and trehalose also functions as a stress protectant [9,10]. So, while investigating the role of storage carbohydrate pools during a feast-famine regime in *P. chrysogenum*, it should be taken into account that storage carbohydrates can have various metabolic functions.

In this study, a more thorough and comprehensive analysis of the intracellular metabolic effects of the intermittent feeding regime is made. Therefore the physiological behavior of intermittently fed cultures is compared to that of control chemostat cultures, whereby the medium composition and the (cycle-averaged) dilution rate are the same for the two cultivation regimes. Special attention is paid to the fate (storage and release) of carbon and electrons in reserve carbohydrates and other intracellular metabolite pools, to investigate their role as buffer pools for carbon and electrons from substrate.

## 2 Materials and methods

### 2.1 Strain and cultivation details for chemostat and intermittently fed cultures

The high yielding industrial production strain *Penicillium chrysogenum* DS17690 [11] was kindly donated by DSM Anti-Infectives (Delft, the Netherlands) as spores on rice grains.

The composition of the used media (which supported a biomass concentration of about 5.7 g<sub>DW</sub>/L), the bioreactor setup and controls were exactly as described in [5]. The bioreactor, which was operated at a working volume of 4.0 L and at 0.30 bar overpressure, was inoculated with the fungal spores (prepared by submerging approximately 10 g of rice grains in 100 mL of demineralized water for 1 h at room temperature), and after a batch phase of approximately 60 h, just before all glucose was consumed, feeding was started either in chemostat mode (continuous feeding) or in an intermittent feeding mode. In the chemostat regime, medium was supplied continuously at a rate of 0.20 L/h. The intermittent feeding regime consisted of cycles of 360 s, in which medium was supplied only during the first 36 s at a rate of 2.0 L/h. This cyclic feeding pattern, which was controlled by an industrial timer (PTC-1A Programmable Timing Controller, Omega Engineering Inc.,

USA), was maintained throughout the cultivation. In both feed regimes, the overall dilution rate was the same ( $0.05 \text{ h}^{-1}$ ) as well as the supply of nutrients, such as glucose ( $0.75 \text{ g/L/h}$ ). While the mixing time of the used lab-scale bioreactor was at least much less than 5 seconds [12], the aim of the intermittent feeding regime was to mimic the alternation of high and low substrate concentration experienced by mycelia travelling along the recirculation flows of an industrial fed-batch bioreactor ( $>150 \text{ m}^3$ ) with mixing times of several minutes [13].

## 2.2 Labeling experiments

For one cultivation of both feeding regimes, a labeling experiment with  $\text{U-}^{13}\text{C}$  labeled glucose was performed. A bottle with 100-300 mL of medium was prepared with the same composition as the normal medium, only the naturally labeled glucose was replaced by  $\text{U-}^{13}\text{C}$  labeled glucose at the same molar concentration ( $83.3 \text{ mM}$ ). The bottle was connected to the bioreactor via a separate feed line which was primed until just a few cm before the medium would drop from the headplate into the culture. For the standard chemostat, the labeling experiment started, approximately 232 h after feeding had started, by stopping the pump flow of the medium with naturally labeled glucose and starting the flow of the medium with  $\text{U-}^{13}\text{C}$  labeled glucose at the same time. In the case of the intermittent feeding regime, the experiment started, approximately 175 h after the start of the intermittent feeding regime, by starting a feeding cycle with pumping the medium with labeled glucose. During the labeling experiment, samples were collected at time intervals to measure the labeling enrichment of intracellular and extracellular metabolites. The labeling period was 60 minutes for the standard chemostat and 18 minutes for the intermittently fed culture (3 cycles).

## 2.3 Sampling procedures

The biomass dry-weight was determined daily in triplicate by filtering 5 mL of broth over a glass fiber filter (Pall Corporation, East Hills, USA; 47 mm in diameter,  $1 \mu\text{m}$  pore size) which was washed twice with 10 mL of demineralized water. The filters were dried for approximately 24 hours at  $70 \text{ }^\circ\text{C}$  both before use and after the filtration before weighing them on a microbalance.

Samples for determining extracellular metabolite concentrations were obtained by the cold steel-bead method [14]. About 2 mL of broth was sampled through a thin port in the side of the reactor. The broth sample, which flowed quickly through the port (residence time  $<1$  second) due to the overpressure in the reactor, was collected in a syringe with steel beads which was pre-cooled ( $-20^\circ\text{C}$ ) to cool down the broth sample immediately to close to  $0^\circ\text{C}$  to drastically slow down metabolic activity. The collected broth was then quickly filtered

(0.45  $\mu\text{m}$ ) and 20  $\mu\text{L}$  of the filtrate was immediately transferred to a GC glass vial, to which already 20  $\mu\text{L}$  of  $^{13}\text{C}$  cell extract (see details below) was added as internal standard, and the vial was then immediately submerged in liquid nitrogen to completely stop enzymatic activity, and then stored at  $-80^\circ\text{C}$  until further analysis. For extracellular gluconate measurements, filtrate without  $^{13}\text{C}$  cell extract was used.

Samples for determining the level of intracellular metabolites or the ratio of isotopologues of intracellular metabolites, except those of the penicillin pathway were obtained using a rapid sampling device [15]. Samples of approximately 1.2 mL of broth were collected from the bioreactor in tubes containing 8 mL  $-25^\circ\text{C}$  40% (v/v) aqueous methanol and immediately vortexed for 2-5 seconds [16]. The tubes were centrifuged (5 min, 4800g, pre-cooled swing-out rotor), the pellets washed with 5 mL  $-25^\circ\text{C}$  40% (v/v) aqueous methanol and centrifuged again. If the sample was intended for determining intracellular metabolite levels, 120  $\mu\text{L}$  of  $^{13}\text{C}$  cell extract was added as internal standard to the pellets. [17,18]. Subsequently, extraction was performed by adding 5 mL of preheated (5 min,  $95^\circ\text{C}$ ) 75% aqueous ethanol to the pellets and incubating them for 3 minutes in a water bath at  $95^\circ\text{C}$ . Finally, the extracts were concentrated under vacuum ( $<10$  mbar) at room temperature using a RapidVap (Labconco, USA) until a final volume of approximately 300  $\mu\text{L}$ , and the volume was then adjusted to 600  $\mu\text{L}$  with milli-Q water. Debris was removed by centrifugation and filtration and the sample stored at  $-80^\circ\text{C}$  until analysis. Sampling for intracellular intermediates of the penicillin pathway was done using the cold filtration method [19].

In the case of the  $^{13}\text{C}$  labeling experiments, samples were collected as described above, but no  $^{13}\text{C}$  cell extract was added to the samples.

The  $^{13}\text{C}$  cell extract was obtained from a fed-batch culture of *Penicillium chrysogenum* DS17690 grown on  $>99\%$  U- $^{13}\text{C}$ -labeled glucose (Campro Scientific, Veenendaal, the Netherlands) and  $^{13}\text{C}$ -labeled PAA with all carbon atoms of the aromatic ring labeled (Sigma-Aldrich).

Sampling for glycogen content was also performed using the rapid-sampling device by spraying the broth into  $-25^\circ\text{C}$  40% (v/v) aqueous methanol. After washing by centrifugation, the pellets were extracted for 4 hours at  $95^\circ\text{C}$  in 0.25 M  $\text{Na}_2\text{CO}_3$ , after which the pH of the extract was brought down to 5.2 with an acetate buffer [20].

## 2.4 Analytical procedures

The extracellular gluconate concentration was determined enzymatically. All other metabolites were analyzed using GC-MS and LC-MS methods as described in the following.

Intracellular intermediates of the glycolysis and TCA cycle (G6P, F6P, M6P, FBP, T6P, 6PG, PEP G3P, pyruvate,  $\alpha$ KG, succinate, fumarate, malate, and the combined pools of citrate + isocitrate, 2PG + 3PG and G1P + M1P) were determined using LC-MS/MS. [21].

For GC-MS analysis of R5P, S7P, trehalose, mannitol, erythritol and glucose, 100  $\mu$ L of sample was freeze-dried and subsequently derivatized as described in [5].

The metabolites related to the penicillin pathway were analyzed using the LC-MS/MS method described in [22].

For analysis of the amino acids Ala, Leu, His, Ser, Gly, Tyr, Phe, Trp, Asn, Asp, Met, Thr, Ile, Glu, Gln, Pro and Lys, the GC-MS method was used as described in [23]. The presence of the tripeptide ACV interferes with the analysis of AAA and Val in this latter method, and analysis of Cys is unstable in this method. Therefore, these three amino acids were analyzed by the GC-MS method described in [5].

Metabolite concentrations were determined using the ID-MS method (isotope dilution mass spectrometry), which relies on  $^{13}\text{C}$  labeled internal standards [17,18]. For determining the ratio of metabolite isotopologues, the same derivatization and separation techniques were applied, and the selected ion monitoring (SIM) mode was extended to include the  $m/z$  of all expected isotopologues of the selected metabolite (fragment). Both LC- and GC-MS measurements were corrected for the presence of natural isotopes of non-carbon atoms using the correction tool of Wahl et al.[24].

The carbonate extracts were used to hydrolyze extracted glycogen to glucose using amyloglucosidase (Fluka Biochemika 10115) by incubation at 57°C overnight with shaking. Quantification of glycogen content was done by enzymatic determination of glucose. To measure the labeling enrichment of the glucose monomers derived from the extracted glycogen, the hydrolysate was analyzed by the above-mentioned GC-MS method.

## 2.5 Calculatory procedures

### 2.5.1 Reconstruction of the $q\text{O}_2$ and $q\text{CO}_2$ in the intermittent feeding regime

For the intermittent feeding regime, a reconstruction of the dynamic biomass-specific rates of  $\text{O}_2$  uptake and  $\text{CO}_2$  production from dynamic measurements of the concentrations of dissolved  $\text{O}_2$  and gaseous  $\text{O}_2$  and  $\text{CO}_2$  in the offgas was made following the procedure described in [25].

### 2.5.2 Additional correction of intracellular metabolite levels

One of the datasets of intracellular metabolite levels from an intermittent feeding experiment showed for all metabolites some peculiar elevated and decreased levels which



were out of the time trend at certain time points during the 360 s cycle. These out-of-trend levels were attributed to pipetting errors in the added volume of  $^{13}\text{C}$  cell extract (internal standard), which explains why they were observed for all metabolites. Therefore a correction for the out-of-trend levels was applied as follows. No time pattern was observed in the trehalose level (see section 3.3), and so the average from all sample points of the trehalose level was considered a good estimate of the trehalose level at each sample time point. All other metabolite levels in the dataset were then corrected by multiplying them by the ratio of the average trehalose level and the non-averaged trehalose level at the same sample time point.

### 2.5.3 Estimation of turnover rates of storage pools from labeling data

The storage pools considered in this study were trehalose, glycogen and mannitol. The approaches taken to estimate the turnover rate of these pools for the chemostat and intermittent feeding regime are explained below.

#### 2.5.3.1 Chemostat regime

The following procedure was followed for the estimation of the turnover rate of storage pools under chemostat regime. By definition in the chemostat regime, the (cell-specific) concentration of each storage pool is constant, and the flux into the pool equals that of the (total) flux out of the pool. The turnover rate  $\phi$  (in  $\text{h}^{-1}$ ) was defined as the ratio of the flux (in  $\mu\text{mol}/\text{g}_{\text{DW}}/\text{h}$ ) to the pool concentration (in  $\mu\text{mol}/\text{g}_{\text{DW}}$ ) and is also constant. A simple model was set up to describe the dynamic change of the fully unlabeled and fully labeled fraction of a storage pool by the influx of its fully unlabeled and fully labeled precursor. This influx occurs at turnover rate  $\phi$  ( $\text{h}^{-1}$ ) which can be estimated by minimization of the error between the simulated and measured (see section 2.2) changes of the labeling fractions (fractions of isotopologues) of the storage pool. In the simulation, the magnitude of the fully unlabeled and fully labeled fractions of the precursor were based on the labeling measurements of the precursors, and in between sample time points they were calculated by linear interpolation between the values measured at the sample time points.

Only in the case of trehalose, its direct metabolic precursor T6P was measured in the experiment and used as such in the calculations outlined above. However, the metabolic network connections of the mannitol pathway are not completely elucidated and in this case it was assumed for the calculations that F6P was its precursor. The labeling of the direct precursor of glycogen, UDP-glucose, was not measured and the closest measured precursor G6P was used for the calculations instead.

The labeling state of the metabolites was measured in this experiment by GC-MS and therefore only information about the molecular fragment detected by the GC-MS was obtained (C6 for trehalose, C6 for T6P, C4 for mannitol, C3 for F6P, C4 for glucose derived from glycogen and C4 for G6P). In view of the fact that during the labeling experiment naturally labeled glucose in the medium was exchanged for fully labeled glucose, the predominant fractions in the relevant metabolites were the fully unlabeled and fully labeled ones. For the purpose of estimating the turnover rates it was therefore considered acceptable to perform the calculations using the measurements on the fully unlabeled and fully labeled molecular fragments of the metabolites detected by the GC-MS.

### 2.5.3.2 Intermittent feeding regime

#### *Trehalose*

The labeling enrichment of trehalose was measured by GC-MS on a C6 fragment containing the six carbons of one of the two glucose moieties. The labeling enrichments of 13 isotopologues (m+0 to m+12) of T6P were measured by LC-MS.

To estimate the turnover of trehalose, the following reasoning and assumptions were made. A molecule of T6P m+12 will be formed into a molecule of trehalose m+12 by T6P phosphatase, and is detected by the used GC-MS method as an m+6 isotopologue. However, after dephosphorylation, T6P m+11 will be detected as trehalose m+6 in only about half of the cases. The fractions of T6P m+6 to m+10 will contribute to trehalose m+6 formation in even smaller ratios. In view of the fact that fully labeled glucose was used as substrate in this experiment, the predominant fractions of G6P, G1P and UDP-glc were m+0 and m+6, so the likelihood is high that a molecule of T6P m+6 consisted of a glucose moiety m+0 and a glucose moiety m+6. Therefore, for modeling purposes it was assumed that T6P m+6 contributed in half of the cases to a trehalose m+6 detection. The T6P fractions m+7 to m+10 were assumed not to contribute to trehalose m+6 detection, which is justified in view of their small pool size (only 17% of the T6P was in these fractions).

A model was set up describing the dynamic change of the fraction of the detected trehalose m+6 isotopologue, based on a dynamic flux through the trehalose pool from T6P and based on the labeling fractions of the m+6, m+11 and m+12 isotopologues of T6P. It was assumed that the influx into and efflux from the trehalose pool were always equal, because no significant concentration changes in the measured trehalose pool were observed. These considerations lead to the following ODE:

$$\frac{df_{\text{treh},m+6}}{dt} = \frac{v(t)}{c_{\text{treh}}} \cdot \left( f_{\text{T6P},m+12} + \frac{1}{2} f_{\text{T6P},m+11} + \frac{1}{2} f_{\text{T6P},m+6} - f_{\text{treh},m+6} \right) \quad (1)$$

The influx and efflux  $v(t)$  was modeled as a piecewise linear flux with knots at the cycle times 0, 36, 72 ... 324 seconds [26]; the flux in between the knots were obtained by linear interpolation. An estimation of the flux  $v(t)$  was obtained by minimizing the error between the simulated (eq. 1) and measured  $m+6$  fraction of trehalose, allowing to vary the magnitude of the flux at the knots. Finally, the average flux was obtained by the following calculation:

$$v_{\text{average}} = \frac{\int_{t=0}^{360s} v(t)dt}{360s} \quad (2)$$

### *Mannitol*

The same approach as for trehalose was taken to calculate the turnover of the mannitol pool during the intermittent feeding regime using labeling data. The dynamic changes in the fully labeled and fully unlabeled fractions of mannitol were modeled with the measured fully labeled and unlabeled fractions of F6P as input and varying the flux as a piece-wise linear flux, analogously to the ODE in equation 1.

#### 2.5.4 Flux balance analysis for uptake, secretion and intracellular reaction rates

Classical flux balance analysis was performed on data from an intermittently fed culture. The macroscopic rates which form the input for the calculation were cycle-averaged and subsequently reconciled with respect to elemental conservation balances. The metabolic network presented by Van Gulik et al. [4] was used, with an adaptation to the biomass formation reaction to reflect differences in trehalose and mannitol levels in mycelia grown under intermittent feeding conditions, as reported in the results section of this chapter.

## 3 Results and discussion

The concentration profile of extracellular glucose during the feeding cycles of the intermittently fed cultures is given in Figure 3 in [5]. Per cycle, 75 mg/L (or 73  $\mu\text{mol/g}_{\text{DW}}$ ) of glucose was fed, which was apparently all taken up, as the concentration of glucose between 200 and 360 seconds was practically zero. Nevertheless, the dissolved oxygen concentration varied much less dynamically (Figure 1 in [5]) compared to the glucose consumption rate, which suggested that a significant amount of the consumed glucose was accumulated during the feast and consumed during the famine period of each cycle.

### 3.1 Excreted metabolites in the feast/famine regime

To investigate how *P. chrysogenum* organizes its carbon and electron flows during the alternating periods of glucose excess and glucose depletion in the intermittent feeding

regime, various measurements were done in the culture filtrate, to check if any metabolites were accumulating in large amounts extracellularly and were subsequently consumed and thus would act as external carbon buffers.

It is well known that *P. chrysogenum* converts glucose to gluconate if glucose is present at high concentrations. However, measurements revealed that only low concentrations of gluconate were present in the culture filtrate of cultures subjected to the intermittent feeding regime: at  $t=51$  s after the cycle start the measured concentration was  $48\pm 19$   $\mu\text{mol/L}$ , at  $t=120$  s  $59\pm 25$   $\mu\text{mol/L}$  and at  $t=272$  s  $31\pm 39$   $\mu\text{mol/L}$ . Based on the standard deviations of these measurements, it's not possible to determine if the concentration changed during the cycle. However, based on the low concentrations found it can be concluded that, even though there might be a fast flux through the pool, gluconate is not used as extracellular carbon buffer during the intermittent feeding regime.

In addition, relatively high concentrations of some metabolites related to penicillin biosynthesis were measured in the culture filtrate, including the side chain precursor PAA (present in the feed medium), PenG, 6-APA and OPC (see Table 1). Multiple samples were analyzed during the cycle (16 or more, depending on the experiment/culture), but the measured concentrations did not change significantly. Furthermore, low concentrations of other metabolites were measured in the culture filtrate, namely erythritol (80  $\mu\text{M}$ ), mannitol (150  $\mu\text{M}$ ), trehalose (8  $\mu\text{M}$ ), fumarate (0.7  $\mu\text{M}$ ) and succinate (0.9  $\mu\text{M}$ ). Also their concentrations did not vary noticeably during the cycle.

No metabolites were found which are usually associated with overflow metabolism in certain bacteria or yeasts, such as lactate, acetate or ethanol. This is in line with a very early observation that *P. chrysogenum* does not excrete lactate in the presence of glucose [27]. From measured TOC contents of the culture filtrate it could be calculated that the filtrate contained about  $36\pm 5$   $\text{mCmol/L}$  of unknown (unidentified) compounds at any time during the cycle. It is very likely that this pool consisted mainly of cell debris, excreted proteins and carbohydrates, because significant amounts of these were also found in conventional chemostat cultures of the same strain of *P. chrysogenum* [4,5].

All in all, no specific compounds were measured in the extracellular liquid which accumulated to significant levels. This can also be expressed in terms of rates: glucose was fed at 25  $\text{mCmol/L/h}$ , while organic carbon in the culture filtrate which was unrelated to penicillin production was produced at only 1.9  $\text{mCmol/L/h}$ , which is only 7.6% of the carbon fed as glucose. This indicates that the feast-famine regime did not incite *P. chrysogenum* to exhibit extracellular overflow metabolism.

**Table 1** Extracellular concentrations in culture filtrate of intermittently fed cultures. Expressed in  $\mu\text{mol/L}$ ,  $\text{mCmol/L}$  and  $\mu\text{Cmol/g}_{\text{DW}}$ .

Extracellular compound	$\mu\text{mol/L}$	$\text{mCmol/L}$	$\text{mCmol/g}_{\text{DW}}$
PAA	3.1E3	25	4.3
PenG	0.69E3	11	1.9
6-APA	0.30E3	2.4	0.41
OPC	0.62E3	3.7	0.64
Trehalose	8	0.096	0.016
Mannitol	0.15E3	0.90	0.15
erythritol	80	0.32	0.055
gluconaat	45	0.27	0.046
TOC filtrate	NA	80	14
Unknown compounds	NA	36	6.2

### 3.2 Dynamic biomass-specific rates for $\text{O}_2$ uptake and $\text{CO}_2$ production

The dissolved  $\text{O}_2$  tension and the off-gas concentrations of  $\text{O}_2$  and  $\text{CO}_2$  were clearly fluctuating in a periodic pattern of 360 seconds (Figure 1 in [5]). These measurements indicate that the biomass specific oxygen uptake and carbon dioxide production rates ( $q_{\text{O}_2}$  and  $q_{\text{CO}_2}$ ) were very dynamic during the cycle. To calculate from the dynamic off-gas measurements in which way the two rates fluctuated during the cycle is not a simple task: the measured responses in the off-gas concentrations are distorted due to the mixing and dispersion of the gas in the off-gas system, and the measured DO is lagging behind the real DO due to probe lag. Moreover, a substantial amount of the dissolved  $\text{CO}_2$  which is produced by the cells may be converted to bicarbonate, which is a big pool (same order of magnitude as the dissolved  $\text{CO}_2$ ) at the working pH of 6.5. All these distortions were taken into account to reconstruct the actual  $\text{O}_2$  uptake and  $\text{CO}_2$  production rates by calculation using a recently developed approach [25]. The reconstruction results of a representative data set from one particular cultivation covering measurements from fifteen cycles are presented in Appendix 1. The average patterns of  $q_{\text{O}_2}$  and  $q_{\text{CO}_2}$  of these fifteen cycles are presented in Figure 1. It can be seen that both  $q_{\text{O}_2}$  and  $q_{\text{CO}_2}$  rise quickly at the start of the cycle, when glucose is supplied and thus the glucose uptake rate is high. The rates remain high for approximately 180 seconds, and then begin to decrease slowly. However, respiration continues throughout the cycle, also when the glucose is completely exhausted (200 s after the start of the cycle). Interestingly, the respiratory quotient is somewhat higher than average during the first 180 seconds, and lower after that. This could indicate that the glucose that is taken up, is (at least partially) first converted into compounds which are

more reduced than glucose, which are oxidized later on in the cycle. Potential candidates for these reduced compounds are reduced carbohydrates like polyols, such as mannitol, erythritol and arabitol, which could accumulate during the feast period and be consumed thereafter.

The integral amount of carbon released in the form of  $\text{CO}_2$ , calculated from the reconstructed  $q_{\text{CO}_2}$  in Figure 1, is  $203 \mu\text{Cmol/g}_{\text{DW}}$  per cycle, while per cycle  $430 \mu\text{Cmol/g}_{\text{DW}}$  of glucose is taken up. So, about 47% of the consumed glucose is released as  $\text{CO}_2$ , while the remaining part is converted to biomass, PenG and byproducts. This matches very well with the ratio of averaged rates reported earlier in Table 1 in [5]. In addition,  $189 \mu\text{mol/g}_{\text{DW}}$  of  $\text{O}_2$  is consumed per cycle to accept  $756 \mu\text{mol/g}_{\text{DW}}$  of electrons, while  $1718 \mu\text{mol/g}_{\text{DW}}$  of electrons were consumed in the form of glucose, which represents a ratio of 44% of  $q_{\text{O}_2}$  to  $q_{\text{glc}}$ . This also matches the cycle-averaged ratio.

In the feast period of the cycle (between  $t=0$  and  $200$  s),  $126 \mu\text{Cmol/g}_{\text{DW}}$  of  $\text{CO}_2$  was produced, while in the famine period, in which no glucose was taken up (between  $t=200$  s and  $t=360$  s),  $77 \mu\text{Cmol/g}_{\text{DW}}$  of  $\text{CO}_2$  was produced. In the next sections it will be discussed in which intermediate form (after it was taken up as glucose and before it was released as  $\text{CO}_2$ ) this carbon was stored in the cells.

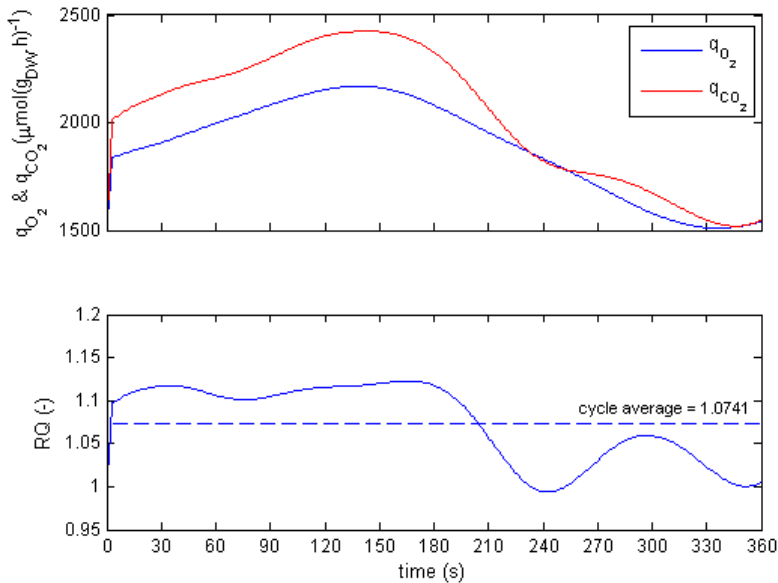


**Figure 1** Reconstructed  $q_{\text{O}_2}$ ,  $q_{\text{CO}_2}$  and RQ (respiratory quotient).

### 3.3 Storage carbohydrate pools: need for $^{13}\text{C}$ -labeling

The intermittently fed cultures consumed carbon in the form of glucose during the first 200 seconds of each 360 second cycle, and excreted carbon in the form of  $\text{CO}_2$  throughout each cycle (see Figure 1). Overall, 44% of the consumed carbon was excreted as  $\text{CO}_2$ , 40% was used to produce new biomass, 2% was used for PenG formation, and the remaining 14% ended up in extracellular byproducts like excreted proteins, carbohydrates and lysis related byproducts (disintegrated biomass) (Table 1 in [5]). This raises the question in which form the carbon, which was consumed in the first 200 seconds but which was not directly turned into one of these final (by)products, was stored, until it was transformed into one of the final (by)products during the last 160 seconds of each cycle.

Nasution et al. suggested that *P. chrysogenum* shuttles a significant part of glucose into intracellular pools of storage carbohydrates (glycogen, trehalose) when glucose-limited cells grown under a carbon-limited chemostat regime are perturbed by a glucose pulse (chapter 4 in [28]). In the intermittently fed cultures, this might also happen during the feast period. However, in these cultures a high RQ of about 1.1 was observed during the period of glucose-excess (first 200 seconds, see Figure 1), which suggests accumulation of an intracellular compound with a degree-of-reduction higher than that of glucose during this period; therefore trehalose and glycogen (which have a degree of reduction of 4 emol/Cmol, like glucose) don't seem to be the most logical candidates. To investigate their role during the feast-famine regime, the intracellular concentrations of the most important storage carbohydrates and polyols (trehalose, glycogen, mannitol and arabitol) were measured in cells from both the chemostat and intermittently fed cultures. During the intermittent feeding regime, samples were also taken during one feeding cycle. The results are presented in appendix 2. It was found that the intracellular glycogen level was relatively low in both conditions: about 5.7 mg/g<sub>DW</sub> in chemostats and about 3 mg/g<sub>DW</sub> in intermittently fed cultures. The intracellular levels of trehalose, mannitol and erythritol were much higher, but also very different in the two regimes: the trehalose concentration was 3 times higher and the mannitol concentration 4.6 times lower in the intermittent feeding regime. Erythritol showed a different concentration profile over cultivation time in the two feeding regimes, but had a comparable concentration after about 150 hours.

A clear concentration pattern within the cycle was observed for mannitol, which increased from about  $79 \pm 0.8 \mu\text{mol/g}_{\text{DW}}$  at the beginning of the cycle to  $88 \pm 0.8 \mu\text{mol/g}_{\text{DW}}$  in the middle of the cycle, whereafter it decreased again (see Figure 2). However, no dynamic concentration profile could be discerned in the cycle measurements of trehalose, glycogen and erythritol (appendix 2). The (sampling and analytical measurement) error of the measurement of the trehalose level is about 5%, corresponding to  $9 \mu\text{mol/g}_{\text{DW}}$ . Considering

that in every cycle about  $73.5 \mu\text{mol/g}_{\text{DW}}$  of glucose is fed, and assuming that one tenth of that would be converted into trehalose, then such an increase would be smaller than the error of the measurement. So, the direct measurement of the concentration of trehalose is not accurate enough to determine how much of the consumed glucose is shuttled into that pool. Therefore,  $^{13}\text{C}$  labeling experiments were performed, in which medium with fully  $^{13}\text{C}$ -labeled glucose was fed and the labeling enrichment of the intracellular pools of the two presumably most abundant storage metabolites, trehalose and mannitol, were measured during three consecutive cycles. Then, from the concentration and labeling data of these storage pools and the (assumed) metabolic precursors, the fluxes through these pools were calculated; see Figures 4 and 5. In this calculation, the labeling of the (assumed) metabolic precursors was used as input and a flux through the storage pools was allowed to vary over the cycle time. The error between the measured and modeled labeling fraction(s) of the storage carbohydrate was minimized to determine the flux, which was modeled as a piecewise linear model (see section 2.5.3.2 for more details). For both trehalose and mannitol, it was found that the flux increased during the first part of the cycle until 144 seconds, and then decreased (Figures 4 and 5). The flux through the trehalose pool increased 8-fold, and the flux through the mannitol pool also varied highly. The cycle-averaged flux through the trehalose pool was  $32.3 \mu\text{mol/g}_{\text{DW/h}}$ . (The cycle-averaged flux was also calculated in a slightly different approach using the Cmol-enrichment of T6P and trehalose instead of the isotopologue fractions, yielding an averaged flux of  $27.8 \mu\text{mol/g}_{\text{DW/h}}$ , instead of  $32.3 \mu\text{mol/g}_{\text{DW/h}}$ , which is very close and therewith confirms the result. However, the calculation based on Cmol-enrichment is thought to be less accurate, because of the relatively high variance in the measurements of the trehalose isotopologues other than m+6, and therewith the calculated Cmol enrichment.)

A similar labeling experiment was also performed in a conventional chemostat culture to determine the turnover rates of storage pools in that regime. Again with the help of a simple model, the flux through the pools of trehalose, mannitol and glycogen were calculated (see Figure 3), using the measured labeling data of the (nearest) metabolic precursor as an input. A good fit of the model on the measured labeling data could be obtained.

Interestingly, the labeling data of G6P and F6P indicate that after 600 s only about 75% of the pool is fully labeled and this didn't increase much until 3600 s, although only fully labeled glucose was fed to the bioreactor during this period (Figure 3). This indicates that there is a significant turnover of unlabeled storage material, which is in line with the calculated fluxes through the storage pools.

All measured concentrations and calculated (cycle-averaged) fluxes for both feeding regimes are also presented in Table 2.



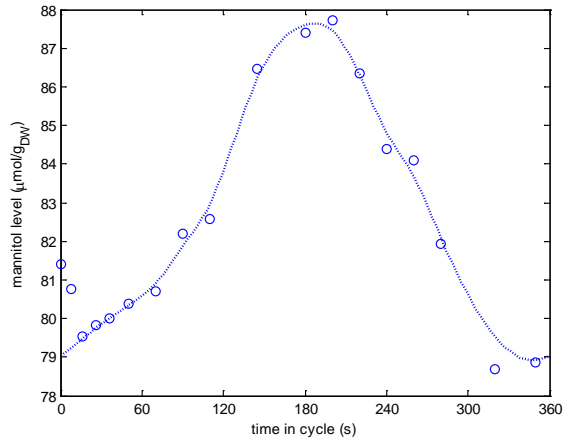


**Figure 2** Intracellular mannitol level during a cycle. Circles represent measured values. Dotted line: spline through data points.

**Table 2** Comparison of the turnover rates of storage carbohydrate pools in the chemostat regime and the intermittent feeding regime

	Chemostat regime			Intermittent feeding regime		
	Concentration (μmol/g <sub>DW</sub> )	Flux (μmol/g <sub>DW</sub> /h)	Turnover rate $\phi$ (h <sup>-1</sup> )	Average concentration (μmol/g <sub>DW</sub> )	Average flux (μmol/g <sub>DW</sub> /h)	Turnover rate $\phi$ (h <sup>-1</sup> )
Trehalose	59.1 ± 9.8	16.4	0.278	177.3	32.3	0.182
Mannitol	374 ± 62	127	0.341	82.4	67.7	0.821
Glycogen*	31.6 ± 3.4	5.5	0.174	16	Not measured	
Arabitol	24.3 ± 4.1	2.2	0.099	Not measured	Not measured	
Erythritol	75.3 ± 13.4	12.6**	0.168**	65.4	Not measured	

\*Glucose-equivalents

\*\*Underestimation: this is a minimal value, based on the assumption that the pre-cursor of erythritol was fully labeled during the labeling experiment.

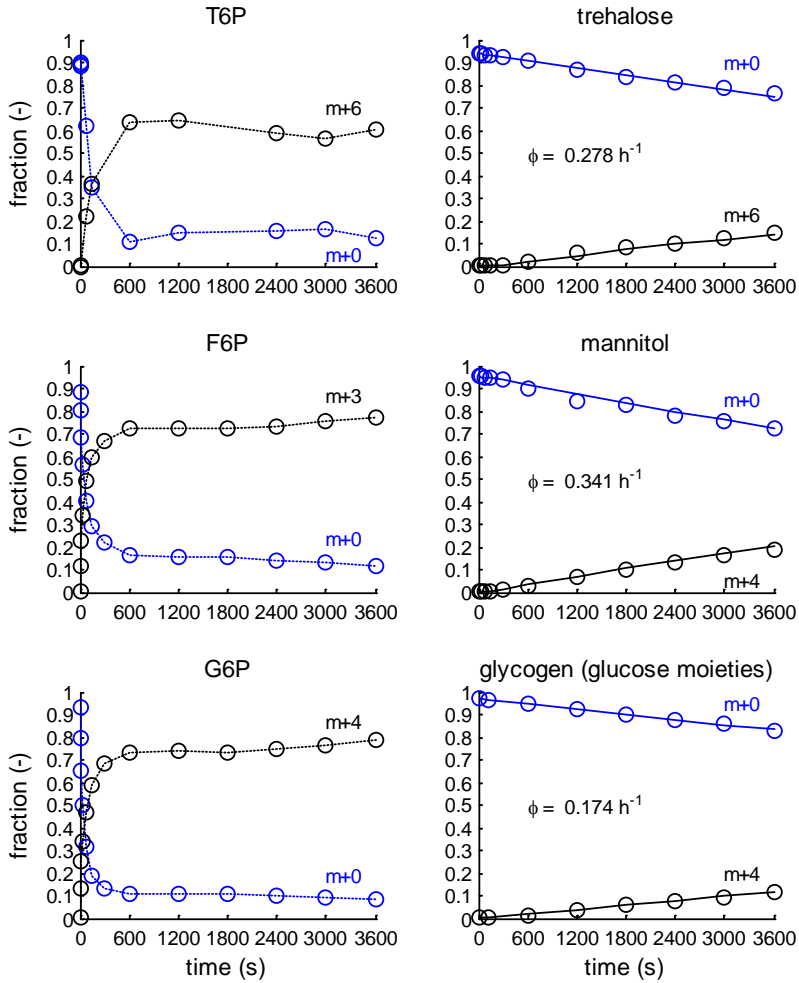


**Figure 3** Labeling of storage pools and their precursors under chemostat regime. Each circle represents the measurement of a fully unlabeled (blue) or fully labeled (black) fraction of the molecular fragment detected by the GC-MS (corrected for natural labeling of the derivatization) for the indicated metabolite. The dotted lines in the plots of the precursors (left) T6P, F6P and G6P indicate the interpolations used for the simulation of the change in labeling of the storage pools (right) trehalose, mannitol and glycogen, respectively. The solid lines in the plots of the storage pools represent the fitted dynamics of the labeling fractions. The turnover rate ( $\phi$ ) obtained by the fitting procedure is indicated for each storage pool.

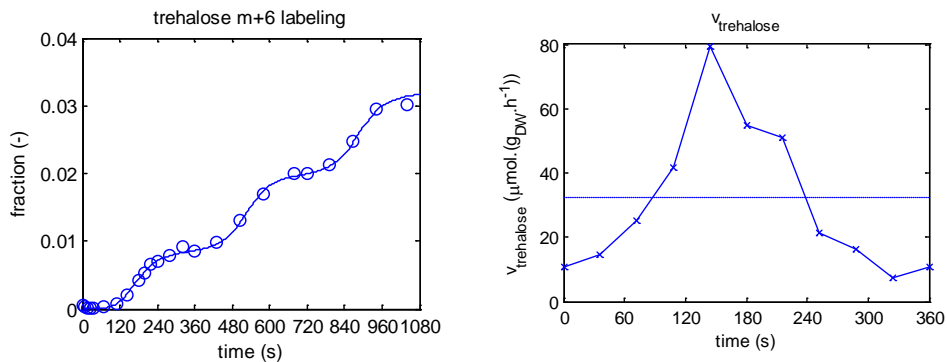


**Figure 4** Labeling of trehalose under the intermittent feeding regime. Left: trehalose m+6 (open circles represent measurements, line represents model output). Right: modeled flux (piece-wise line) through trehalose pool during one feeding cycle, and the average flux (dashed line).

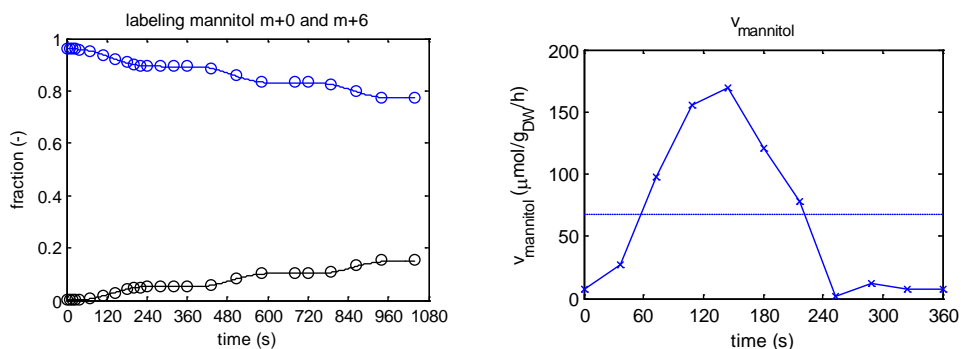


**Figure 5** Labeling of mannitol under intermittent feeding regime. Left: measurements (circles) of fractions of m+0 (black) and m+6 (blue) during three intermittent feeding cycles, and model (line). Right: modeled flux (piecewise line) through the mannitol pool during one feeding cycle, and the average flux (dashed line).

From the combined turnover fluxes of trehalose and mannitol, expressed in glucose equivalents, of 132.3 μmol/ g<sub>DW</sub>/h and the average glucose consumption rate of 735 μmol/ g<sub>DW</sub>/h it can be calculated that in the intermittent feeding regime, 18 % of the consumed glucose passes through the pools of mannitol and trehalose. In the chemostat regime, this is 22%. These two values are very comparable, which means that overall there isn't a higher storage turnover rate in the intermittent feeding regime. Furthermore, Table 2 shows that:

- there are major differences in storage metabolism under the two regimes

- only a fraction of the carbon taken up during glucose excess is shuttled through storage pools. So, in search of the answer to the question where *Penicillium chrysogenum* shuttles the carbon from glucose which has been taken up during the feast period, it can be concluded that carbon is certainly not largely accumulated in the form of trehalose, glycogen and/or mannitol.

### 3.4 Other metabolite levels

#### 3.4.1 Dynamic patterns

Apart from storage and release of carbon, supplied as glucose, in the form of the compounds addressed above, it could be that part of it is accumulated as intermediates of central carbon metabolism and/or other intracellular metabolites. Therefore we quantified a large number of intracellular metabolites during the feast famine cycles. The results are presented in Figures 6 until 14. Furthermore mass action ratios for a selection of enzymatic reactions are presented in Figure 15.

It can be seen from Figure 6 that the pools of hexose-phosphates are very dynamic and are almost exhausted at the start of each cycle. For G6P and F6P there is a delay of about 10 to 20 seconds before their levels start increasing rapidly, whereas M6P and G1P seem to increase immediately once glucose is in excess. The increase in FBP is even more delayed, about 40 seconds. Interestingly, the levels of the hexose-phosphates start to decrease as from about 120 seconds, whereas glucose is still in excess at that moment. However, the glucose uptake rate is also decreasing in this period [5]. The 2PG, 3PG and PEP levels decrease during glucose excess and return to their original level when the extracellular glucose is depleted. These patterns are expected, because the reactions between 2PG, 3PG and PEP are reversible and the enzyme pyruvate kinase is feed-forward activated by FBP. Analysis of pyruvate yielded very different levels for three different experiments; it is suspected that this is due to an issue of the analytical method for pyruvate. Anyway, in all three experiments pyruvate levels didn't show pronounced dynamics during the cycles. (Iso)Citrate and  $\alpha$ -ketoglutarate have very peculiar profiles, starting with a slow accumulation (slow response to glucose uptake) and then a fast increase and decrease between 200 and 280 seconds. The succinate profile is not very clear, but the profiles of fumarate and malate are a delayed imitation of those of the hexose-phosphates, although their pools do not get depleted.

Most amino acids don't show any dynamics, which is probably due to their long turnover times (see Table 3). However, there are some exceptions. The dynamics observed in glutamate and aspartate are probably caused by changes in the NAD/NADH ratio [28,29]. The dynamics of alanine can be the result of a high activity of alanine aminotransferase,

under the influence of the dynamics of glutamate and  $\alpha$ -ketoglutarate. The dynamics observed for leucine, isoleucine, tyrosine and glycine may well be explained by the smaller turnover times of these pools (Table 3). On the other hand, the turnover times of valine and histidine (in Table 3) seem to be overestimated, because the intracellular levels of these two free amino acids exhibit clear dynamics during the cycle (Figure 12 and 14), whereas their estimated turnover times are much longer than the cycle time (Table 3). The resemblance of the leucine and isoleucine profiles is remarkable and could feed the hypothesis that there is an isomerase interconverting these two amino acids. During biosynthesis of penicillin, AAA is incorporated into ACV, but released again when for the formation of PenG the side chain formed by AAA in IPN is exchanged for PAA. In view of the high ATP requirements for ACV synthesis, where 3 ATP are hydrolyzed to 3 AMP, it is expected that the activity of ACVS is high during the beginning of the cycle when the energy charge is high (Figure 8), and lower when the energy charge is reduced towards the end of the cycle. In line with this expected dynamic change in ACVS activity, the level of AAA is observed to decrease in the beginning of the cycle, and to return to its original level at the end of the cycle.

**Table 3** Turnover times of metabolite pools in the intermittent feeding regime. Turnover times were calculated from net fluxes obtained from flux balance analysis and cycle-averaged levels.

metabolite pool	turnover time (s)	metabolite pool	turnover time (s)	metabolite pool	turnover time (s)
G6P	7.6	UDP-glc	1570	Pro	417
F6P	1.9	mtl-1P	94	Asn	1999
FBP	5.6	Trehalose	70331	Asp	1911
23PG	3.2	Mannitol	70838	Met	63
PEP	2.9	Erythritol	104883	Glu	599
pyr	20	Ribose5P	144	Phe	92
cit	5.8	S7P	127	AAA	83
aKG	3.1	Ala	16149	Cys	60
succ	2.8	Gly	681	Gln	1160
fum	4.3	Val	563	Lys	324
mal	19	Leu	269	His	746
G1P	137	Ile	246	Tyr	168
6PG	0.61	Thr	2142	Trp	96
G3P	242	Ser	619	ATP	3.1
T6P	437			ADP	0.43

Measurement of the adenine nucleotides yielded very different levels for three different intermittent feeding experiments. The reason for this could not be found, but it might be due to errors made in the preparation of calibration standards. Nevertheless, the sum of ATP, ADP and AMP seem equally constant in the three experiments and the dynamics of the energy charge were equal for two experiments. UTP shows an opposite trend compared to ATP, which may be related to the formation of UDP-glc. UDP mimics ADP. The mass action ratio of myokinase is not constant, so there is no equilibrium at this time scale.

The mass action ratios for PGI, PGM, PMI, fumarase, “enolase” and Mtl1P-DH are not constant during the cycle and pseudo-equilibrium for these reactions can't be assumed on this time-scale.

The (normalized) NAD/NADH ratio was calculated from assuming (lumped) near equilibrium reactions in which the NAD/NADH couple was involved. First, equilibrium was assumed in the pool of FBP, GAP, DHAP and 2PG+3PG, and secondly, equilibrium was assumed in the reactions of aspartate transaminase, malate dehydrogenase and fumarase. When the (normalized) NAD/NADH ratio was calculated from these two equilibrium pools, a decrease in the (normalized) NAD/NADH ratio was found in the beginning of the cycle (see Figure 8), in line with expected higher fluxes through glycolysis and the TCA cycle in that part of the cycle, and an increase in the famine phase. Although the trend obtained from the two equilibrium pools is similar, the obtained normalized ratios are different; especially in the later part of the cycle the profiles of the ratios behave differently, mainly due to the peculiar profile of  $\alpha$ -ketoglutarate. This may indicate different behavior of the NAD/NADH ratio in the cytosol as compared to that in mitochondria. The observed decrease in the NAD/NADH ratio during the beginning of the cycle is in line with the observed accumulation of other reduced compounds, such as mannitol (Figure 2). If, however, the NAD/NADH ratio is calculated from assuming fast equilibrium between F6P and mtl1P by the mtl1P-DH reaction, the opposite trend in NAD/NADH ratio is obtained (Figure 15). Possibly, the fast equilibrium assumption is incorrect in this case, which may be due to a very low activity of the mtl1P-DH in this organism/strain or under the current conditions.

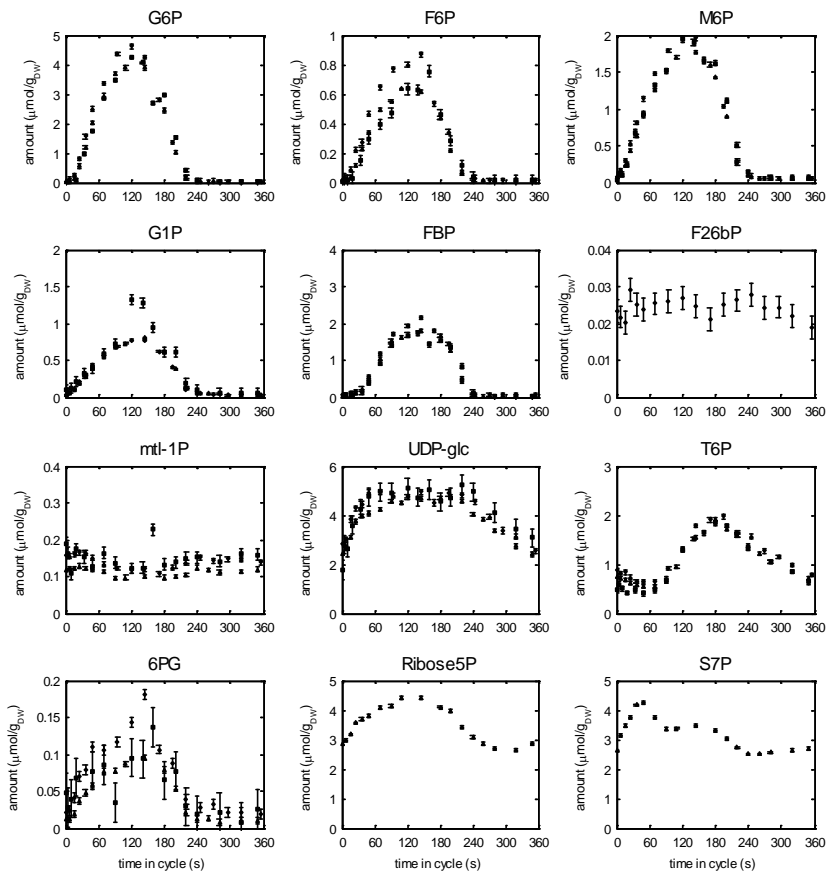


**Figure 6** Metabolite pools from upper glycolysis, hexose-phosphates, intermediates of storage metabolism and PPP. The three different symbols represent measurements from three independent cultures.

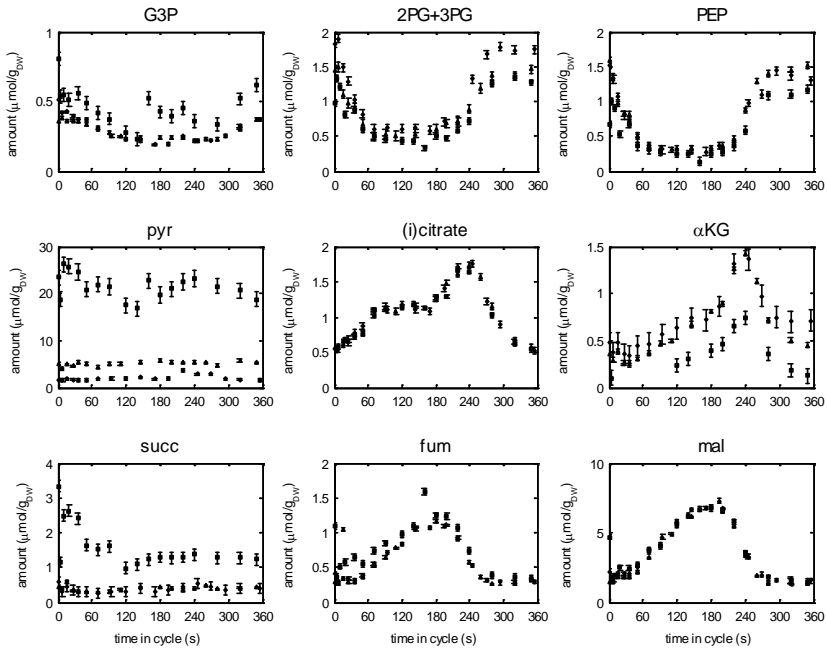


**Figure 7** Metabolite pools of lower glycolysis, TCA cycle and G3P.



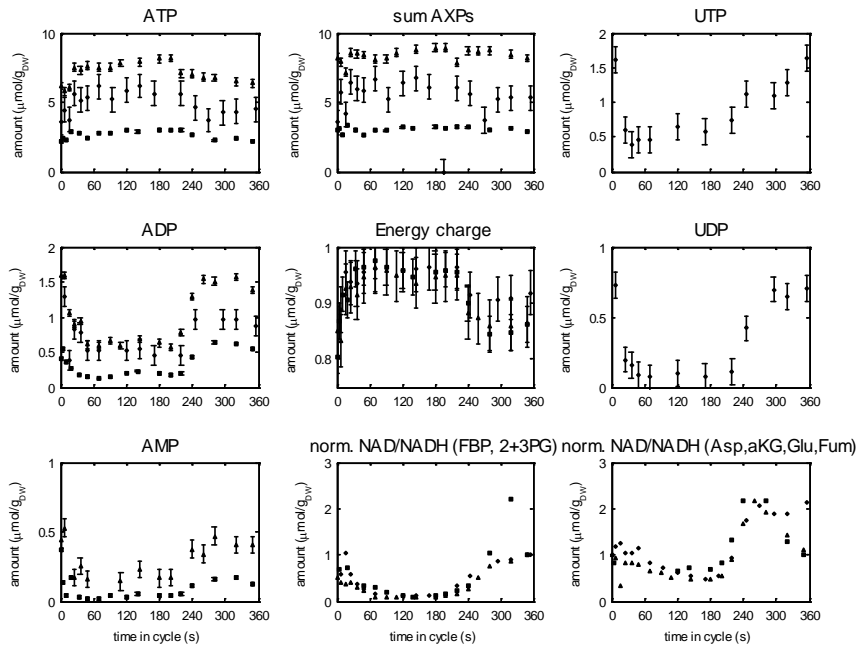


**Figure 8** Nucleotide pools, energy charge and calculated normalized NAD/NADH ratio.

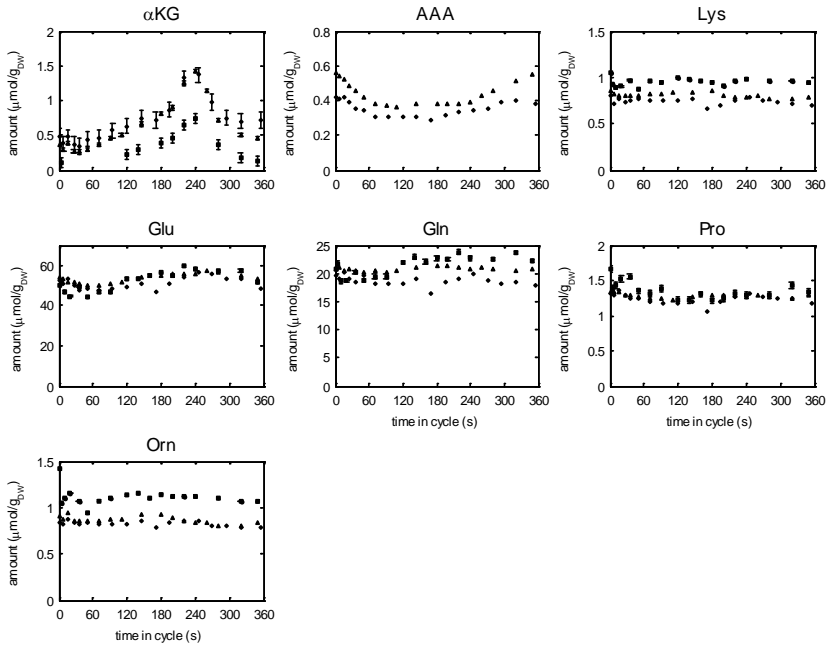


**Figure 9** Pools of amino acids from the glutamate family, with precursor  $\alpha$ KG.

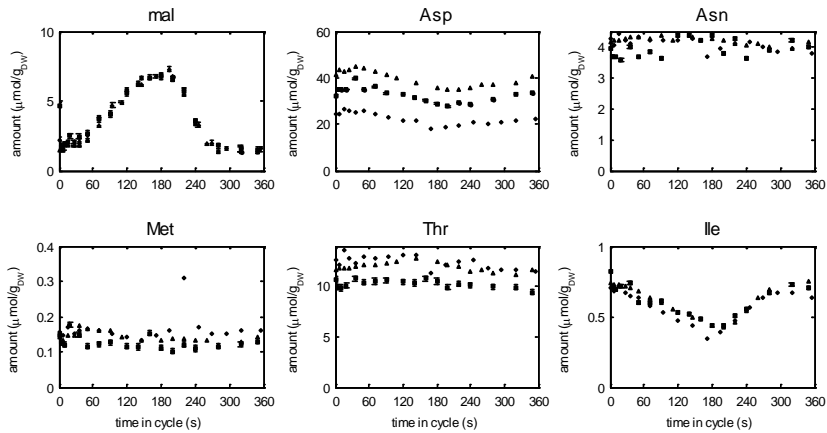


**Figure 10** Pools of amino acids from the aspartate family, with malate (precursor OAA not analyzed).

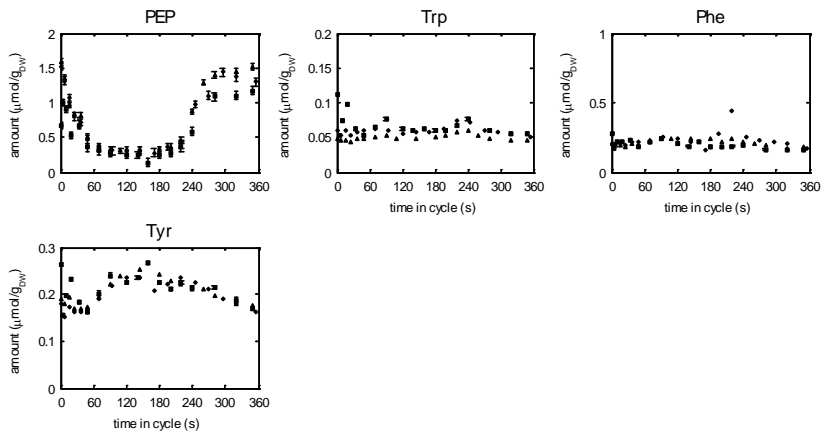


**Figure 11** Pools of amino acids of the aromatic family, with precursor PEP (precursor E4P not analyzed).

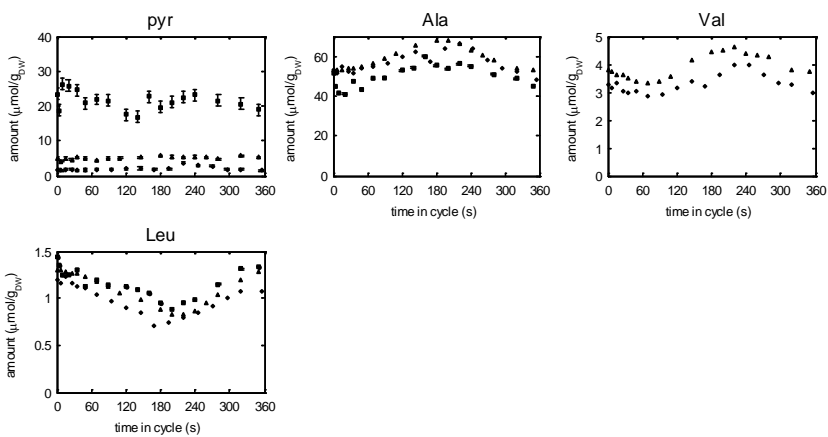


**Figure 12** Pools of amino acids of the pyruvate family, with precursor pyruvate.

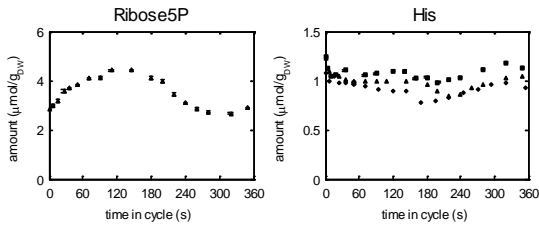


**Figure 13** Pool of histidine, with precursor Ribose5P.

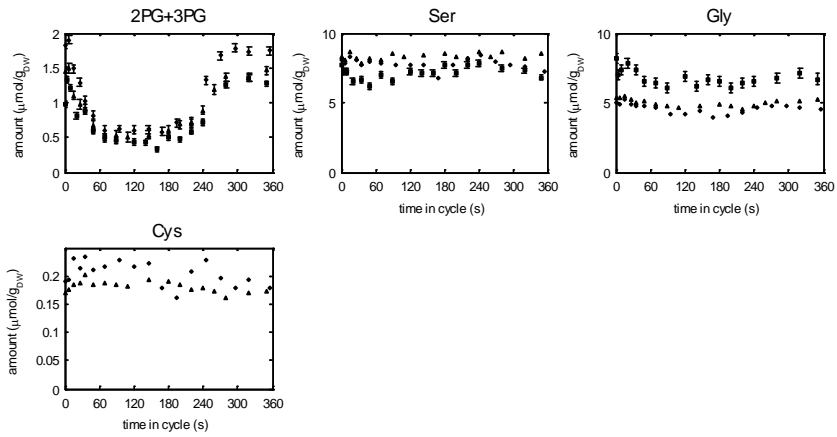


**Figure 14** Pools of amino acids of the serine family, with precursor pool 2PG+3PG.

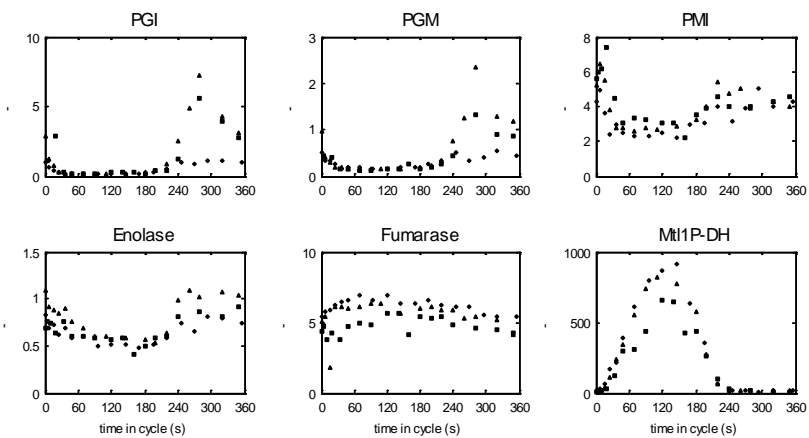


**Figure 15** Mass action ratios for several enzymatic reactions.

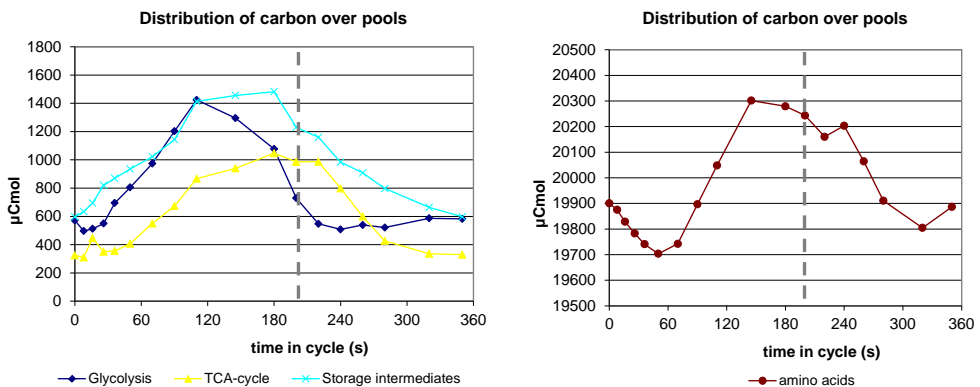
### 3.4.2 Dynamic patterns of metabolite groups

Figure 16 shows the dynamic profiles of the amount of carbon in groups of metabolites, grouped per metabolic pathway (glycolysis, TCA-cycle) or class (amino acids, precursors of storage carbohydrates). As may be expected, there is a faster accumulation of carbon at the start of the cycle in the metabolite groups which are close to glucose (the carbon substrate in these experiments) in the metabolic network, like in intermediates of the PPP and glycolysis, while the accumulation is slower in groups further away in the network, like in the TCA-cycle intermediates. Amino acids even show a decrease at the start of the feast phase.

At the end of the feast period ( $t = 200$  s) there is a surplus of about  $1458.4 \mu\text{Cmol} / (4\text{L} \times 5.7\text{g}_{\text{DW}}/\text{L}) = 63.7 \mu\text{Cmol}/\text{g}_{\text{DW}}$  of carbon in glycolysis, TCA-cycle, PPP and storage precursors compared to the start/end of the cycle. In addition, mannitol accumulated to  $50.5 \mu\text{Cmol}/\text{g}_{\text{DW}}$  at the end of the feast period. These are carbon pools which are easy to mobilize and easy to oxidize in the TCA cycle to  $\text{CO}_2$ . As was calculated in section 3.2,  $77.3 \mu\text{Cmol}/\text{g}_{\text{DW}}$  of  $\text{CO}_2$  was produced during the famine period. So it appears that there is enough carbon in easy-to-mobilize pools at the end of the feast period to account for the amount of  $\text{CO}_2$  produced in the famine period.

During the famine period the free intracellular amino acid level decreased from 20243 to 19886  $\mu\text{Cmol}$  per ( $4\text{L} \times 5.73 \text{g}_{\text{DW}}/\text{L}$ ); so,  $350 \mu\text{Cmol}/\text{g}_{\text{DW}}/\text{h}$ . This decrease could be caused by the consumption of amino acids to synthesize proteins for growth. *P. chrysogenum* mycelium consists for about 45% (w/w) of protein [30]. If the reduction of the amino acid pool in the famine period would only be caused by the synthesis of biomass protein, then the mycelial growth rate would be  $778 \mu\text{Cmol}/\text{g}_{\text{DW}}/\text{h}$  or  $0.022 \text{h}^{-1}$ . This is much less than the cycle-averaged growth rate of  $0.05 \text{h}^{-1}$ . This indicates that there is either still amino acid synthesis during the famine phase, or that the growth rate during the famine phase is lower than the cycle-averaged growth rate of  $0.05 \text{h}^{-1}$  and, consequently, higher during the feast phase. A similar calculation can be made based on the degree of reduction of the measured metabolite pools: during the famine phase the intracellular metabolite pools (central pathways, amino acids, storage) were reduced by  $12210 \mu\text{mol}$ , of which  $6495 \mu\text{mol}$  were used to reduce oxygen to water, and approximately  $1515 \mu\text{mol}$  ended up in excreted cell debris. So,  $4200 \mu\text{mol}$  per ( $4\text{L} \times 5.73 \text{g}_{\text{DW}}/\text{L}$ ) were available for cell growth, which represents a specific cell growth rate of  $0.029 \text{h}^{-1}$ . These results could indicate that the growth rate is indeed reduced during the famine phase, and should therefore be higher than the cycle-average during the feast phase.

From Figure 16 it also follows that  $1800 \mu\text{Cmol} / (4\text{L} \times 5.73 \text{ g}_{\text{DW}}/\text{L}) = 78.5 \mu\text{Cmol}/\text{g}_{\text{DW}}$  of carbon accumulated during the feast period (0 to 200 seconds) in the central metabolic pathways. This represents 18% of the carbon taken up as glucose during this feast period. Together with the amount accumulated as mannitol ( $50.7 \mu\text{Cmol}/\text{g}_{\text{DW}}$ , Figure 2), and the amount released as  $\text{CO}_2$  ( $126 \mu\text{Cmol}/\text{g}_{\text{DW}}$ ; section 3.2), a total of 59% of the consumed carbon is accounted for in measured metabolites (in intracellular metabolite pools and released  $\text{CO}_2$ ) at the end of the feast period ( $t = 200 \text{ s}$ ). This means that a significant part of the carbon taken up as glucose during the feast period is just shuttled to and accumulated in the central metabolic pathways.



**Figure 16** Distribution of carbon over measured pools. (The unit is total  $\mu\text{Cmol}$  in the culture.) The dashed vertical line indicates the moment of depletion of extracellular glucose at approximately 200 seconds after the cycle start.

### 3.5 Balances of carbon, degree of reduction and oxygen

In dynamic conditions it is not obvious which metabolic processes are running at which rate. One way to help to identify those processes is by setting up balances and to analyze the gaps that are left after quantifying the effects of known (or assumed) processes on those balances. Comparing the gaps of different balances gives information on the nature of material of which the gap consists and the metabolic process which produces that material.

The carbon and degree-of-reduction balances are two balances that are informative and easily set up. A third balance that is often set up is that of ATP. Under aerobic conditions, when oxygen is the final electron acceptor, this requires knowledge of the P/O ratio. However, in eukaryotes like yeast and *Penicillium* the P/O ratio is not a fixed parameter, but dependent on the metabolic processes that are running, as explained in [31]. (Briefly, this is because different amounts of protons are translocated when electrons are transferred

through the different proton-translocating systems of the electron transport chain depending on the electron donor, which can be mitochondrial NADH, cytosolic NADH or mitochondrial FADH<sub>2</sub>.) As the purpose of setting up the balances is to identify the rates of metabolic processes, it is therefore required when setting up an ATP-balance to assume a fixed P/O ratio to calculate the amount of ATP produced by oxidative phosphorylation. This approach was for example followed in [32].

In order to avoid making assumptions on the P/O ratio, it is possible to set up a (molecular) oxygen balance. Under the condition that all consumed cofactors are regenerated and under aerobic and fully respiratory conditions, each metabolic process consumes oxygen. All processes either produce NADH, or consume ATP, or both, and the regeneration of those cofactors consumes oxygen. Even the formation of reduced compounds like mannitol and erythritol, which consumes NADH, requires some oxygen to regenerate the consumed ATP. This is of course not true for fermentative catabolic products, but in the case of *Penicillium* they can be neglected.

For setting up the oxygen balance, each metabolic reaction (growth, (by)product formation, accumulation of intermediates, etc.) should now be formulated as consuming only extracellular glucose, oxygen, ammonium, sulfate, phosphate, and producing only CO<sub>2</sub> and water. This can be achieved by lumping reactions of a stoichiometric model, in this case we used the one published by [4], with some adaptations (biomass defined as biomass\_cc6, oxidative phosphorylation reactions with  $\delta=1.85$  (see [31])). Please note that the uptake of 1 mol of glucose costs 1 mol of ATP in this model. For the phosphorylated metabolic intermediates, no costs for import of a phosphate group were counted, because in view of the periodic concentration changes of these metabolites it was assumed that the phosphate was obtained from a conserved intracellular pool and no specific costs for phosphate import had to be made.

In addition to the amounts of energy (ATP, or O<sub>2</sub>) consumed in these lumped reactions which are known from the stoichiometry, there are amounts of energy consumed in unknown (unspecified) processes. These latter processes can be divided as maintenance, growth-related and product formation-related, as explained in [31]. To calculate the O<sub>2</sub> balance, these three ATP stoichiometry parameters are needed, as well as a parameter for the P/O ratio. Values for these parameters for the same strain of *P. chrysogenum* were published in [31]. However, it was found that the O<sub>2</sub> balance could not be closed for the chemostat cultures reported here. Therefore the measured rates of the two chemostat cultures were reconciled, the intracellular fluxes calculated by classic MFA, and these were used to re-estimate the P/O ratio parameter delta. It was re-estimated to be 1.28 mol(ATP)/mol(O); the values of the other parameters were not re-estimated.

The higher oxygen requirements may be explained from the fact that a different fermentor with a larger stirrer was used in the current experiments compared to the experiments reported by Van Gulik et al. [4,31]. Therefore there was likely more vigorous agitation in the cultivations of the current experiments. It has been reported that the specific uptake rate for oxygen increases with more vigorous agitation [33]. This is probably due to the destruction of biomass by the agitator, and therefore more energy is required for biomass formation and maintenance.

Cumulative C-,  $\gamma$ - and O<sub>2</sub>-balances were set up for a feast/famine cycle, assuming that the rates for growth, penicillin production and byproduct formation remained constant throughout the cycle (Figure 17). The balances also include the accumulation of mannitol (Figure 2). Due to the mannitol accumulation the balances close quite well at around 180 seconds, but there are gaps before and after this time point, and there is a deficit in the O<sub>2</sub> balance before 180 seconds.

The energy charge is high until 220 seconds and based on that it could be expected that the biomass formation rate is higher in that period. Calculations shown at the end of section 3.4 also suggested that there was a lower biomass growth rate during the famine phase. Therefore, the balances were also calculated using a growth rate of 0.0668 h<sup>-1</sup> during the first 200 s, and a growth rate of 0.029 h<sup>-1</sup> was used for the last 160 seconds (giving a cycle average of 0.05 h<sup>-1</sup>), and the results are presented in Figure 18. The C- and  $\gamma$ -balance in Figure 18 close better, but the gaps in the O<sub>2</sub> balance have become bigger. So, the measurements of the metabolite levels and the reconstructed O<sub>2</sub> uptake rate are contradictory with respect to the hypothesis that the biomass growth rate varies during the cycle.

It should be realized that only a limited set of carbon pools has been measured. Relatively small dynamic changes in very large intracellular pools of protein, RNA and lipids would have big effects on the balances. However, it was not attempted to measure these other pools.



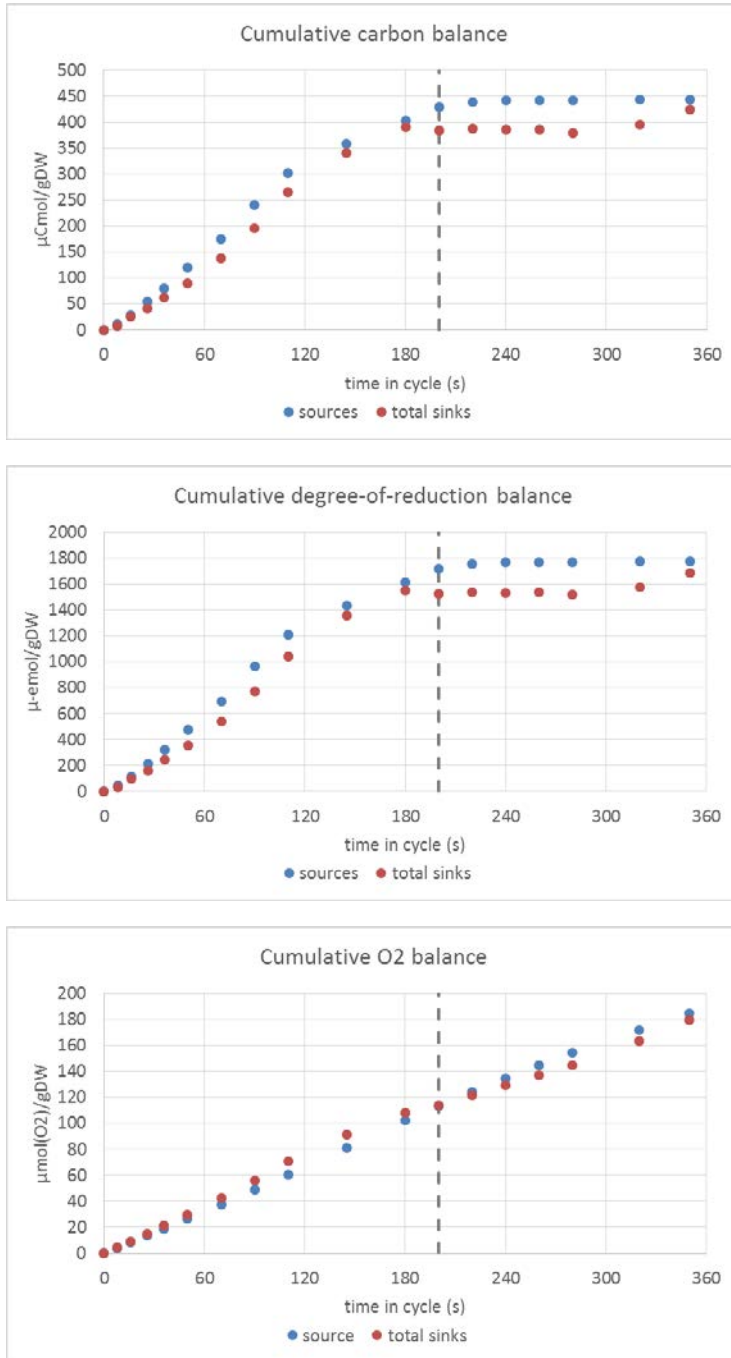


**Figure 17** C-,  $\gamma$ - and O<sub>2</sub>-balances feast/famine cycle. A constant growth rate of 0.05 h<sup>-1</sup> was assumed in the calculations.

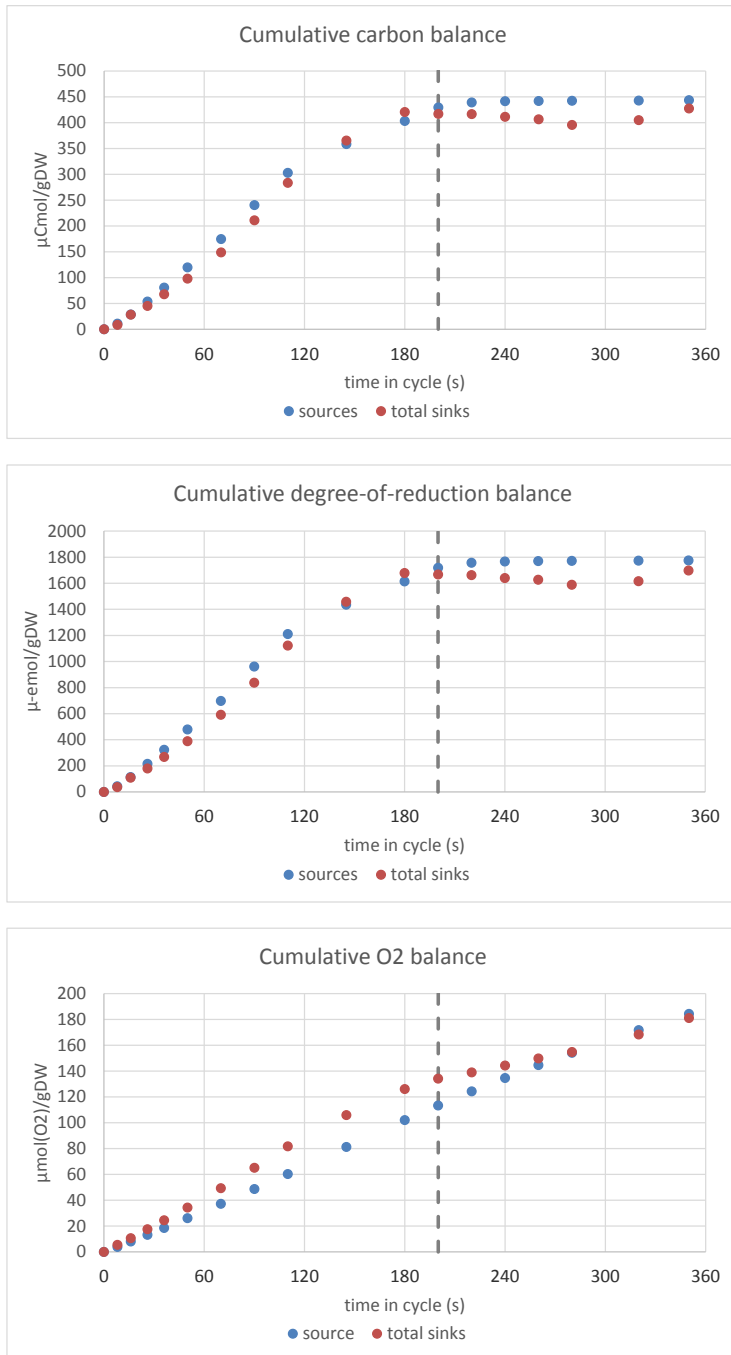


**Figure 18** C-,  $\gamma$ - and O<sub>2</sub>-balances feast/famine cycle. The growth rate was assumed to be 0.0668 h<sup>-1</sup> until 200 s, and 0.029 h<sup>-1</sup> from 200 to 360 seconds.

### 3.6 Relation to intermittent feeding of other microorganisms

The effect of intermittent feeding has also been investigated for other micro-organisms. As was found in this study, the filamentous fungus *Aspergillus oryzae*, showed no significant difference in biomass yield when it was fed in a pulsed way, compared to a continuous feeding regime [34], but it was observed that the size of mycelia was considerably reduced, which reduced broth viscosity. Also no difference in biomass yield was observed for *C. glutamicum* when it was subjected to fluctuations in the concentrations of substrate and dissolved oxygen [35], but this micro-organism did show extracellular overflow metabolism. In a comparison of *S. cerevisiae* and *C. utilis*, pulsewise feeding led to a decrease in biomass yield for *S. cerevisiae*, but not for *C. utilis* [1]. This was attributed to a difference in the affinity of the glucose uptake system of the two yeast species [1].

## 4 Conclusion

*P. chrysogenum* was subjected to a feast/famine regime of 360 second cycles to investigate how it organizes its requirements for carbon and electrons under such conditions. It was verified that there was no accumulation of extracellular metabolites, so (extracellular) overflow metabolism was not exhibited. The  $q_{O_2}$  and  $q_{CO_2}$  were found to behave dynamically during the cycles, but respiration was active throughout the cycle. All carbon that was fed as glucose was taken up within the first 200 seconds of each cycle. It was found that this carbon was not immediately converted into the final metabolic (by)products, but carbon accumulated in various intracellular pools: a part was shuttled into, and accumulated in storage carbohydrate pools, but a significant part also accumulated as intermediates of central metabolic pathways. So, to cope with the feast/famine regime, carbon consumed during the period of glucose excess was only partially stored in storage carbohydrate pools, and a significant part of the carbon was absorbed in central metabolic pathways and distributed from there.

These results imply that for a mathematical model describing growth and product formation of *P. chrysogenum* under dynamic conditions (fluctuating substrate concentration), it will be necessary to describe this accumulation of carbon in the central metabolic pathways in order to describe rates of growth, product formation,  $CO_2$  production and  $O_2$  consumption.

## References

- [1] B.H.A. Van Kleeff, J.G. Kuenen, and J.J. Heijnen, Heat flux measurements for the fast monitoring of dynamic responses to glucose additions by yeasts that were subjected to different feeding regimes in continuous culture, *Biotechnol. Prog.* 12 (1996) pp. 510-518.
- [2] F.V. Soltero and M.J. Johnson, The Effect of the Carbohydrate Nutrition on Penicillin Production by *Penicillium-Chrysogenum* Q-176, *Applied Microbiology* 1 (1953) pp. 52-57.
- [3] A.A. Brakhage, P. Sprote, Q. Al-Abdallah, A. Gehrke, H. Plattner, and A. Tuncher, Regulation of penicillin biosynthesis in filamentous fungi, *Adv. Biochem. Eng. Biotechnol.* 88 (2004) pp. 45-90.
- [4] W.M. van Gulik, W.T.A.M. De Laat, J.L. Vinke, and J.J. Heijnen, Application of metabolic flux analysis for the identification of metabolic bottlenecks in the biosynthesis of penicillin-G, *Biotechnol. Bioeng.* 68 (2000) pp. 602-618.
- [5] L.P. de Jonge, N.A.A. Buijs, A. ten Pierick, A. Deshmukh, Z. Zhao, J.A.K.W. Kiel, J.J. Heijnen, and W.M. Gulik, Scale-down of penicillin production in *Penicillium chrysogenum*, *Biotechnology Journal* 6 (2011) pp. 944-958.
- [6] L. de Jonge, N.A.A. Buijs, J.J. Heijnen, W.M. van Gulik, A. Abate, and S.A. Wahl, Flux response of glycolysis and storage metabolism during rapid feast/famine conditions in *Penicillium chrysogenum* using dynamic C-13 labeling, *Biotechnology Journal* 9 (2014) pp. 372-385.
- [7] D.H. Lewis and D.C. Smith, Sugar Alcohols (Polyols) in Fungi and Green Plants .I. Distribution Physiology and Metabolism, *New Phytol.* 66 (1967) p. 143-&.
- [8] A. Diano, S. Bekker-Jensen, J. Dynesen, and J. Nielsen, Polyol synthesis in *Aspergillus niger*: Influence of oxygen availability, carbon and nitrogen sources on the metabolism, *Biotechnol. Bioeng.* 94 (2006) pp. 899-908.
- [9] J. Francois and J.L. Parrou, Reserve carbohydrates metabolism in the yeast *Saccharomyces cerevisiae*, *FEMS Microbiol. Rev.* 25 (2001) pp. 125-145.
- [10] J.W.G. Paalman, R. Verwaal, J.H. Slofstra, A.J. Verkleij, J. Boonstra, and C.T. Verrips, Trehalose and glycogen accumulation is related to the duration of the G(1) phase of *Saccharomyces cerevisiae*, *FEMS Yeast Res.* 3 (2003) pp. 261-268.
- [11] D.M. Harris, J.A. Diderich, Z.A. van der Krogt, M.A.H. Luttik, U.M. Raamsdonk, R.A.L. Bovenberg, W.M. van Gulik, J.P. Van Dijken, and J.T. Pronk, Enzymic analysis of NADPH metabolism in beta-lactam-producing *Penicillium*

- chrysogenum: Presence of a mitochondrial NADPH dehydrogenase, *Metab. Eng.* 8 (2006) pp. 91-101.
- [12] U. Nasution, W.M. van Gulik, R.J. Kleijn, W.A. Van Winden, A. Proell, and J.J. Heijnen, Measurement of intracellular metabolites of primary metabolism and adenine nucleotides in chemostat cultivated *Penicillium chrysogenum*, *Biotechnol. Bioeng.* 94 (2006) pp. 159-166.
- [13] A.R. Lara, E. Galindo, O.T. Ramirez, and L.A. Palomares, Living with heterogeneities in bioreactors, *Mol. Biotechnol.* 34 (2006) pp. 355-381.
- [14] M.R. Mashego, W.M. van Gulik, J.L. Vinke, and J.J. Heijnen, Critical evaluation of sampling techniques for residual glucose determination in carbon-limited chemostat culture of *Saccharomyces cerevisiae*, *Biotechnol. Bioeng.* 83 (2003) pp. 395-399.
- [15] H.C. Lange, M. Eman, G. van Zuijlen, D. Visser, J.C. van Dam, J. Frank, M.J.T. de Mattos, and J.J. Heijnen, Improved rapid sampling for in vivo kinetics of intracellular metabolites in *Saccharomyces cerevisiae*, *Biotechnol. Bioeng.* 75 (2001) pp. 406-415.
- [16] L.P. de Jonge, R.D. Douma, J.J. Heijnen, and W.M. van Gulik, Optimization of cold methanol quenching for quantitative metabolomics of *Penicillium chrysogenum*, *Metabolomics* 8 (2012) pp. 727-735.
- [17] M.R. Mashego, L. Wu, J.C. van Dam, C. Ras, J.L. Vinke, W.A. Van Winden, W.M. van Gulik, and J.J. Heijnen, MIRACLE: mass isotopomer ratio analysis of U-C-13-labeled extracts. A new method for accurate quantification of changes in concentrations of intracellular metabolites, *Biotechnol. Bioeng.* 85 (2004) pp. 620-628.
- [18] L. Wu, M.R. Mashego, J.C. van Dam, A.M. Proell, J.L. Vinke, C. Ras, W.A. Van Winden, W.M. van Gulik, and J.J. Heijnen, Quantitative analysis of the microbial metabolome by isotope dilution mass spectrometry using uniformly C-13-labeled cell extracts as internal standards, *Anal. Biochem.* 336 (2005) pp. 164-171.
- [19] R.D. Douma, L.P. de Jonge, C.T.H. Jonker, R.M. Seifar, J.J. Heijnen, and W.M. van Gulik, Intracellular Metabolite Determination in the Presence of Extracellular Abundance: Application to the Penicillin Biosynthesis Pathway in *Penicillium chrysogenum*, *Biotechnol. Bioeng.* 107 (2010) pp. 105-115.
- [20] J.L. Parrou and J. Francois, A simplified procedure for a rapid and reliable assay of both glycogen and trehalose in whole yeast cells, *Anal. Biochem.* 248 (1997) pp. 186-188.

- [21] J.C. van Dam, M.R. Eman, J. Frank, H.C. Lange, G.W.K. van Dedem, and J.J. Heijnen, Analysis of glycolytic intermediates in *Saccharomyces cerevisiae* using anion exchange chromatography and electrospray ionization with tandem mass spectrometric detection, *Anal. Chim. Acta* 460 (2002) pp. 209-218.
- [22] R.M. Seifar, Z. Zhao, J. van Dam, W. van Winden, W. van Gulik, and J.J. Heijnen, Quantitative analysis of metabolites in complex biological samples using ion-pair reversed-phase liquid chromatography-isotope dilution tandem mass spectrometry, *J. Chromatogr. A* 1187 (2008) pp. 103-110.
- [23] A.B. Canelas, A. ten Pierick, C. Ras, R.M. Seifar, J.C. van Dam, W.M. van Gulik, and J.J. Heijnen, Quantitative Evaluation of Intracellular Metabolite Extraction Techniques for Yeast Metabolomics, *Analytical Chemistry* 81 (2009) pp. 7379-7389.
- [24] S.A. Wahl, M. Dauner, and W. Wiechert, New tools for mass isotopomer data evaluation in C-13 flux analysis: Mass isotope correction, data consistency checking, and precursor relationships, *Biotechnol. Bioeng.* 85 (2004) pp. 259-268.
- [25] L.P. de Jonge, J.J. Heijnen, and W.M. van Gulik, Reconstruction of the oxygen uptake and carbon dioxide evolution rates of microbial cultures at near-neutral pH during highly dynamic conditions, *Biochem. Eng. J.* 83 (2014) pp. 42-54.
- [26] A. Abate, R.C. Hillen, and S.A. Wahl, Piecewise affine approximations of fluxes and enzyme kinetics from in vivo <sup>13</sup>C labeling experiments, *International Journal of Robust and Nonlinear Control* 22 (2012) pp. 1120-1139.
- [27] D.J.D. Hockenhull, M. Herbert, A.D. Walker, G.D. Wilkin, and F.G. Winder, Organic Acid Metabolism of *Penicillium-Chrysogenum* .1. Lactate and Acetate, *Biochem. J.* 56 (1954) pp. 73-82.
- [28] U.D. Nasution, A Dynamic and Steady State Metabolome Study of Central Metabolism and Its Relation With the Penicillin Biosynthesis Pathway in *Penicillium Chrysogenum*, PhD Thesis, Delft University of Technology, 2007.
- [29] U. Nasution, W.M. van Gulik, A. Proell, W.A. Van Winden, and J.J. Heijnen, Generating short-term kinetic responses of primary metabolism of *Penicillium chrysogenum* through glucose perturbation in the bioscope mini reactor, *Metab. Eng.* 8 (2006) pp. 395-405.
- [30] C.M. Henriksen, L.H. Christensen, J. Nielsen, and J. Villadsen, Growth energetics and metabolic fluxes in continuous cultures of *Penicillium chrysogenum*, *J. Biotechnol.* 45 (1996) pp. 149-164.

- [31] W.M. van Gulik, M.R. Antoniewicz, W.T.A.M. Delaat, J.L. Vinke, and J.J. Heijnen, Energetics of growth and penicillin production in a high-producing strain of *Penicillium chrysogenum*, *Biotechnol. Bioeng.* 72 (2001) pp. 185-193.
- [32] L. Wu, J. van Dam, D. Schipper, M.T.A.P. Kresnowati, A.M. Proell, C. Ras, W.A. Van Winden, W.M. van Gulik, and J.J. Heijnen, Short-term metabolome dynamics and carbon, electron, and ATP balances in chemostat-grown *Saccharomyces cerevisiae* CEN.PK 113-7D following a glucose pulse, *Appl. Environ. Microbiol.* 72 (2006) pp. 3566-3577.
- [33] J.J. Smith, M.D. Lilly, and R.I. Fox, The Effect of Agitation on the Morphology and Penicillin Production of *Penicillium-Chrysogenum*, *Biotechnol. Bioeng.* 35 (1990) pp. 1011-1023.
- [34] S. Bhargava, M.P. Nandakumar, A. Roy, K.S. Wenger, and M.R. Marten, Pulsed feeding during fed-batch fungal fermentation leads to reduced viscosity without detrimentally affecting protein expression, *Biotechnol. Bioeng.* 81 (2003) pp. 341-347.
- [35] F. Kass, I. Hariskos, A. Michel, H.J. Brandt, R. Spann, S. Junne, W. Wiechert, P. Neubauer, and M. Oldiges, Assessment of robustness against dissolved oxygen/substrate oscillations for *C-glutamicum* DM1933 in two-compartment bioreactor, *Bioprocess Biosystems Eng.* 37 (2014) pp. 1151-1162.

## Appendix 1. Reconstruction of $q_{O_2}$ and $q_{CO_2}$

The dynamic measurements of the dissolved oxygen concentration and the gaseous concentrations of oxygen and  $CO_2$  in the offgas from an intermittently fed culture over 15 feeding cycles were used to reconstruct the biomass-specific rates of  $O_2$  uptake and  $CO_2$  production using the procedure described in [25]. The reconstruction results are shown in Figure A1.

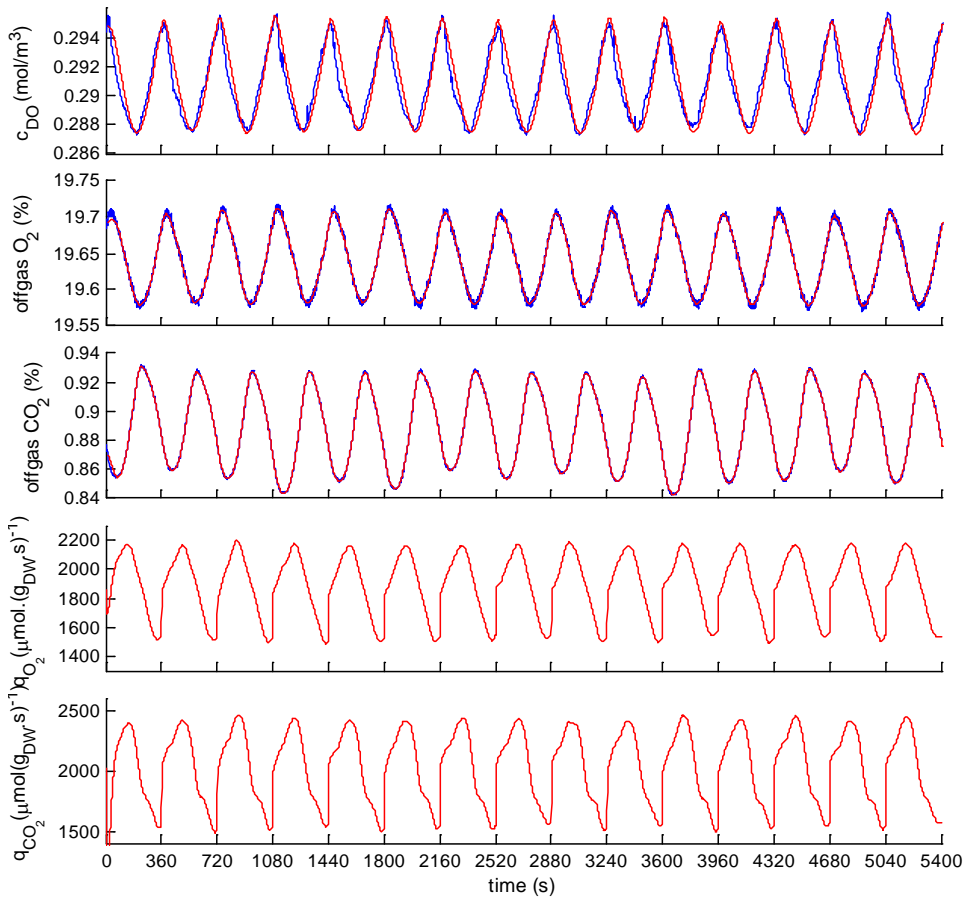


**Figure A1** Reconstruction results from measurements of DO, offgas  $O_2$  and offgas  $CO_2$  over 15 cycles from an intermittently fed culture. Measurements are indicated in blue and model output in red.



## Appendix 2. Storage carbohydrates

Storage carbohydrate levels were measured during cycles of intermittent feeding (see Figure A2).

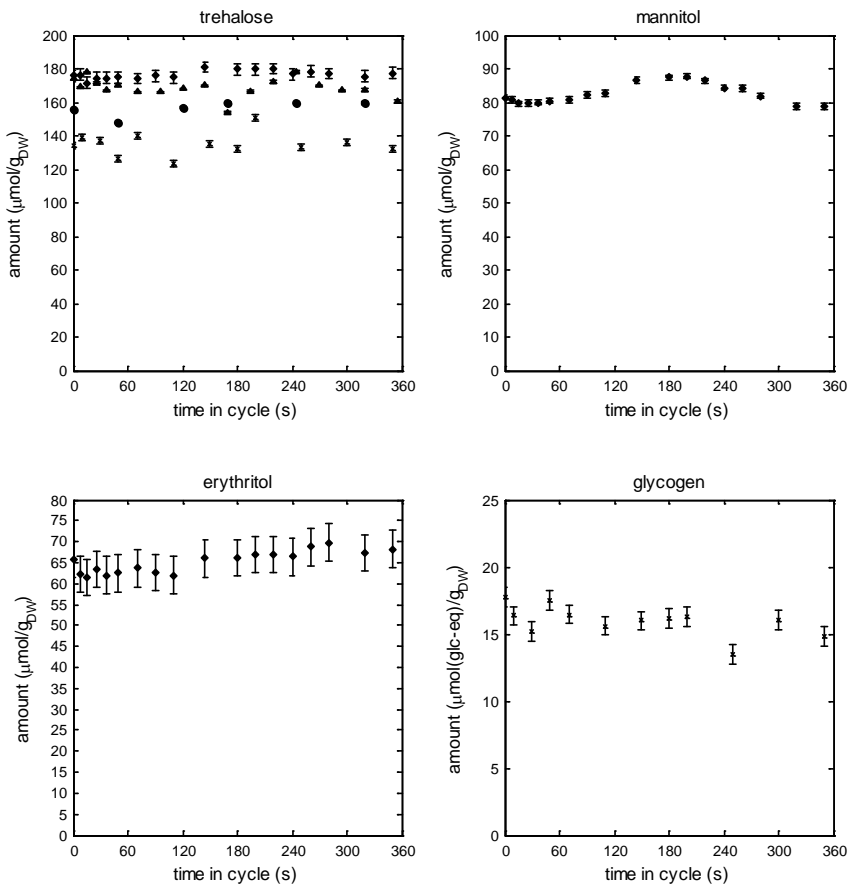


**Figure A2** Storage carbohydrate levels during a cycle of intermittent feeding. Different symbols represent different cultures. Error bars represent the standard deviation of analytical replication.

Changes in levels of storage carbohydrate levels with culture age were measured in intermittently fed cultures and chemostat cultures (see Figure A3).

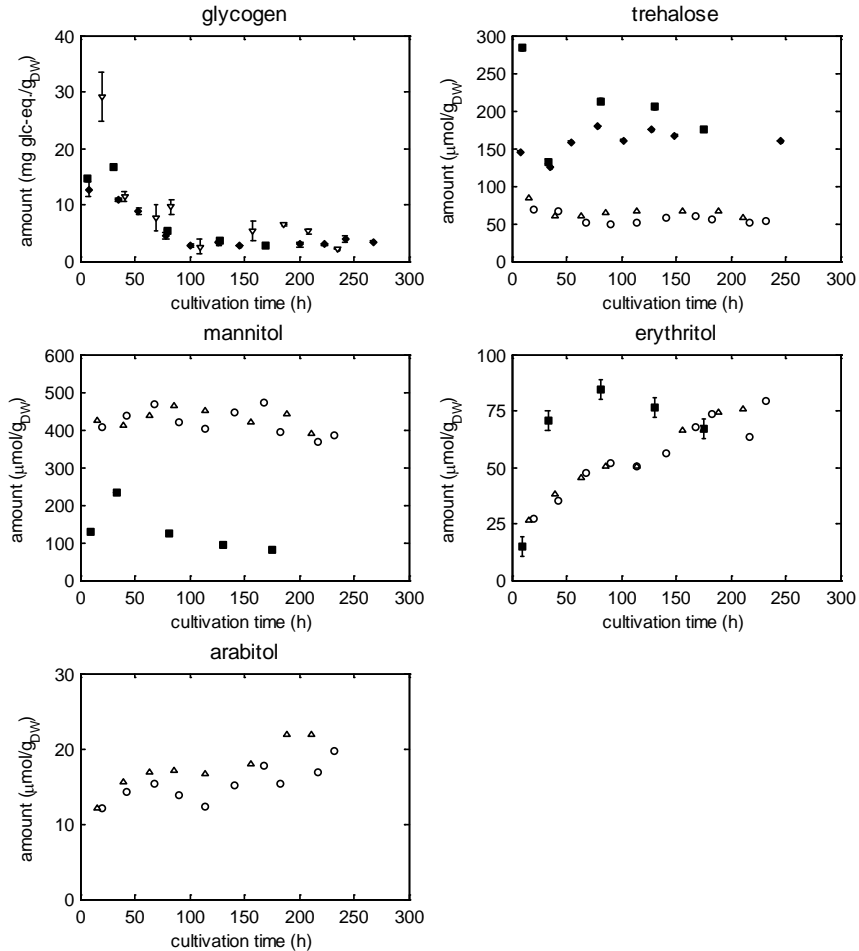


**Figure A3** Storage carbohydrate levels as a function of culture age in intermittently fed cultures (solid symbols) and control chemostat cultures (open symbols). Different symbols represent different cultures. For each cultivation, time 0 represents the start of the carbon limited phase.



## **Chapter 7**

---

### Outlook

---

## 1 Introduction

The range of products that is produced through fermentation is continuously expanding and increasingly more fermentation processes will be executed at industrial production scale. All of these processes are developed first at small laboratory scale and are subsequently scaled up. Inevitably, a large part of these processes will also face heterogeneities and gradients in concentrations of substrate and dissolved oxygen in the bioreactor at the industrial production scale. The focus of the research presented in this thesis was the penicillin fermentation using *Penicillium chrysogenum* because it is both an industrially-relevant process and an important model process. The results from this research provide more insight into the effects that substrate gradients can have on the behavior of central metabolism in terms of metabolic fluxes and metabolite levels and the consequences this can have on metabolic product pathways. This insight raises new questions which may be the subject of future research, both with respect to penicillin fermentations and with respect to other fermentation processes. Some suggestions for future research are given below.

## 2 Metabolism of *P. chrysogenum*

Sugar alcohols have important metabolic roles in many species of fungi, for example as storage for carbon, redox buffer and osmo-regulator [1-3]. One of these sugar alcohols, mannitol, was also found to be present in high quantities in *P. chrysogenum* in the present studies, and it was possible to show that there was a significant metabolic flux through the pool of mannitol. Remarkably, the connectivity and stoichiometry of the metabolic reactions leading to the formation and degradation of mannitol in *P. chrysogenum* are not fully understood. Therefore an assumption had to be made during the analysis of the measured metabolite levels in the present study regarding the metabolic precursor for mannitol formation. Knowledge of the correct type of cofactor(s) (NADH or NADPH) involved in the formation and degradation of mannitol would allow a deeper understanding of its metabolic role under various conditions. The use of <sup>13</sup>C labeling may be an approach to elucidate the connectivity of the mannitol pathway.

The quantitative metabolomics techniques which are available for the study of *P. chrysogenum* were refined by the improvements described in chapters 2 and 3 of this thesis. They permit the most accurate quantification of metabolite levels in biomass of *P. chrysogenum* to date. Knowledge of the metabolite levels, and dynamic changes in them, are highly informative for the analysis and understanding of the metabolic state of a culture. Yet, the current techniques have drawbacks which limit the information contained in their results. First, metabolite levels are usually an average of an entire population due to the

nature of the sample treatment, whereas it is known that metabolite levels and metabolic fluxes differ from one cell to another within a cell population, for example depending on the cell cycle phase [4]. In the case of *P. chrysogenum*, the hyphae are differentiated, and metabolite levels and metabolic fluxes probably vary with the differentiation. To be able to study the impact of differentiation on hyphal metabolism and product formation, new sample treatment techniques are needed by which metabolite levels of individual types of differentiated hypha can be determined.

Furthermore, in eukaryotes enzymes are localized in specific subcellular compartments. This implies that certain metabolites have a higher concentration in one compartment than in another. Currently it is not possible to determine metabolite concentrations within subcellular compartments. There is a need for experimental techniques which enable that, because knowledge of metabolite concentrations, in combination with knowledge of the affinities of enzymes, would improve the understanding of metabolic behavior of cells.

Compartmentation also plays a role in penicillin biosynthesis, because the reactions are partly localized in the cytosol and partly in peroxisomes. This means that some metabolites need to be transported over the peroxisomal membrane. The proteins involved in these intracellular transport steps start to become identified [5]. It will be interesting to study whether these enzymatic steps are limiting the penicillin biosynthesis formation rate under any condition.

During the intermittent feeding experiments, the extracellular glucose concentration in culture supernatant was determined to quantify the glucose uptake rate. The determination of the glucose concentration in the culture supernatant was complicated by the presence of one or more reactions which formed glucose, and special experimental measures had to be taken to quench these reactions by quick freezing in liquid nitrogen. It is suspected that this formation of glucose is the result of enzymatic degradation of dead biomass, for example hydrolysis of glucans from cell walls of dead mycelial fragments, or trehalose released from dead hyphae. It is known that shear forces from the agitator cause partial destruction of some hyphae. From the results obtained in the current studies the rate of this glucose release could not be quantified. In view of the concentration of lysed biomass in the culture it is likely that this rate is insignificant compared to the glucose feed rate. Nevertheless it may be worthwhile to attempt to quantify this release rate and to identify the exact source(s). This should provide a more realistic estimate of the glucose uptake rate, which is important for studies involving metabolic flux estimates. This is likely relevant for other filamentous fungi as well.

### 3 Approaches to resolve the effects of gradients at large scale

There are several solutions possible for the problem of the reduced penicillin formation rate as a result of the presence of substrate concentration gradients. First, it could be attempted to replace the substrate uptake system of *P. chrysogenum* by one with a lower affinity for the substrate. This could be achieved either by protein engineering of the involved *P. chrysogenum* enzymes, or by replacing it by enzymes from another micro-organism. This approach has been followed for other organisms [6].

Another solution may be to feed glucan polymers to the fermentor, and to add glucanases. The glucans can reach homogeneous mixing throughout the bioreactor, and by hydrolysis of the glucans at every point in the bioreactor an even supply of glucose should be achieved. The challenge of this approach probably lies in the control of the hydrolysis rate.

To enhance the understanding of the behavior of *P. chrysogenum* in large scale fermenters and the impact of the presence of gradients in concentrations (substrate, oxygen and CO<sub>2</sub>) and shear stress, kinetic models of the metabolism of *P. chrysogenum* are useful. The characteristic responses of the organism should continue to be studied in scale-down experiments and this should be the input for a kinetic model. The kinetic model should then be combined with Computational Fluid Dynamics (CFD) to design and optimize the production bioreactor and process [7]. Ideally, the model should also contain the response to the effects of varying shear stress [8-11].

---

## References

- [1] P.S. Solomon, O.D.C. Waters, and R.P. Oliver, Decoding the mannitol enigma in filamentous fungi, *Trends Microbiol.* 15 (2007) pp. 257-262.
- [2] L. Adler, A. Pedersen, and I. Tunblad Johansson, Polyol Accumulation by 2 Filamentous Fungi Grown at Different Concentrations of NaCl, *Physiol. Plant.* 56 (1982) pp. 139-142.
- [3] A. Diano, S. Bekker-Jensen, J. Dynesen, and J. Nielsen, Polyol synthesis in *Aspergillus niger*: Influence of oxygen availability, carbon and nitrogen sources on the metabolism, *Biotechnol. Bioeng.* 94 (2006) pp. 899-908.
- [4] R. Costenoble, D. Muller, T. Barl, W.M. van Gulik, W.A. Van Winden, M. Reuss, and J.J. Heijnen, C-13-Labeled metabolic flux analysis of a fed-batch culture of elutriated *Saccharomyces cerevisiae*, *FEMS Yeast Res.* 7 (2007) pp. 511-526.
- [5] M. Fernandez-Aguado, J.F. Martin, R. Rodriguez-Castro, C. Garcia-Estrada, S.M. Albillos, F. Teijeira, and R.V. Ullan, New insights into the isopenicillin N transport in *Penicillium chrysogenum*, *Metab. Eng.* 22 (2014) pp. 89-103.
- [6] A.R. Lara, L. Caspeta, G. Gosset, F. Bolivar, and O.T. Ramirez, Utility of an *Escherichia coli* strain engineered in the substrate uptake system for improved culture performance at high glucose and cell concentrations: An fed-batch cultures, *Biotechnol. Bioeng.* 99 (2008) pp. 893-901.
- [7] S. Schmalzriedt, M. Jenne, K. Mauch, and M. Reuss, Integration of Physiology and Fluid Dynamics, *Adv. Biochem. Eng. Biotechnol.* 80 (2003) pp. 19-68.
- [8] J.J. Smith, M.D. Lilly, and R.I. Fox, The Effect of Agitation on the Morphology and Penicillin Production of *Penicillium-Chrysogenum*, *Biotechnol. Bioeng.* 35 (1990) pp. 1011-1023.
- [9] J.C. Van Suijdam and B. Metz, Influence of Engineering Variables Upon the Morphology of Filamentous Molds, *Biotechnol. Bioeng.* 23 (1981) pp. 111-148.
- [10] J. Nielsen and P. Krabben, Hyphal Growth and Fragmentation of *Penicillium-Chrysogenum* in Submerged Cultures, *Biotechnol. Bioeng.* 46 (1995) pp. 588-598.
- [11] S. Kelly, L.H. Grimm, C. Bendig, D.C. Hempel, and R. Krull, Effects of fluid dynamic induced shear stress on fungal growth and morphology, *Process Biochem.* 41 (2006) pp. 2113-2117.





## Summary

To make optimal use of fermenter capacity and to obtain high volumetric conversion rates, the biomass concentration in industrial fermentation processes is usually optimized to high levels. At the same time, many industrial bioprocesses are operated in fed-batch mode in which a concentrated feed substrate stream, often a concentrated solution of some kind of sugar, is added to the fermenter during the process. In this way, substrate is supplied to the biomass at the optimal rate, while the substrate concentration in the fermenter is kept low. This is important for bioprocesses in which product formation is repressed by a high substrate concentration, a phenomenon called catabolite repression. Another reason to operate in fed-batch mode, as opposed to batch mode, can be that it allows to control the biomass-specific growth rate through the substrate feed rate. This can be important in case the maximum biomass-specific production rate is obtained at a biomass-specific growth rate which is lower than maximum.

Large-scale industrial fermenters have mixing times in the order of several minutes, due to their size (volumes can go up to several thousands of cubic meters) and sometimes due to high broth viscosity. The combination of the long mixing time, operating in fed-batch mode and having a high volumetric substrate conversion rate leads to the formation of steep substrate concentration gradients inside the fermenter: there is a high concentration close to the entry point of substrate into the fermenter, but the substrate can be depleted in parts of the fermenter which are far away from this entry point. The cells in the fermenter follow the liquid circulation flows through the zones of high and low substrate concentration and thus experience fluctuations in the substrate concentration. Depending on the micro-organism used in the bioprocess, this can have various effects. Often it results in a decreased product yield compared to the process developed at lab scale using well-mixed fermenters in which a constant substrate concentration can be well maintained.

The problem of substrate concentration gradients in large-scale fed-batch fermentations is the subject of this thesis, which was investigated using the penicillin fermentation as a model process. Production of penicillin by the filamentous fungus *Penicillium chrysogenum* is one of the first modern industrial bioprocesses. The industrial production started around the 1940s and continues to be widely applied. The main topic of the research described in this thesis is the effect of substrate concentration gradients in large scale penicillin fermentations, mimicked in scale-down experiments, on the primary and secondary metabolism of *P. chrysogenum*, mainly in terms of metabolic fluxes and metabolite levels.

Such research has become possible thanks to recent improvements in techniques to quantify intracellular metabolite levels (quantitative metabolomics).

Appropriate methods to quantify the intracellular metabolite levels of the penicillin biosynthesis pathway were essential for these studies. A number of these metabolites are not only present intracellularly, but are also abundantly present extracellularly. This is especially the case for the product of the pathway, penicillin-G, and the side chain precursor phenylacetic acid which is supplied in the medium, and to a lesser extent also for some by-products of the pathway. **Chapter 2** presents the development of a method which efficiently removes these large extracellular amounts from the sample, which allows the accurate quantification of the intracellular amounts. The new method employs fast filtration instead of washing by centrifugation, using a cold aqueous methanol solution to keep metabolic reactions quenched.

Quenching of metabolic activity is crucial during sampling and sample treatment for quantitative metabolomics. Instant quenching is usually achieved by sampling into a quenching liquid. Various quenching liquids are in use for this purpose, but cold aqueous methanol solutions are especially popular, because they leave the biomass intact, which allows washing of the biomass before the intracellular metabolites are extracted. In recent years, however, it has become apparent that intracellular metabolites may leak away from cells into the quenching solution. In **chapter 3**, the use of cold aqueous methanol as a quenching liquid for *P. chrysogenum* was re-evaluated and optimized to reduce metabolite leakage. Minimal leakage was obtained for a methanol content of 40% (v/v) while keeping the temperature at or below -20 °C. Under this condition, the average metabolite recovery was 95.7% ( $\pm 1.1\%$ ) for a set of diverse metabolites including amino acids, phosphorylated metabolites and organic acids. Although the exact mechanism of metabolite leakage remains unclear, some observations seem to suggest that metabolites are lost from quenched mycelia of *P. chrysogenum* by diffusion over the cell membrane.

Information about the metabolic state of an aerobic culture can also be obtained from the rates of O<sub>2</sub> uptake and CO<sub>2</sub> production, and under steady state conditions these can be calculated from measurements of the concentrations of O<sub>2</sub> and CO<sub>2</sub> in the offgas. In dynamic conditions these rates can also be reconstructed from the measurements of the changing concentrations of O<sub>2</sub> and CO<sub>2</sub> in the offgas and the dissolved O<sub>2</sub>, but it requires a mathematical model which describes the mass transfer between liquid and gas phase, the dispersion of O<sub>2</sub> and CO<sub>2</sub> in the offgas system and sensor dynamics. In addition, if the cultivation is performed at near-neutral pH levels, like in the case of penicillin fermentations, the interconversion of dissolved CO<sub>2</sub> and bicarbonate needs to be taken into account. Such a mathematical model was developed in **chapter 4**. It was found that for the

bioreactor system used, the model should not only describe mass transfer between sparged gas bubbles and broth, but also between headspace gas and broth. Furthermore, the dispersion, distortion and delay of the offgas signals by the offgas system itself could be conveniently described by the impulse response of the offgas system. The model was applied successfully to reconstruct the dynamic changes in the rates of O<sub>2</sub> uptake and CO<sub>2</sub> production of a glucose-limited chemostat culture of *P. chrysogenum* which was perturbed by a glucose pulse to the culture.

The methods developed in chapters 2, 3 and 4 were then applied to study the influence of substrate concentration gradients on the metabolism and physiology of a high-producing strain of *P. chrysogenum*. The effects of substrate concentration gradients in large-scale fermenters were mimicked in scale-down experiments carried out in well-mixed lab scale bioreactors by applying an intermittent feeding regime of 360 seconds cycles in which substrate was only fed during the first 36 seconds. As described in **chapter 5**, the penicillin production was reduced by a factor two in the intermittent feeding regime compared to control chemostat cultures with constant feeding. The biomass yield, however, was the same. Measurement of the levels of intermediates and enzymes of the penicillin biosynthesis pathway suggested that the reduction of the penicillin production was mainly caused by a reduction of the influx into the pathway. This could potentially be explained by the dynamic metabolite levels of adenosine monophosphate, pyrophosphate and adenosine triphosphate, because the intracellular levels of these metabolites were unfavourable for the enzymatic activity of the first enzyme in the pathway during a part of the intermittent feeding cycle in comparison to the levels of these metabolites in control chemostat cultures.

The results of the scale-down experiments were further investigated in **chapter 6** with focus on the effects of intermittent feeding on primary metabolism and storage carbohydrate metabolism. All substrate in the form of glucose was consumed during the first 200 seconds of each cycle, and there was no glucose during the last 160 seconds. There was no carbon excreted by the culture which could serve as a reserve carbon source during these 160 seconds of glucose depletion. Yet, respiration continued during this period, which indicates that the glucose consumed in the period of glucose excess was stored intracellularly in some form until it was converted to one of the final (by)products. Indeed, approximately 11% of the carbon consumed in the form of glucose accumulated temporarily as intracellular mannitol during the period of glucose excess. Although there were remarkable differences in the storage carbohydrate metabolism of intermittently fed-cultures and chemostat cultures, the overall turnover rate of material in their trehalose and mannitol pools were very comparable (18% versus 22% of the glucose uptake rate). Finally, from the measurement of intracellular metabolite levels in central metabolic pathways it

was found that another 18% of the consumed glucose was accumulated in the form intermediates of central metabolism. In conclusion, to cope with periods of substrate excess and substrate depletion, *P. chrysogenum* has the capacity to absorb a large amount of carbon in intracellular pools of storage carbohydrates and central metabolic pathways during substrate-available periods, from which it can release carbon during periods of substrate depletion.

# Samenvatting

Om optimaal gebruik te maken van fermentorcapaciteit en om hoge volumetrische omzettingssnelheden te verkrijgen wordt de biomassaconcentratie in industriële fermentatieprocessen doorgaans geoptimaliseerd naar hoge waarden. Tegelijkertijd worden veel industriële bioprocessen uitgevoerd in fed-batch modus waarbij een geconcentreerde stroom voedingssubstraat, vaak een geconcentreerde oplossing van een vorm van suiker, toegevoerd wordt naar de fermentor tijdens het proces. Op die manier wordt substraat naar de biomassa gebracht op de optimale snelheid, terwijl de substraatconcentratie in de fermentor laag gehouden wordt. Dat is belangrijk voor bioprocessen waarin productvorming onderdrukt wordt door een hoge substraatconcentratie, een verschijnsel dat kataboliet-repressie genoemd wordt. Een andere reden om in fed-batch modus te werken, in tegenstelling tot batch modus, is dat dan de biomassa-specifieke groeisnelheid gecontroleerd kan worden door middel van de toevoersnelheid van substraat. Dat kan belangrijk zijn als de maximale biomassa-specifieke productiesnelheid verkregen wordt bij een lagere dan de maximale biomassa-specifieke groeisnelheid.

Grootschalige industriële fermentoren hebben mengtijden in de orde van grootte van enkele minuten, veroorzaakt door hun omvang (volumes kunnen oplopen tot enkele duizenden kubieke meters) en soms door een hoge viscositeit van de fermentorinhoud. De combinatie van de lange mengtijd, het werken in fed-batch modus en het hebben van een hoge volumetrische substraatomzettingssnelheid leidt tot het ontstaan van steile gradiënten in substraatconcentratie in de fermentor: de concentratie is hoog dicht bij het punt waar substraat de fermentor binnenkomt, maar het substraat kan volledig opgebraakt zijn in delen van de fermentor die ver van dat punt weg zijn. De cellen in de fermentor volgen de vloeistofcirculatiestromen door zones met hoge en lage substraatconcentratie en ervaren dus fluctuaties in de substraatconcentratie. Afhankelijk van het micro-organisme dat in het bioproces gebruikt wordt, kan dit verscheidene effecten hebben. Vaak resulteert het in een verlaagde productopbrengst in vergelijking met het proces dat ontwikkeld was op laboratoriumschaal in goed gemengde fermentoren waarin de substraatconcentratie goed constant gehouden kan worden.

Het probleem van gradiënten in de substraatconcentratie in grootschalige fed-batch fermentaties is het onderwerp van dit proefschrift. Dit is onderzocht in de penicilline-fermentatie als modelproces. Productie van penicilline door de filamenteuze schimmel *Penicillium chrysogenum* is één van de eerste moderne industriële bioprocessen. De industriële productie begon rond de jaren '40 van de 20<sup>e</sup> eeuw en blijft op grote schaal

toegepast worden. Het hoofdonderwerp van het onderzoek dat in dit proefschrift beschreven staat is het effect van gradiënten in substraatconcentratie in grootschalige penicilline-fermentaties, nagebootst in schaalverkleiningsexperimenten, op het primaire en secundaire metabolisme van *P. chrysogenum*, voornamelijk in termen van metabole fluxen en metabolietniveau's. Dergelijk onderzoek is mogelijk geworden dankzij recente verbeteringen in technieken waarmee intracellulaire metabolietniveau's gekwantificeerd kunnen worden (kwantitatieve metabolica).

Voor dit onderzoek waren geschikte methoden waarmee de intracellulaire metabolietniveau's van de penicilline-biosynthese route gekwantificeerd kunnen worden essentieel. Een aantal van deze metabolieten is niet alleen intracellulair aanwezig, maar ook in ruime mate buiten de cel. Dit geldt vooral voor het product van de route, penicilline-G, en de zijketenprecursor fenylazijnzuur die in het medium geleverd wordt, en in mindere mate ook voor enkele bijproducten van de route. In **hoofdstuk 2** wordt de ontwikkeling van een methode gepresenteerd waarmee die grote extracellulaire hoeveelheden efficiënt uit monsters verwijderd kunnen worden, waardoor de intracellulaire hoeveelheden nauwkeurig gekwantificeerd kunnen worden. De nieuwe methode maakt gebruik van snelle filtratie in plaats van wasstappen middels centrifugatie, en van een koude oplossing van methanol in water om metabole reacties stil te leggen.

Het stilleggen van de metabole activiteit is cruciaal tijdens de monsternamen en monsterbehandeling voor kwantitatieve metabolica. Dit instantaan stilleggen ("quenching") wordt gewoonlijk bereikt door te bemonsteren in een quenching-vloeistof. Er zijn verscheidene quenching-vloeistoffen in omloop voor dit doel, maar koude oplossingen van methanol in water zijn bijzonder populair, omdat ze de biomassa intact laten, waardoor het mogelijk is de biomassa te wassen voordat de intracellulaire metabolieten eruit geëxtraheerd worden. Maar in de afgelopen jaren is aan het licht gekomen dat intracellulaire metabolieten weg kunnen lekken uit cellen in de quenching-vloeistof. In **hoofdstuk 3** is het gebruik van de koude oplossing van methanol in water als quenching-vloeistof voor *P. chrysogenum* opnieuw geëvalueerd en geoptimaliseerd om het weglekken van metabolieten te verminderen. De lekkage was het minst als het methanolgehalte 40% (v/v) bedroeg en de temperatuur op of onder -20 °C gehouden werd. Onder deze omstandigheden werd gemiddeld 95.7% ( $\pm 1.1\%$ ) van een diverse verzameling metabolieten, waaronder aminozuren, gefosforyleerde metabolieten en organische zuren, teruggevonden in de biomassa. Het precieze mechanisme waardoor metabolieten weglekken blijft onduidelijk, maar enkele observaties duiden erop dat het verlies van metabolieten uit stilgelegde mycelia van *P. chrysogenum* plaatvindt door diffusie over de celmembraan.

Informatie over de metabole toestand van een aerobe cultuur kan ook verkregen worden uit de snelheden van zuurstofopname en CO<sub>2</sub> productie, en in stationaire omstandigheden kunnen die berekend worden uit metingen van de concentraties O<sub>2</sub> en CO<sub>2</sub> in het afgas. In dynamische omstandigheden kunnen deze snelheden ook gereconstrueerd worden uit de metingen van de veranderende concentraties O<sub>2</sub> en CO<sub>2</sub> in het afgas en de opgeloste O<sub>2</sub>, maar hiervoor is een mathematisch model nodig dat de massa-overdracht tussen vloeistof- en gasfase, de dispersie van O<sub>2</sub> en CO<sub>2</sub> in het afgassysteem en de dynamiek van de sensoren beschrijft. Als er bij een vrij neutrale pH gekweekt wordt, zoals in het geval van penicilline-fermentaties, moet bovendien rekening gehouden worden met de interconversie van opgeloste CO<sub>2</sub> en bicarbonaat. Een dergelijk mathematisch model is ontwikkeld in **hoofdstuk 4**. Het bleek dat voor het bioreactorsysteem dat gebruikt was het model niet alleen massa-overdracht tussen gasbellen en vloeistof, maar ook tussen gas in de bovenruimte van de bioreactor en vloeistof moest beschrijven. Verder konden de dispersie, vervorming en vertraging van de afgassignalen door het afgassysteem zelf makkelijk beschreven worden door de impulsrespons van het afgassysteem. Het model is met succes toegepast voor de reconstructie van de dynamische veranderingen in de snelheden van zuurstofopname and CO<sub>2</sub> productie van een glucose-gelimiteerde chemostaatcultuur van *P. chrysogenum* die verstoord was door een glucosepuls toegevoegd aan de cultuur.

De methoden die in de hoofdstukken 2, 3 en 4 zijn ontwikkeld zijn vervolgens toegepast voor de bestudering van de invloed van gradiënten in substraatconcentratie op het metabolisme en de fysiologie van een stam van *P. chrysogenum* die veel penicilline-opbrengst geeft. De effecten van gradiënten in substraatconcentratie in grootschalige fermentoren werden nagebootst in schaalverkleiningsexperimenten die uitgevoerd werden in goed gemengde laboratoriumschaal bioreactoren. Daarbij werd een onderbroken voedingsregime opgelegd bestaande uit cycli van 360 seconden waarin substraat alleen werd gevoed tijdens de eerste 36 seconden. In **hoofdstuk 5** staat beschreven dat de penicilline productie een factor twee lager was onder het onderbroken voedingsregime in vergelijking met controle chemostaatculturen met een constante voeding. De opbrengst van biomassa was echter gelijk. Meting van de niveau's van metabolieten en enzymen van de penicilline-biosyntheseroute duiden erop dat de verlaging van de penicillineproductie voornamelijk werd veroorzaakt door een verlaging van de flux die de route ingaat. Een mogelijke verklaring hiervoor vormen de dynamische metabolietniveau's van adenosine monofosfaat, pyrofosfaat en adenosine trifosfaat, omdat de intracellulaire niveau's van deze metabolieten gedurende een deel van de onderbroken voedingscyclus ongunstig waren voor de enzymactiviteit van het eerste enzym in de route in vergelijking met de niveau's van deze metabolieten in de controle chemostaatculturen.



De resultaten van de schaalverkleiningsexperimenten zijn verder onderzocht in **hoofdstuk 6** met de nadruk op de effecten van onderbroken voeding op het primair metabolisme en het metabolisme van opslagkoolhydraten. Al het substraat in de vorm van glucose werd volledig opgenomen tijdens de eerste 200 seconden van elke cyclus, en er was geen glucose over tijdens de laatste 160 seconden. Er werd door de cultuur geen koolstof uitgescheiden wat als reserve koolstofbron zou kunnen dienen tijdens de 160 seconden van glucose-uitputting. Toch ging de ademhaling in deze periode gewoon door, wat erop duidt dat de glucose die opgenomen werd in de periode waarin glucose in overdaad beschikbaar was intracellulair in één of andere vorm werd opgeslagen totdat het werd omgezet in één van de uiteindelijke (bij)producten. Zo hoopte ongeveer 11% van de koolstof die in de vorm van glucose werd opgenomen tijdens de periode van glucose-overdaad tijdelijk op als intracellulaire mannitol. Hoewel er opmerkelijke verschillen waren in het metabolisme van opslagkoolhydraten tussen onderbroken gevoede culturen en chemostaatculturen, was de totale omloopsnelheid van materiaal in hun reservoirs van trehalose en mannitol erg vergelijkbaar (18% versus 22% van de glucoseopnamesnelheid). Tot slot bleek uit de meting van de intracellulaire metabolietniveau's in de routes van het centraal metabolisme dat nog eens 18% van de opgenomen glucose ophoopte in de vorm van tussenproducten van het centraal metabolisme. Concluderend, om om te kunnen gaan met perioden van substraat-overdaad en substraat-uitputting heeft *P. chrysogenum* de capaciteit om tijdens perioden waarin substraat beschikbaar is een grote hoeveelheid koolstof te absorberen in intracellulaire reservoirs van opslagkoolhydraten en van de centrale metabole routes, waarvandaan het koolstof kan vrijmaken tijdens perioden van substraat-uitputting.

## List of publications

**de Jonge LP**, Heijnen JJ, van Gulik WM. Reconstruction of the oxygen uptake and carbon dioxide evolution rates of microbial cultures at near-neutral pH during highly dynamic conditions. *Biochem Eng J* 2014;83:42-54.

**de Jonge L**, Buijs NAA, Heijnen JJ, van Gulik WM, Abate A, Wahl SA. Flux response of glycolysis and storage metabolism during rapid feast/famine conditions in *Penicillium chrysogenum* using dynamic <sup>13</sup>C labeling. *Biotechnol J* 2014;9(3):372-85.

Zhao Z, ten Pierick A, **de Jonge L**, Heijnen JJ, Wahl SA. Substrate cycles in *Penicillium chrysogenum* quantified by isotopic non-stationary flux analysis. *Microb Cell Fact* 2012;11.

**de Jonge LP**, Douma RD, Heijnen JJ, van Gulik WM. Optimization of cold methanol quenching for quantitative metabolomics of *Penicillium chrysogenum*. *Metabolomics* 2012;8(4):727-35.

Douma RD, Deshmukh AT, **de Jonge LP**, de Jong BW, Seifar RM, Heijnen JJ, van Gulik WM. Novel insights in transport mechanisms and kinetics of phenylacetic acid and penicillin-G in *Penicillium chrysogenum*. *Biotechnol Prog* 2012;28(2):337-48.

van Gulik WM, Canelas AB, Taymaz-Nikerel H, Douma RD, **de Jonge LP**, Heijnen JJ. Fast sampling of the cellular metabolome. *Methods Mol Biol* 2012;881:279-306.

**de Jonge LP**, Buijs NAA, ten Pierick A, Deshmukh A, Zhao Z, Kiel JAKW, Heijnen JJ, van Gulik WM. Scale-down of penicillin production in *Penicillium chrysogenum*. *Biotechnol J* 2011;6(8):944-58.

Douma RD\*, **de Jonge LP\***, Jonker CTH, Seifar RM, Heijnen JJ, van Gulik WM. Intracellular metabolite determination in the presence of extracellular abundance: Application to the penicillin biosynthesis pathway in *Penicillium chrysogenum*. *Biotechnol Bioeng* 2010;107(1):105-15.

\*These authors contributed equally to this work.

Aboka FO, Yang H, **de Jonge LP**, Kerste R, van Winden WA, van Gulik WM, Hoogendijk R, Oudshoorn A, Heijnen JJ. Characterization of an experimental miniature bioreactor for cellular perturbation studies. *Biotechnol Bioeng* 2006;95(6):1032-42.



## Curriculum vitae

Lodewijk Philip de Jonge was born in Leiden, The Netherlands on the 28th of December 1981. After graduating from the Stedelijk Gymnasium Leiden in 2000, he started his study Life Science & Technology, a BSc and MSc program which was offered jointly by Leiden University and the Delft University of Technology. He performed a 3 months' BSc research project in the Enzymology group at the Delft University of Technology on the "Purification, characterization and cloning of a hydrolase from the archaeon *Pyrococcus furiosus*". He received his BSc degree cum laude in 2003. During the MSc program Lodewijk developed an interest in the analysis of fermentation processes, which resulted in performing the 9 months' MSc research project "Biological experiments for the validation of a biosystem for controlled uptake rate variation experiments (biocurve)" in the Bioprocess Technology group at the Delft University of Technology. He received his MSc degree cum laude in 2006.

Lodewijk started as a PhD student in the Bioprocess Technology group at the Delft University of Technology under the supervision of dr. W.M. van Gulik and prof. dr. ir. J.J. Heijnen in 2006. His research focused on the physiological and metabolic response of *Penicillium chrysogenum* to substrate concentration gradients in large scale penicillin fermentations. The results are described in this thesis.

Since April 2012, Lodewijk works as scientist in the upstream process development group at Janssen Infectious Diseases and Vaccines (formerly Crucell) in Leiden, The Netherlands. There he is involved in the development and scale up of platform technologies for the production of various human vaccines.



# Acknowledgements

Now that the writing of my thesis has come to an end, it is time to thank the many people who have contributed in one way or another to the completion of this thesis.

First and foremost, I would like to thank Sef, my promotor. Your enthusiasm for scientific research, and your passion for biotechnological processes and the analysis of metabolic networks have persuaded me to start this research project. Thank you for instructing me in your research approach, in which you always strive not only for abundance, but also precision of measurements, so that the obtained data sets can always be checked for consistency and correctness. Thank you also for your patience with me. On (too) many occasions, I got stuck in my analyses or in my writing process and didn't know how to proceed, and I am deeply impressed by the fact that you were able to provide a way out for me on each of these occasions. Secondly, I am very much indebted to Walter, my co-promotor, for many years of supervision and for providing a range of valuable small suggestions and big ideas. Thank you for all of your critical notes which improved my research proposals. Most importantly, I am grateful for your tireless improvements of my manuscripts with your exceptional writing skills, which were an instructive example for me.

I enjoyed the various bigger and smaller collaborations I had around *Penicillium chrysogenum* and penicillin fermentations during my research project. Starting around the same time with our projects, I profited greatly from the help, exchange of results and discussions within the “pen clan”. Rutger and Zheng, thank you for an unforgettable time in the lab, at conferences and during a holiday in Mexico. I am grateful for the work of Uly, which formed the basis for all the quantitative metabolomics work I did. Amit is thanked for our joined effort to generate reference fermentation data. Thanks go out to Aljoscha, for his interest in my experimental setup and results, which, combined with his modelling skills, yielded an interesting article. I am also grateful for all the valuable discussions with colleagues, partners and experts in the IMB group in Delft, at the University of Groningen and at DSM.

Especially important for the results described in this thesis were the effort and dedication of the analytical team. Cor, Angie, Jan, Johan, Zhen and Reza, thank you for the development of high quality methods, and for your accurate way of working while analyzing my enormous sets of samples. Equally essential was the maintenance of the fermentation labs, for which I thank Rob, Dirk, Mario and Susan. Many thanks also to everyone in the Kluyverlab who worked in any support function.

A number of students worked with me in my research project. I want to thank Folkert, Luke, Bouke, Caspar, and Klaas for their contributions to my projects. I enjoyed working with you, and I learned a lot from you.

I want to thank all colleagues of the Bioprocess Technology group (now Cell Systems Engineering) as well as those in the rest of the Kluuyverlab for a stimulating scientific environment, and for enjoyable moments of diversion.

I want to thank Wim de Laat for lending me his copy of Jens Nielsen's book "Physiological Engineering Aspects of *Penicillium chrysogenum*" back in November 2005, when we worked together at Nedalco, as soon as he learned about the topic of my PhD project that I was about to start then. I used the book so often during the past years to look up details about the metabolism of *Penicillium chrysogenum*, that it will be a little hard for me to return it to you. Of course, I am much obliged to Jens Nielsen for writing the book in the first place.

Many thanks for my current manager, Bas Diepenbroek, for continuing to encourage me to finalize this thesis, as you believed this was important for me, and for my personal growth. I have to admit that I felt extremely nervous each time you enquired about the status of my thesis, but you always managed to strike the right note when we discussed this sensitive topic. I believe I couldn't be luckier than to have you as my manager at this point in my career, and I am grateful for all the opportunities I'm offered to develop as a professional. I also thank all my other colleagues at Janssen for their interest in my PhD project.

In 2011, I was working on chapter 4, trying hard to fit the model described there to my experimental data. At that time, I visited the exhibition "Willem Hussem – vormen van ruimte", and as soon as I saw it, I was struck by the painting now displayed on the cover of this book. To me, it expresses very powerfully the tension there can be between two simple lines, just as there can be tension between a model and reality. I'm grateful to Frank Hussem for giving me permission to use the painting, and to John Stoel for providing his photo of it.

The concentration and perseverance that I needed to continue working on this thesis could only be maintained over such a long period of time thanks to regular moments of diversion and relaxation. Playing music and listening to music help(ed) me shift my brain activity. Therefore I want to thank Susanne Gersch, the Zeemanlaantrio, and the members of the Praetorius ensemble for all the times at which we experience(d) how wonderful it is to play music together. I particularly want to thank Dmitri Shostakovich for all the string quartets he composed, which have accompanied me during many hours of data analysis and manuscript writing.

Many thanks also to my friends and family for their interest, encouragement and support. Special thanks go out to my LST friends Suming, Elmar and Rinus, for all the times we have exchanged our experiences of being a PhD student.

Most of all, I want to thank Aletta, for your understanding all those years, for all the times you comforted me, for your encouragement, for your love and support! I am very lucky to be married to you. I am happy for you that I finalized this project. And Daniël, you too incited me to complete this thesis. Thank you for that. It's wonderful that you are here!



